



NTNU – Trondheim
Norwegian University of
Science and Technology

New technologies for purification and carbon capture in hydrogen production from natural gas

Kristin Skrebergene

Master of Energy and Environmental Engineering

Submission date: June 2015

Supervisor: Truls Gundersen, EPT

Co-supervisor: Kristin Jordal, SINTEF
Mari Voldsund, SINTEF

Norwegian University of Science and Technology
Department of Energy and Process Engineering

EPT-M-2015-82

MASTER THESIS

for

Student Kristin Skrebergene

Spring 2015

New technologies for Carbon Capture in Hydrogen Production from Fossil Fuels

*Nye teknologier for karbonfangst i hydrogen-produksjon fra fossile kilder***Background and objective**

Hydrogen is expected to be an important energy carrier in a future carbon constrained energy society according to different scenarios developed by e.g. the International Energy Agency (IEA). In addition to H₂ production from renewable resources, H₂ production from fossil fuels such as natural gas will also be important. In order to prevent CO₂ emissions, H₂ production processes using fossil fuels as feedstock must be integrated with CO₂ separation and capture.

As part of a last year project in the fall of 2014, HYSYS was used to develop different process concepts for H₂ production from natural gas with carbon capture. The main shift from the last year project to this Master thesis project is related to the use of membranes in H₂ production with CO₂ capture. The simulation models developed during the last year project will be used to analyze the effect on process efficiency of utilizing different emerging separation technologies for H₂ and CO₂ such as membranes and low temperature processes.

The main objective of this Master thesis project is to compare membrane solutions and low-temperature solutions for CO₂ capture with established technologies for carbon capture in hydrogen production from natural gas.

The following tasks are to be considered:

1. A brief literature study of the use of membranes and low temperature processes for carbon capture.
2. Extend the ATR hydrogen production case from the last year project to also include a power plant that produces the required amounts of steam and power. Design the heat recovery system using Pinch Analysis.
3. Perform HYSYS simulations of cases with CO₂ separation (e.g. one membrane module, sequential membrane and WGS modules or WGS-MR) and low temperature CO₂ capture.
4. Carry out a parametric study on energy consumption versus membrane area for the membrane process (provided that a membrane model is available from SINTEF Materials and Chemistry).

5. Compare and evaluate the different cases.

-- ” --

Within 14 days of receiving the written text on the master thesis, the candidate shall submit a research plan for his project to the department.

When the thesis is evaluated, emphasis is put on processing of the results, and that they are presented in tabular and/or graphic form in a clear manner, and that they are analyzed carefully.

The thesis should be formulated as a research report with summary both in English and Norwegian, conclusion, literature references, table of contents etc. During the preparation of the text, the candidate should make an effort to produce a well-structured and easily readable report. In order to ease the evaluation of the thesis, it is important that the cross-references are correct. In the making of the report, strong emphasis should be placed on both a thorough discussion of the results and an orderly presentation.

The candidate is requested to initiate and keep close contact with his/her academic supervisor(s) throughout the working period. The candidate must follow the rules and regulations of NTNU as well as passive directions given by the Department of Energy and Process Engineering.

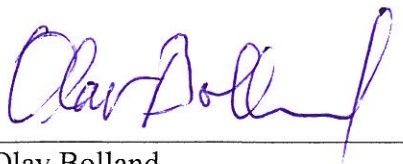
Risk assessment of the candidate's work shall be carried out according to the department's procedures. The risk assessment must be documented and included as part of the final report. Events related to the candidate's work adversely affecting the health, safety or security, must be documented and included as part of the final report. If the documentation on risk assessment represents a large number of pages, the full version is to be submitted electronically to the supervisor and an excerpt is included in the report.

Pursuant to “Regulations concerning the supplementary provisions to the technology study program/Master of Science” at NTNU §20, the Department reserves the permission to utilize all the results and data for teaching and research purposes as well as in future publications.

The final report is to be submitted digitally in DAIM. An executive summary of the thesis including title, student's name, supervisor's name, year, department name, and NTNU's logo and name, shall be submitted to the department as a separate pdf file. Based on an agreement with the supervisor, the final report and other material and documents may be given to the supervisor in digital format.

- Work to be done in lab (Water power lab, Fluids engineering lab, Thermal engineering lab)
 Field work

Department of Energy and Process Engineering, 13 January 2015



Olav Bolland
Department Head



Truls Gundersen
Academic Supervisor

Co-Supervisor(s):

Mari Voldsund, SINTEF Energy Research, E-mail: Mari.Voldsund@sintef.no
Kristin Jordal, SINTEF Energy Research, E-mail: Kristin.Jordal@sintef.no

Preface

This master thesis was completed in the spring of 2015 at the Norwegian University of Science and Technology in Trondheim. The thesis is written at the Department of Energy and Process Engineering as the final part of the study program Energy and Environment. The work extends over a 20-week period, and constitutes 30 credits. The specialization project conducted in the autumn 2014 forms the basis for the work done in the master thesis.

I would especially like to thank my supervisor Truls Gundersen for great guidance during the semester. Further, I would like to express a special thanks to my co-supervisors from SINTEF Energy Research, Mari Voldsund and Kristin Jordal for good support and guidance. I would also like to send my gratitude to David Berstad from SINTEF Energy Research for great help with necessary simulations that were outside the scope of this thesis.



Kristin Skrebergene
Trondheim 09.06.15

Abstract

In a society increasingly concerned with environmentally friendly solutions for energy extraction, hydrogen is expected to be an important energy carrier. Hydrogen can originate from various feedstocks, where fossil fuels represent the largest share. Among the fossil fuels, natural gas outperforms the others regarding environmental considerations in hydrogen production. It is of great interest that hydrogen-producing plants are under constant development, related to improved efficiency and reduced emission. This work therefore focuses on potential improvements of the conventional process for hydrogen production from natural gas.

The Autothermal Reforming process (ATR) for hydrogen production is the process under investigation, due to the possibility of capturing the required amount of CO₂ through a single separation unit. In order to develop a platform for comparing the conventional ATR process with new and possible improved technology, a case study was developed. The base case of this study comprises the conventional ATR process, containing the reformer, the water-gas shift reactors, the Pressure Swing Adsorption (PSA) unit for hydrogen purification and a solvent process for CO₂-removal in front of the PSA. PSA off-gas is sent to a gas turbine for power generation.

Membranes represent a new and optimistic technology when it comes to hydrogen purification. Using membranes for this purpose facilitate CO₂-capture downstream. An interesting process concept is therefore to combine the membrane with a following low-temperature separation process for CO₂. The main objective for this thesis will consequently be to compare the conventional ATR process with the more unconventional processes, concentrating on membrane solutions in various designs and low-temperature separation processes for CO₂-capture.

Four membrane cases are developed, where different solutions for membrane implementation are studied. The cases consider, respectively, implementation of a single membrane module placed after the WGS-unit, a sequential membrane and WGS module, a single membrane case with 20 bar permeate pressure and a combination of the base case and the single membrane case where CO₂ removal occurs in front of the membrane. All developed cases aim to be heat-and power integrated, and two membrane feed pressures were investigated, respectively 36 bar and 66 bar.

HYSYS, version 8.3, is used as the primary simulation tool, where all the developed cases are constructed. The tendency of the simulation results is that the case considering a sequential membrane and WGS module performs better than the other studied cases, regarding both the overall plant efficiency and the total CCR. This case stands out as the best solution for hydrogen production. The single membrane process, however, will not provide any advantageous effects compared to the conventional ATR process, except for the fact that membranes generate entirely clean hydrogen. Elevated permeate pressure makes hydrogen compression superfluous. However, 20 bar permeate pressure leads to an unrealistic large membrane area due to lack of driving forces. This was observed through the membrane parametric study carried out. The results for the case considering CO₂-removal in front of the membrane module, follows approximately the same trend as the single membrane case, and will not provide any great benefits compared to the conventional ATR process. In addition, this case consumes most power in order to produce the same amount of hydrogen as the other cases. However, the required membrane area will decrease significantly for this case. The decision between the single membrane cases, therefore, becomes a tradeoff between investments costs and operating costs. The conclusion of this work is that the case considering a sequential membrane and WGS module, with two steps, gives the best results, and should be the applied process for hydrogen production.

Sammendrag

I et samfunn som i stadig økende grad er opptatt av miljøvennlige løsninger for energiutvinning, er hydrogen forventet å være en viktig energibærer. Hydrogen kan produseres fra ulike råstoff, hvor fossile brenslere utgjør den største andelen. Blant de fossile brenslene utkonkurrerer naturgass de andre med tanke på miljøhensyn. Det er av stor interesse at hydrogenproduserende anlegg er under konstant utvikling for å kunne øke effektiviteten og redusere klimaskadelige utslipp. Denne oppgaven fokuserer derfor på potensielle forbedringer i den tradisjonelle prosessen for hydrogenproduksjon fra naturgass.

Opgaven fokuserer på den Autotermiske Reformerings prosessen (ATR) for hydrogenproduksjon. Grunnen til dette er at denne prosessen har mulighet for å fange den nødvendige mengden CO₂ gjennom en enkelt separasjonsenhet. For å kunne sammenligne den tradisjonelle ATR prosessen med ny og muligens forbedret teknologi, er det nødvendig å opprette et case studie. Basisprosessen i denne studien omfatter den konvensjonelle ATR prosessen som består av selve reformeringsenheten, vann-gass-skiftreaktorer og en renseenhet for hydrogenet. I tillegg inneholder basisprosessen et CO₂-fjerningsanlegg som er plassert foran renseenheten. Avgass fra renseenheten blir brukt som brensel i en gass turbin.

Membraner representerer en ny og optimistisk teknologi når det gjelder hydrogenrensing. Bruk av membraner gjør det lettere å fange CO₂ nedstrøms på grunn av den økende CO₂-konsentrasjonen på gassen etter membranen. Et interessant konsept for hydrogenproduksjon vil derfor være å kombinere membranen med en lavtemperatur separasjonsprosess for CO₂. Hovedmålet for denne oppgaven vil følgelig være å sammenligne den konvensjonelle ATR prosessen med de mer utradisjonelle prosessene, hvor fokuset vil være på ulike membran løsninger og lavtemperatur separasjonsprosesser for CO₂-fangst.

Det ble utviklet fire forskjellige membrancase, hvor ulike metoder for implementering ble studert. Casene betrakter henholdsvis en enkelt membranmodul plassert etter WGS-enheten, en sekvensiell membran og WGS modul, en enkelt membranmodul med 20 bar permeattrykk, samt en kombinasjon av basisprosessen og en enkelt membranmodul hvor CO₂-separasjonen foregår foran membranen. Alle casene har som mål å være varme- og kraftintegreert, og to ulike membran trykk er studert, henholdsvis 36 bar og 66 bar.

Alle de ulike casene ble konstruert og simulert i HYSYS, versjon 8.3. Simuleringsresultatene viser en klar tendens at prosessen som tok for seg en sekvensiell membran og WGS modul presterer best, både med tanke på virkningsgraden for prosessen og den totale CO₂-fangst raten. Når det gjelder prosessen som studerte implementeringen av en enkelt membranmodul, viser imidlertid resultatene at denne prosessen ikke vil gi noen særlig form for forbedringer sammenlignet med den konvensjonelle ATR prosessen, utenom det faktumet at membranprosesser generer helt rent hydrogen. I prosessen som studerte 20 bar permeattrykk ble hydrogenkompresjon overflødig, noe som gjør at kraftbehovet minker. Imidlertid ble arealbehovet i membranen urealistisk stort på grunn av manglende drivende krefter. Dette ble observert ved hjelp av en sensitivetsanalyse utført for membranmodulen i denne prosessen. Prosessen som studerte påvirkningen av CO₂-fjerning før membranmodulen, vil i liten grad endre resultatene til prosessen som implementerte en enkelt membranmodul med påfølgende lavtemperatur CO₂-fangst. I tillegg har denne prosessen det største kraftbehovet av alle de studerte prosessene. Med andre ord vil ikke denne prosessen medføre betydelige forbedringer sammenlignet med basisprosessen. Derimot vil fjerning av CO₂ før membranen redusere det nødvendige membranarealet betydelig sammenlignet med prosessen som fjerner CO₂ etter membranen. Konklusjonen er at prosessen som inkluderer en sekvensiell membran og WGS modul, med to steg, får de beste resultatene og bør være den prosessen som blir anvendt for hydrogen produksjon.

Abbreviations

AEA	Aspen Energy Analyzer
ASU	Air Separation Unit
ATR	Autothermal Reforming
BC	Base Case
BFW	Boiler Feed Water
CCR	Carbon Capture Rate
CCS	Carbon Capture and Storage
CW	Cooling Water
DSU	Desulfurization Unit
EOS	Equation of State
GGC	Grand Composite Curve
GT	Gas Turbine
GWP	Global Warming Potential
HEN	Heat exchanger Network
HHV	Higher Heating Value
HP	High Pressure
HRF	Hydrogen Recovery Factor
HRSG	Heat Recovery Steam Generator
HT	High Temperature
HTS	High Temperature Shift
HX	Heat Exchanger
LP	Low Pressure
LT	Low temperature
LTS	Low Temperature Shift
MMscfd	Million Metric Standard Cubic Feet per Day
MP	Medium Pressure
MR	Membrane Reactor
NCS	Norwegian Continental Shelf
NG	Natural Gas
POX	Partial Oxidation Reforming
PSA	Pressure Swing Adsorption
SMR	Steam Methane Reforming
ST	Steam Turbine
TIT	Turbine Inlet Temperature
TSA	Temperature Swing Adsorption
WGS	Water Gas Shift

Table of Contents

1. Introduction.....	1
1.1 Background and Objective.....	1
1.2 Outline	2
2. Motivation - Why hydrogen?	3
3. Hydrogen production from natural gas	4
3.1 Why hydrogen from natural gas?.....	4
3.2 Steam Methane Reforming Process	5
3.3 Partial Oxidation Process.....	6
3.4 Autothermal Reforming Process	6
3.5 Thesis focus	6
4. Conventional Autothermal Reforming – a literature review	8
4.1 Concept overview	8
4.2 Unit description	9
5. Alternatives studied	27
5.1 Concept overview	27
5.2 Use of membranes in hydrogen production	27
5.3 Low temperature process for carbon capture	34
6. Process integration fundamentals.....	37
6.1 Pinch Analysis	37
6.2 Grand composite curve	38
7. Process Description	40
7.1 Process characterization.....	40
7.2 Heat- and power integration	46
8. Methodology, Design basis and HYSYS implementations	53
8.1 Design Basis	53
8.2 Applying Aspen Energy Analyzer	57
8.3 HYSYS simulations.....	58
9. Analysis and resulting heat-integrated processes	64
9.1 Heat – and power integrated base case.....	64
9.2 Heat – and power integrated membrane cases with 36 bar inlet pressure.....	69
9.3 Heat and power-integrated membrane cases with 66 bar inlet pressure	83
9.4 Overview of results.....	88
10. Results.....	90
10.1 Calculations	90
10.2 Process results.....	91
10.3 Parametric study of the membrane module – results and analysis.....	96
11. Discussion and analysis of process results	101
12. Discussion of process simulations	108
13. Conclusion	110
14. Further work.....	112
15. References.....	114
16. Appendix	118
Appendix A - Derivations.....	118
Appendix B – Unit Specifications.....	119
Appendix C - Calculations.....	121
Appendix D - Power distribution	138
Appendix E – Stream Data.....	143
Appendix F – LT-process simulation results	155
Appendix G – HYSYS screenshots	159
Appendix H – Grand Composite Curves and AEA – networks.....	160

1. Introduction

1.1 Background and Objective

The world is facing a tremendous task trying to limit the emissions that can lead to climate changes. Environmentally friendly solutions in the energy sector will become more important than ever in the future carbon-constrained society. Hydrogen is expected to be an important energy carrier as the concern regarding the environment increases. Using pure hydrogen in combustion or in fuel cells to get an energy output, only releases water vapor, which has no negative effect on the environment. However, production of hydrogen requires energy. The used energy may stem from renewable sources, like wind and solar, but the largest proportion of the produced hydrogen today originates from fossil fuels. Among the fossil fuels, natural gas outperforms the others in terms of climate impact due to reduced emissions of greenhouse gasses. With that in mind, hydrogen production from natural gas could prove to be a very important step towards a more environmentally friendly society.

This master thesis focuses on hydrogen production from natural gas. For hydrogen production, originated from natural gas, to be environmentally friendly, the manufacturing needs to implement carbon capture. This is due to the large amount of CO₂ generated throughout the process. The thesis builds on the work presented in the specialization project, conducted during the fall 2014, where the objective was to develop different concepts for hydrogen production from natural gas, with carbon capture, in HYSYS. Based on the conventional Autothermal Reforming (ATR) process developed in the project work, the objective of this thesis is to compare the conventional ATR process with an ATR process using less matured technology. More precisely, the objective is to compare membrane solutions and low-temperature CO₂ capture with established technologies for respectively hydrogen purification and carbon capture in hydrogen production from natural gas, which is further described throughout the next section.

1.1.1 Problem description

The objective of this thesis is to develop a case study, where different cases of the ATR process are under investigation. This study intends to clarify the possible advantages of utilizing new technology for hydrogen production. With that in mind, the thesis work looks at cases where conventional technology is used, and compare them with cases where new and more modern technology is applied. The conventional ATR process creates this work's base case. The base case uses established technologies for hydrogen purification and carbon capture, referring to PSA and solvent processes.

Membranes represent a new and optimistic technology when it comes to hydrogen purification. Membrane separation is interesting due to the low energy consumption, the possibility for simple and continuous operation, the cost effectiveness and the reduced investment costs compared to the PSA unit (Ockwig and Nenoff, 2007). In addition, using membranes for this purpose ensures pure hydrogen due to the membranes 100% selectivity towards hydrogen (Atsonios et al., 2012). This is of great importance if the hydrogen shall be liquefied. Membranes also facilitate the use of low temperature carbon capture. The alternative cases are, accordingly, based on membranes for purification purposes and low temperature CO₂ capture instead of the more conventional solvent-process for CO₂ capture.

All cases aim to be self-sustained. This implies that the process should not have any external heat- or power supply, but be able to generate the required amount throughout the process. Fundamental process

integration techniques are applied in order to obtain heat- and power integrated processes. The cases and the basis behind the self-sustained processes are further discussed in Chapter 6 and 7.

The thesis also aims to investigate the membrane design further throughout a sensitivity analysis. This parametric study is carried out through a membrane module borrowed from SINTEF Materials and Chemistry. The intention is to study the impact of increased membrane feed- and permeate pressure. Variations to either the feed pressure or the permeate pressure affects the driving forces in membrane. The focus of the parametric study will be to investigate how changes in driving forces affect the membrane area. Two different feed pressures are studied, respectively 36 bar and 66 bar, for the membrane cases.

1.2 Outline

This report consist of two main parts, respectively a literature study and a case study, where the case study represent the largest part of the thesis. The overall structure of the report is as illustrated in Figure 1.1. The first part of the thesis contains a literature review, where fundamental theory based on the work done in this thesis is reviewed. Important theory is the characterization of the ATR process, described through two chapters. The first chapter focuses on the conventional ATR process, while the second chapter concentrates on the studied alternatives. In addition, the literature review also considers fundamental process integration theory.

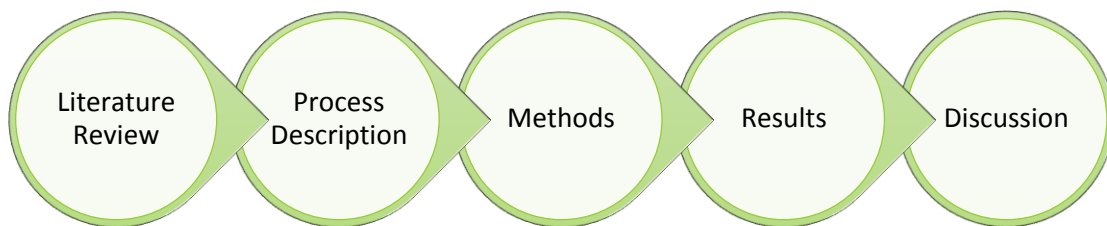


Figure 1.1: Thesis outline

In the next part of the thesis, the focus is directed towards the developed cases. As an introduction to this part of the report, the process description introduces the case study, and gives an overview of the developed cases. Throughout the method section, it will be described how the different cases are implemented in HYSYS, and how the additional simulation program Aspen Energy Analyzer is employed in this thesis. A design basis is also included under the methods part, where specifications regarding the processes are conducted. The result part contains a description of the resulting heat-and power integrated processes, process results from HYSYS simulations as well as a part considering a parametric study, where the results are given and analyzed. Results given in this part form the basis for the discussion provided in the next part. Process results are discussed in addition to a section covering a discussion of the HYSYS simulation. Finally, there will be a conclusion based on the findings in this study.

2. Motivation - Why hydrogen?

As the world's population is continuing to grow alongside the improving standard of living, the worldwide energy demand is rapidly increasing. Transportation and heating currently represent 2/3 of the primary energy demand in the world, and most of the energy supply to these sectors comes from fossil fuels (Gupta, 2008). Fossil fuels are easy to utilize, store and transport compared to many renewable energy sources. As the energy demand increases, the world needs new solutions for energy production in order to maintain the standards of living and at the same time consider the environmental issues by using fossil fuels. Hydrogen stands out as an environmentally friendly solution since it is considered as a nonpolluting energy carrier. Many environmentalists and industrial organizations claim that hydrogen can be the solution for the energy challenge the world is facing today (Gupta, 2008). However, this depends on what type of energy that is used in the production of hydrogen.

Primarily, one has to be aware of the fact that hydrogen is not an energy source, but an energy carrier. Hydrogen has to be produced from a hydrogen feedstock, usually water/steam. This process requires energy input. The type of energy used in hydrogen production determines whether the hydrogen is environmentally friendly or not. Hydrogen will be 100% renewable if the energy used in the production was renewable. For hydrogen produced from fossil fuels, which is most common, the process requires CCS for the hydrogen to be environmentally friendly.

When utilizing hydrogen in a fuel cell or directly in combustion, the only product, along with energy, is water vapor. This makes hydrogen an interesting field of study for a global strategy to reduce emission of greenhouse gasses. Hydrogen may prove to be a very important source for a low-carbon transportation system, but is facing big competition from electrical vehicles. One of the reasons is the lack of infrastructure for hydrogen in the transportation sector, and the fact that fuel cells are still very expensive. As fuel cell technology becomes more mature, the price might decrease, which would be a step towards a hydrogen driven transportation system. When it comes to infrastructure, this depends on the political engagement.

In addition to hydrogen being a very environmentally friendly energy carrier, it is also very flexible. There are multiple ways of producing hydrogen and it has potential applications across all end-use sectors (IEA, 2012). Hydrogen can produce energy by combustion to produce heat and pressure in an industrial process, or electricity by using a fuel cell. This implies that hydrogen can be used as energy input in all types of sectors, from big industrial plants to small households.

A big challenge within the energy sector is storage of energy over a longer period. Hydrogen can provide important storage capacity for energy. However, hydrogen is a very light gas, with a low energy density in gas phase (0.089 kWh/m³) (Energilink, 2008a). For comparison, natural gas has a relatively high energy density, respectively 11.11 kWh/m³ (Energilink, 2008a). In order to store large amount of energy, the hydrogen either has to be compressed, cooled down to liquid phase or stored in solid materials. These operations requires energy, but makes it possible to store clean energy over extended periods of time.

To summarize, production of hydrogen can be an important step towards a cleaner energy extraction, and thus to a more environmentally friendly society. It is necessary to make the energy utilization in the world today more environmentally friendly, and that is why hydrogen is an interesting topic for discussion.

3. Hydrogen production from natural gas

This thesis focuses on hydrogen production from natural gas. Natural gas reforming is the most important technique for hydrogen production today, and stands for around 48% of the hydrogen produced on a global scale (IEA, 2012). Reforming occurs when natural gas together with either steam and/or oxygen reacts by being transported over catalyst beds at high temperatures. What natural gas is mixed with, either steam, oxygen or both, decides whether the process is a steam methane reforming process, a partial oxidation process or an autothermal reforming process. This chapter briefly explains the mentioned techniques for hydrogen production, as well as an introduction to why it is beneficial to produce hydrogen from natural gas.

3.1 Why hydrogen from natural gas?

Despite the growing focus on using renewable energy sources, fossil fuels are still by far the most important energy source in the world today (IEA, 2014). The renewable energy production is not able to satisfy the current energy demand, leaving the world completely dependent on fossil fuels. To cope with such a trend, it becomes more important to utilize the fossil fuels in the most sustainable way. With that in mind, using fossil fuels to produce hydrogen can utilize the energy in the hydrocarbons more efficient than many other applications (Liu et al., 2010).

As much as 96% of the produced hydrogen today originates from fossil fuels (IEA, 2012). Among the fossil fuels, natural gas is the most environmentally friendly. Due to the growing concern for the environment, natural gas outperforms the other fossil fuels, and is likely to be favored in the future.

Natural gas has a higher hydrogen/carbon ratio than the other fossil fuels. This ratio is an indicator of energy content in the fuel, per mass, and the amount of CO₂ released under combustion. Hydrogen has a much higher energy content per mass than carbon, meaning that fuels with higher H/C-ratio contain more energy per mass. The “lighter” the fuel is, the higher H/C-ratio it will have, since it will be richer in hydrogen. Coal contains high values of carbon, typical 60-100% (Manum, 2009), thus have a lower H/C-ratio. Table 3.1 below shows the correlation between the H/C-ratio, energy content and CO₂ released for hydrogen and various hydrocarbons.

Table 3.1: H/C – ratio (Western Oregon University, 2006)

	<i>H/C- ratio</i>	<i>Energy Content (kJ/g)</i>	<i>CO₂ released (mole/10³ kJ)</i>
<i>Hydrogen</i>	-----	120	-----
<i>Natural Gas</i>	4/1	51.6	1.2
<i>Petroleum</i>	2/1	43.6	1.6
<i>Coal</i>	1/1	39.3	2.0
<i>Ethanol</i>	3/1	27.3	1.6

The CO₂ released is reversely proportional to the H/C-ratio, meaning that lighter hydrocarbons emit less CO₂, which favors natural gas.

Figure 3.1 depicts that using natural gas for hydrogen production instead of heavier hydrocarbons gives a higher hydrogen yield. Hydrogen yield is a measurement of how many moles of produced hydrogen there

will be per mole of fuel input. Since heavier hydrocarbons have a lower H/C – ratio, less hydrogen is available for reforming. In other words, you need more fuel when using heavier hydrocarbons compared to natural gas to produce the same amount of hydrogen. This means that less energy is required for producing the same amount of hydrogen when using natural gas instead of heavier hydrocarbons.

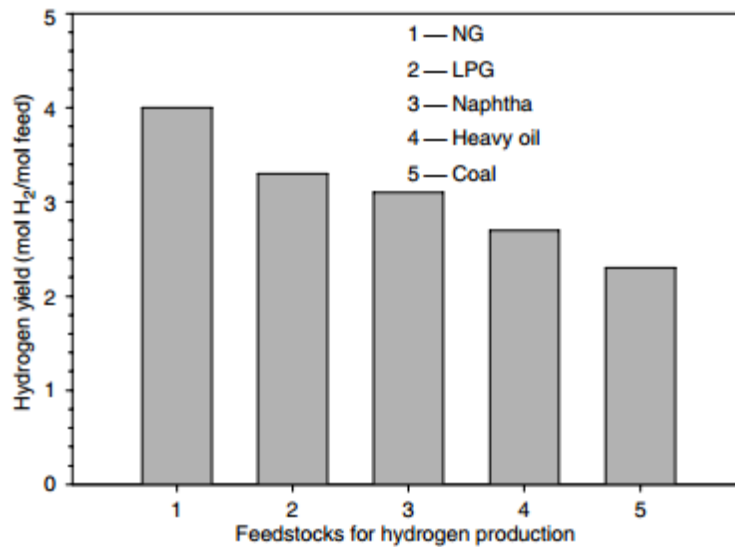


Figure 3.1: Maximum theoretical yield for hydrogen production by steam reforming (gasification) of different feedstock's (Gupta, 2008)

Due to the environmental profile of hydrogen production from natural gas, it will be of major interest in the future. The next sections consider the main processes for natural gas reforming for hydrogen production.

3.2 Steam Methane Reforming Process

A three-step process characterizes the Steam Methane Reforming (SMR) process. The first step contains a reformer where methane and heavier hydrocarbons react with steam and create carbon monoxide and hydrogen (3.1). This reaction is endothermic, meaning it requires heat to take place. Further, the carbon monoxide reacts with steam to generate carbon dioxide and hydrogen in the water-gas shift (3.2). This reaction is exothermic, meaning it releases heat. After this step, the gas enters the hydrogen purification stage, like illustrated in Figure 3.2.

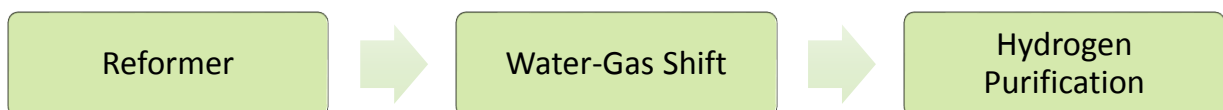
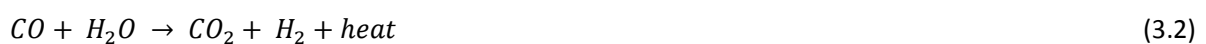


Figure 3.2: Overview SMR process

SMR is by far the most used process for natural gas reforming in manufacturing of hydrogen and stands for around 40% of the total world production (Gupta, 2008). The technology is mature and available for a wide range of plant sizes. All type of plants can use the SMR process, from small decentralized units to large-

scale syngas manufacturing plants. Syngas is a mixture of mainly carbon monoxide and hydrogen, sometimes some carbon dioxide as well (Liu et al., 2010).

3.3 Partial Oxidation Process

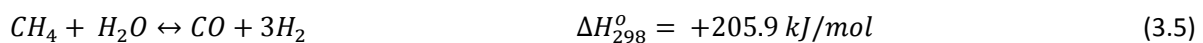
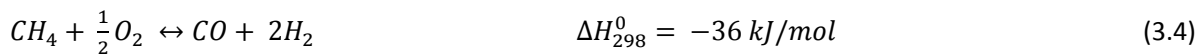
This technique for producing hydrogen is similar to the SMR process, except for the first step. The first step consists of partial combustion of methane with pure oxygen. The products from this reaction is carbon monoxide and hydrogen. This reaction is exothermic, and is as followed.



After partial combustion of methane, the gas enters the water-gas shift step, where carbon monoxide reacts with steam and creates carbon dioxide and hydrogen (3.2). The last step is hydrogen purification.

3.4 Autothermal Reforming Process

Autothermal reforming process is a combination of the Steam Methane Reforming process (SMR) and the Partial Oxidation Process (POX). Inside the ATR, natural gas reacts with steam to provide syngas, as in the SMR process, and in addition, parts of the fuel react with oxygen (3.5). The fundamentals of ATR are summarized in the given reaction equations.



After the reforming unit, the steps equal the SMR process. This work focuses on the ATR process, as will be argued for throughout the next section.

3.5 Thesis focus

This thesis focuses only on the ATR process. Natural gas reforming is an endothermic reaction, meaning it requires heat. The difference between a SMR process and an ATR process is how this heat is supplied. The SMR process uses so-called external combustion. This implies that combustion occurs outside the reforming tubes where the reforming takes place. In an ATR process, on the other hand, heat supply occurs through internal combustion, where the oxidation (3.5) produces the required amount of heat for the steam methane reforming (3.4), inside the reforming tubes. The benefit of using internal combustion is that the reforming unit do not discharge two separate CO₂-containing streams. See Figure 3.3 for an illustration.

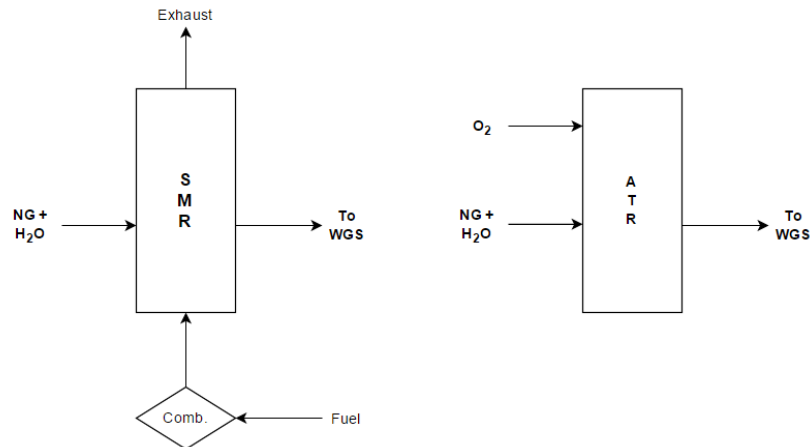


Figure 3.3: overview heat supply SMR contra ATR

As Figure 3.3 depicts, the reforming occurring in the SMR reactor has two discharge points of CO₂. The gas leaving the reformer to proceed the process contains a large share of CO and CO₂. Carbon monoxide reacts further in the WGS-reactors and generates CO₂. In addition, the exhaust from the fuel combustion contains CO₂. This makes it necessary with two CO₂ capturing units in the SMR process to be able to capture most of the CO₂. For the ATR process, where heat supply occurs inside the tubes, the generated CO₂ and CO during reforming and oxidation follow the rest of the gas through the process. It is therefore possible to capture most of the CO₂ through one capturing unit, normally placed after the WGS-stage. Due to the increased concern for the environment, CO₂-capture implementation is of great importance. Building one unit for this purpose, instead of two, reduces the penalty.

As the reformer in the ATR process utilizes the heat from oxidation to cover the heat requirements for steam-methane reforming, the reformer unit becomes more compact and simple, which reduces the capital cost. In addition, the ATR reforming can take place at increased pressure levels compared to the SMR process, making the compression work required for the syngas less (Gupta, 2008).

The ATR process is a very interesting process for hydrogen production, and is because of the mentioned reasons the focusing process in this work. The next chapters provide a literature survey on the conventional ATR process, as well as an introduction to the more immature technologies available for hydrogen production through an ATR process.

4. Conventional Autothermal Reforming – a literature review

4.1 Concept overview

The conventional ATR process studied in this thesis contains the units illustrated in Figure 4.1. Natural gas and steam go through pre-reforming before the mixture enters the main reformer along with oxygen from an Air Separation Unit, ASU. After the reformer stage, the gas contains considerable amounts of CO. In order to improve the hydrogen yield, the process includes Water-Gas Shift, WGS, where CO reacts with steam and generates water vapor and hydrogen. This hydrogen plant contains an absorption process for CO₂ capture, which is located in front of the purification unit. The hydrogen plant modeled in this work sends the PSA off-gas to a gas turbine, while the pure hydrogen goes to the liquefaction unit. The next section goes systematically through the process, and describes each unit in detail.

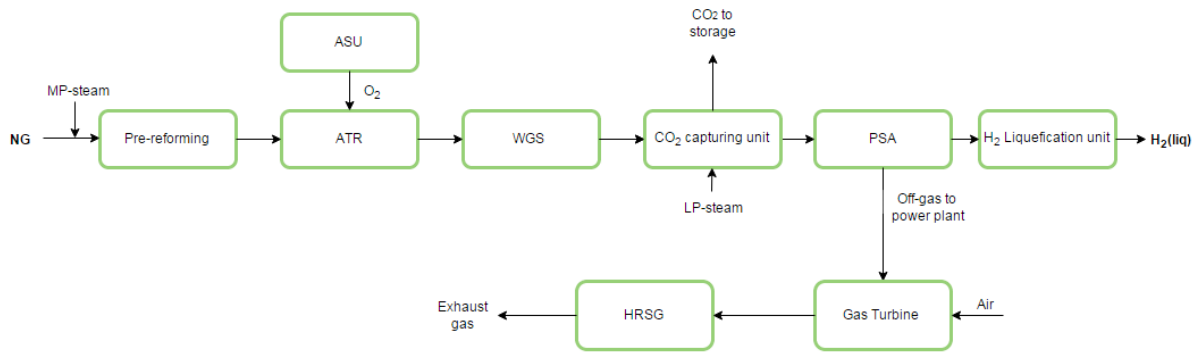


Figure 4.1: Overview conventional ATR process

All considered cases developed in this thesis aim to be self-sustained. To achieve a self-sustained process, all heating- and cooling requirements must be in balance, and the process must be able to produce the amount of required power. Figure 4.2 below gives a sketch of the process control volume. As the figure illustrates, the streams entering the process are natural gas, oxygen from the air separation unit, steam and air. Streams leaving the process are the captured and liquefied CO₂, the liquefied hydrogen and the exhaust gas from the gas turbine. In a self-sustained process, these are the only streams entering and leaving the hydrogen producing plant. This control volume applies to all hydrogen producing plants considered in this thesis.

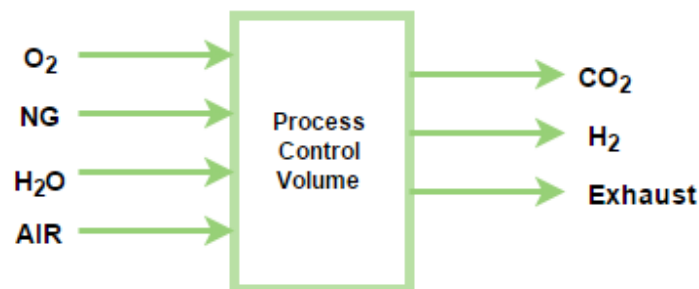


Figure 4.2: Control volume

4.2 Unit description

This section intends to give a more complementary description of the units in the conventional ATR process, which forms this works base case. The block diagrams in the previously section shows that the main units in the ATR process are the pre-reformer, the main reformer, the air separation unit, the water-gas shift, the purification unit and the carbon capturing unit. In addition, this ATR process contains a power plant and a liquefaction unit. A common unit in all hydrogen production facilities is pretreatment of the gas. This unit is however not implemented in this thesis, but will be briefly described.

4.2.1 Pretreatment

Natural gas contains, in various amounts, sulfur compounds. Sulfur damages the catalysts in the reformer and in the water-gas shift reactors. Sulfur will also harm the membranes, if membranes are used for hydrogen purification. In addition, if the produced hydrogen is intended for use in fuel cells, even traces of sulfur in the feed gas can damage the anode catalyst. The first step in any hydrogen producing plant is therefore to remove the sulfur. This occurs in a desulfurization unit (DSU) (Gupta, 2008).

This thesis do not consider pretreatment of the gas. Primarily since natural gas from the Norwegian Continental Shelf (NCS) contains small amounts of sulfur. Pretreatment complicates the process and it is therefore assumed that the entering natural gas is absent of all sulfur compounds.

4.2.2 Air separation unit

Air separation is required in order to provide the reformer with the necessary amount of oxygen. Separation of air takes place in the Air Separation Unit, ASU. The ASU splits air into its primary components, mainly nitrogen and oxygen. Currently, the most efficient and cost-effective technology for oxygen production is through cryogenic air separation (Smith and Klosek, 2001). This method involves compression and cooling of the air until it is in liquid form. The components can then be separated by selectively distilling at their various boiling point temperatures. Cryogenic air separation is a mature technology and produces high purity gases. The purity of the oxygen entering the ATR is 95%. The remaining 5% consists of 1.76% N₂ and 3.24% argon (Jones et al., 2011). However, the process is very energy intensive.

The ASU is not modelled in HYSYS due to its complexity. However, estimated values are used for specific separation energy and compression energy to get the energy requirement for this unit involved in total energy consumption for the plant. The values are summarized in Table 4.1. Specific separation energy is defined in industry as the energy required for producing 1 ton pure O₂ at ambient conditions, which is 15°C, 1atm and 60% relative humidity for air (Fu, 2015). This study applies a simple ASU design, which consists of a standard double-column distillation design. The choice of design depends on, among others, site conditions, air supply technology, air supply pressure, required purity and pressure of O₂ (Higginbotham et al., 2011). Double column design is usually preferred when there is limited use of the remaining nitrogen, as in this case. Processes that use nitrogen to supply the gas turbine usually prefers a triple column design (Higginbotham et al., 2011). When applying a double-column distillation design, a value of 225kWh/ton of produced O₂ seems reasonable according to Chao Fu, postdoctoral fellow at NTNU.

Table 4.1: Specific separation energy and compression energy for ASU

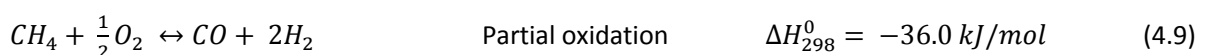
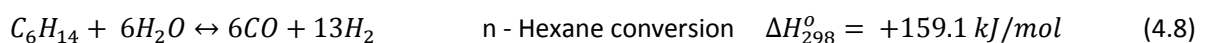
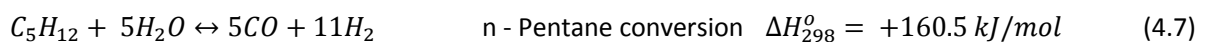
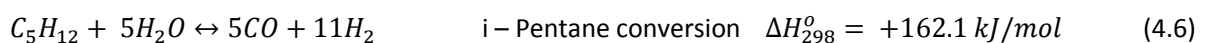
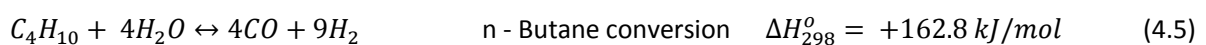
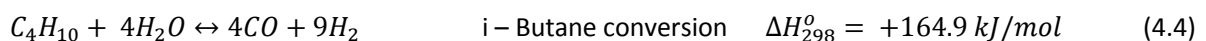
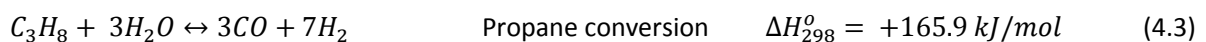
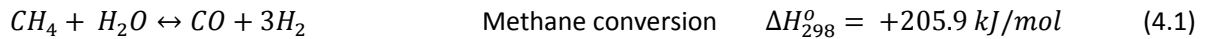
<i>Energy consumption ASU</i>	
<i>Specific separation energy (kWh/ton O₂)</i>	225
<i>Compression energy (kWh/ton O₂)</i>	84.9

Normally, when talking about air separation units, the focusing parameter is the specific energy consumption, which is the total energy consumption per ton pure O₂ produced and compressed. The

specific energy consumption is equal to the specific separation energy plus the compression energy. The compression energy represents the power needed to compress the oxygen up to the desired level before it enters the ATR.

4.2.3 Reforming unit

Steam supplies the process before the gas enters the reformer stage. Production of syngas occurs in the reformer, where hydrocarbons react with steam and oxygen and create syngas with help from catalysts. The chemical equilibriums in the reformer stage are the following (Moulijn et al., 2013) :



Depending on the amount of heavier hydrocarbons (C₂+) present in the natural gas, the reformer may consist of two stages, respectively a pre-reformer and a main reformer (Gupta, 2008).

Pre-reformer

Natural gas consists of mainly methane, but heavier hydrocarbons are present at various amounts. The main purpose of a pre-reformer is to convert the heavier hydrocarbons into a mixture of CH₄, CO, CO₂, H₂ and H₂O. Even though the amount of heavier hydrocarbons are limited in natural gas, it is normally sufficiently large to require a pre-reformer. The chemical reactions taking place in the pre-reformer are listed above. However, the partial oxidation only occurs in the main reformer, and the shift reaction mainly occurs in the WGS-reactors.

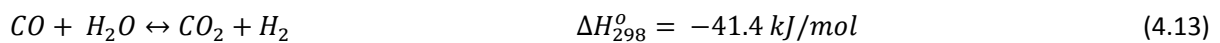
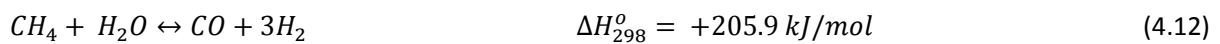
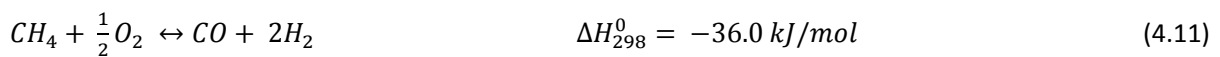
Implementation of a pre-reformer reduces the risk of carbon deposition in the main reformer since heavier hydrocarbons are converted before the gas enters the main reformer. Heavier hydrocarbons are more reactive than methane, resulting in more easily decomposition over the catalysts, which might lead to deactivation. Carbon deposition can destroy the catalysts by either encapsulation or dissolving and diffusion inside the catalyst pellet. This reduces the activity of the catalyst and the pressure drop in the reformer increases due to plugging of the catalyst. The pre-reformer operates at a lower temperature than the main reformer, which enables the pre-reformer to work properly without carbon deposition problems. Since the pre-reformer reduces the chances for carbon deposition in the main reformer, the overall S/C-ratio can be reduced. S/C-ratio is a reflection of how many moles of steam there are, compared to moles of carbon. Steam is used to avoid carbon deposition. Meaning that the steam requirements for the main reformer would be higher if the pre-reformer was not included. When reducing the S/C-ratio, the overall plant efficiency increases since steam production requires energy. This is further discussed in the next section.

In addition to reducing the overall S/C-ratio, a pre-reformer increases the opportunity for using feed gas of various quality. If the natural gas consists of almost pure methane, this step would be of less use than if the feed gas contains large quantities of heavier hydrocarbons. The pre-reformer also works as a “sulfur guard”. If some small concentrations of sulfur dioxide persist in the feed gas after the sulfur removal, it will react in the pre-reformer and not do any damage downstream. Having a pre-reformer result in stable and mild operating conditions for the downstream reformer.

The reactions in the pre-reformer are normally operated under temperatures between 450-500°C with Ni-catalyst present (Ebner and Ritter, 2009). The reactions are endothermic, causing the temperature to drop through the reactor. Since the chemical reactions are endothermic, the reactor prefers high operating temperature.

Main reformer

The gas leaving the pre-reformer enters the main reformer, the ATR, together with pure oxygen from the air separation unit. The gas is now virtually absent of all heavier hydrocarbons and the reactions taking place in the main reformer are summarized in 4.11 - 4.13 (Moulijn et al., 2013).



The latter reaction is the shift-reaction, which mainly occurs in the WGS reactors. However, some CO and H₂O will react in the reformer as well.

When natural gas, steam and oxygen enters the ATR, it goes into reforming tubes where the reactions take place. These reforming tubes consist of catalysts to make the reforming more rapid. Heat produced by oxidation, equation 4.11, fulfils the heat requirements for the endothermic steam methane reforming reaction (4.12). Consequently, no additional heat is required when using an ATR (Liu et al., 2010). This way of supplying heat to the reformer is called internal combustion, as discussed in Chapter 3.

An ATR reactor consists of three zones, respectively a combustion zone, a thermal zone and a catalytic zone, as Figure 4.3 indicates (Gupta, 2008). The burner provides proper mixing of the entering streams, and hydrocarbons and oxygen are gradually combusted throughout the combustion zone. Proper mixing is essential for preventing soot formation. Further conversion of the gas occurs gradually down the reactor, where the final conversion of hydrocarbons takes place in the catalyst zone. The most used catalyst in the reforming process for hydrogen production is alumina-supported nickel based (Ni-based) catalysts (Gupta, 2008). Due to the high temperature in the reforming process, the catalysts must have high thermal stability. The main reason for using Ni is the low cost, and that it has sufficient activity. Even though Ni has been used in the industry for a long time, research is still being conducted trying to find an even better suited catalyst for this process.

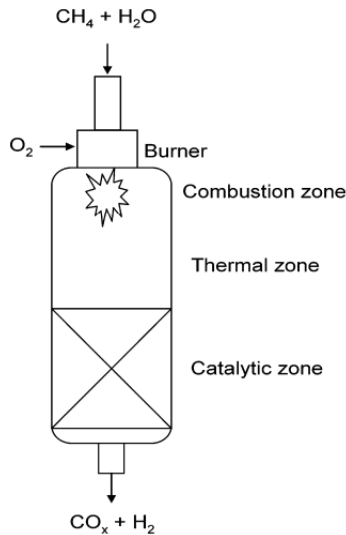


Figure 4.3: ATR unit (Navarro et al., 2007)

The oxidant do not need to be pure oxygen, it can also be air or enriched air. Which oxidant that is optimal, depends on the purification requirements downstream (Liu et al., 2010). If the produced hydrogen is intended for i.e. ammonia production, air gives sufficient purity. When using an air-blown ATR, the need of energy input increases due to the large amount of inert gases in air. On the other hand, when applying an O₂-blown ATR, it is necessary to separate air through an air separation unit to get pure oxygen, which requires power. This thesis concentrates on an O₂-blown ATR process.

Parameters that effect the performance of the reforming process are temperature, pressure, S/C-ratio and O₂/C – ratio, of which is considered throughout the next sections. Typical operational conditions for an ATR are summarized in Table 4.2.

Table 4.2: Typical ATR operating conditions

<i>ATR operational conditions characteristics (Liu et al., 2010), (Gupta, 2008) & (Moulijn et al., 2013)</i>	
<i>Reformer temperature (°C)</i>	900-1150
<i>Inlet pressure (bar)</i>	< 80
<i>Pressure drop (% of inlet pressure)</i>	3-5
<i>S/C</i>	1-2
<i>O₂/C</i>	0.6 – 0.65

Effects of temperature and pressure

The steam methane reforming (4.12) in the ATR is an endothermic reaction, meaning it favors high temperature. Actually, the only limiting factor for the reformer temperature is the material constraints. In the ATR, the temperature-increase occurs through partial oxidation of methane, which is an exothermic reaction and therefore generates heat. Figure 4.4 below illustrates the effect of increased temperature on the steam methane reforming in the ATR. As can be interpreted from Figure 4.4, the concentration of hydrogen increases rapidly with increased temperature and the increase in produced hydrogen is quicker at 1 bar than at 30 bar, indicating that low pressure is favorable for this reaction.

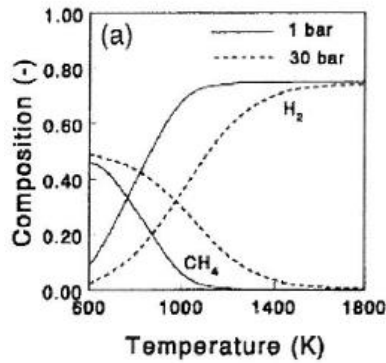


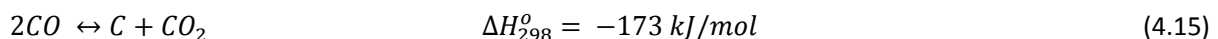
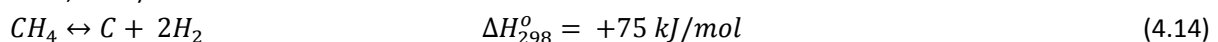
Figure 4.4: Effects of temperature and pressure on steam reforming reaction (Moulijn et al., 2013)

The reason why reforming of natural gas desires low pressure can be explained by Le Chateliers principle. For the reformer equations given above (4.1 – 4.9), the number of moles on the product side of the equilibrium is larger than the number of moles on the reactant side. How an equilibrium works when the pressure increases, is that it tries to counteract this by shift the equilibrium towards the place with lower pressure, which is the side with the fewest moles. Opposite, if the pressure decreases, the equilibrium reacts by shift towards the place with high pressure, which in the reformer is the product side. If there were equal amounts of mole on both sides of the equilibrium, change in pressure would have no effect (Zumdahl, 2009). Even though the reformer process prefers low pressure, it is desired to operate the reformer at elevated pressure. Pressurized syngas removes the requirement for a compressor, and then removes an energy-demanding unit. In addition, the size of the units decreases with higher pressure, which means lower investment costs.

The derivation that argues for using high temperatures in the reforming unit is attached in Appendix A. The reason is the connection between the equilibrium constant, K , and the Gibbs free energy equation.

Effects of steam/carbon ratio

A major problem within reforming is carbon deposition, which is a result of the following reactions (Moulijn et al., 2013):



Pre-reforming reduces the risk for carbon deposition in the main reformer. Nevertheless, it can arise and the reason might be a too small S/C-ratio. In order to avoid carbon formation in the reformer, the S/C-ration needs to be sufficiently high. One could believe that injecting a huge amount of steam to the reformers will solve all problems, but steam is expensive to produce since it requires large amounts of heat. This indicates that minimizing the S/C-ratio is important for maximizing the efficiency of the plant. A decrease in the S/C-ratio gives a higher amount of unconverted methane (methane slip) in the reformers, as can be observed in Figure 4.5. Counteraction of this is possible by driving the process at either higher temperature and/or lower pressure. Lower pressure leads to larger equipment, and higher temperature means an increased demand for heat input. Consequently, there is a tradeoff between investment costs and operating costs in the decision of the optimal S/C-ratio. For conventional ATR processes, the S/C-ratio is in the range 1-2 (Moulijn et al., 2013).

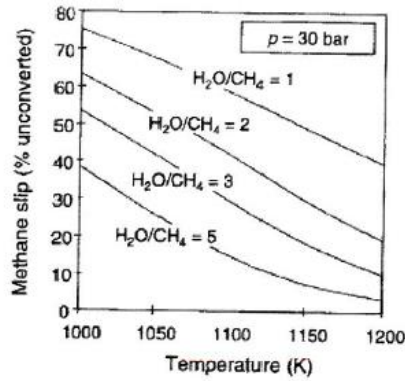


Figure 4.5: Effects of S/C-ratio on methane slip (Moulijn et al., 2013)

Effect of oxygen/carbon ratio

The amount of O₂ fed into the reformer determines the reactor temperature. By proper adjustment of the O/C- and the S/C-ratio in the reformer, the partial combustion provides the heat needed for steam reforming. The ATR prefers excess O₂ in the combustion, meaning there must be a sufficient amount of oxygen entering the reformer such that the combustion becomes complete.

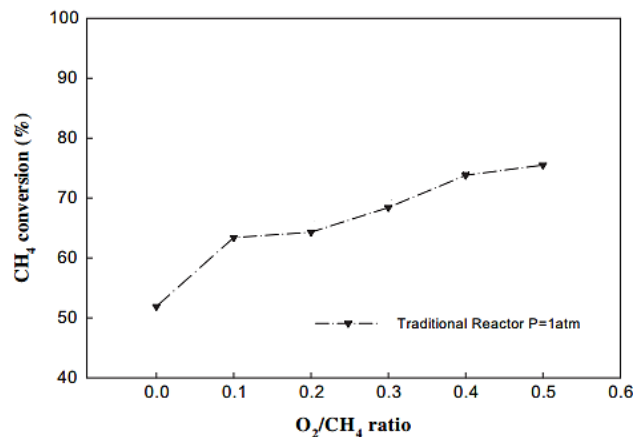


Figure 4.6: Experimental graphic view of methane conversion vs. O/C-ratio at different pressures (Chang et al., 2010)

The amount of produced H₂ per CO at the outlet of the reformer can be adjusted by changing the S/C-ratio and/or the O/C-ratio (Navarro et al., 2007). The product gas composition is fixed thermodynamically through the pressure, exit temperature, S/C-ratio and O/C-ratio (Gupta, 2008), see Figure 4.6. Even though the ATR demands a rather high oxygen flow, due to the simultaneous steam reforming, it uses less oxygen than the POX process, making the ATR process less sensitive to oxygen prices. The O/C-ratio is usually in the range of 0.6-0.65 (Gupta, 2008).

4.2.4 Water-Gas Shift unit

The syngas entering the water-gas shift units typically contains CH₄, H₂O, CO₂, H₂ and CO in chemical equilibrium at high temperatures. The gas may also contain some N₂ and Argon along with some minor sulfur compounds like H₂S (not in this study). Carbon monoxide is highly toxic. It will reduce the hydrogen productivity and it can poison the catalysts in the downstream processes (Liu et al., 2010). It is therefore desirable to convert as much CO as possible. This is done by letting CO react with steam over a catalyst bed and generate CO₂ and H₂, like given in equation 4.16.



Conversion of CO and H₂O into H₂ and CO₂ increase the hydrogen yield for the plant. How many stages of WGS needed, mainly depends on the acceptable levels of CO in the produced hydrogen. Normally a two-stage WGS in series are used. The gas from the reformer is pre-cooled and enters the high temperature water-gas shift unit (HTS). HTS operates at typical temperatures between 315 – 439°C (Ebner and Ritter, 2009). The catalysts used in this stage is normally iron-chromium-based (Gupta, 2008). Typical operating pressures range above 20 bar (Liu et al., 2010). The gas is further cooled before it enters the low temperature water-gas shift unit (LTS). Favorable temperatures for the LTS is between 205 - 230°C (Ebner and Ritter, 2009). LTS squeezes out the rest of the CO in the gas and converts it to H₂ and CO₂. Typically, around 92% of the CO in the gas entering HTS is converted when using both HTS and LTS (Gupta, 2008).

As for the reformer stage, temperature and S/C-ratio affect the conversion rate in the WGS stage. Since the shift-reaction have no change in number of moles, the pressure do not have any significant influence on the equilibrium. Nevertheless, with elevated pressure, the devise can be smaller and the reaction rate increases. Low temperatures are favorable in the WGS units. This is due to the shift-reaction being exothermic. It is favorable with as high equilibrium constant as possible, since the equilibrium will then shifts towards the product, see Appendix A for derivation of this claim. Figure 4.7 shows that for an exothermic reaction the equilibrium constant, K, increases with lower temperatures. It should be mentioned that it is not desirable to go below 200°C in the water-gas shift reactor, due to the dew point of water at the operating conditions (Liu et al., 2010). Generation of condensed water in the reactors introduce a substantial risk of damaging the catalyst. In addition, catalyst prefers elevated temperatures, meaning that the temperature in the WGS reactors becomes a tradeoff between conversion of CO and speed of the reaction.

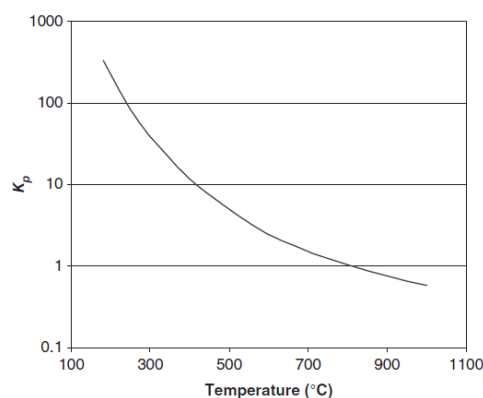


Figure 4.7: WGS equilibrium constant variations with temperature (Liu et al., 2010)

The S/C- ratio strongly influences the amount of unconverted CO from the WGS units. As Figure 4.8 depicts, hydrogen production increases as the S/C-ratio increases, but flattens out when the value reaches around two. This figure is for operating temperature of 400°C.

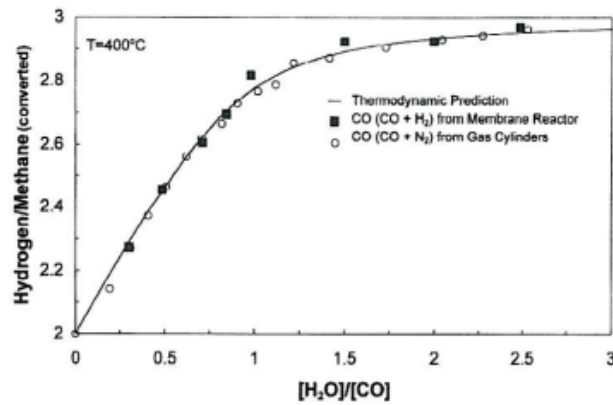


Figure 4.8: Converted methane to hydrogen vs. S/C – ratio (Maiya et al., 2000)

Carbon deposition can occur in the WGS units as well. Sufficient amount of steam in the feed gas can avoid this problem.

4.2.5 CO₂-Capturing unit

A growing concern for the environment has evolved over the recent years, resulting in stricter rules for emitting pollutants into the atmosphere. CO₂ is the biggest contributor to the greenhouse effect and represents almost 84% of the total greenhouse gas emissions from Norway (Miljødirektoratet, 2014). Hydrogen production from natural gas generates substantial amounts of CO₂. In general, each ton of produced hydrogen also produces 9-12 tons of CO₂, depending on the quality of the feedstock (natural gas, rich gas, naphtha, etc.) (Collodi, 2010).

The requirements for carbon capture increases as the world becomes more aware of the climate impact of CO₂. According to the Intergovernmental Panel on Climate Change (Intergovernmental Panel on Climate Change, 2005), the world needs to reduce the CO₂ emission by 50-85% to be able to reach the goal of maximum 2-2.4°C average global temperature increase from pre-industrial times. The International Energy Agency (IEA, 2012), estimated that implementation of CCS in industry and power generation accounts for slightly more than 1/5 of the needed emission reductions between 2015 and 2050 in order to reach the 2°C scenario.

For the industry to consider implementation of carbon capture, it is of great concern that the capturing process is as energy efficient, simple and cheap as possible, but at the same time fulfills the desired requirements. Carbon capture technology is a hot research topic as the process has great impact on the overall efficiency of the plant.

Currently, there are three main technologies available for carbon capture, respectively post-combustion capture, pre-combustion capture and oxyfuel combustion (Zero Emission Resource Organisation, 2014). The focus of this thesis is to compare the conventional ATR process containing pre-combustion carbon capture with the less mature low-temperature carbon capture process. This section focusses on the conventional pre-combustion CO₂ capture, as this is used in the base case.

Pre-combustion capture

The most mature technology for carbon capture is post-combustion capture, which captures the carbon from the flue gas after combustion. Pre-combustion carbon capture, on the other hand, captures the carbon upstream the combustion. The separation technology is equal for the two capturing methods, but pre-combustion carbon capture has an advantage of higher pressure, which leads to lower energy consumption.

Figure 4.9 gives an overview of a plant using pre-combustion carbon capture. The separation process occurs in the scrubber column.

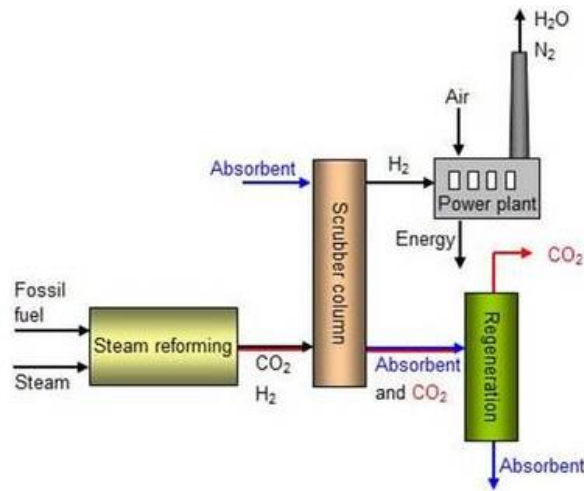


Figure 4.9: Principal sketch, pre-combustion capture (Bellona, 2014)

CO₂ capture can occur through chemical absorption, physical absorption, physical adsorption or by membranes. In absorption, the molecules connect to a liquid, while in adsorption they connect to a solid. Membranes represent new technology, and will not be considered for this purpose in this study. Absorption is the most common process, and therefore the chosen technology for the ATR base case. The choice of chemical or physical absorption depends on the partial pressure of CO₂ and the composition of the feed stream. Chemical absorption prefers low partial pressure for CO₂, while physical absorption is preferred when the partial pressure of CO₂ is high (Intergovernmental Panel on Climate Change, 2005). Figure 4.10 gives an indication of when to use the different solvents. Typical chemical solvents are amines (e.g. MEA, MDEA), while selexol is a typical physical solvent.

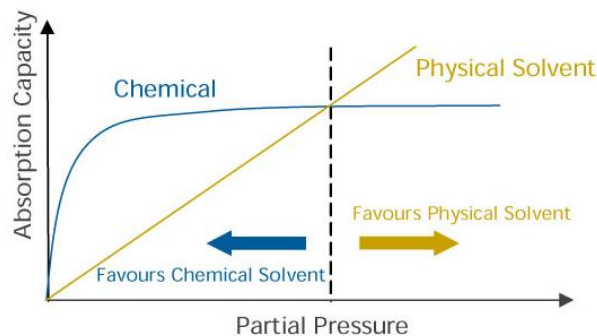


Figure 4.10: Correlation between CO₂ partial pressure and type of solvent (IEAGHG, 2012)

The pressure is typically lower in the exhaust gas, meaning chemical solvents are more appropriate in post-combustion capture. Pre-combustion carbon capture can be designed with either of the two types of solvents (Intergovernmental Panel on Climate Change, 2005). This task focuses, however, on chemical solvents, more particularly amines. The same result of carbon capturing rate could be achieved by using physical solvents as well, but since amines are expected to have less energy requirements it has been chosen. Figure 4.11 gives a more detailed illustration of how the amine process works. Lean amines flow downwards, while the exhaust gas flows upwards through the scrubber. Amines will react with CO₂ and form a bonding. Rich amines, saturated with CO₂, flow to a stripper unit. Heat supplies the stripper in order to split the amines and the CO₂. A pure stream of CO₂ leaves at the top of the stripper, while the lean amines go back to the absorption unit.

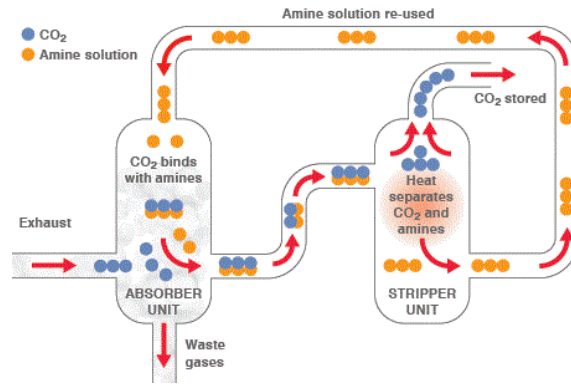


Figure 4.11: Amine process

In addition to heat input to the stripping unit, this process contains pumping units and therefore requires an energy input in form of power as well. Figure 4.12 below gives a control volume for the relevant CO₂-capturing unit.

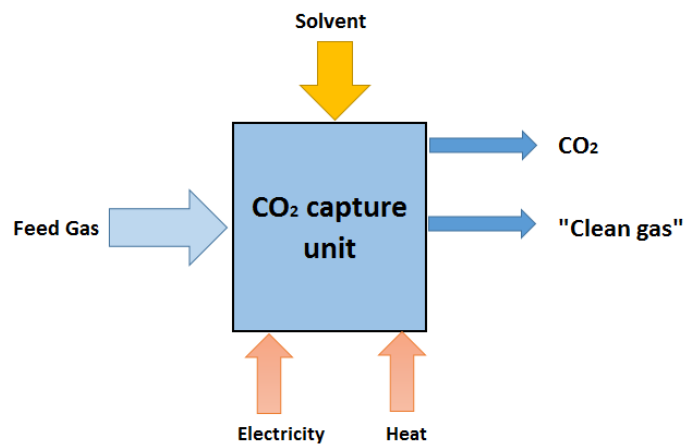


Figure 4.12: Control volume CO₂ capturing unit

Pre-combustion CO₂ capture has to be integrated in the process, which makes this technology only applicable for new plants. Unlike post-combustion carbon capture that relatively easy can be retrofitted into a process, pre-combustion capture has to be integrated from the start, otherwise, the retrofitting will be complicated.

4.2.6 Hydrogen purification unit

Even though hydrogen stands for the largest share of the gas when it leaves the CO₂-capturing unit, a higher hydrogen purity is often needed for the final product. For this purpose, the process includes a hydrogen purification unit. It exists several different methods for purifying the gas. As of today, there are three main technologies used for this aim, respectively membranes, adsorption (PSA/TSA) and cryogenic separation by partial condensation or methane wash (Besancon et al., 2009). Over 85% of the hydrogen production facilities around the world uses Pressure Swing Adsorption (PSA). PSA is the state-of-the-art technology when it comes to hydrogen purification if the feed gas contains 60-90mole% hydrogen, as it typically does after the WGS-stage (Liu et al., 2010). PSA will be the focus in this section since the base case of this study applies this technology as purification method.

The main objective for the PSA unit is to purify the gas stream so it contains 98-99.999mole% hydrogen (Liu et al., 2010). The PSA unit is characterized by pressure variations, and is a cyclic process. Feed gas enters the PSA unit at relatively high pressures, 4-30atm (Liu et al., 2010), and flows over solids in multiple adsorption beds. These solids adsorb the impurities in the gas, while the hydrogen will flow relatively untouched through the column. When the solids become saturated, desorption is necessary. Desorption is achieved by lowering the pressure inside the column and let a flow of pure hydrogen go through. The impurities connected to the solids will let go from the surface of the solid, and connect to the hydrogen again. This cyclic process needs a multicolumn adsorption system to ensure continuous purification. All the installed columns follow the same cyclic process, but with a time delay. The PSA unit works at approximately constant temperature, which typically is around 20-50°C (Ebner and Ritter, 2009).

The PSA unit operates as a cyclic process, and has four basic process steps of which will be further described:

- Adsorption
- Hydrogen recycling / depressurization
- Regeneration
- Repressurization

Adsorption

Adsorption occurs when gas comes in touch with the solids in the packed column due to physical interaction forces between the surface of the solid and the molecules in the gas. The surface area of the adsorbents are large, around 1000 m² per gram of adsorbent (Liu et al., 2010). This makes it possible for the adsorbents in the column to pick up large amounts of gas.

Adsorption is an exothermic phenomena (Liu et al., 2010), meaning low temperature is preferable for effective adsorption. The adsorption process in the PSA unit is best suited at high pressure (Liu et al., 2010). High gas pressure provides high partial pressure of the gas components, meaning a greater quantity of adsorbed components, which Figure 4.13 visualizes. This figure interprets the basic principle for PSA and TSA in an adsorption process. TSA, Temperature Swing Adsorption, will however not be discussed here. The secondary-axis represents the total weight of the adsorbed material in percent, in other words, the equilibrium adsorption capacity. The primary-axis indicates the pressure.

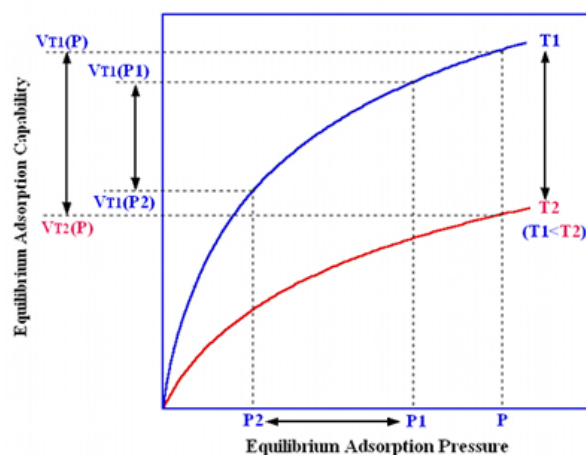


Figure 4.13: Conceptual diagram of PSA and TSA (Jechem, 2014)

In a PSA unit, the pressure varies from adsorption phase to regeneration phase. Indicating to Figure 4.13, at pressure P1 and temperature T1, the column is adsorbing, and the capacity of adsorption is $V_{T_1}(P_1)$. At regeneration, the pressure drops to P2. The adsorption capacity falls to $V_{T_1}(P_2)$, meaning a reduction in

quantity adsorbed. When lowering the pressure, the adsorbents will not hold on to the adsorbed molecules since the solution is not in equilibrium any more. The difference between $V_{T1}(P1)$ and $V_{T1}(P2)$ is the amount of adsorbed molecules diluted into the gas again.

Regeneration

Regeneration of the column starts when the mass transfer zone reaches approximately half of the columns height/length, and occurs through two depressurization steps. The first step is recycling of the hydrogen inside the adsorption column at the end of the adsorption step. This step uses co-current depressurization (from the bottom to the top). The impurity front proceeds against the top of the column, meaning a margin is necessary at the end of the column such that the impurities do not flow together with the pure hydrogen out of the column.

After recycling of the hydrogen left in the column, regeneration of the adsorbents start. This step uses counter-current depressurization (from the top to the bottom). By lowering the pressure and letting pure hydrogen flow through the column, the impurities will go back into the gas, and leave the PSA as a residual gas. The pure hydrogen used for this regeneration, is the hydrogen taken out in the previous step. When the adsorbents are ready for a new round of adsorption, the pressure will again increase and feed gas enters the PSA. Usually several columns like these are present in a production facility, such that if one column is in adsorption phase, two or three are recycling hydrogen, one or more is under regeneration while the remaining columns are under repressurization. To maintain a continuous hydrogen supply from the plant, a minimum of four adsorbing columns are required (Linde, 2009). Figure 4.14 visualizes the four steps in the PSA process. The pure H_2 stream is produced at elevated pressure, the same as inlet pressure minus the pressure drop in the in the column, while the off-gas is delivered at low pressure.

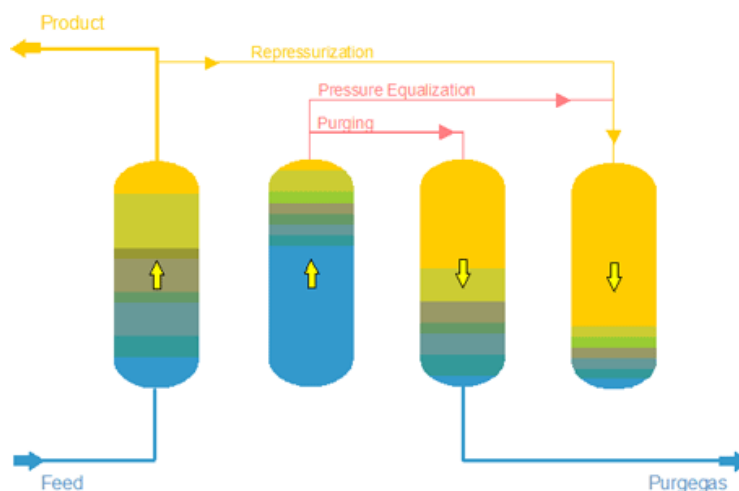


Figure 4.14: PSA Cycle (The McIlvane Company, 2014)

4.2.7 Power Plant

The ATR process includes a power plant for production of the required steam and power. The power plant consists of a gas turbine in combination with a steam cycle. The objective is to align the power production from the gas turbine and the steam turbines such that the total power production covers the power consumption in the process. The units of the combined cycle are briefly described throughout this section.

Gas Turbine

The installed gas turbine is a Siemens SGT6-PAC 5000F. More information regarding this unit can be found on the Siemens web page (Siemens, 2015). A gas turbine essentially consists of a compressor, a combustion

chamber and a turbine, as Figure 4.15 depicts. The compressor sucks in ambient air, and compresses it to a pressure in the range 10-35 bar (Bolland, 2013). Pressurized air is used as combustion air in the combustion chamber where burning of the fuel takes place. The most commonly used fuel for gas turbines is natural gas, which is used in about 80% of all gas turbines (Bolland, 2013). The gas turbine depends on having constant suitable fuel supply for producing the required amount of power. In this case, the off-gas from the purification unit contains components with high heating value, which makes the off-gas suitable for combustion. Burning this gas, together with air, increases the gas temperature and enables power production through gas expansion. However, if the off-gas do not give a sufficient amount of produced power, the fuel must be supplemented, which in this case is decided to be covered by natural gas.

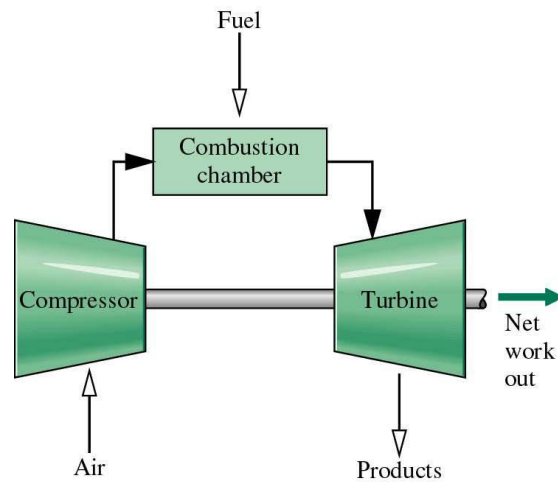


Figure 4.15: Simple sketch of a gas turbine (Moran and Shapiro, 2010)

Inside the combustion chamber, there is constant combustion of fuel and air at high pressures. The outlet temperature from the combustion chamber can reach around 1500°C (Bolland, 2013). This temperature is often referred to as Turbine Inlet Temperature, TIT, and represents an important factor for the gas turbine efficiency. It is beneficial to have as high TIT as possible, but the materials and the cooling system of the gas turbine limit the temperature. In order to get an appropriate TIT, the combustion takes place with an excess air ration of around 2.5-3, which is rather high (Bolland, 2013).

The net work out from the turbine is the total power produced in the turbine minus the required power for compression. In general, the turbine generates around twice the power consumed by the compressor (Bolland, 2013). The excess work can be used to produce power through an electric generator that is coupled to the shaft. The turbine expands the gas down to a pressure level slightly above the atmospheric pressure. The temperature of the gas leaving the turbine is in the range 450-650°C, depending upon type of gas turbine (Bolland, 2013). For the chosen gas turbine in this thesis, the exhaust gas temperature is set to approximately 595°C. Instead of emitting the flue gas, the energy in flue gas is used to raise steam through the HRSG.

Heat Recovery Steam Generation and Combined Cycle

The gas turbine and the steam turbines connect via the Heat Recovery Steam Generator (HRSG), as Figure 4.16 indicates. The heat from the exhaust gas is utilized due to three main reasons in this study: (i) to improve the plant efficiency, (ii) to generate the required amount of steam in the process and (iii) to generate power through steam turbines in order to meet the power requirements of the process. As the aim is to achieve a self-sustained process, the remaining power requirements, after utilization of the power from the gas turbine, must be achieved from the steam turbines. If the process is in power deficit, more

natural gas needs to be added either directly into the gas turbine or to a supplementary firing of the exhaust gas.

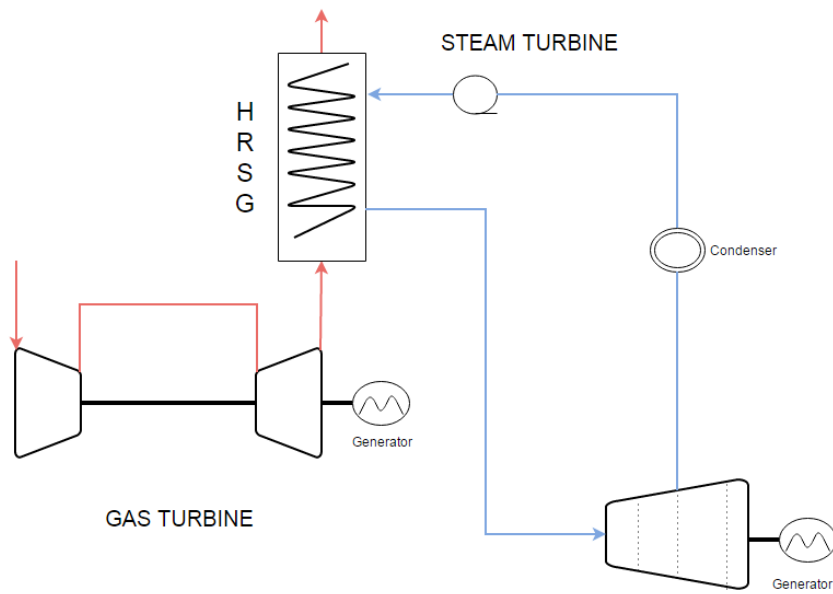


Figure 4.16: Combined gas turbine and steam turbine – combined cycle

The temperature of the flue gas decreases to around 80-100°C before it is emitted, depending on the type of HRSG (Bolland, 2013). The generated steam in the HRSG may be produced at multiple pressure levels. This thesis operates with three pressure levels, respectively high-pressure steam, medium-pressure steam and low-pressure steam. The produced steam enters the steam turbines, as Figure 4.17 illustrates.

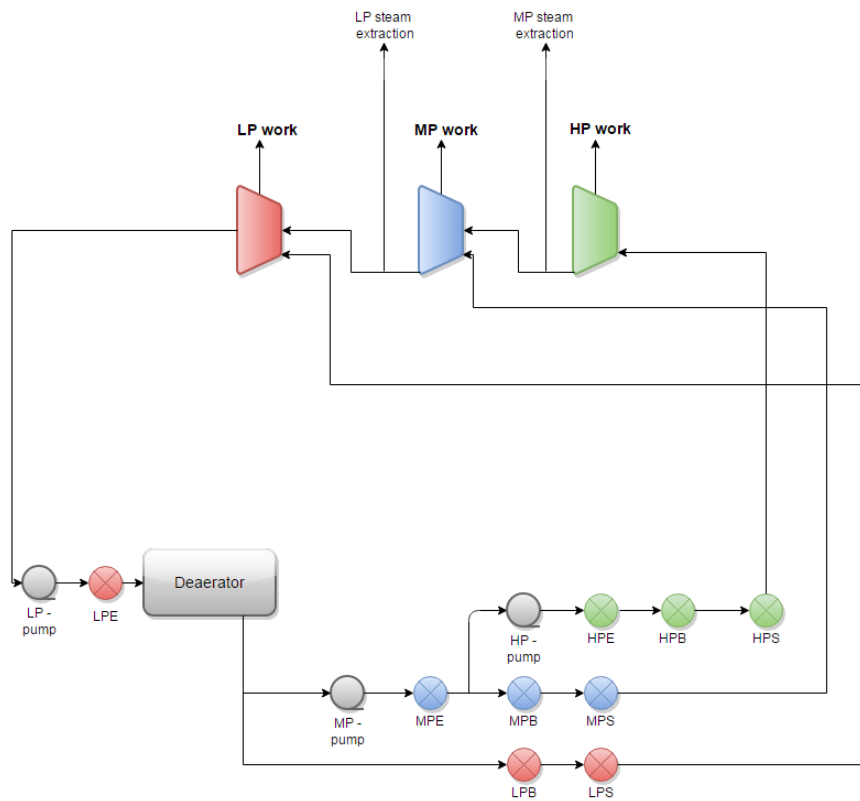


Figure 4.17: Steam turbine cycle

The colors indicate the production and expansion of the different steam levels, respectively red for LP-steam, blue for MP steam and green for HP steam. Steam generation occurs when water is exposed to a sufficient amount of heat, which depends on the pressure. The decided pressure levels in this study are summarized, along with the boiling point of water at the given pressure, in Table 4.3.

Table 4.3: Steam Levels

	Pressure [bar]	Boiling point [°C]	Superheated temperature [°C]
LP – steam	3	134,2	290
MP – steam	35	242,4	445
HP – steam	131	330,5	473

Expansion of pressurized steam through a turbine generates power. The power output from the steam turbine increases as the temperature of the steam increases, meaning that the steam should be superheated before entering the turbine (Bolland, 2013). The respective steam temperature decided for superheating in this thesis is given in Table 4.3. As indicated in Figure 4.17, each steam level has three heat exchangers where heat is transferred from the process to the Boiler Feed Water (BFW). The first heat exchanger is referred to as the economizer, and heats the water to just below the boiling point at the given pressure. The next heat exchanger, the evaporator, boils the water such that the output is saturated steam at the given pressure. The temperature is constant during boiling. The third heat exchanger superheats the steam before it enters the turbine. A typical TQ-diagram for heat transfer between water/steam and excess heat from the process looks like indicated in Figure 4.18.

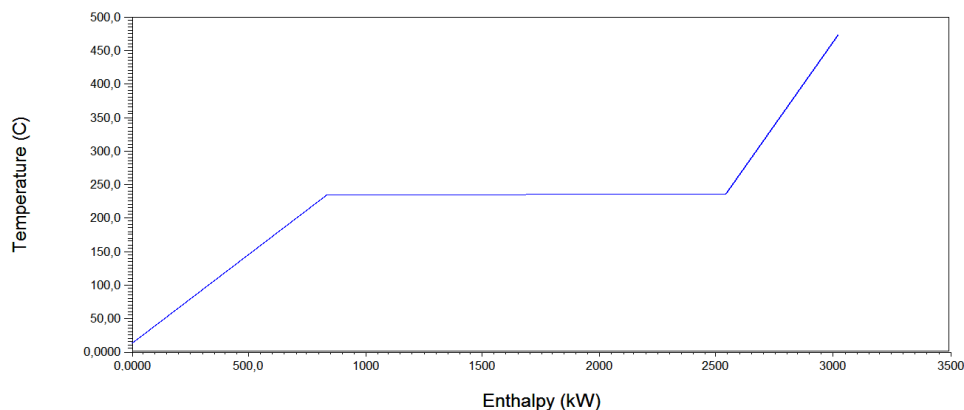


Figure 4.18: Example of a TQ-diagram for steam generation (from HYSYS simulation)

Heat supply must occur through three different units. Boiling cannot take place in the economizer because it will destroy the heat exchanger. The same applies for superheating, since it cannot take place in the boiler as it destroys the heat exchanger.

As mentioned, the process requires input of MP steam for the reforming process and LP steam for the reboilers in the CO₂-capturing unit. The needed amount of steam is extracted as indicated in Figure 4.17. The reforming process utilizes the MP steam, meaning that the steam cycle needs to be constantly supplied with the same amount of water that leaves in form of MP steam. The LP steam, on the other hand, circulates as it is transferred to the reboiler where it delivers the required amount of heat, before it goes back to the steam cycle again. Even though the process requires MP-steam and LP-steam, the focus should be on produce as much HP-steam as possible. Expansion of HP-steam down to MP-steam generates power, and the required amount of MP steam can be extracted after the HP-turbine. The remaining MP-steam is

expanded down to LP-steam, where the required amount is extracted. This way the power generation is maximized.

Figure 4.17 includes a deaerator. A deaerator, or a feed water tank, is almost universally practiced in steam systems like this. The primary reason for installing a deaerator is to avoid corrosion in the system. Feed water to the steam generating heat exchangers is often a mixture of pure water and returned condensate from the steam cycle, and it contains varying amounts of carbon dioxide and oxygen. Dissolved oxygen and carbon dioxide in the feed water form a great risk of corrosion. Dissolved oxygen is extremely corrosive in boiler tubes. The dissolved carbon dioxide is not corrosive when the water is in steam condition, but as soon as steam starts to condense, the carbon dioxide connects with water and forms a very corrosive carbonic acid. Carbon dioxide is not as corrosive as oxygen, such that a small amount of carbon dioxide will not make as much damage as a small amount of oxygen. However, if both oxygen and carbon dioxide are present, the condensate becomes approximate four times more corrosive than if oxygen or carbon dioxide were presented alone (Bolland, 2013). Installing a deaerator improves the lifetime of the steam system dramatically as it protects the process equipment from corrosion. In addition to reducing the risk of corrosion, installing a deaerator also improves the heat transfer as it removes the non-condensable gasses oxygen and carbon dioxide. Non-condensable gasses will reduce the heat transfer across the tube wall and as a result make the heat transfer poorer. A typical deaerator design is given in Figure 4.19.

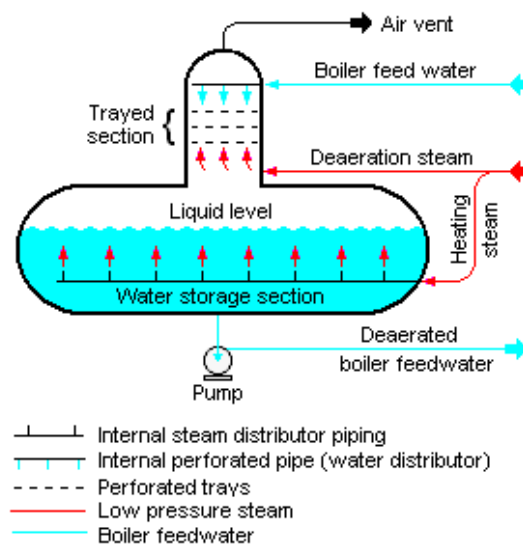


Figure 4.19: A typical deaerator (Bolland, 2013)

4.2.8 Hydrogen Liquefaction unit

The produced hydrogen aims for liquefaction in this study. The reason for liquefying hydrogen is to increase the energy density. Even though hydrogen has a relatively high heating value, the density is low. This makes it necessary either to compress the hydrogen or to liquefy it to make it comparable with other fuels available, like fossil fuels. Gaseous hydrogen at 200 bar and 15°C has about 17 times lower energy density than liquid gasoline (Walnum et al., 2012). However, liquefying hydrogen makes the energy density increase with approximately 5 times compared to the gaseous hydrogen at 200 bar and 15°C (Walnum et al., 2012). Liquefaction of hydrogen increases the hydrogen trucking capabilities, as Figure 4.20 indicates, since liquid hydrogen occupies less space than gas. This gives a benefit of fewer distribution trucks on the road.

Hydrogen trucking capacities

- > Liquid: ± 4000 kg 
- > 200 bar gas: ± 400 kg
- > 500 bar gas: ± 900 kg 

Figure 4.20: Hydrogen trucking capacities (Berstad et al., 2013c)

Liquefaction of hydrogen is, however, an energy demanding process. Hydrogen has the second lowest boiling point of all substances, accordingly -252.9°C at atmospheric pressure. Gaseous hydrogen must therefore undergo excessive cooling before it becomes liquid. A typical temperature for liquid hydrogen is -254°C (Energilink, 2008b). This cooling process can appear in many different designs. One generic design is given in Figure 4.21.

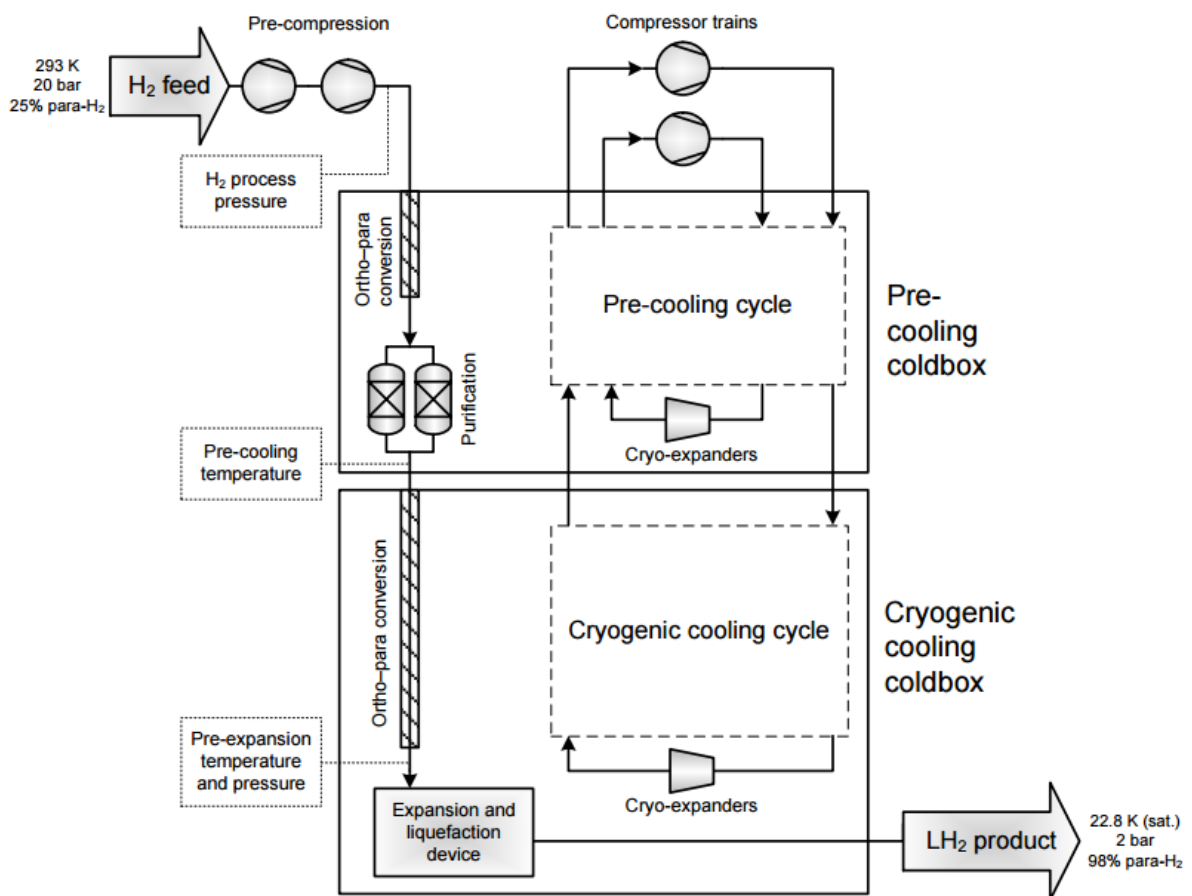


Figure 4.21: Generic hydrogen liquefaction process (Walnum et al., 2012)

The first step is pre-compression of the incoming hydrogen. Inlet specifications for this process is pure hydrogen at 20 bar and 30°C , which is used as boundaries in this thesis as well. The hydrogen pressure is typically around 20 bar when it leaves the PSA unit. When membranes are used for purification, additional compression is necessary, as the pressure of the hydrogen is almost atmospheric. Pre-compression makes the cooling process cheaper as parts of the cooling demand can occur at higher temperature. This reduces the required refrigerant work.

The cooling appears in so-called cold boxes, which contains cooling cycles where refrigerants cool the hydrogen. These cooling cycles can appear in many different arrangements. All existing large-scale plants for hydrogen liquefaction apply liquid nitrogen as cooling media for pre-cooling. However, there exist other

possibilities, as utilization of mixed refrigerants in cascade systems. It is anticipated that an eventual transition to using mixed refrigerant can improve the process efficiency (Berstad et al., 2009). This is not further discussed as it exceeds the scope of this work. In the cryogenic cooling cycle, hydrogen is further cooled, down to a pre-expansion temperature. This typically occurs through a hydrogen-claude cycle, or a purely reversed Brayton cycle with helium (Walnum et al., 2012). The last step is expansion of the hydrogen down to the liquid region.

5. Alternatives studied

This chapter gives a brief introduction to the concept overview of the cases considering new and alternative technology for hydrogen production, as well as a thoroughly review of the membrane technology and the low-temperature separation technology for CO₂ capture.

5.1 Concept overview

Figure 5.1 gives an overview of the basic membrane process discussed throughout this thesis. As Figure 5.1 depicts, the main difference between the membrane cases and the conventional ATR process discussed in the latter chapter, is the order of the purification unit and the CO₂-separating unit. In the conventional ATR process, the purification unit is placed after the CO₂-separating unit. This is due to the reduced size requirements for the PSA unit when most of the CO₂ is removed upstream. However, for ATR processes using membranes for purification, the most common way of implementation is to combine the membrane unit with a following low-temperature CO₂-separating unit.

The reforming of the natural gas occurs in the same manner for this concept as for the conventional process. It is only the purification unit and the CO₂-separating unit that deviates the two concepts. The new components are described throughout the next sections.

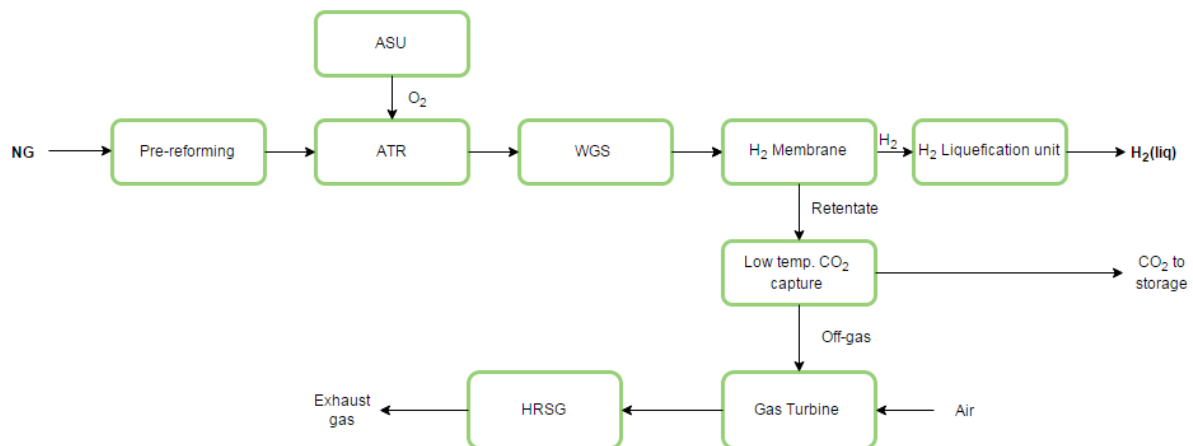


Figure 5.1: Overview membrane concept

5.2 Use of membranes in hydrogen production

Implementation of membranes are an alternative to the conventional PSA for hydrogen purification. The great advantage of utilizing membranes for this purpose, is that the hydrogen stream becomes completely clean. This chapter provides the reader with a short introduction to general membrane technology before a more thesis related section describes how membranes are used in hydrogen production.

5.2.1 Introduction to membrane separation

Separation is an essential process in chemical industry, and membranes are one of the many available techniques for this purpose. A membrane works as a separator as it divides the feed stream into two streams, like Figure 5.2 indicates. The membrane off-gas is referred to as retentate, while the permeate substances are called permeate. Figure 5.2 gives a basic overview of a membrane module.

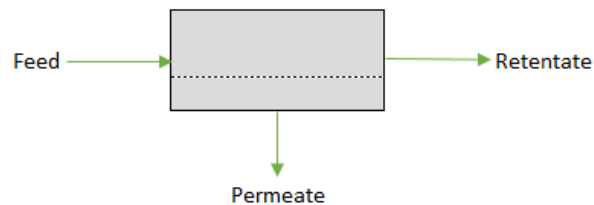


Figure 5.2: Membrane principle

Membranes are selective barriers, meaning that only selective species passes through, while the residuals remain on the feed side. Selectivity is one of two parameters that decides the performance of a membrane. The other important factor is *flux*, which relates to the volume flowing through the membrane per area and time (Mulder, 1996).

Separation in a membrane occurs due to forces acting on the molecules in the feed stream. These forces are denoted driving forces for the separation, and are differences in chemical potential between the feed and the permeating side of the membrane (Ormestad, 2009). Typical driving forces are gradients in concentration, pressure, temperature or electrical potential. The driving force of a membrane separation can be defined as the gradient in chemical potential across the membrane (ΔX) divided by the thickness of the membrane (l), as shown in (5.1) (Mulder, 1996).

$$\text{Driving force} = \frac{\Delta X}{l} \quad (5.1)$$

Transport of components through the membrane can be passive or active, depending on whether or not external power is applied. In passive transport, components in the feed mixture are transferred through the membrane due to potential differences between the feed side and the permeate side. See Figure 5.3.

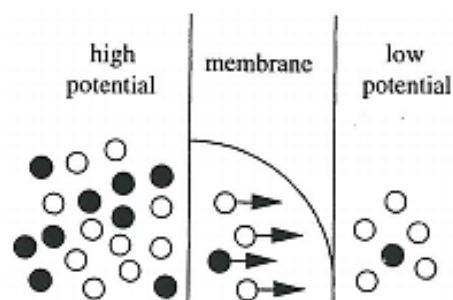


Figure 5.3: Passive membrane transport (Mulder, 1996)

Driving forces are closely related to the flux of the membrane, meaning, stronger driving forces gives higher flux. In fact, the flux is proportional with the driving forces, as displayed in equation 5.2 (Mulder, 1996).

$$\text{Flux (J)} = \text{proportionality factor (A)} \cdot \text{driving force (X)} \quad (5.2)$$

Membrane structure

The structure of the membrane is a decisive factor for the membrane performance. The desired separation decides the construction design of the membrane, which will be different for each purpose of the membrane. A change in the membrane structure will change the functionality of the membrane, as it affects what types of components that pass through the membrane. There are numerous ways of classifying membranes, depending on the viewpoint. One common way to classify membranes is by nature, as indicated in Figure 5.4.

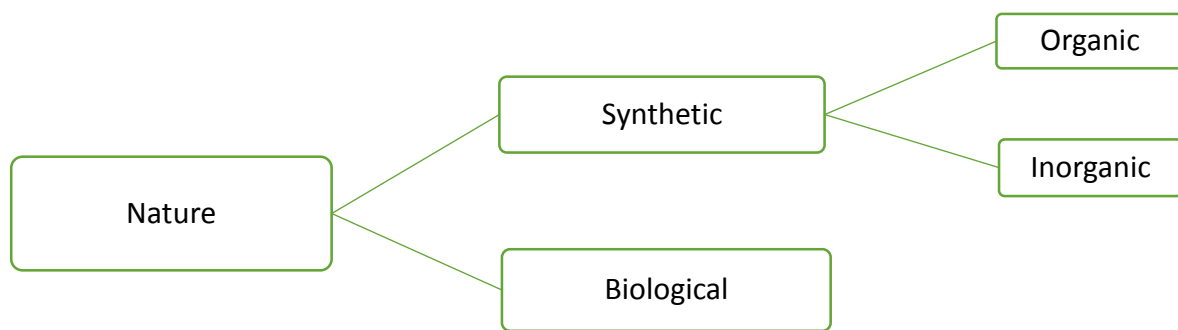


Figure 5.4: Fundamental classifications of membrane types

This distinction is the most fundamental in terms of membrane structure and functionality, as biological and synthetic membranes differ completely from each other. Biological membranes will not be discussed further due to the lack of relevance according to this thesis. Synthetic membranes, on the other hand, form the fundament for further work in this thesis. Synthetic membranes are usually intended for separation in industry, and can be subdivided into organic- and inorganic membranes depending on what material the membrane is created from.

A more reasonable way of classifying the membranes considering the scope of this work, is to restrict it to synthetic membranes, and divide these membranes into groups. As Figure 5.4 displayed, synthetic membranes can be divided into organic or inorganic membranes, but another possible way is to classify the membranes according to its structure and separation principles. A common way of classifying the membranes based on these factors is to divide between porous membranes, nonporous membranes and carrier membranes. For porous membranes, the size of the pores determines which particles from the feed that is allowed to pass through the membrane. Nonporous membranes can separate molecules of approximately the same size, as separation is determined by difference in solubility and diffusivity. Carrier membranes uses a specific carrier molecule that picks up the desired molecule on one side of the membrane, and transport it through the membrane before it releases it on the permeate side (Mulder, 1996).

5.2.2 Membrane separation in hydrogen production

As an attempt to increase the plant efficiency, the use of H₂ – selective membranes have become a frequently proposed alternative for excretion of pure hydrogen. Using membranes for hydrogen purification gives 100% pure hydrogen on the permeate side, which is an advantage compared to using PSA, especially if the hydrogen shall be liquefied. Even though the PSA gives very pure hydrogen, 99.99%, it is still not pure enough for liquefaction. Because hydrogen liquefaction requires 100% pure hydrogen, the PSA hydrogen must be further purified before the cooling starts (Bracha et al., 1994).

In hydrogen production, membranes based on palladium and its alloys, can successfully replace the PSA unit. Hydrogen can then be separated from the feed gas through the permselective pd-alloy membrane, while the residual gas goes as retentate. Pd-alloys has high hydrogen permeability, meaning that the membrane only allows hydrogen to pass through. A promising membrane temperature for this purpose range between 250 and 500°C (Ockwig and Nenoff, 2007). A principal sketch of how the palladium (Pd) membrane work is given in Figure 5.5. Using Pd-alloyed membranes in hydrogen production possesses the advantages of high hydrogen selectivity and permeability, easy operation, low maintenance requirements, low energy consumption, which lower the facility cost, and long lifetime. These factors give membranes a potential competitive advantage compared to other solutions for the excretion of hydrogen in hydrogen production. However, Pd-alloyed membranes are very vulnerable when it comes to unwanted gas compounds in the feed gas, as sulfur. Small amounts of sulfur can destroy the membrane quite quickly, and it is therefore of great concern to remove all sulfur before the membrane reactor (Chen and Ma, 2010).

One major advantages of using membrane for hydrogen separation is that the hydrogen flow from the membrane do not contain any CO or CO₂ components, which makes the hydrogen well suited for use in fuel cells (Kyriakides et al., 2013).

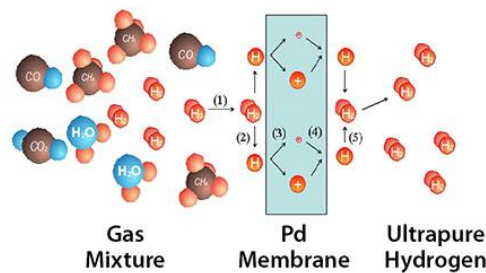


Figure 5.5: Simple schematic of a typical hydrogen membrane (National Energy Technology Laboratory, 2014)

Driving forces

The driving force in membranes used for hydrogen production is the difference in hydrogen partial pressure on the feed side and the permeate side. Feed gas enters the membrane with elevated pressure, while the pressure on the permeate side is low. Due of Chateliers principle, the equilibrium shifts towards the product when the product side has lower pressure that the reactant side. This favor hydrogen separation. To increase the pressure difference, sweep gas is occasionally used to carry away the hydrogen from the membrane reactor. This ensures a high level of driving forces. The use of sweep gas is, however, not further discussed since the scope of this work is to produce as pure hydrogen as possible due to liquefaction, and it is therefore undesirable to use sweep gas.

FLUX

As mentioned previously, one of the important factors for the membrane performance is flux. Equation 5.1 gives the flux of hydrogen through a Pd-alloy membrane:

$$F_{H_2} = \frac{S \cdot D}{L} [(P^f_{H_2})^n - (P^p_{H_2})^n] = \frac{Q}{L} [(P^f_{H_2})^n - (P^p_{H_2})^n] \quad (5.1)$$

The solubility and the diffusivity of the membrane are denoted S and D, respectively, in equation 5.1. These two factors multiplied give the hydrogen permeability of the membrane, which is denoted Q. $P^f_{H_2}$ and $P^p_{H_2}$ represent the partial pressure of hydrogen on the feed and permeate side, respectively. L is the

thickness of the membrane, and n is the hydrogen pressure exponent. This pressure exponent changes relative to variations in solubility and diffusivity with pressure. It is also affected by contaminants on the membrane surface. Ideally this value is equal to 0.5, but a more realistic value based on experimental data provides a value of 0.63 (Caravella et al., 2013).

The flux through the membrane also depends on the effect called concentration polarization, which refers to the change in hydrogen concentration at the membrane interface. Transport of hydrogen molecules through the membrane reduces the concentration of hydrogen close to the membrane surface on the feed side. As a hydrogen-depleted layer builds up on the feed-side, the partial pressure of hydrogen decreases at the membrane surface, which results in poorer flux.

Possible solutions for use of membranes in hydrogen production

It exist different solutions for including membranes in hydrogen production. Possible solutions are the advanced membrane reformer system and the WGS Membrane reactor. However, this thesis will not focus on these advanced types of membranes, but simpler membrane modules, as a single-membrane module and a sequential membrane and WGS module. Nevertheless, the next sections introduce all relevant solutions.

Advanced membrane reformer system

The advanced membrane reformer system merge the reforming unit, the WGS-units and the PSA into one single reactor, as Figure 5.6 depicts.

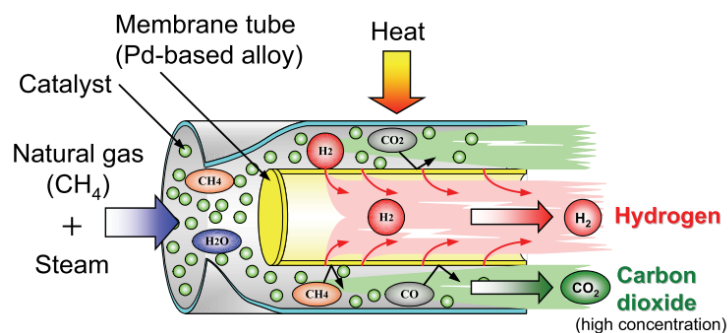


Figure 5.6: Membrane Reformer (Kurokawa et al., 2011)

One of the benefits of applying the membrane reformer is the reduced complexity of the process. This technology manage to combine the reformer stage with the WGS-stage and the purification stage, which gives this unit an advantage when it comes to energy efficiency and space requirements.

Natural gas enters the membrane reformer along with steam, and reacts over catalyst beds. The membrane allows only hydrogen to pass through, providing a pure hydrogen stream, as indicated in Figure 5.6. Reforming of natural gas occurs simultaneously as extraction of hydrogen takes place through the membrane, meaning the reforming reactions happen without limitation of chemical equilibrium, which makes this technology more energy effective than the conventional processes for natural gas reforming (Kurokawa et al., 2011). The retentate from the membrane has high CO₂ concentration, around 70-90% (Kurokawa et al., 2011). This gives the membrane reformer an advantage in terms of CO₂-capturing as well. High concentration of CO₂ reduces the cost of a CO₂ capturing plant as the specific work reduces, which is further described in Section 5.3.

This technology is not yet commercialized, but represents a promising technology that will make hydrogen production more energy effective, and at the same time reduce the drawback of carbon capture.

WGS-MR

WGS-MR stands for Water-Gas Shift Membrane Reactor, and this technology integrates the WGS-unit and the hydrogen separation unit. Hydrogen production occurs simultaneously as it is removed through the membrane. This shifts the reaction towards the product and gives a better hydrogen conversion in the WGS unit. Figure 5.7 indicates the basic design of a water-gas shift membrane reactor. This thesis will not go into further detail regarding the WGS-MR technology, even though it is an interesting topic for future work.

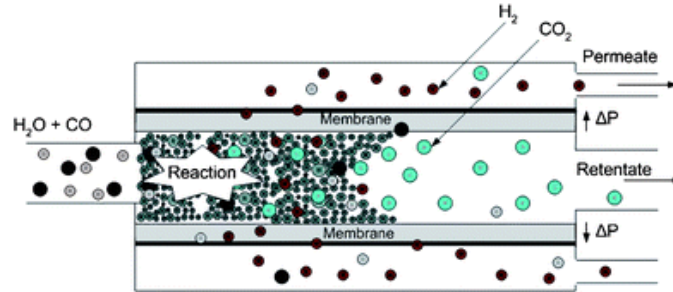


Figure 5.7: WGS-MR (Smart et al., 2010)

Membrane modules

This work focuses on the use of a single membrane module, and a sequential membrane and WGS module. In the case considering a single membrane module, the membrane is installed right after the LT-WGS unit, like depicted in Figure 5.8.

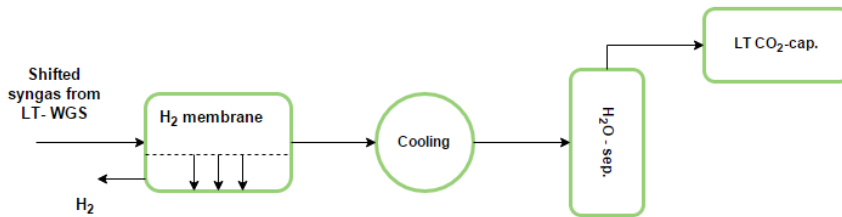


Figure 5.8: Single membrane module

The shifted syngas should optimally have a temperature of around 400°C when it enters the membrane module to ensure high H₂ flux. However, as WGS reactors favor low temperature it can be necessary to preheat the gas before it enters the membrane.

The rate of hydrogen going through the membrane compared to the total amount in the feed gas is denoted as Hydrogen Recovery Factor, HRF. By increasing the pressure difference across the membrane, the HRF increases. There is, however, a practical limit. In cases where the syngas pressure is too low to obtain the desired HRF, the process must include a compressor in front of the membrane.

It is of interest to look at a sequential membrane and WGS module as well. Instead of having just one membrane module after the LT-WGS stage, this technology uses two membrane modules, like depicted in Figure 5.9.

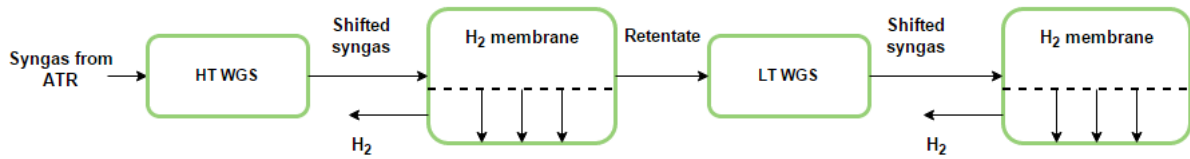


Figure 5.9: Sequential membrane and WGS module, two steps

It is also possible to install more membrane modules, but it would not give any significant advantage. This can be observed from Figure 5.10. This figure gives an indication of the plant efficiency and the required membrane area for a certain HRF value. The plant efficiency will not be affected greatly by the choice of technology. The required membrane area, on the other hand, shows a great reduction when a two- or three-stage membrane module is used. Implementation of a third membrane module complicates the process without giving any great advantages. It is therefore decided to only focus on a two-step membrane separation technology in addition to a single step.

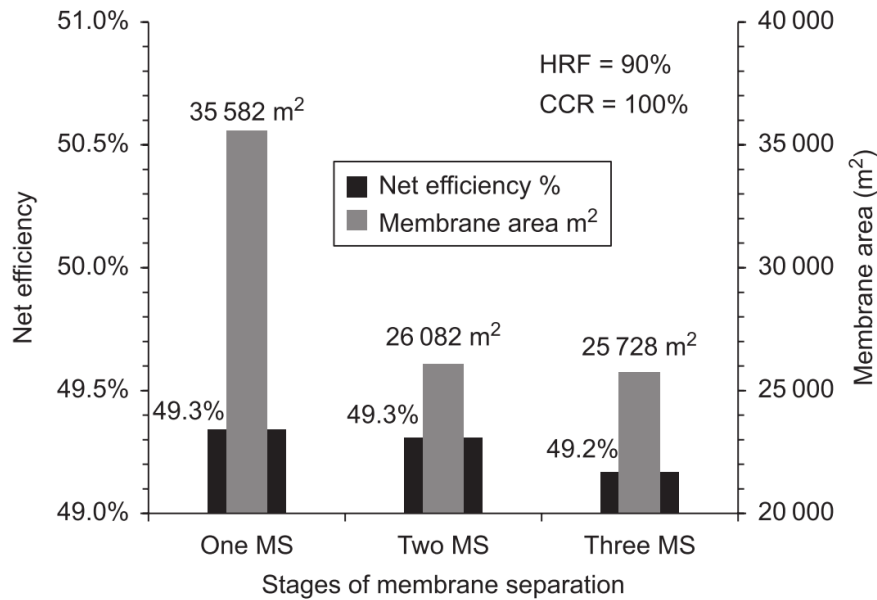


Figure 5.10: Comparison of one- two- and three-stage membrane modules (Atsonios et al., 2015)

5.3 Low temperature process for carbon capture

The basic principle of a low-temperature carbon capturing process is to separate CO₂ through phase separation. Phase separation can occur through gas-liquid separation where the liquid is CO₂ rich, gas-solid separation where CO₂ becomes solid or a combination of the two, referred to as CO₂ slurry separation (Berstad et al., 2013b). In cases where separation of CO₂ occur from synthesis gas, as in this thesis, the partial pressure of CO₂ is above the triple point pressure of CO₂, which means that liquefaction can be done through cooling and partial condensation. This appears in Figure 5.11 below.

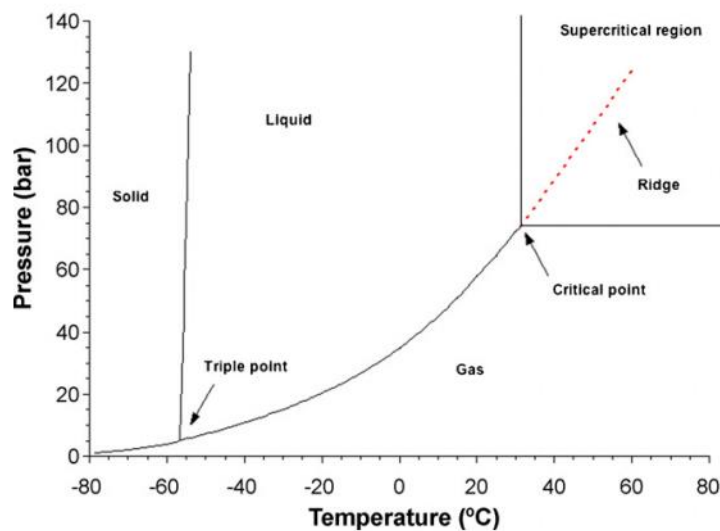


Figure 5.11: CO₂ phase diagram (Pasquali and Bettini, 2008)

The main components in the gas after the membrane and water separation are H₂ and CO₂. Other limited compounds are CH₄, H₂O, N₂ and Ar. Among these compounds, except H₂O, CO₂ has the highest dew point temperature. All H₂O is removed before cooling, meaning that CO₂ liquefies first when the gas is cooled. The dew point temperature and the boiling point temperature is equal for a single component, and Table 5.1 summarizes the values for the respective gas mixture.

Table 5.1: Dew point temperatures at atmospheric pressure (The Engineering ToolBox, 2015) & (LENNTECH, 2015)

<i>Dew point temperature at atmospheric pressure</i>	
H ₂	-253°C
CH ₄	-161°C
N ₂	-196°C
Ar	-186°C
CO ₂	-78.5°C
H ₂ O	100°C

It is favorable that the LT separation occurs at high pressure. As pressure increases, the dew point temperature of the compounds decrease, meaning get closer to 0°C in this case. The cooling requirements for liquefaction will then decrease, and the process gets less challenging. The synthesis gas is therefore

compressed in one or several stages, depending on the desired pressure level, before the cooling starts, typically around 30 bar (Berstad et al., 2013b).

Three main parameters affect the Carbon Capture Rate, CCR, in the LT processes. These are the CO₂ concentration for the entering gas, pressure level at partial condensation and phase separation and the separation temperature (Berstad et al., 2013b). The CO₂ concentration has great impact on the CCR since CO₂ separation gets easier as the CO₂ concentration increases. As the CO₂ concentration in the syngas increases, the specific separation and compression work for the LT process decreases, as depicted in Figure 5.12.

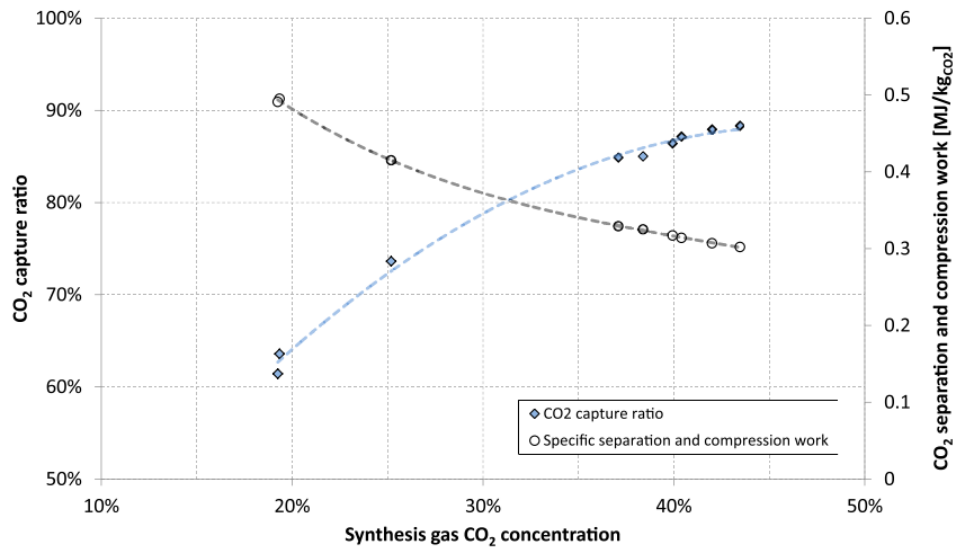


Figure 5.12: “Results specific CO₂ separation and compression work and capture ratio for a selection of natural gas derived synthesis gas with varying CO₂ concentration. For uniformity, synthesis gas feed pressure and phase separation pressure have been fixed to 35 bar and 110 bar, respectively.” (Berstad et al., 2013b)

Process design for LT carbon capture

There exist several different opportunities for designing the LT carbon capture process. Even though the scope of this thesis do not consider the details of this design, a brief description will be of interest. A typical process scheme is given in Figure 5.13. The temperature in the separation process goes way below the freezing point of water. It is therefore very important that the water amount in the LT process is extremely limited such that freeze out is avoided. Solid water may cause destruction of the system. A common way of remove smaller amounts of water is by adsorption, typically with molecular sieves as adsorbents (Solbraa, 2013). Once the water compounds are removed, the pre-compression of the gas starts. Figure 5.13 depicts a two-stage compression with intercooling where the gas is cooled down to approximately 30°C by an ambient cooling medium. The gas then enters the first low-temperature heat exchanger, HX1, where it is cooled by other process streams. The gas is further cooled by a propane cycle and an ethane cycle. In HX2, the gas is typically cooled down to around -39°C and subsequently down to around -55°C through HX3 and HX4 (Berstad et al., 2013a). The phase separator splits the liquefied CO₂ and the gas. Liquid CO₂ goes back to HX3 where it is heated such that impurities evaporate and goes back to the start phase. The purpose is to purify the CO₂. The liquid CO₂ is then pumped up to a pressure suitable for transport. The gas from the first phase separator, on the other hand, contains considerable amounts of hydrogen, which make this gas suitable for combustion in a gas turbine. Expansion of this gas, down to an appropriate pressure for combustion, ensures some power production.

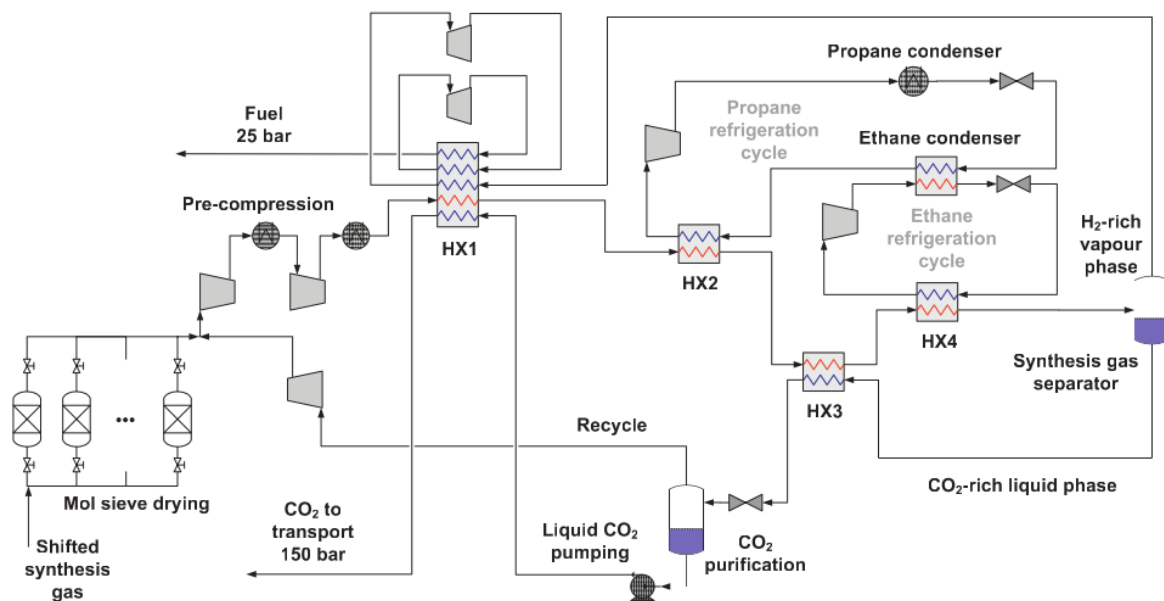


Figure 5.13: Possible LT carbon capture design (Berstad et al., 2013a)

6. Process integration fundamentals

All developed cases aim to be heat- and power integrated. The intention of process integration is to utilize the heat and cold available in the process in the most sustainable manner, in order to reduce the external use of hot- and cold utilities. An integrated process reuses heat internally instead of using external heat. In contrast to an analytical approach to the process, where individual units are attempted to be optimized separately, process integration employs a holistic approach to the system where the aim is to optimize the whole system and not necessarily each unit. Process integration is advantageous in terms of operating costs since the external use of utilities reduce as the process becomes heat integrated. A common way of achieving the process design of an integrated system is to use the pinch design method. As the pinch design method is fundamental in further thesis work, this chapter serves as a theory background for the work done while integrating the processes.

6.1 Pinch Analysis

Pinch analysis is a technique for finding the network design that gives minimum external heating- and cooling requirements. In other words, using pinch design analysis ensures that the heat integration in the network is optimal, such that external requirements for heating and cooling are minimized. When applying pinch analysis to a set of process streams, the pinch point has to be defined. The definition of the pinch point is the point of closest approach between the hot and cold composite curves. Hot and cold composite curves represent all individual hot and cold streams, respectively, in one single stream, often illustrated graphically, like Figure 6.1. The composite curve also illustrates the minimum required hot – and cold utility requirements as it highlights the gap between available heat and cold. It has to be mentioned that there can be practical limitations making it impossible to achieve the minimum use of utilities.

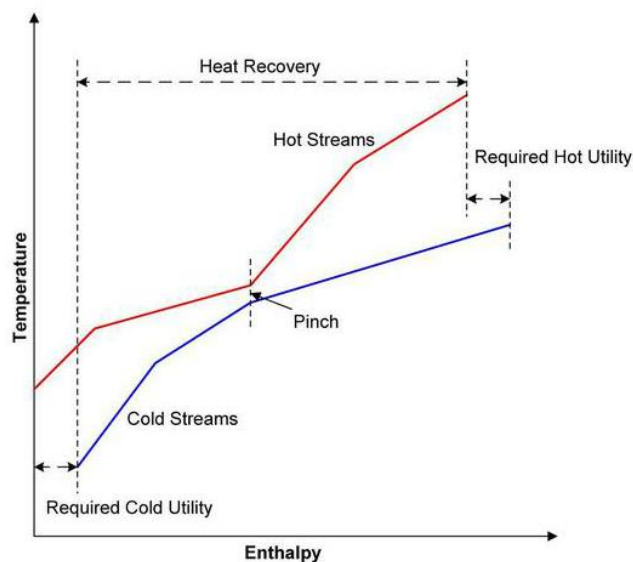


Figure 6.1: Hot and cold composite curve (The University of Waikato, 2014)

Figure 6.2 is an example of a small system with three hot streams and two cold streams. To be able to perform a pinch analysis, the supply temperature, T_s , the target temperature, T_T , and the mCp -value of each stream must be defined, in addition to the pinch point. The mCp -value for a stream expresses the change in enthalpy divided by the change in temperature, and is normally given as $kW/^\circ C$. If the network is simple, as in Figure 6.2, the pinch analysis can be done by hand.

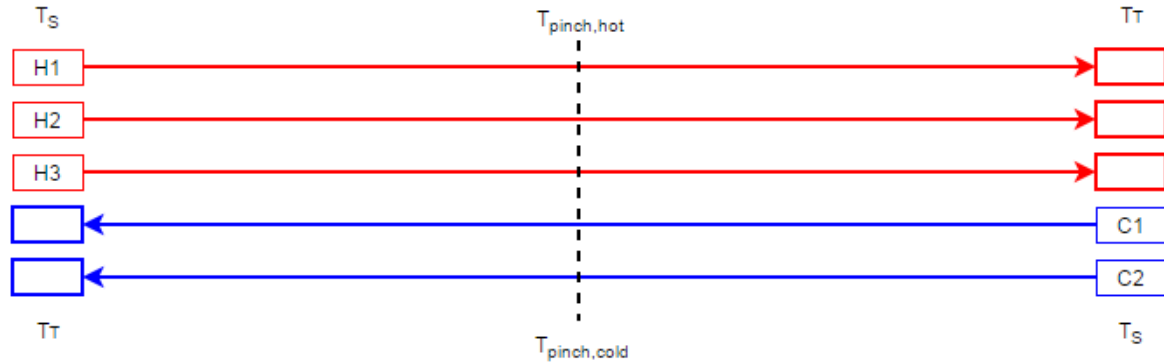


Figure 6.2: Simple stream network

When applying the pinch design method, one starts the design of the network at the pinch point, and moves away from the pinch as the most constrained area of the network is completed. There are certain rules to follow when designing the pinch heat exchangers (situated immediately above or below the pinch point). Above the pinch point, the pinch heat exchanger can only include streams where the mCp -value of the cold stream is equal or larger than the mCp -value of the hot stream, see (6.1). Otherwise, the temperature difference becomes smaller moving away from the pinch, which is infeasible (Smith, 2005). The same applies to the pinch exchangers below the pinch point. The mCp -value of the hot stream must be equal or larger than the mCp -value of the cold stream, see (6.2).

$$mCp_H \leq mCp_C \text{ (above pinch)} \quad (6.1)$$

$$mCp_H \geq mCp_C \text{ (below pinch)} \quad (6.2)$$

In the current work, the stream network is more complex than the one in Figure 6.2. It therefore becomes complicated to use the pinch design method by hand. However, the pinch design method can be applied to the current work through computer help, which is further described in Chapter 7. Another important feature related to process integration is the grand composite curve, which is further described throughout the next section.

6.2 Grand composite curve

A tool to recognize the heating and cooling demands in a process is to look at the grand composite curve of the network. The grand composite curve depicts the net heat flows in a process against the shifted temperature. Once the grand composite curve is drawn, it has the ability to illustrate where the process can utilize the internal heat flows and where external heating and cooling are needed. Figure 6.3 gives an example of how a typical grand composite curve for a process looks like. The pinch point is identified and marked.

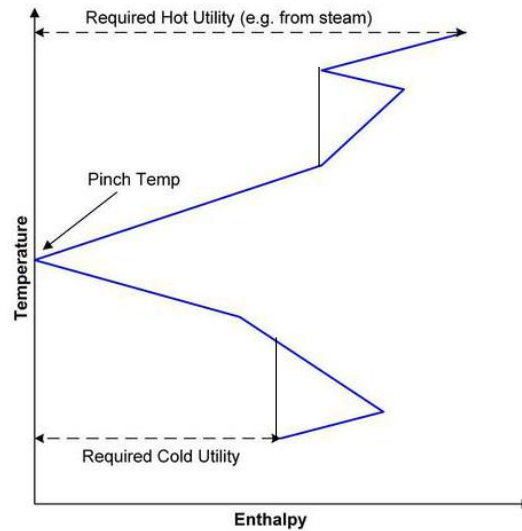


Figure 6.3: Typical GCC (The University of Waikato, 2014)

A process generally acts as a heat sink above the pinch point temperature, and a heat source below pinch. This is also the case in Figure 6.3. The grand composite curve in Figure 6.3 indicates the total required hot utility and cold utility needed. It also shows the so-called heat pockets. Heat pockets indicate where the process can utilize internal heat, in other words the process-to-process heat transfer. The grand composite curve not only informs about the required amount of heating and cooling in the process, but the graph also indicates at which temperature level the hot and cold utilities are needed. The graph can therefore imply the desired temperature levels for steam consumption and, if possible, steam production. Figure 6.4 gives an example of how the grand composite curve can be used for identification of desired temperature levels.

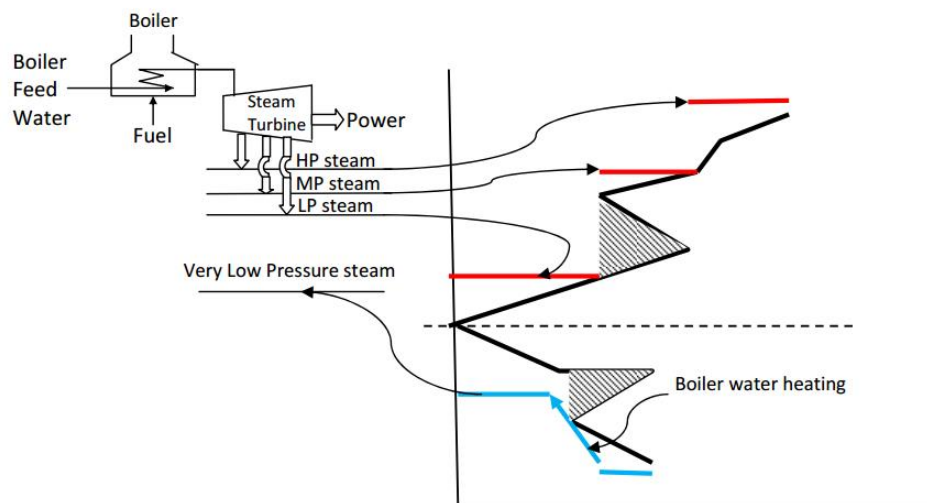


Figure 6.4: Multiple utilities in Grand Composite Curve (National Programme on Technology Enhanced Learning, 2012)

Instead of using high pressure steam to cover the entire heat demand, different steam levels can provide the suitable temperature level with heat. Generation of HP-steam requires more energy than generation of lower pressure level steam, which makes it beneficial to use as little HP-steam as possible, and instead try to distribute the heat requirements as in Figure 6.4. The heat available below pinch can be used for generation of steam if the temperature is sufficient. The grand composite curve gives an indication of the required utility use, but when it comes to network design that achieves these targets, a pinch design analysis is necessary.

7. Process Description

The main objective for this thesis is to develop fundamental process designs for the chosen concepts for hydrogen production. A comparison of the developed cases form the basis for discussion. The aim is to achieve self-sustained processes, where the only input is natural gas and the only output is liquefied hydrogen and carbon dioxide. Two main cases are developed, which will be further described throughout this chapter.

7.1 Process characterization

This sections intention is to describe the chosen case study. The traditional ATR process forms the base case, while the more unconventional technologies constitutes the second case.

All cases contain both High Temperature Shift (HTS) and Low Temperature Shift (LTS). The benefit of using both is that the hydrogen yield increases since more carbon monoxide reacts with steam and creates hydrogen. This is especially important if deposition of the off-gas occurs directly to atmosphere, as carbon monoxide is very harmful to the environment. In the current case, off-gas goes directly to combustion, which reduces the risk of emitting carbon monoxide since it reacts with oxygen and forms carbon dioxide during the complete combustion. However, including both HTS and LTS ensures a higher hydrogen concentration in the gas. This may lead to a reduced required area in the hydrogen purification unit. In the membrane cases, an increased hydrogen concentration can improve the hydrogen flux through the membrane and therefore obtain the same HRF with a reduced membrane area. On the other side, implementation of the LTS unit makes it, in some cases, necessary to heat the gas again before it enters the membrane, which makes the heat-integration slightly more complicated.

The entering gas is an all cases assumed to be absent of all sulfur containing components, meaning there is no need for a sulfur removing unit.

7.1.1 Base Case

Development of a base case is necessary. The conventional ATR process consists of pre-reforming, main reforming, water-gas shift, CO₂-capturing and hydrogen purification, like Figure 7.1 depicts, and as described throughout Chapter 4. An O₂-blown ATR is chosen, meaning an air separation unit is required.

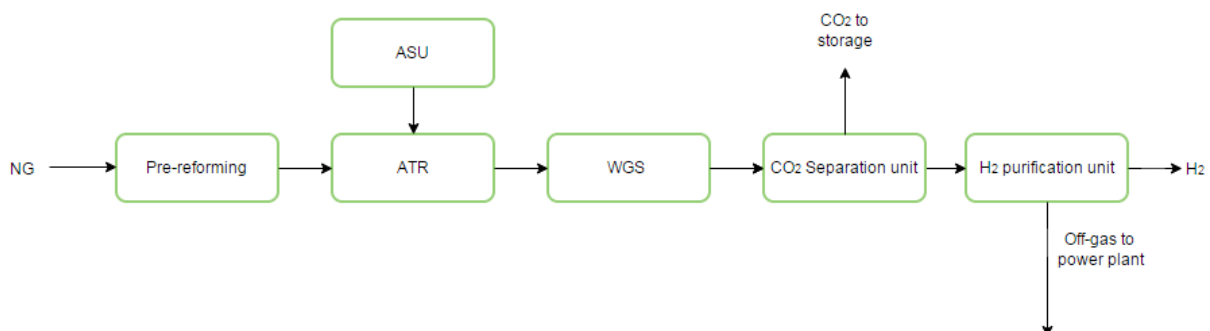


Figure 7.1: Conventional ATR process

The PSA off-gas is suitable for combustion since it primarily contains hydrogen along with some methane, which both have high heating value. The off-gas is therefore sent to a power plant where it enters a gas turbine. The purpose of the power plant is to supply the process with the required amount of power. Utilization of the hot exhaust gas from the gas turbine occurs through a Heat Recovery Steam Generation, HRSG, unit. The produced hydrogen is liquefied for transporting purposes. The base case becomes as Figure 7.2 depicts.

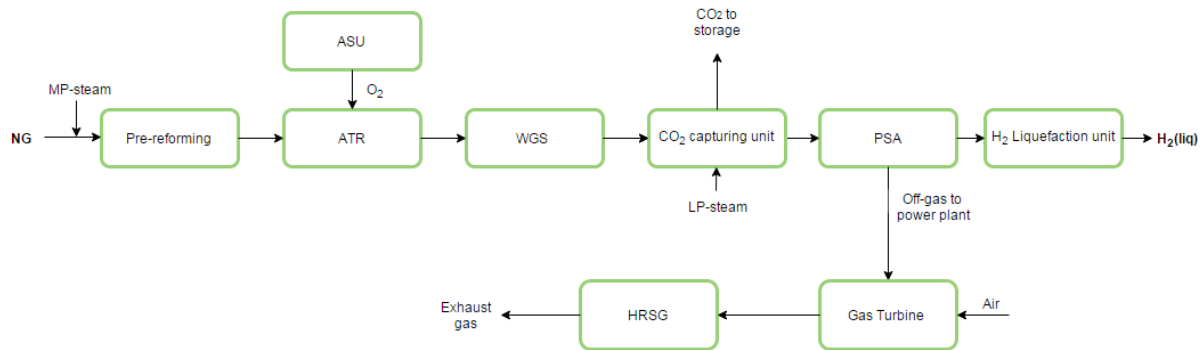


Figure 7.2: Overview base case

Process review

Natural gas enters the pre-reformer immediately after arriving the plant since pre-treatment of the gas is not considered. Supply of MP steam takes place at 330°C and 35 bar through a stream mixer. Natural gas enters the plant at 70 bar. As discussed, the reformer process is best suited at low pressure and high temperature. It is therefore desirable to throttle the gas, and preheat it before it enters the pre-reformer. Oxygen from the air separation unit is preheated to 500°C, same as natural gas, and enters the reformer. The gas from the reformer is exposed to cooling before it goes to the HT-WGS where CO reacts with H₂O and generates hydrogen. To squeeze out the last CO, the gas is further cooled after the HT-WGS and enters the LT-WGS. After the LT-WGS, the gas contains considerable amounts of carbon dioxide, water and hydrogen. Water is removed by phase separation after cooling the gas down to 25°C, where most of the water has condensed. Before hydrogen purification, the gas goes through the CO₂ separating unit, where approximately 95% of the CO₂ is extracted from the gas and enters a four-stage compression and cooling process to become liquid. Liquid CO₂ is then pumped up to the desired transport pressure, accordingly 110 bar in this thesis. Rest of the gas from the CO₂ capturing unit goes to hydrogen purification. The hydrogen after the PSA unit is ready for liquefaction. The PSA off-gas, on the other hand, contains considerable amounts of combustible compounds and works as fuel for the gas turbine. The complete combustion in the gas turbine ensures power output and hot exhaust gas capable of raising steam. Generation of steam occurs through process excess heat and through the HRSG.

7.1.2 Case II

The aim for this master thesis is to compare membrane solutions for hydrogen purification and low-temperature solutions for CO₂-capture with established technologies for hydrogen production from natural gas. With that in mind, case II adopts new technology, and replaces the PSA with a hydrogen selective membrane and the pre-combustion carbon-capturing unit with a low-temperature process for CO₂ capture.

The membrane cases are studied with various HRF-values. Adjustment of the HRF-value changes the possible power output from the gas turbine, as it changes the amount of fuel supply. The higher HRF, the

less work is extracted from the gas turbine since it gets less useful fuel. It will not necessarily be optimal to maximize the HRF-value due to the aim of self-sustained processes.

The desired temperature level for a membrane is around 400°C (Ockwig and Nenoff, 2007). The pressure difference between the feed side and the permeate side is the driving force of the membrane, and can vary to adjust the HRF.

Hydrogen selective membranes facilitate CO₂ capture as the CO₂ – concentration of the gas increases after the membrane. The higher CO₂ – concentration, the less work is required for the separation process (Berstad et al., 2013b). In the base case, the CO₂ separating unit is located in front of the hydrogen purification unit, which leads to a lower CO₂-concentration of the gas entering the capturing unit. One of the goals is therefore to find out how this affects the CCR compared to the membrane cases applying LT – process for CO₂ separation, and how it affects the efficiency of the plants.

There exists several opportunities for membrane implementation in a hydrogen producing facility, which Chapter 5 looked into. This thesis looks at two alternatives, respectively a single membrane module and a sequential membrane and WGS module. For the single membrane case, there will be developed three different subcases. Accordingly, a basic case, a case where the permeate pressure is equal to the required pressure in the liquefaction unit, and a combination of the base case and the single membrane module case where the CO₂ capturing unit is placed in front of the membrane. All membrane cases are also considered with two different feed pressures, respectively 36 bar and 66 bar. The reason is to investigate how the increased driving forces affect the membrane performance and the power integration of the plant. The following sections provide an overview of the studied membrane cases.

Case II-1

Case II-1 represents implementation of a single membrane module. This membrane module is located right after the LT-WGS. An overview of this case is given in Figure 7.3.

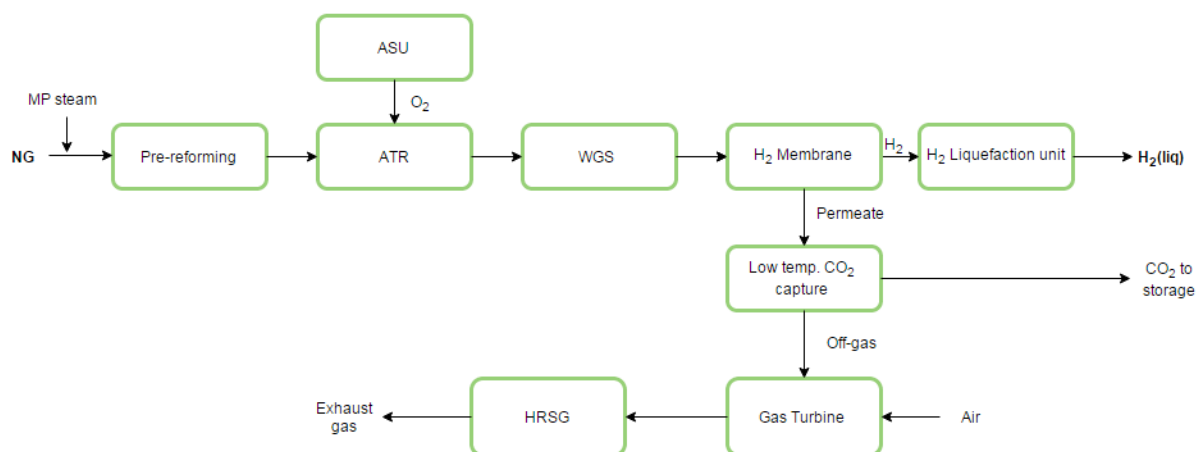


Figure 7.3: Overview case II-1

Case II-2

This case considers two membrane modules, one placed between the HT-WGS and the LT-WGS and one after the LT-WGS, as Figure 7.4 depicts. This technology is assumed to require less membrane area to achieve the same results as the single membrane module, which was seen in Chapter 5.

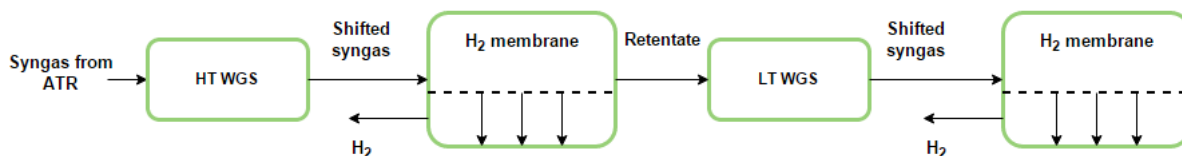


Figure 7.4: Sequential membrane and WGS module - case II-2

Case II-3

One of the benefits of using PSA for hydrogen purification is the elevated pressure of the hydrogen leaving the PSA unit. The cases described all consider a permeate pressure of 1 bar. To be able to achieve the required liquefaction specifications, respectively 20 bar and 30°C, the hydrogen must be compressed after leaving the membrane. Hydrogen compression requires huge amounts of power. It would therefore be of interest to see how it affects the process if the permeate pressure is defined to be 20 bar, such that compression is avoided. How this is done in reality is uncertain, but it is interesting to see how this process performs compared to the other cases. A third membrane case is therefore created, denoted case II-3, and will be studied with both 36 bar and 66 bar inlet pressure, like the other membrane cases. This case will only be considered with the single membrane module since this will give sufficient comparative basis. The process design equals the design of case II-1.

Case II-4

Another interesting idea for the hydrogen producing plant is to move the CO₂-capturing unit upstream the membrane. This reduces the amount of gas entering the membrane, which will affect the membrane properties. The assumption is that less membrane area is required to complete the separation when less gas enters the membrane. This is beneficial considering the investment costs. However, the operating costs for removing CO₂ will increase, and there will be a tradeoff between these factors.

The process will be simulated in HYSYS, as the other cases. In order to see the changes in the membrane properties once the hydrogen fraction of the incoming membrane gas increases, this case is, as the others, also analyzed through the parametric study carried out in the membrane model borrowed from SINTEF Materials & Chemistry. Both 36 and 66 bar inlet pressure are studied, but this case only considers the single membrane module. This membrane case is denoted case II-4, and Figure 7.5 gives an overview of the process plant.

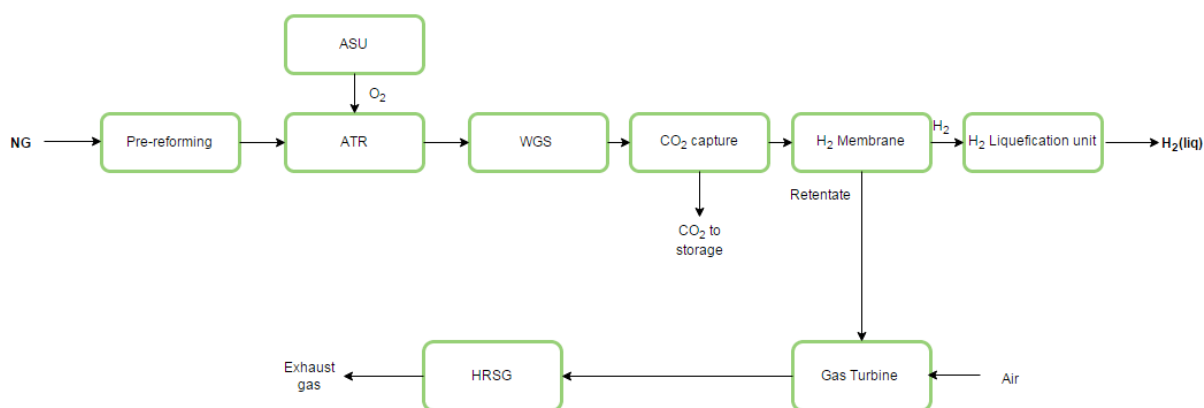


Figure 7.5: Overview case II-4

Membrane case overview

Different subcases are developed for the membrane cases, where the HRF-value is varied. The main membrane cases are designed to produce exactly the same amount of hydrogen as the base case. Meaning, the HRF-value in the membranes are adjusted such that the same amount of hydrogen is produced in all cases, which makes the comparison easier. In some cases, this result in an extra demand of fuel supply to the gas turbine in order to accomplish the power balance. This is covered by injecting natural gas to the combustion chamber in the gas turbine. Alternatively, it could also be of interest to study the impact on the hydrogen production if the HRF-values are adjusted such that power consumption and production are in exact balance without any supplementary fuel to the gas turbine. In addition to vary the HRF-value, the cases are also analyzed with two different feed pressures for the membrane, respectively 36 bar and 66 bar. Table 7.1 provides an overview of the different membrane cases developed, and how they are accomplished.

Table 7.1: Overview membrane cases

	Same hydrogen amount as base case (main case)		Power balance with no additional NG to the gas turbine	
	36 bar membrane feed pressure	66 bar membrane feed pressure	36 bar membrane feed pressure	66 bar membrane feed pressure
Case II-1	-	Adjust HRF	-	Adjust HRF
Case II-2	-	Adjust HRFs	-	Adjust HRFs
Case II-3	-	Adjust HRF	-	Adjust HRF
Case II-4	-	Adjust HRF	-	Adjust HRF

Figure 7.6 gives an alternative overview of the developed membrane cases.

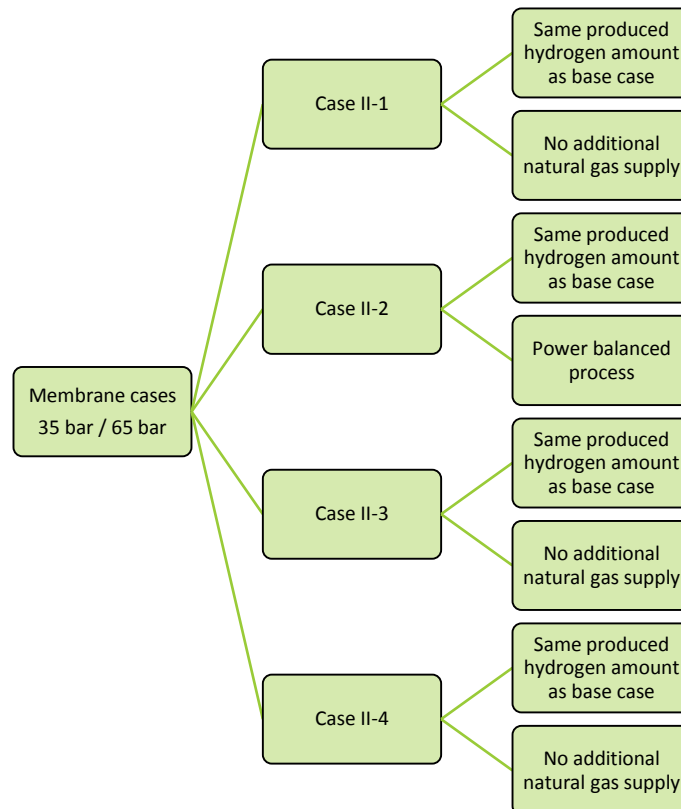


Figure 7.6: Overview membrane cases

Process review

The membrane cases are similar to base case until the HTS unit. Oxygen and natural gas are preheated in the same manner and the heat available after the ATR is utilized to generate HP steam and to supply other heat demanding units in the process. For case II-1, with a single membrane module, the stage between the HTS and LTS is also equal to base case. After the LTS, however, the process starts to deviate from the base case. The gas leaving the LTS is compressed and pre-heated (not necessary in the 66 bar inlet case) in order to obtain the desired membrane pressure and temperature. The hydrogen leaving the membrane has the same temperature as the feed gas since the membrane is assumed to operate with no temperature loss. The pressure, however, has diminished to atmospheric conditions and must undergo compression in order to obey the hydrogen liquefaction specifications. Pre-cooling of the hydrogen in front of the compressor ensures a less energy demanding compression. The gas temperature increases as it is compressed and must be cooled significantly to achieve the desired liquefaction specifications of 20 bar and 30°C. The membrane retentate contains mostly H₂O, H₂ and CO₂. Before LT-separation of CO₂, it is crucial that the gas is absent of all water compounds. Cooling of the gas down to 25°C appears immediately after the outlet of the membrane, followed by a phase separator for extraction of liquid water. The gas then enters the low temperature CO₂-capturing unit, where slightly less than 95% of the CO₂ content in the gas leaves. The CO₂ is in liquid form and at the desired transport pressure when it leaves the LT-unit. The remaining gas primarily contains hydrogen, along with smaller parts of CH₄, CO, CO₂, N₂ and Ar. This gas is suitable for combustion in the gas turbine.

Case II-2 has much in common with case II-1. The only thing deviating the two cases occurs between the HTS and the LTS units. Instead of cool the gas from around 450°C to 200°C after the HTS reactor, it is only cooled to 330°C in the case of 36 bar membrane inlet pressure, and 230°C for the 66 bar membrane inlet pressure case. The gas is then compressed and the temperature increases to 400°C as it enters the first membrane module. After the first membrane, the retentate gas is cooled to 200°C to obtain a good shift reaction in the LTS reactor. The LTS outlet gas must again be heated to 400°C before it can enter the second membrane. From this stage, the gas undergoes the same process as described above.

Case II-3 is only considered with a single membrane module, and the process is equal to case II-1 except for the hydrogen treatment after the membrane. Since case II-3 introduces the possibility for pressurized permeate gas, the hydrogen compression becomes superfluous and is therefore removed. This causes less available heat from this stage, and thus reduces the possible steam generation.

Case II-4 differs from the other membrane cases since the CO₂-capturing unit is placed in front of the membrane module. The process equals the base case including the CO₂-capturing unit. After the CO₂-capturing unit, the gas temperature is 27°C and the pressure is approximately 25 bar. To achieve the desired membrane pressure, a compressor is installed in front of the membrane, ensuring a pressure increase and at the same time a temperature increase. However, the temperature of the gas do not reach 400°C in any of the inlet pressure cases, and a heater is therefore necessary in order to achieve the desirable membrane temperature. The CO₂ capturing unit captures the CO₂ in an amine process, and sends it to a four stage cooling and compression process before it is pumped up to the desired transport pressure. The hydrogen from the membrane is pre-cooled in front of the hydrogen compression. Membrane retentate goes as fuel to the gas turbine.

7.2 Heat- and power integration

When designing the cases, the objective is to achieve an integrated ATR process where the only feed is natural gas and the only outlet is liquefied hydrogen and carbon dioxide. To be able to accomplish such a system, the internal heat and cooling demands, as well as power production and consumption, must be in balance. The cloud in Figure 7.7 visualizes the idea for the ATR process. Figure 7.7 is not a control volume for the process, but only illustrates the desired concept for the process plant.

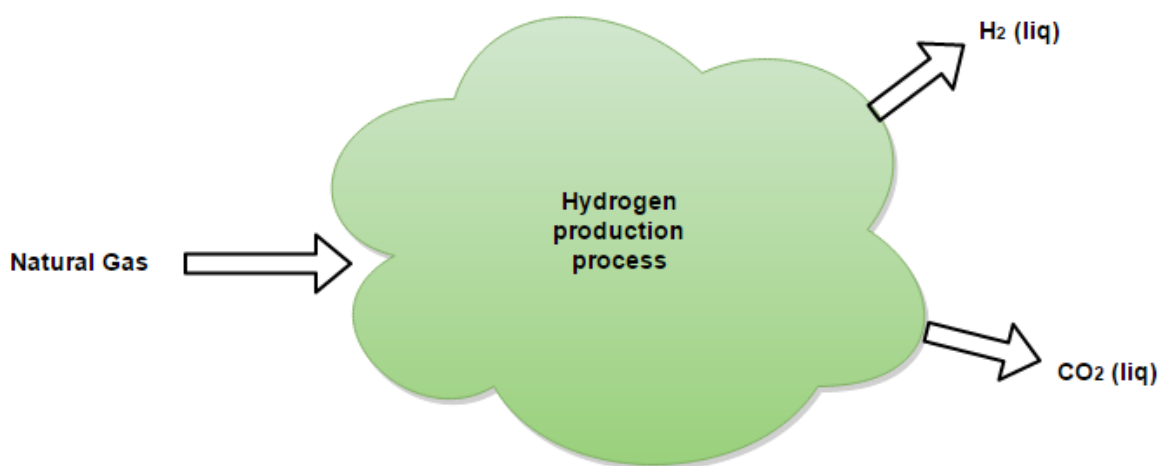


Figure 7.7: Objective for self-sustained ATR process

This section aims to clarify how the heat- and power integration has been conducted for the various cases. The heating and cooling demands in the different cases are much the same, but differ in some parts of the process. This chapter is therefore divided into two, where the first part considers the heat- and power integration for the base case, while the second part considers integration of the membrane cases. Since some of the issues highlighted in the first part also applies for the second part, only the things done differently in the membrane cases are emphasized in the second part.

7.2.1 Heat- and power integration of Base Case

Heat Integration

The process has internal heating- and cooling requirements, as indicated in Figure 7.8. The first red arrow indicates the heat requirement for pre-heating of natural gas. Pre-heating of oxygen is indicated as a red arrow between the ASU and ATR. The temperature of the gas leaving the ATR is high, more precisely 950°C, because of the partial oxidation taking place during the reforming. Since the chemical reactions occurring in the water-gas shift units are exothermic, they favor low temperature. It is therefore beneficial to cool the gas between the reforming stage and the WGS stage. Further cooling of the gas is necessary after the WGS stage in order to separate out water before the carbon-capturing unit. The capturing unit requires LP steam for the reboilers, and the compression and liquefying of CO₂ requires cooling water. The exhaust gas is cooled in the HRSG as it raises steam.

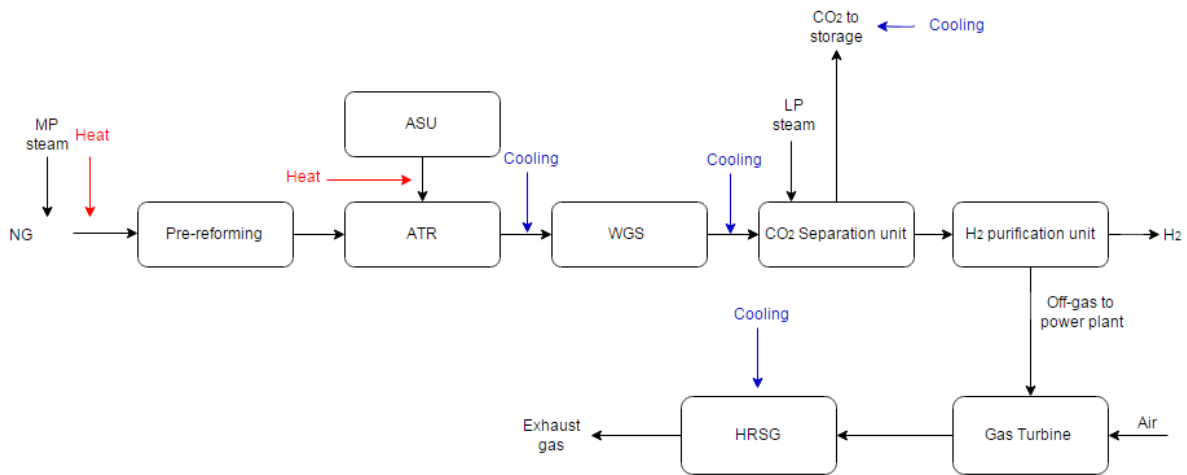


Figure 7.8: Overview of heat and cooling demand ATR process with pre-combustion carbon capture and PSA for purification

Because of the hot gas leaving the reformer and the warm exhaust gas from the gas turbine, the cooling demand represents a greater value than the heating demand, resulting in excess heat from the process. When the heat requirements in the process are fulfilled by process-to-process heat exchange, the remaining heat will be used for steam production. Steam production is necessary for supplying the process with the required amount of MP-and LP steam. The minimum produced steam must therefore be the amount that exactly covers the needs in the process. However, steam production is also desirable due to possible power production in steam turbines.

A tool to recognize the heating and cooling demands in a process is to look at the grand composite curve of a network. Figure 7.9 gives the grand composite curve of the base case. Observations from the GCC is that the process has a great cooling demand, while the small heating demand will be covered by the process heat available, as can be seen from the small heat pocket at the right in the picture. The GCC gives an indication of how much steam the process can produce, and at which steam level. However, it must be kept in mind the simplifications by assuming steam generation through a straight line in the GCC. Steam generation occurs through heating of the BFW, boiling and superheating. Drawing a straight line at the boiling point temperature in the GCC gives only an indication of the amount of possible steam generation. There can also be practical limitations that reduce the indicated amount, like metal dusting in the superheater.

Grand Composite Curve

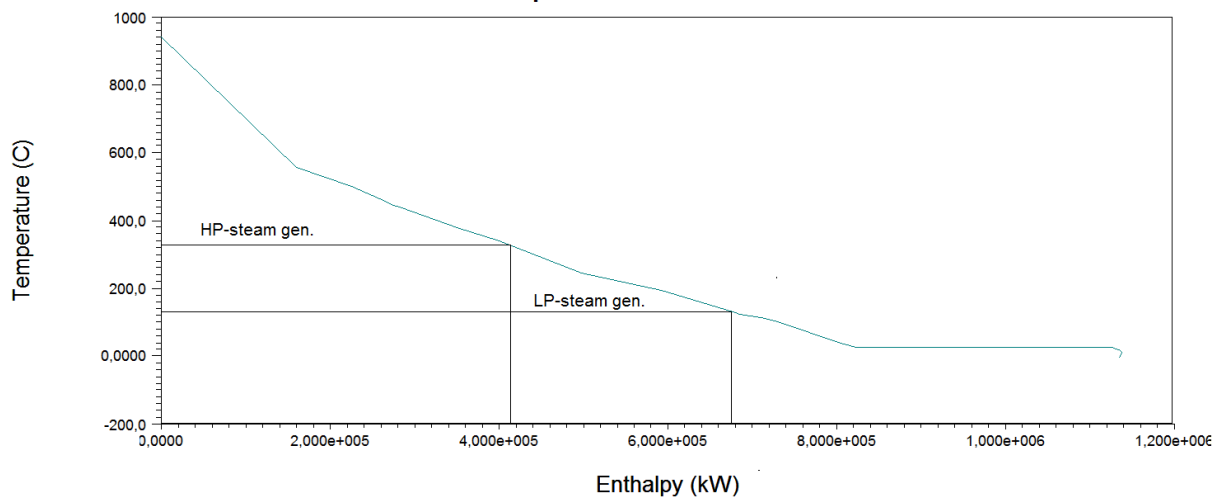


Figure 7.9: Grand Composite Curve and steam production

When designing the heat-integrated system, there are, basically, two things that has to be obeyed:

- The ΔT_{\min}
- Forbidden matches

The minimum delta T is a decided value for the minimum allowable temperature approach in heat exchangers. This value is decided by evaluating the tradeoff between capital costs and operating costs for the heat exchangers. Increasing ΔT increases the driving forces in the heat exchanger, and the heat exchanger area can therefore be reduced. The assumption in the current work is that $\Delta T_{\min} = 10^{\circ}\text{C}$ gives a reasonable tradeoff.

Forbidden matches are a designer's choice to disallow heat exchange between a pair of streams in the network. Reasons for employing forbidden matches can for example be that the streams are located in different parts of the process plant, making it impossible to exchange heat. It can also be in order to avoid corrosion problems or it can be because of safety issues. The reasons can be many. Imposing forbidden matches might affect the optimal network design, which can lead to a process penalty in form of extra utility requirements. Regarding this thesis work, there will be forbidden matches in the process due to the risk of metal dusting occurrence. Metal dusting can destroy the heat exchangers, and it is therefore crucial to avoid. This is further described in Chapter 8.

Power Integration

Power production occurs through the gas turbine and the steam turbines. Heat integration and power integration are closely related as they affect each other. Changes in the heat-integrated network may influence the amount of produced steam, which will affect the production of power and thus the power integration. Adjustment of the produced power occurs through modification of the power output from the turbines. The amount of fuel supplied determines the power output from the gas turbine, while the available excess heat in the process determines the power output from the steam turbines. The power output from the gas turbine affects the power output from the steam turbines, which makes these two variables interdependent. An increase in fuel supply to the gas turbine increases the potential for steam generation through the HRSG unit since the mass flow of the exhaust gas increases. In case of deficit power production when the gas turbine uses all its fuel supply and there is maximum steam generation, one alternative is to supply the gas turbine with extra natural gas, which will increase the power output from both the gas turbine and the steam turbines.

Figure 7.10 gives an impression of where the power production and consumption are located in the base case. The most energy intensive unit is the H₂-liquefying unit.

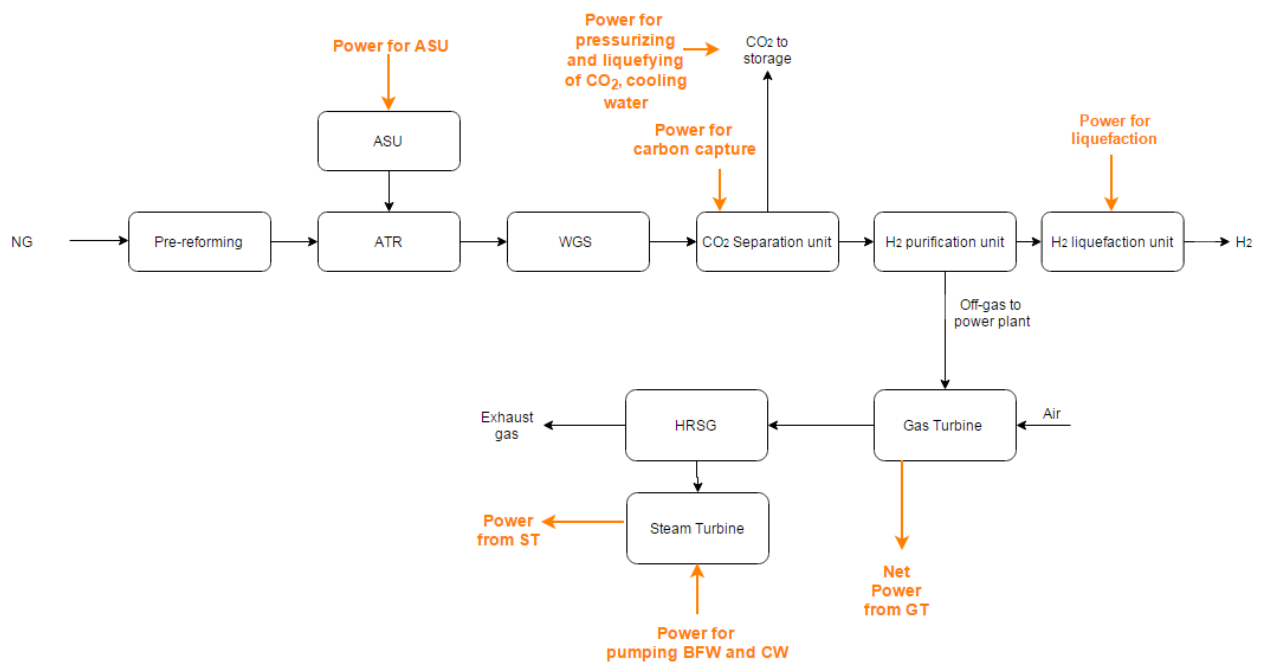


Figure 7.10: Power production and consumption

7.2.2 Heat- and power integration membrane cases

The four membrane cases differ to some extent when it comes to heat- and power integration. However, for case II-1, II-2 and II-3, the differences are not significant and the description in this section is therefore covering these cases simultaneously. Case II-4, on the other hand, deviates from the other cases as it combines the base case and the membrane cases. This case is therefore considered in a separate section.

Heat Integration of case II-1, II-2 and II-3

The membrane cases considering 36 bar inlet membrane pressure has the heating and cooling demands as illustrated in Figure 7.11. As the base case, the process has heat surplus. Again, the first priority is to cover the process needs. Once this is done, rest of the heat is used to raise steam.

The membrane retentate goes to the low temperature CO₂-separating unit. Observations from Figure 7.11 shows that this unit is not heat integrated with rest of the process. Cooling in this unit primarily occurs through internal heat exchangers and separated cooling circuits, and is therefore not implemented. However, before the retentate goes to the LT-unit, it is cooled down to 25°C for condensing out liquid water. This cooling is heat integrated in the process. Further, the exhaust gas is cooled through steam generation in the HRSG.

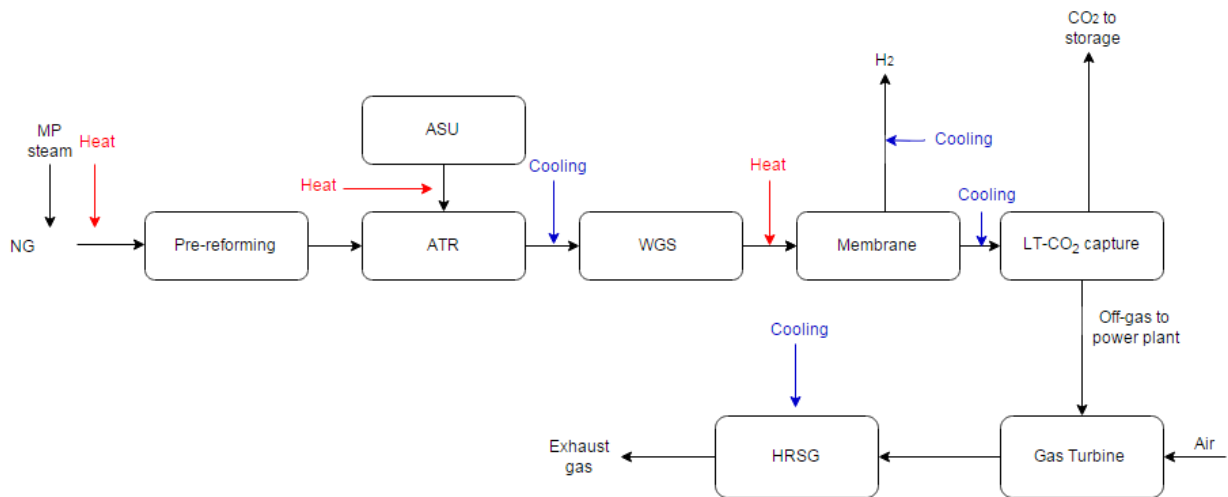


Figure 7.11: Heating- and cooling requirements for membrane cases with 36 bar membrane feed pressure

The distribution of heating and cooling demands are equal for the cases considering 66 bar membrane inlet pressure except for the heat requirement in front of the membrane. When the pressure increases, the temperature increases which leads to a sufficient temperature increase without any preheating in front of the membrane. It becomes as depicted in Figure 7.12.

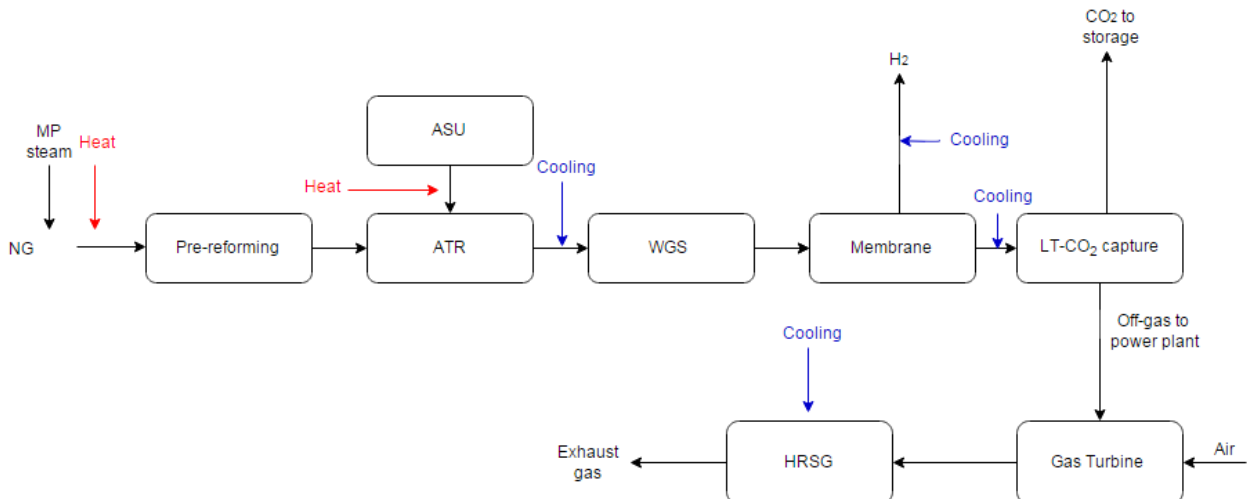


Figure 7.12: Heating- and cooling requirements for membrane cases with 66 bar membrane feed pressure

Grand composite curves for the respective membrane cases can be found in Appendix H.

Heat Integration of case II-4

The heat demand and heat production in case II-4 are as depicted in Figure 7.13. The gas is cooled down to 25°C in front of the CO₂-capturing unit in order to separate liquid water from the process. This means that the gas must be heated again before it enters the membrane. The same distribution of the heating- and cooling requirements occur for the case considering 66 bar inlet pressure. The grand composite curve for this case is attached in Appendix H.

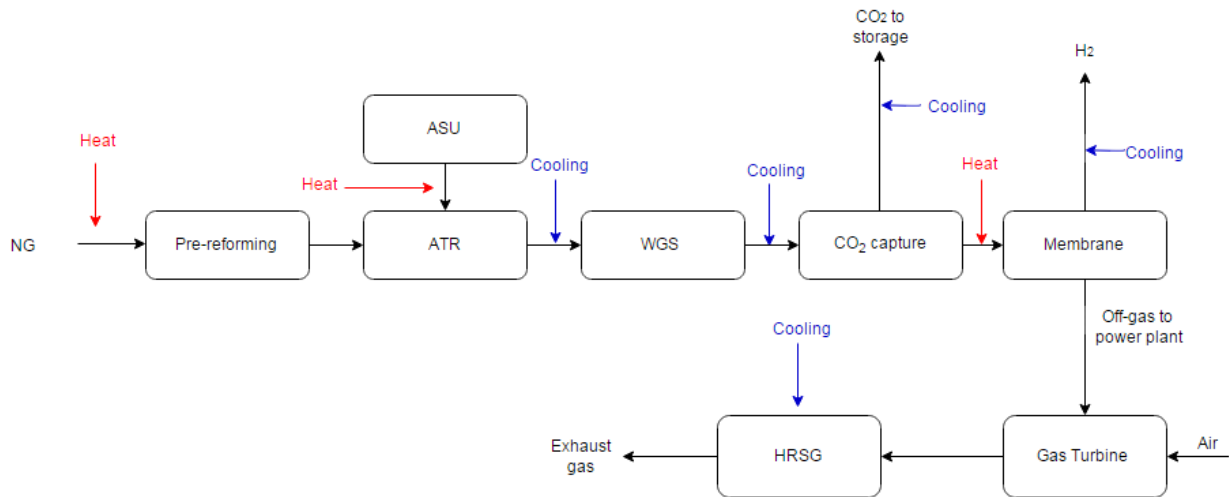


Figure 7.13: Heating- and cooling requirements for case II-4

Power Integration of case II-1, II-2 and II-3

Like the base case, the membrane cases need power supply to the ASU, the liquefaction unit and the steam cycle pumps. In addition, the membrane cases introduce some new energy demanding units. The gas must be compressed before entering the membrane modules, as pressure is the driving force in these installations. How much power is needed for this purpose depends on the decided feed pressure. The hydrogen from the membrane must be compressed to prepare for liquefaction. The low temperature CO₂ separating process requires work for the compressors and pumps. Figure 7.14 gives an overview of the power consuming- and producing units in these membrane cases.

In the case with two membrane modules installed, the same energy demands are identified. This thesis uses only one compressor in front of the first membrane module to raise the pressure. The rationale for this choice is the small pressure drop between the membranes. It would be costly to install two compressors for this purpose. The inlet pressure for the first membrane is therefore 69 bar, and the inlet pressure of the second membrane is 66 bar. For case II-3, which considers pressurized permeate gas, the energy requirement for hydrogen compression is absent. The other power demands are however equal to the other cases.

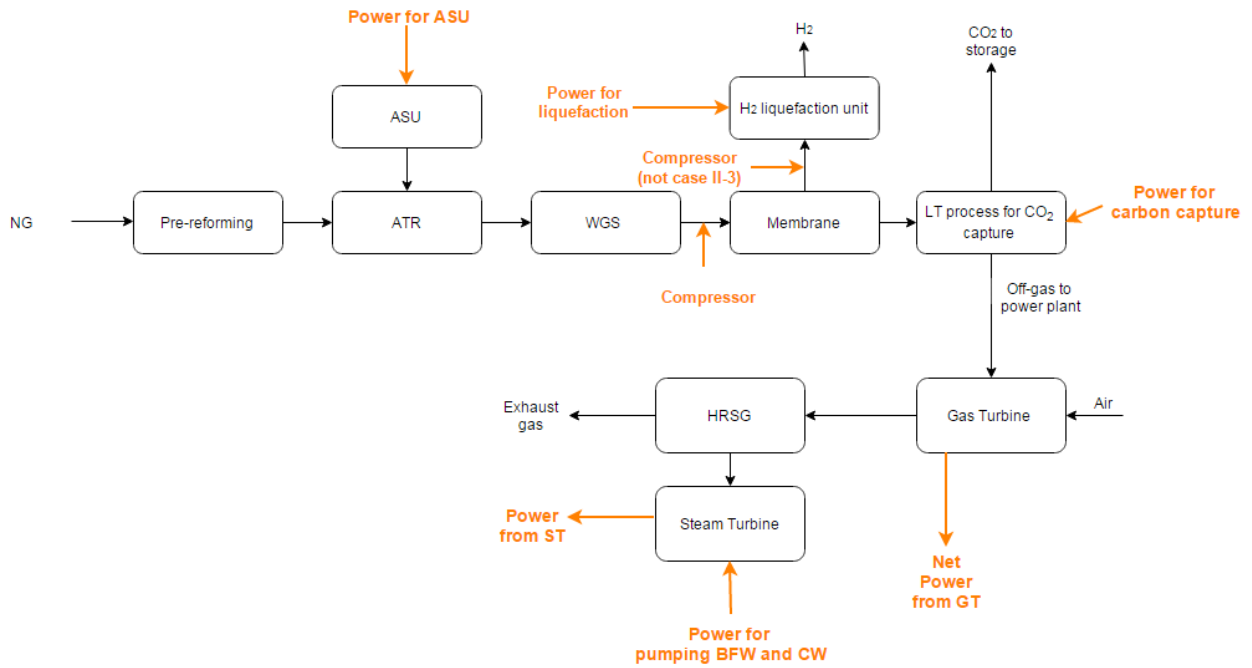


Figure 7.14: Power distribution for case II-1, II-2 and II-3

Power Integration of case II-4

The power consuming-and producing units in case II-4 are as illustrated in Figure 7.15. This case will require a larger CO₂-capturing work, but in return, this case needs less power for membrane compression since a big share of the gas is removed in the CO₂ capturing unit. Chapter 9 provides the resulting heat- and power-integrated processes.

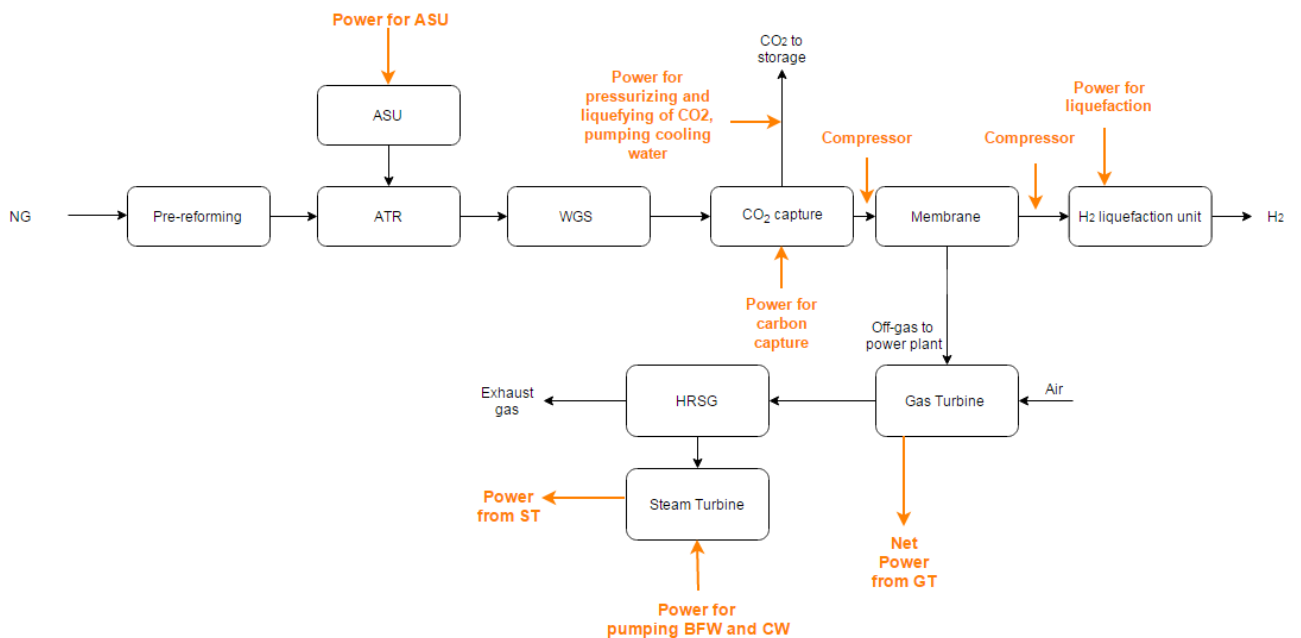


Figure 7.15: Power distribution case II-4

8. Methodology, Design basis and HYSYS implementations

This chapter describes the methodology deployed in the simulations of the relevant case study. The purpose of this chapter is to provide the reader with essential insight in the methods used for achieving the objectives. This study uses Aspen HYSYS as primary simulation tool. Simulations performed in HYSYS form the basis for comparing the cases, which makes HYSYS a completely necessary tool for reaching the targets of this thesis. As a supplementary simulation tool, Aspen Energy Analyzer is used. Using Aspen Energy Analyzer allows the user to get insight in the energy saving potentials in the process as the program uses pinch analysis to identify the utility targets for the process. Before going into detail regarding the applied simulation tools, and how the respective process units are implemented in HYSYS, this chapter initially informs the reader of relevant process specifications. Throughout the design basis section, all relevant process specifications are reviewed as well as argumentation for the choice of Equation of State (EOS) in HYSYS.

8.1 Design Basis

This section provides specifications and relevant design information regarding the simulations done in HYSYS. Information concerning the use of equation of state is also discussed in this section. HYSYS stream data for the relevant case study is provided in Appendix E.

8.1.1 Process specifications

In order to achieve a comparable design, the process must follow some defined specifications. These specifications work as constraints and form system boundaries for the process. All cases developed throughout this study must abide these specifications. This section provides the reader with the relevant energy streams specifications. All units implemented in HYSYS need to work within decided specifications as well. All process units are operated according to the specifications given in Appendix B. The unit specifications are a result of discussions with the supervisors and values from the DeCARBit's manual (DECABRit, 2009).

Energy streams specifications

According to the process control volume, given in Figure 4.2 and rendered in Figure 8.1 below, the energy streams of the system are accordingly the entering natural gas, oxygen, air and water, while the energy streams leaving are the hydrogen and the carbon dioxide. Exhaust gas is a product of the process and is not considered as an energy stream. This section provides the respective specifications for these streams.

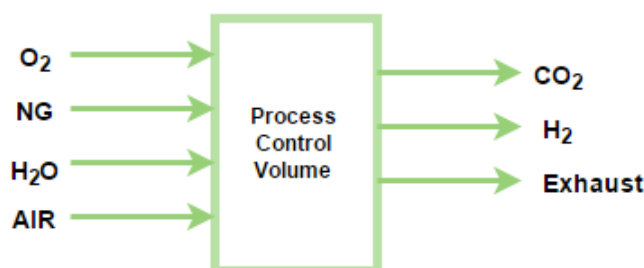


Figure 8.1: Process control volume

Natural gas

Table 8.1 provides the specified composition, temperature, pressure and calorific values for natural gas.

Table 8.1: Natural gas specifications (DECABRit, 2009)

<i>Natural gas specifications</i>	
<i>Pressure [bar]</i>	70
<i>Temperature [°C]</i>	10
<i>Entering molar flow [kgmole/h]</i>	9000
<i>Corresponding entering mass flow [kg/s]</i>	45.06
<i>Composition [mole%]</i>	
<i>Methane</i>	0.89001
<i>Ethane</i>	0.07
<i>Propane</i>	0.01
<i>i-Butane</i>	0.0005
<i>n-Butane</i>	0.0005
<i>i-Pentane</i>	5,00E-05
<i>n-Pentane</i>	4,00E-05
<i>n-Hexane</i>	0
<i>H₂O</i>	0
<i>CO</i>	0
<i>Hydrogen</i>	0
<i>CO₂</i>	0.02
<i>Nitrogen</i>	0.0089
<i>Oxygen</i>	0
<i>H₂S</i>	0
<i>M-Mercaptan</i>	0
<i>SO₂</i>	0
<i>Argon</i>	0
<i>NO</i>	0
<i>NO₂</i>	0
<i>HHV [kJ/kg]</i>	5.113*10 ⁴
<i>LHV [kJ/kg]</i>	4.650*10 ⁴

Hydrogen

The pure hydrogen is produced according to the specifications for hydrogen liquefaction. The specific work for H₂ liquefaction assumes that hydrogen enters at 20 bar and 30°C. This specification applies even if liquefaction is included or not, and the specifications are summarized in Table 8.2.

Table 8.2: Hydrogen specifications

<i>Hydrogen specifications</i>	
<i>Pressure [bar]</i>	20
<i>Temperature [°C]</i>	30

Carbon dioxide

The different cases uses different types of technology for carbon capture. The Carbon Capture Ratio, CCR, is one of the values to be investigated for the various cases. Whatever technology used, the CO₂ must be liquefied and compressed before transportation. The specifications are summarized in Table 8.3.

Table 8.3: Carbon dioxide specifications

<i>Carbon capture specifications</i>	
<i>Pressure, to storage [bar]</i>	110
<i>CO₂ content in stream to storage [mole %]</i>	95

Ambient conditions

The process requires cooling water, BFW and ambient air. The specifications for the respective streams are as followed in Table 8.4.

Table 8.4: Ambient air - and water specifications

<i>Cooling- and boiler feed water specifications</i>	
<i>Temperature [°C]</i>	15
<i>Pressure [bar]</i>	1

<i>Ambient air specifications</i>	
<i>Temperature [°C]</i>	15
<i>Pressure [bar]</i>	1
<i>Air composition [mole%]</i>	
<i>N₂</i>	77.288
<i>CO₂</i>	0.033
<i>O₂</i>	20.733
<i>Ar</i>	0.924
<i>H₂O</i>	1.022

The reference temperature in the system is decided to be 15°C and 1 bar, meaning cooling water and air comes in at reference conditions, and then by definition contains no energy.

8.1.2 Equation of state

To obtain a correct model, the choice of Equation of State, EOS, is important. This thesis uses two different EOS to make the process as valid as possible. The hydrogen producing plant uses the Kabadi-Danner EOS. The Kabadi-Danner EOS is a modification of the original SRK equation of state. This fluid package uses the Kabadi-Danner method to calculate vapor-liquid equilibriums and SRK for calculating enthalpy and entropy. An alternative EOS that could be employed in this study, is the Peng-Robinson EOS. To see if there are any significant differences between the two alternatives, the LT-separation process for CO₂ were studied with both EOS, and Table 8.5 provides the results, respectively. As observed, not much separates the two alternatives.

Table 8.5: Overview results EOS testing

	Kabadi-Danner	Peng-Robinson
CCR [%]	91.96	91.31

The steam cycle uses ASME steam as an equation of state. The steam cycle was tested with both the Kabadi-Danner and the ASME-steam EOS, and the results deviated to some extent. It was therefore decided to use two different EOS in the same model. Compared with the Kabadi-Danner EOS, the steam turbines generally produced more power once the ASME-steam EOS were used. The results are summarized in Table 8.6.

Table 8.6: Overview results of EOS testing - II

	Kabadi-Danner	ASME steam	Increase [%]
HP turbine [kW]	$5.515 \cdot 10^4$	$5.922 \cdot 10^4$	7.4
MP turbine [kW]	$5.521 \cdot 10^4$	$5.630 \cdot 10^4$	1.97
LP turbine [kW]	$1.087 \cdot 10^5$	$1.091 \cdot 10^5$	0.37

8.2 Applying Aspen Energy Analyzer

Aspen Energy Analyzer is a software for computation and design of optimal heat exchanger networks. An optimal heat exchanger network has minimum use of utilities, making the process design as integrated as possible. Aspen Energy Analyzer, AEA, can import flow sheets directly from Aspen HYSYS or the streams can be developed directly in the program. The program identifies hot and cold streams of the process as the supply and target temperature of a stream is defined. In addition to the temperatures, the program needs to ascertain the mC_p -value of the stream to be able to design a proper network. Figure 8.2 gives an example of how the interface of the program appears when the streams are defined.

Name	Inlet T [C]	Outlet T [C]	MCp [kJ/C-h]	Enthalpy [kW]	Segm.	HTC [kJ/h-m ² -C]	Flowrate [kg/h]	Effective Cp [kJ/kg-C]	DT Cont. [C]
ATR to HT	950,0	350,0	1,509e+00E	2,515e+005		720,00	----	----	Global
HT to LT	455,0	200,0	1,451e+00E	1,028e+005		720,00	----	----	Global
LT to cooled	253,3	25,0	2,737e+00E	1,736e+005		720,00	----	----	Global
PreCCS to 1	45,0	20,0	3,293e+00E	2287		720,00	----	----	Global
first comp to cooled CO ²	137,8	20,0	3,462e+00E	1,133e+004		720,00	----	----	Global
second comp to 8	120,6	30,0	3,559e+00E	8958		720,00	----	----	Global
third comp to 10	134,1	30,0	3,890e+00E	1,125e+004		720,00	----	----	Global
comp co2 to 11	138,0	16,0	9,963e+00E	3,376e+004		720,00	----	----	Global
O2 ASU to O2 ATR	22,0	450,0	1,709e+00E	2,032e+004		720,00	----	----	Global
to prereformer	450,0	500,0	1,147e+00E	1,593e+004		720,00	----	----	Global
NG in to heated NG	-8,3	435,0	4,539e+00E	5,590e+004		720,00	----	----	Global
37-O2 to ATR	450,0	500,0	1,793e+00E	2490		720,00	----	----	Global
With steam to 73	375,7	450,0	1,127e+00E	2,326e+004		720,00	----	----	Global
To exhaust	564,7	80,0	2,769e+00E	3,728e+005		720,00	----	----	Global
ST	32,5	32,0	2,292e+00E	3,438e+005		720,00	----	----	Global
New									

Figure 8.2: Screen shot of Aspen Energy Analyzer interface

Once the process streams and feasible utilities are defined, the program calculates the energy targets, the minimum numbers of heat exchangers possible, known as $U_{\min, MER}$, area targets and cost index targets. In addition, the program creates composite curves and grand composite curves for the actual case.

Performing a pinch analysis on the current processes requires computer help, which in this thesis is accomplished by Aspen Energy Analyzer. Once the process streams and feasible utilities are defined in Aspen Energy analyzer, the program recommends different network solutions. Some of the recommended networks are attached in Appendix H. However, as this program intends to minimize the cost of a process, and not necessarily the utility use, even though these appear to go hand in hand, the program did not give the desirable result when it came to network design. This software has the industry as their intended audience, which makes it beneficial to design the network based on economic reasons instead of only concentrating on reaching the targets. In order to test if the software gave the desired network design, a simple process, with two hot and two cold streams were implemented to the program. In this stream network, the supply- and target temperature were known, as well as the mC_p -value for each stream. Finding the minimum values for external utility use, the pinch point and the network design that achieved the targets were part of an assignment in the subject TEP4215, process integration, lectured at NTNU by Truls Grundersen. The answer of the indicated problems were therefore already known. AEA gave the correct targets for both the external heating- and cooling demand. However, the recommended network design achieved from AEA was not close to satisfying the targets and the network was more complex than necessary compared to the solution given in the course. With that in mind, and based on discussions with my supervisors, Aspen Energy Analyzer should just work as a supplementary simulation program, where the calculated targets work as indicators when the heat integration is done manually.

8.3 HYSYS simulations

Aspen HYSYS is a process-modeling tool used to simulate all the analyzed cases in this thesis. HYSYS enables the user to draw and simulate an entire process. The process gets realistic and accurate if losses are taken into consideration. This section goes through how the different process units are implemented in HYSYS, and how HYSYS has dealt with heat- and power integration. For information, this thesis uses HYSYS version 8.3.

8.3.1 Unit implementation base case

Simplifications to some of the process equipment is necessary, as designing would be demanding in HYSYS. Besides, implementation of some of the more complex units goes beyond the scope for this work. This section discuss the HYSYS implementation of the different process equipment in the base case.

Pre-reformer

The pre-reformer is implemented as an equilibrium reactor, where the set of chemical reactions, shown in Section 4.3.3, except the partial oxidation equilibrium, are assigned. An equilibrium reactor let the assigned chemical equilibriums react.

Main reformer

A Gibbs reactor works as the main reformer in this case. According to Aspentech (Aspentech, 2004), the Gibbs reactor calculates the composition of the stream leaving the reformer such that it is in phase- and chemical equilibrium by using the fact that the Gibbs free energy of the reacting system is at minimum at equilibrium.

Water-gas-shift reactors

Both HT – and LT- WGS reactors are simulated as equilibrium reactors in HYSYS, where only the shift reaction is assigned to the reactors.

Carbon – capturing unit

The CO₂-removing unit chosen in this work is a conventional amine process. Separating CO₂ occurs in a component splitter in HYSYS in order to simplify the process. It is assumed that the CO₂-capturing plant can capture 95% of the CO₂ content in the gas. In addition, the amine process will absorb small parts of other components, mainly H₂O but also very small amounts of CO, H₂ and N₂. Table 8.7 summarizes the assumed split ratio for the CO₂-capturing unit.

Table 8.7: Split-ratio pre-combustion CO₂ capture

	"clean gas"	CO ₂ gas
Hydrocarbons	1	0
H ₂ O	0.0340	0.9660
CO	0.9955	0.0045
H ₂	0.9955	0.0045
CO ₂	0.0494	0.9506
N ₂	0.9968	0.0032
O ₂	1	0
H ₂ S	1	0
M-Merceptan	1	0
SO ₂	1	0
Ar	1	0
NO	1	0
NO ₂	1	0

Even though implementation of the carbon-capturing unit occurs as a component splitter in HYSYS, the required heat and work for the separation must be taken into account when considering the total heat and power demands for the process. The separation process requires heat to the reboilers, in form of LP steam, and power to supply the pumps. In cooperation with the supervisors, the decided values for specific reboiler duty and specific energy consumption are as given in Table A.1, in Appendix B.

PSA

Like the carbon-capturing unit, the purification unit is also implemented as a component splitter, due to the complicated design of a PSA. The PSA splits the stream according to the specifications given in Table A.1 in Appendix B. The hydrogen leaving the PSA has the correct temperature and pressure for direct input to the liquefaction unit, respectively 30°C and 20 bar.

Liquefaction unit

Liquefying hydrogen is a complicated process, and exceeds the scope of this work. Consequently, implementation of this process only occurs as a power demand according to the specifications given in Table A.1 in Appendix B. The current state-of-the-art technology for this process has a specific power demand of around 12 kWh/kgH₂(liq). However, it is stated by IDEALHY, (Berstad et al., 2013c), that future liquefaction units for hydrogen can diminish down to around 6.4 kWh/kgH₂(liq), which is assumed to be achievable in this thesis.

Gas turbine

The PSA off-gas is sent to the gas turbine where it is mixed with compressed air and feeds the combustion chamber, implemented as a Gibbs reactor in HYSYS. Figure 8.3 shows how the gas turbine looks in HYSYS.

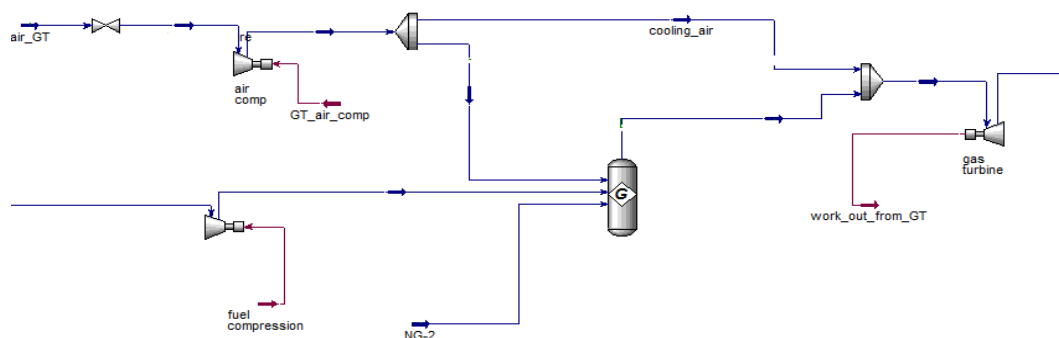


Figure 8.3: Gas turbine in HYSYS

Extra natural gas supplies the combustion chamber in cases where the PSA off-gas do not satisfy the requirements for power production through the gas turbine. In the membrane cases, the retentate gas feeds the gas turbine. The design of the gas turbine is done according to the specifications provided in Table A.1, in Appendix B.

Steam Cycle and HRSG

Excess heat from the process, as well as heat from the exhaust gas, generates steam through process heat exchangers. It is important to obey the ΔT_{\min} -rule and consider metal dusting before exchanging heat. This is further described in the next section. A picture of the steam cycle designed in HYSYS is attached in Appendix G.

ASU

Implementation of the ASU is done in the same manner as implementation of the liquefaction unit. The actual process is not implemented, as it exceeds the scope of this work, but the work required for separation and compression up to the desired level are taken into account. The values are as stated in Table A.1 in Appendix B.

8.3.2 HYSYS heat integration base case

Heat integration of the base case process is done partly with help from Aspen Energy Analyzer and partly by hand. By plotting all streams into AEA, with the correct enthalpy change in the stream and the supply- and target temperature, the program calculates the corresponding mC_p -value and the targets for the system. The program allows for implementation of forbidden matches, which is the case for some of the streams in this process. The targets generated from AEA are used as a measure of how good the heat integration done by hand is, as the program did not give the desired design for the HEN.

When calculating the change in enthalpy for the different streams, it is assumed that the enthalpy follows a straight line, like illustrated in Figure 8.4. This is however not the case for all streams, especially for the streams with phase change. If the h-curve for a stream is very bended, it should be divided into segments for minimizing the errors. Therefore, when implementing HP-, MP- and LP-steam generation to AEA, the streams were divided into three segments. The first segment is the economizer, where BFW is heated. The second segment is the boiling, and the third segment is the superheating. The other streams, however, was assumed to follow the straight line. This can cause some errors in the calculations done by AEA.

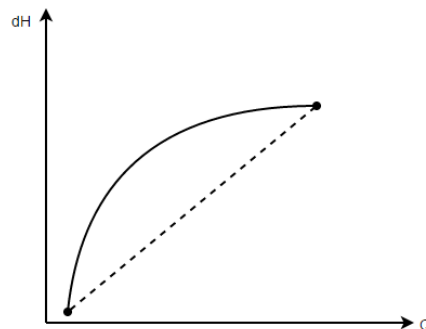


Figure 8.4: Simplifications done to the h-curve

Metal dusting and forbidden matches

An important phenomenon to have in mind when designing a HEN is metal dusting. Metal dusting is a kind of corrosion and can destroy heat exchangers. To develop metal dusting, carbon monoxide must be present and the metal temperature in the heat exchangers must be in the range of typically 450-800°C (Martelli et al., 2012). The literature does not completely agree on the exact temperature range for metal dusting. Some articles claim that metal dusting can appear between 400-800°C (Chun and Ramanarayanan, 2009), while others claim that it can appear between 400-650°C (Grabke, 2003). However, the range of 450-800°C is applied during heat integration of the current case study.

Metal dusting complicates the heat integration as it puts restrictions on what streams that can exchange heat. The hot gas leaving the ATR has a temperature of 950°C before it is cooled down to 350°C and enters the WGS-stage. This gas contains considerably amounts of CO, which makes this stage critical for metal

dusting inside the heat exchangers. To avoid a metal temperature in the range of 450-800°C, it is crucial to cool this gas with a cold medium, like cooling water. The heat available in this stage can for instance not be used for superheating of steam, which would give a metal temperature in the risky area. This gives the process so called forbidden matches.

Cold streams that need to be heated up to a temperature above 450°C cannot exchange heat with the ATR stream as it introduces risk of metal dusting in the heat exchangers. This applies to two streams, respectively preheating of natural gas before it enters the pre-reformer and preheating of O₂ before it enters the ATR, which are both heated to 500°C. However, to utilize the heat as good as possible, these streams are divided into two segments, as Figure 8.5 depicts. This way the ATR stream can be used for heating up the first part of the streams while the final heating from 450°C to 500°C must occur through heat exchange with other heat sources in the plant.

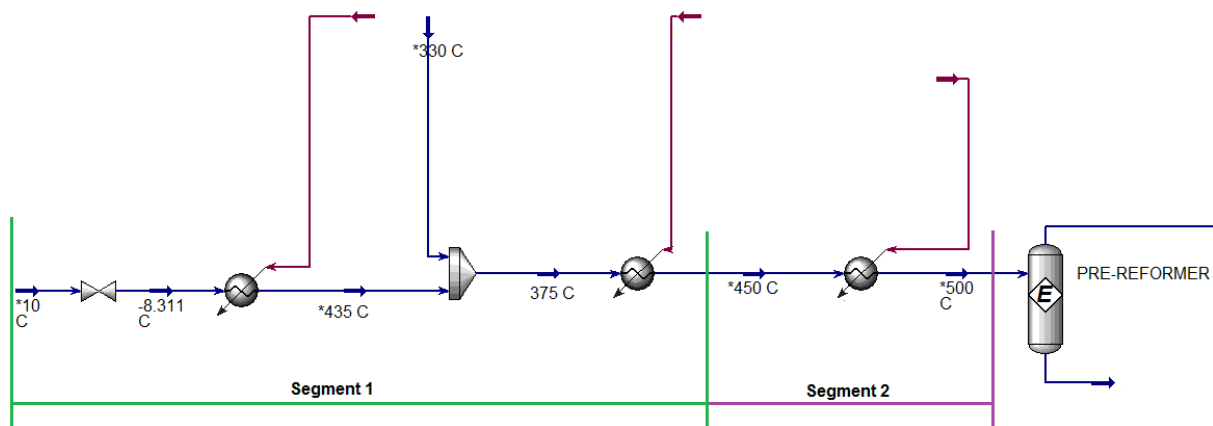


Figure 8.5: Preheating of NG before entering of pre-reformer

Similar for the preheating of O₂. Heat from the ATR can be used to preheat the O₂ up to 450°C, but heating from 450°C to 500°C must be covered by other heat sources where CO is not present. This is a simplification done in this theses. If the hot gas from the ATR is used to heat up natural gas and oxygen to 450°C, the metal temperature will exceed 450°C and the process is in danger of develop metal dusting. It is, however, assumed that this heat exchange is all right. The resulting heat integrated networks are presented in the Chapter 9.

8.3.3 Unit implementation membrane cases

Most of the units used in the membrane cases are similar to the ones used in the base case, and is implemented in the same manner. However, this case introduces the use of membranes and a low temperature CO₂ capture process.

Membrane

Membranes are initially implemented as component splitters, as the actual design is rather complicated. The basics of a membrane is to split the stream, where the permeate contains pure hydrogen. This can be obtained by using a simple component splitter in HYSYS.

One of the drawback about using a component splitter for membrane implementation is the fact that the membrane design is not affecting the results. How well the membrane separation occur depends on several membrane elements, like its thickness, length and area. This is, however, not taken into consideration when the membrane appears as a component splitter. For example, the developed membrane cases analyze two different feed pressures for the membrane, accordingly 36 bar and 66 bar. In HYSYS, the component splitter will not behave any different once the feed pressure increases. In reality, this pressure-increase affects the design and performance of a membrane. The effect of changing the pressure and other parameters concerning the membrane will be further analyzed through a membrane model borrowed from SINTEF Material & Chemistry. This study is further discussed in Chapter 10.

Low-temperature carbon capturing unit

Designing the low temperature carbon-capturing unit goes beyond the scope of this work, and is therefore simplified when implemented in HYSYS. A typical design of a LT-process for CO₂ capture were given in Figure 5.13. Figure 8.6, on the other hand, shows the process implementation in HYSYS for this purpose.

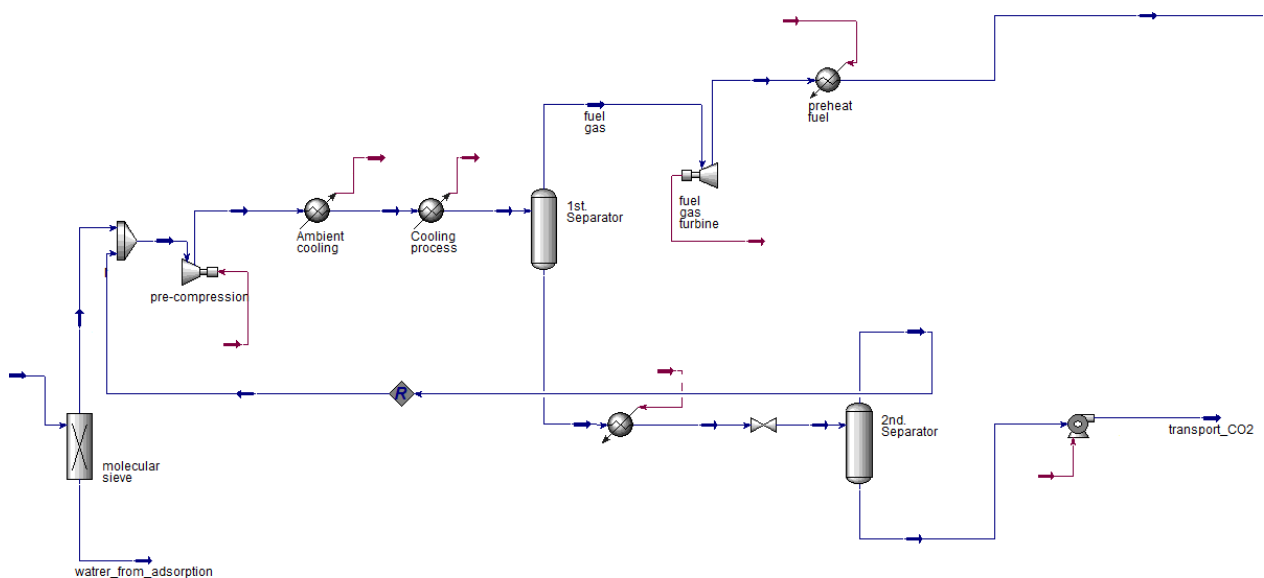


Figure 8.6: LT-process in HYSYS

Instead of designing the cooling process, which uses ethane and propane as mediums, the cooling appears in a single heat exchanger that cools the gas down to the desired separation temperature, accordingly -55°C in this case. The HYSYS model do not use any of the internal heat exchangers as Figure 5.13 illustrated.

The liquid from the first separator is in reality heated through an internal heat exchanger, but is implemented as a single heater in HYSYS. The temperature increases to about - 43°C, before it is throttled down to around 8.5 bar and enters the second phase separator. The temperature of the second separator should be approximately - 55°C as well. The CO₂ – capturing rate is calculated by dividing the amount of CO₂ leaving the process as liquid, with the amount of incoming CO₂.

The LT-process requires work in order to cover the demands for pre-compression, the compressors in the cooling circuit and pumps. Due to the simplifications done to the process in HYSYS, the total work demand cannot be calculated from the simulations. Figure 5.12, indicates that the specific work required in the LT-separation unit depends on the CO₂-concentration of the entering gas. In the current case study, the CO₂-concentration of the gas entering the LT-separation process is generally higher than the provided concentrations in Figure 5.12. To be able to estimate the required work for this unit, David Berstad at SINTEF, which was one of the writers behind the relevant figure (Berstad et al., 2013b), conducted some simulations with the relevant gas composition and inlet pressures for this thesis. SINTEF has developed a HYSYS model for the LT-process described. The results can be found in Appendix F. Interpolation between the values were used in order to find the correct value for the specific work required in each case. HYSYS calculates the CCR in the LT-separation process through a spreadsheet, and the relevant CO₂-concentration can be found in HYSYS. Once these values are known, the table can provide the correct specific work. However, there will be small errors due to rounding adjustment etc. Nevertheless, interpolation in a table gives more correct values than reading from a figure. The specification given in Table A.1 in Appendix B is therefore the specification David Berstad used in the simulations of the LT-process. As observed from Table A.1, the initial pressures used for the simulation are respectively 35 bar and 65 bar. This is why the feed pressure for the membranes are respectively 36 bar and 66 bar, since the pressure drop through the membrane is assumed to be 1 bar.

9. Analysis and resulting heat-integrated process

This chapter provides an analysis of the resulting heat- and power integrated processes. The chapter is divided into three, where the first part considers the base case. Part two and three, consider the membrane cases, respectively for 36 bar and 66 bar membrane inlet pressure. Four main membrane cases are developed, and all are analyzed under each section. The heat-integration is conducted by hand, with some inspiration from AEA. Examples of recommended network provided by AEA is attached in Appendix H. All relevant stream data from the HYSYS simulations are attached in Appendix E.

9.1 Heat – and power integrated base case

The resulting heat integrated process for the base case is sketched in Figure 9.1. Figure 9.1 uses colors to illustrate which streams that exchange heat. In addition, it indicates the different streams considered when designing the heat exchanger network, noted with numbers. As discussed in the previous chapter, the hydrogen producing plant contains some forbidden matches due to the metal dusting issues. Pre-heating of natural gas in front of the pre-reformer and pre-heating of oxygen, both from 450-500°C cannot exchange heat with the heat available after the main reformer. Table 9.1 summarizes the forbidden matches. The stream numbers are taken from Figure 9.1.

Table 9.1: Forbidden matches, referring to Figure 9.1

Stream	Forbidden match
8-9	3-4
8-9	6-7

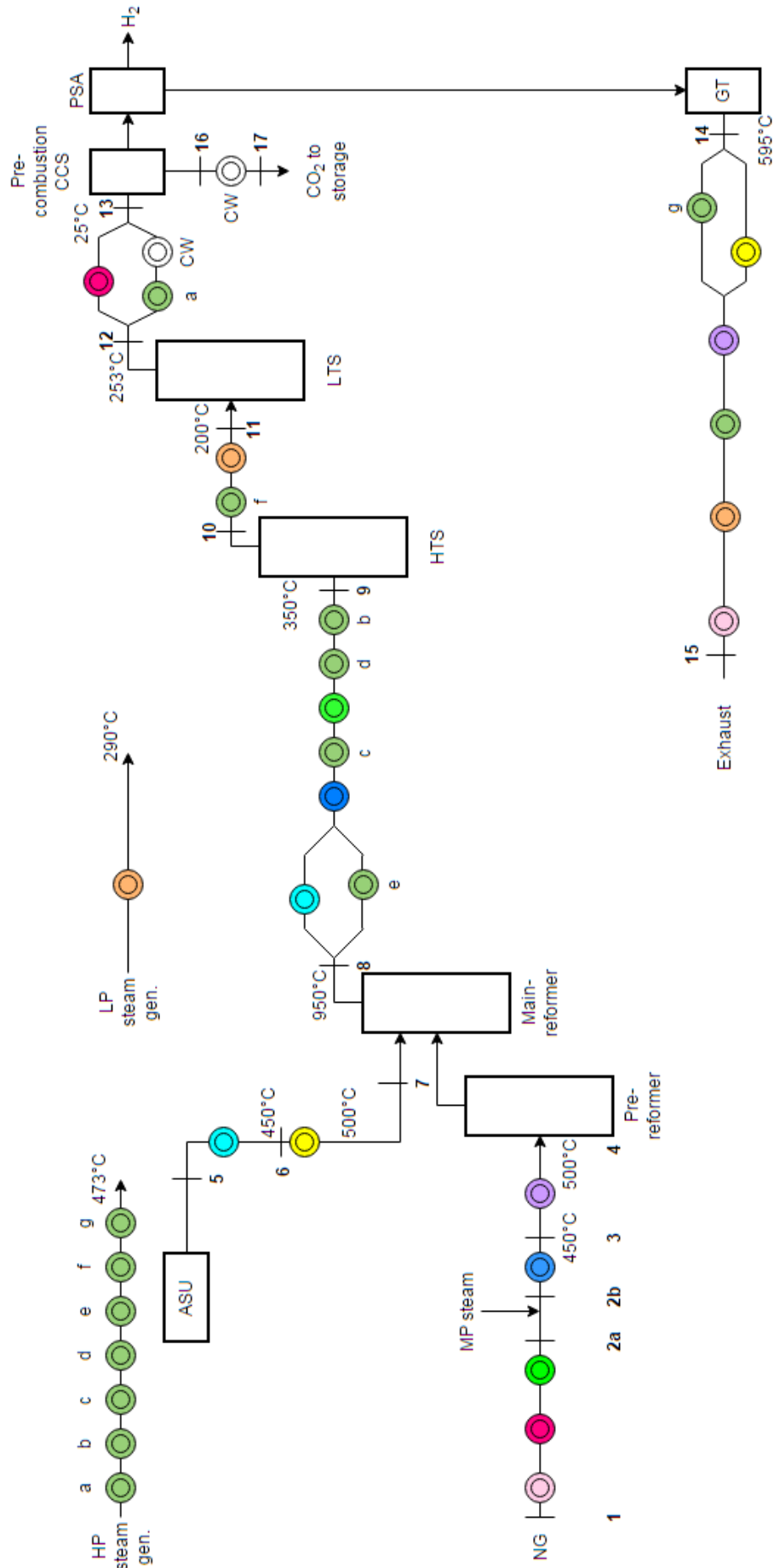


Figure 9.1: Color-coded heat-integrated conventional ATR process

The corresponding heat exchanger networks becomes as depicted in Figure 9.2. The grey heat exchangers illustrate the process-to-process heat exchangers, while the green ones represent HP-steam generation and the orange represent LP-steam generation. The blue heat exchangers indicate the use of cooling water. Stream numbers are taken from Figure 9.1.

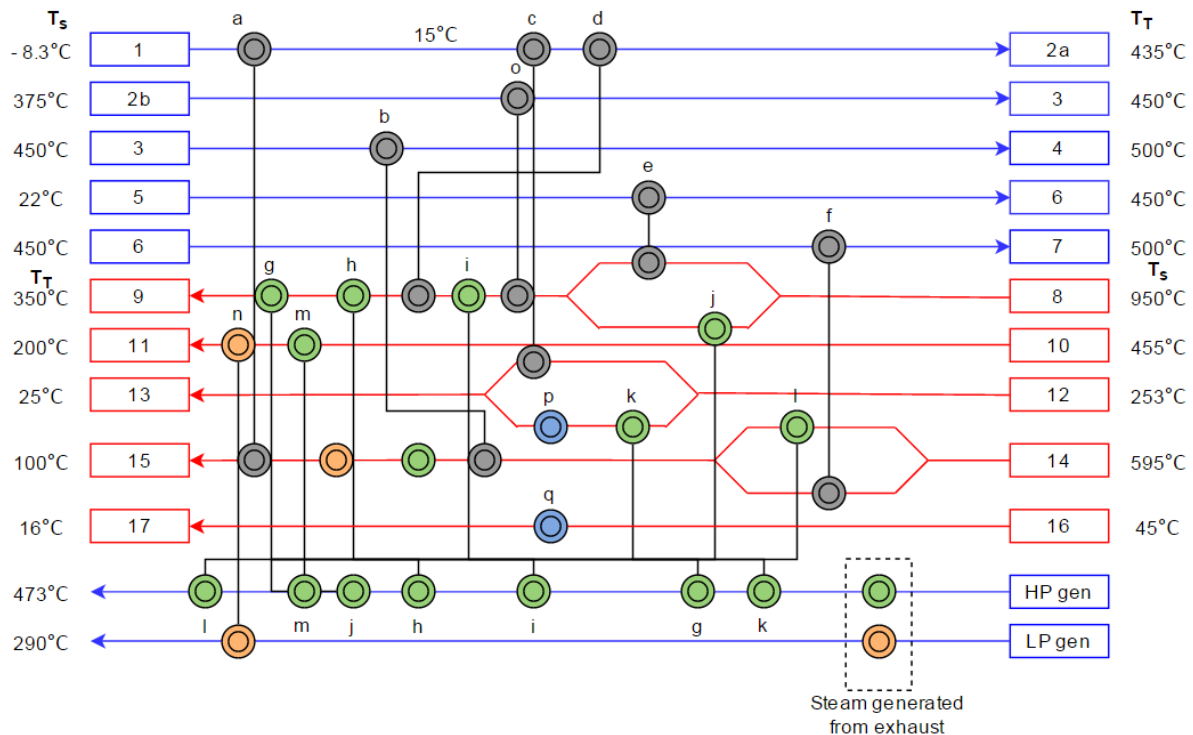


Figure 9.2: HEN for base case with H₂ liquefaction

It has to be mentioned that steam generation is simplified in these drawings, like for LP steam generation. This does not occur through one single heat exchanger, but at least through three different exchangers due to the reason described in Chapter 4. However, for simplicity, these drawings illustrate that the heat available in for example stream 10-11 is sufficient for generation of superheated LP steam. The quantity of produced steam depends on the amount of available heat, which is decided by an adjuster in HYSYS.

Cooling and compression of the captured CO₂ occurs through four steps. The heat taken away from this stream could potentially be utilized to partly generate LP steam. It would, however, not be high enough temperatures to superheat LP steam. Utilization of this heat would not provide considerable benefits, and it is therefore decided that cooling water is used in this stage. The CO₂ liquefaction is stream 16-17 in Figure 9.2.

HP steam generation occurs through excess process heat and through the HRSG. As observed from Figure 9.1, the HP steam generated from the process heat must be superheated by the exhaust gas. This is due to the forbidden matches in this process. The temperature out from the ATR is sufficiently high for superheating HP steam, but due to metal dusting issues, this exchange is not allowed. The same applies for preheating of natural gas and oxygen, from 450 to 500°C, before it enters the reformer.

In addition to the HP- and LP steam generated from the process heat, this case also generates HP – and LP steam through the HRSG. HP steam is expanded through a turbine down to MP-level, where the required amount of MP steam to the process is extracted. The remaining steam is expanded down to LP-level, where some of the steam goes to the pre-combustion carbon-capturing unit before it returns and mixes with the

remaining steam and gets pressurized and heated again. Appendix G gives a picture of the HYSYS steam cycle for the base case. Figure 9.3 shows how the HRSRG looks like in HYSYS.

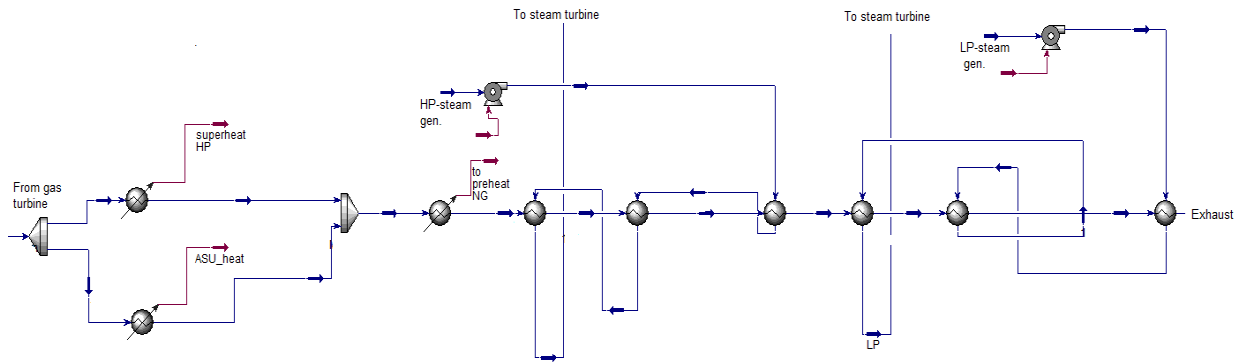


Figure 9.3: HRSRG, case with H₂ liquefaction

Results

Table 9.2 provides the AEA energy targets compared with the achieved targets in HYSYS. As observed, not much differ the two results, meaning that the given heat-integrated process is rather close to the optimum. The value from AEA is assumed to be the correct target value, and the deviation between the two values is therefore calculated in percent of the AEA value. A possible reason for the deviation is further described in Chapter 12.

Table 9.2: Energy targets in AEA vs. achieved in HYSYS

	Heating [kW]	Cooling [kW]	Deviation [%]
Aspen Energy Analyzer	0	1.137e+006	3.34
HYSYS	0	1.099e+006	

Power Integration

Figure 9.4 depicts the energy demanding units in the base case, and it illustrates the relative consumption.

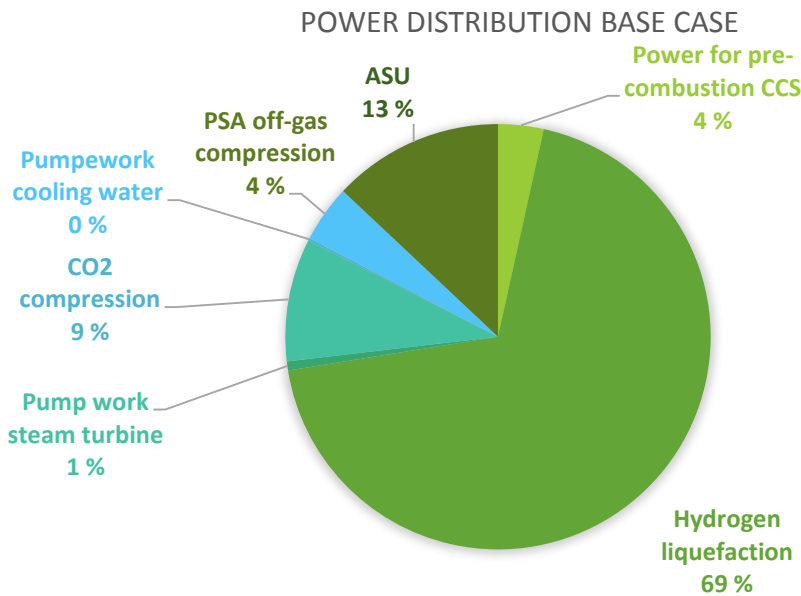


Figure 9.4: Energy consumption base case

Figure 9.4 illustrates the relative energy consumption for all energy demanding units in the plant. However, the compressor in the gas turbine is not included since this unit is supplied by power generated from the gas turbine, as they are connected on the same shaft. As observed from Figure 9.4, hydrogen liquefaction is responsible for the greatest energy consumption in this case. Due to the large energy demand for hydrogen liquefaction, the gas turbine requires additional fuel supply to be able to produce the required amount of power. Meaning, the PSA off-gas do not provide the gas turbine with the sufficient amount of fuel. To resolve this problem, additional natural gas was fed into the combustion chamber in the gas turbine. The amount of required extra NG supply was decided by balancing the energy production from the gas turbine and steam turbines with the total energy demand. To ensure complete combustion in the gas turbine, the compressor needs to suck in huge amounts of air. The exact values for the energy consumption for the various units, alongside with the energy output from the gas turbine and steam turbines are found in Appendix D. Table 9.3 gives the amount of extra NG supply needed for achieving a power balanced process.

Another possibility to provide the gas turbine with the required fuel supply would be to adjust the hydrogen yield in the PSA. In the current work, this value is decided to be 85%. By lowering this value, the PSA off-gas will contain a bigger amount of hydrogen, and thus provide the gas turbine with a more energy rich fuel. There would, however, been produced less hydrogen. This case is not considered.

In order to study the impact of the liquefaction unit, there was developed a case without it. In this case, the PSA off-gas gives adequate fuel supply to the gas turbine. Meaning, there is no need for external NG supply to accomplish a power-balanced process. The actual values are given in Appendix D. However, the heat available in the exhaust gas is larger in the case with hydrogen liquefaction due to the extra NG supply. In the case not considering the liquefaction unit, the heat available in the exhaust gas is not sufficient to cover both superheating of HP steam generated from the process excess heat and preheating of natural gas and oxygen. This means, in the case without liquefaction, the excess heat from the process can only be used to generate superheated MP steam. This reduces the power output from the steam cycle. Nevertheless, this case has excess power, which can be seen from Appendix D, and in Table 9.3.

Table 9.3: Overview results, heat-integration base case

	H ₂ -prod [kg/s] - power balanced process	Additional NG supply to complete power balance[kg/s]	Energy deficit / surplus when no NG supply [MW]
Base Case with H ₂ liq.	11.72	5.14 (11.4% increase in NG supply)	-133.7
Base Case without H ₂ liq.	11.72	0	+ 124.6

9.2 Heat – and power integrated membrane cases with 36 bar inlet pressure

This section focuses on all membrane cases considered with 36 bar inlet membrane pressure, and concentrates on giving the resulting heat-integrated process scheme and the results of the analyzed power integration. Each case is studied with two different approaches. The first approach is to adjust the HRF-value such that the process produces the same amount of hydrogen as the base case. The second approach is to adjust the HRF-value such that the process reaches a power-balanced plant without any surplus or deficit in power, meaning, no excess power or no need for extra NG supply to the gas turbine.

In the membrane cases, except for case II-3, there are a lot of excess heat available when the compressed hydrogen from the membrane needs to be cooled down to 30°C before liquefaction. Instead of preheat the incoming natural gas and oxygen, from 450-500°C, with exhaust gas, as done in the base case, the membrane cases open up for utilizing the heat available after hydrogen compression for this purpose. This is more appropriate since the location of the streams are closer to each other in practice, and the exhaust gas can unaffected be used for steam generation.

All membrane cases share the same forbidden matches as the base case due to the risk of metal dusting.

9.2.1 Case II-1 heat- and power integration

Heat integration of Case II-1 is, as the base case, done manually with inspiration from Aspen Energy Analyzer.

Figure 9.5 gives the resulting heat integrated process scheme. The colors indicate which streams that exchange heat. Again, it must be clarified that this is a simplified scheme when it comes to steam generation. This figure just indicates that heat is taken from the process and is used to generate steam.

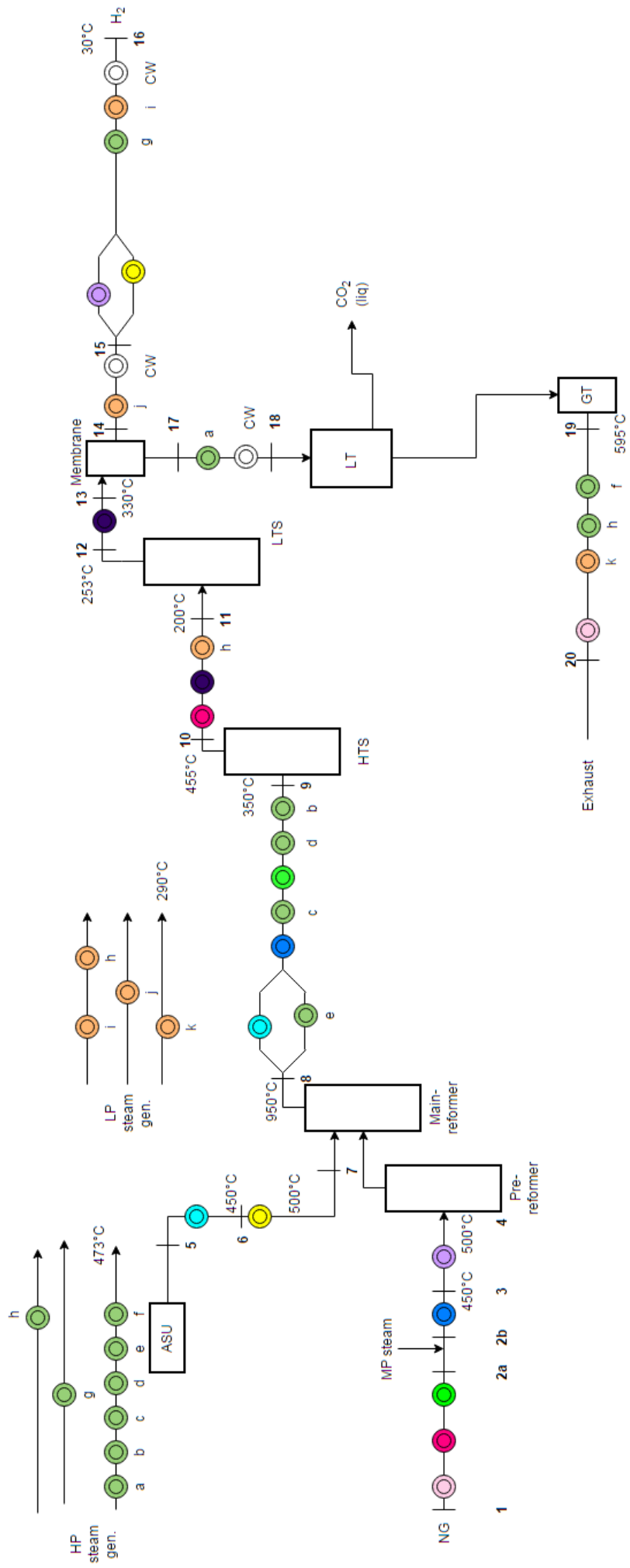


Figure 9.5: Color-coded heat integrated ATR process with a single membrane module

The corresponding heat exchanger network becomes as depicted in Figure 9.6. Stream numbers are taken from Figure 9.5.

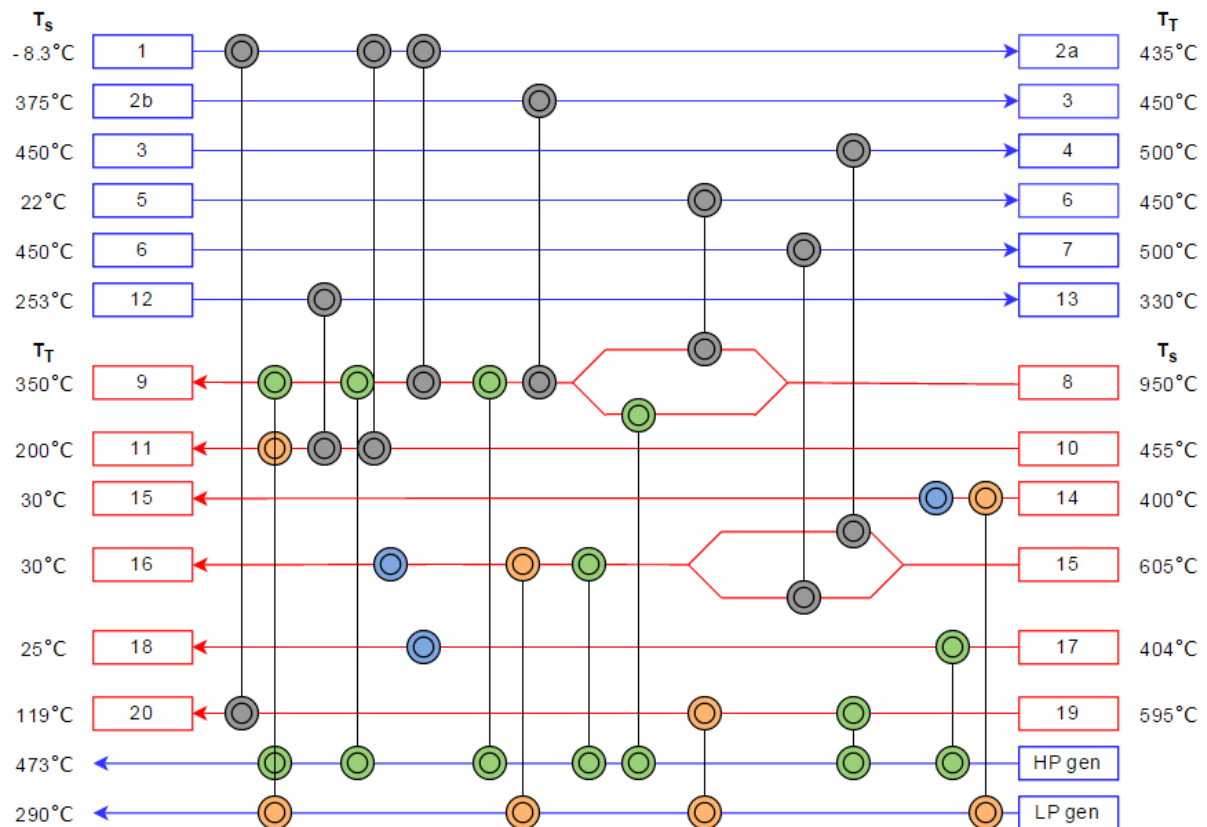


Figure 9.6: HEN, case II-1

Case II-1 generates steam at several locations in the process. Heat available between the reformer stage and the membrane stage covers the heat requirements for the process, except heating of natural gas and oxygen from 450-500°C due to forbidden matches, and generates HP steam up to 444°C. Superheating of this HP steam occurs in the HRSG. Process heat between the ATR and the membrane also partly raise LP steam. The heat removed after the membrane and in front of the hydrogen compression (stream 14-15), generates LP steam. Heat available after compression of the hydrogen is used to cover the natural gas and oxygen needs between 450-500°C, raise HP steam and partly generate LP steam (stream 15-16). In addition, the HRSG ensures generation of HP- and LP-steam.

Cooling water is used when the preferred gas temperature gets below 40°C, like before the hydrogen compression and the final hydrogen product. The BFW temperature is more or less 30°C for the different cases, meaning there would not be enough driving forces if this were used to cool the gas down to 30°C, which is required in the mentioned places.

Results

Table 9.4 provides the target values from AEA and the targets obtained in HYSYS after heat integration. As for the base case, the deviation is calculated as a percentage between the two values where the AEA-value is assumed to be the correct value. The process implemented in AEA, and the HYSYS process used for comparison is the case considering equal amount of hydrogen as base case. A possible reason for the deviation is further described in Chapter 12.

Table 9.4: Results heat-integration case II-1

	Heating [kW]	Cooling [kW]	Deviation [%]
Aspen Energy Analyzer	0	1.265e+006	4.42
HYSYS	0	1.209e+006	

Power Integration

The HRF-value of the membrane is adjusted such that the amount of produced hydrogen equals the amount in the base case. Even though this case produces more steam than the base case, the total power output do not cover the total demand. To achieve a power-balanced process the gas turbine requires extra supply of fuel, in form of natural gas. The exact value is given in Table 9.5.

Figure 9.7 shows the distribution of the power demanding units in this scenario. The total energy demand in this case is greater than in the base case, due to the power requirements for hydrogen compression and compression of the syngas in front of the membrane. Appendix D provides all values.

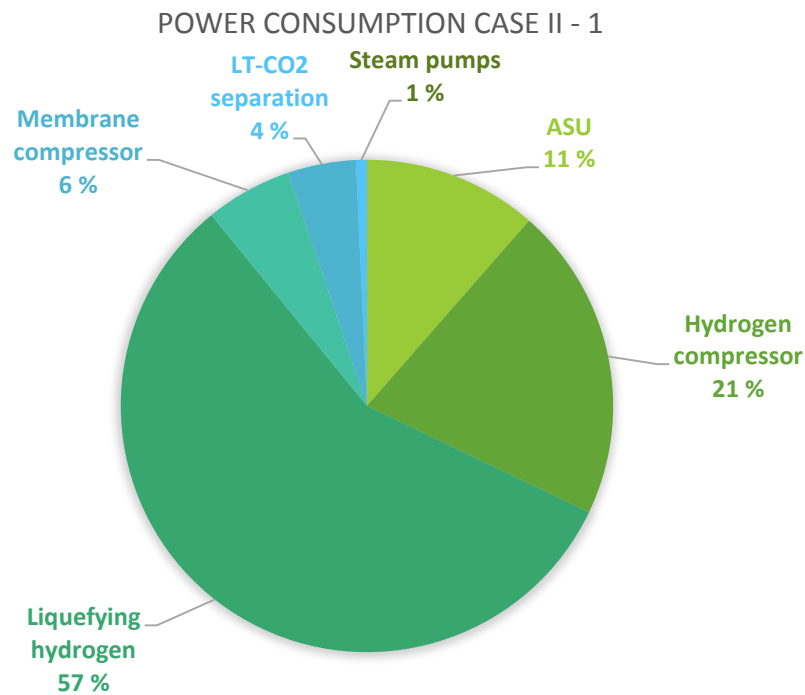


Figure 9.7: Power distribution case II-1

This case was also considered without any additional supply of natural gas. To achieve a power-balanced process without extra fuel supply, the HRF-value in the membrane was adjusted, such that the retentate from the membrane contained a bigger hydrogen share, and therefore provided the gas turbine with a more energy rich fuel. However, as illustrated in Table 9.5, this sacrifices the amount of produced hydrogen.

Table 9.5: Overview results, case II-1, 36 bar

	HRF	Hydrogen production [kg/s]	Amount of external NG supply when equal H ₂ production as base case	Possible excess power [MW]
Case II-1	0.8461	11.72	5.57 (12.38% increase in total NG supply)	-----
Case II-1 (no additional NG)	0.7405	10.26	0	-----
Case II-1 without H ₂ liquifaction	0.8461	11.72	0	130.2

9.2.2 Case II -2 heat- and power integration

The heat integration of this case is very much similar to the heat integration of case II-1. However, this case contains two membrane modules, which complicates the heat integration a bit. Both membranes need a feed temperature of 400°C. The temperature out from the HT-WGS reactor is around 450°C, which roughly corresponds to the desired membrane temperature. However, the gas is cooled down to 400°C before the first membrane module. The retentate temperature after the first membrane is still 400°C, which means that the gas needs to be cooled before it enters the LT-WGS stage. When the gas leaves the LT-WGS, the temperature is around 250°C. The gas must therefore be heated again to obtain a temperature of 400°C before it enters the second membrane. The corresponding heat integrated process becomes as illustrated in Figure 9.8.

The pressure of the gas entering the LT-separation process is defined to be 35 bar, as described in Chapter 8. Because the pressure drop across the membrane is assumed to be 1 bar for the feed gas, this case needs to compress the gas to a higher level to ensure that the pressure is 35 bar when it enters the LT-process because this case consists of two membranes. With that in mind, the compressor in front of the first membrane compresses the gas up to 39 bar. After the first membrane, the pressure is 38 bar. Some pressure drop will accrue in front of the second membrane, ensuring a pressure of 36 when the gas enters. Even though the inlet pressure of the first membrane is 39 bar, this case is, as the other membrane cases, considered as a 36 bar case, for simplicity.

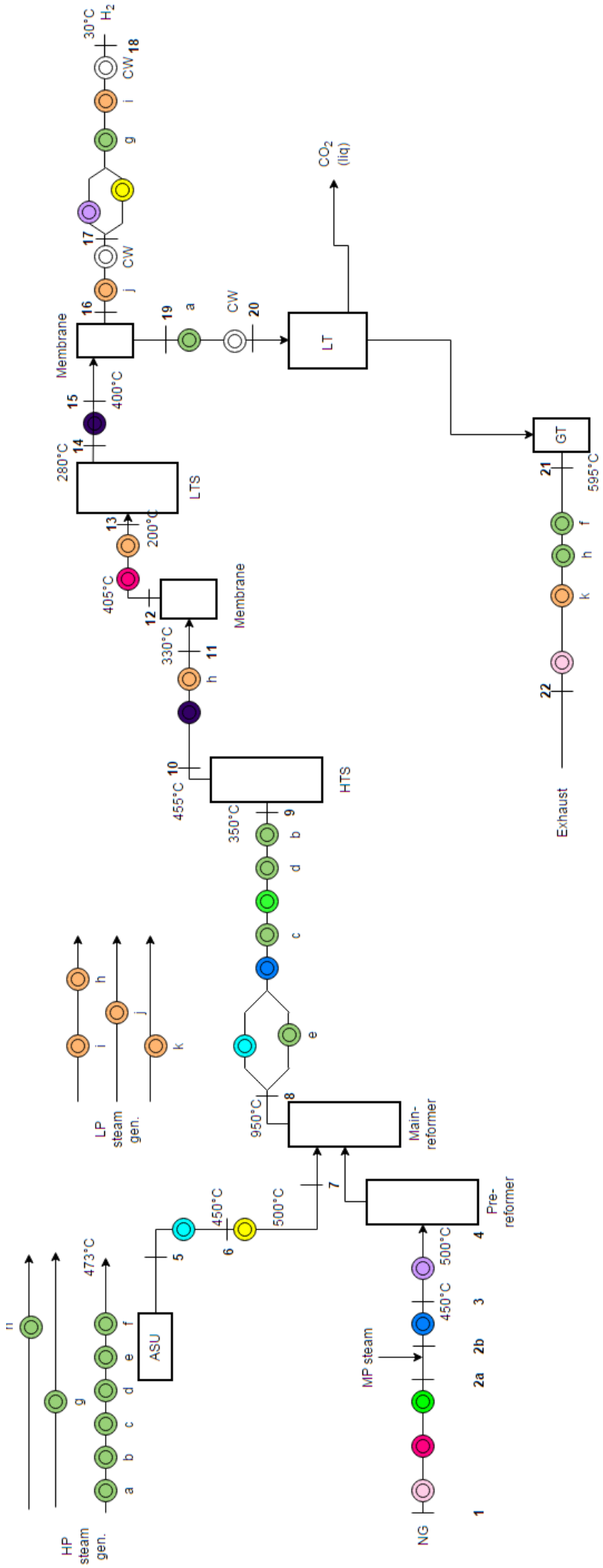


Figure 9.8: Heat-integrated case II-2

The heat exchanger network for this case becomes as illustrated in Figure 9.9.

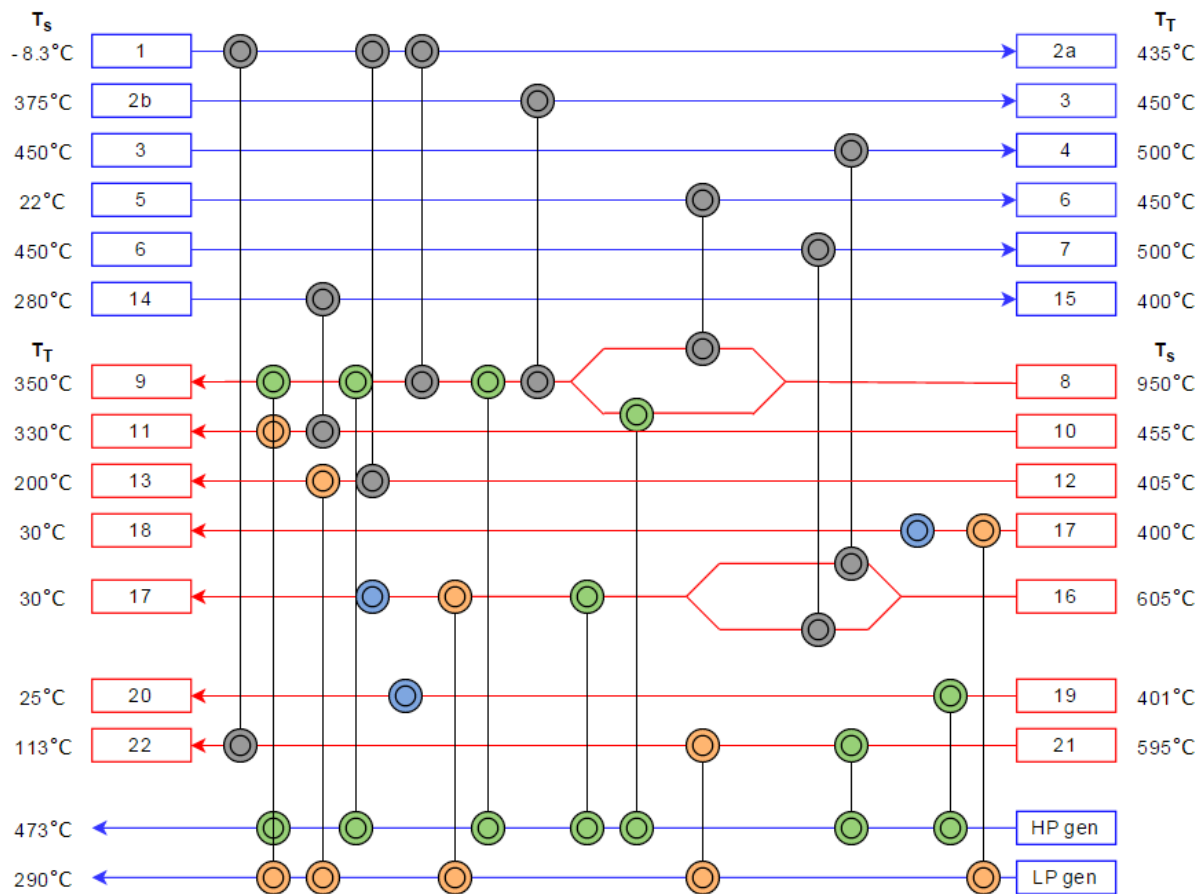


Figure 9.9: HEN, case II-2

The membrane in front of the LT-WGS remove parts of the produced hydrogen. How much depends on the HRF-value, which is decided to be 0.7 in this case. This shifts the shift reaction in the LT-WGS unit towards the product and causes a higher hydrogen conversion rate in this case than the other cases. Respectively, the hydrogen conversion rate for the whole WGS stage in this case is 96.68% compared to 94.46% for the other cases. This result in a potentially reduction in the cooling requirements in front of the LT-WGS and consequently a reduced heating demand after the LT-WGS, to obtain the same hydrogen conversion rate as the other cases. This was investigated in order to see if it had any advantageous effects. It was first tested to remove the cooling in front of the LT-WGS. This was however not a god idea since it gave a poorer hydrogen conversion than the other cases. Consequently, it was tested to adjust the inlet temperature of the LT-WGS to obtain the same hydrogen conversion rate as the other cases. This reduced the required cooling upstream and heating downstream the LT-WGS. However, it resulted in less steam production in total, since the heat taken away before the LT-WGS is of greater amount than the heat supply after the LT-WGS. It is therefore decided that this process cools the gas down to 200°C in front of the LT-WGS. Another argument for doing so is that the HRF value in the second membrane can be reduced in order to obtain the same amount of produced hydrogen as the other cases. This gives a more energy rich fuel supply to the gas turbine, since more hydrogen is produced.

Power Integration

This case deviates from the other cases since the gas turbine manage to produce the required amount of power without any additional supply of natural gas. The HRF-values in the membranes are adjusted such that the hydrogen production equals the base case. The required amount of power in this case is in fact slightly larger than in the case with one membrane module. This is primarily due to the larger power demand in the membrane compressor since it has to compress to a higher pressure than in the previous case. Nevertheless, this process has excess power ready for export.

The reason for this is partly the fact that removing some hydrogen before the LT-WGS shifts the equilibrium towards the product, which leads to more produced hydrogen. Then the HRF value can be reduced which means that more hydrogen is sent to the gas turbine. All relevant values for this purpose is found in Appendix D, and Figure 9.10 gives the power distribution.

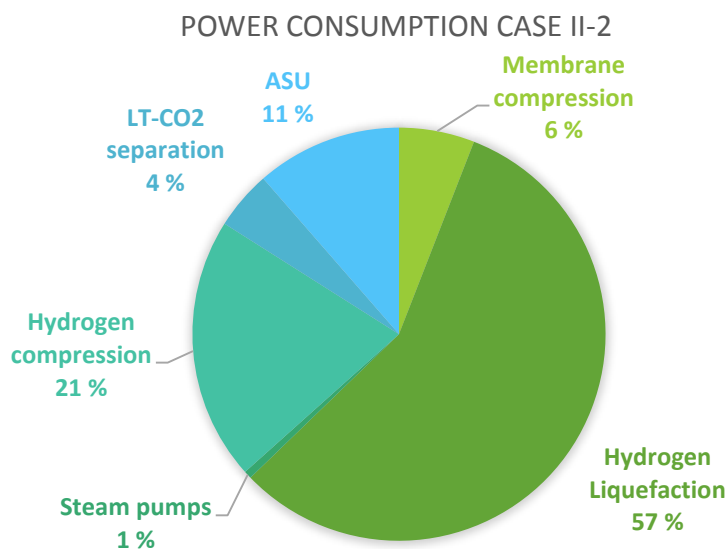


Figure 9.10: Power distribution case II-2

The HRF-value in the membranes can be adjusted to produce more hydrogen in this case since it has excess power. This was done, and the results were an increase of 3.32% in produced hydrogen when the system was in power balance. All results are summarized in Table 9.6.

Table 9.6: Overview results case II-2 with 36 bar

	HRF	H ₂ production [kg/s] (increase [%])	Power deficit / surplus [MW]
Case II-2 with equal amount of produced H ₂	0.7 / 0.5572	11.72	+ 71.53
Case II-2 with power balance	0.7 / 0.6360	12.11 (3.32%)	0

Results

Table 9.7 gives the deviation between the AEA targets and the achieved targets in the HYSYS simulations. These values are calculated from case II-2 with power balance, since this is the most likely process to be built. Excess power from the hydrogen plant should be used to produce more hydrogen, since it after all is a hydrogen producing plant. It has to mentioned, the heat-integrated design of the process is equal for both approaches to case II-2.

Table 9.7 : Result heat-integration case II-2

	Heating [kW]	Cooling [kW]	Deviation [%]
Aspen Energy Analyzer	0	1.025e+006	12.05
HYSYS	0	9.015e+005	

9.2.3 Case II -3 heat- and power integration

The main difference between this case and the other membrane cases is that less heat is available at the permeate side of the membrane due to the lack of compression requirements. This makes it impossible to preheat the incoming natural gas and oxygen from this stage, since the gas temperature leaving the membrane is 400°C. Preheating of these streams must therefore occur through heat exchange with the exhaust gas, as done in the base case. This redesign affects the amount of generated steam. The produced HP- and LP steam from the exhaust gas reduces as exhaust heat must provide preheating of natural gas and oxygen as well. Excess process heat raises HP steam up to 444°C, as the other cases, and is superheated by the exhaust gas. The heat available after the membrane generates LP steam. The heat integration network is provided in Figure 9.12, on the next page. The corresponding HEN is given in Figure 9.11 below.

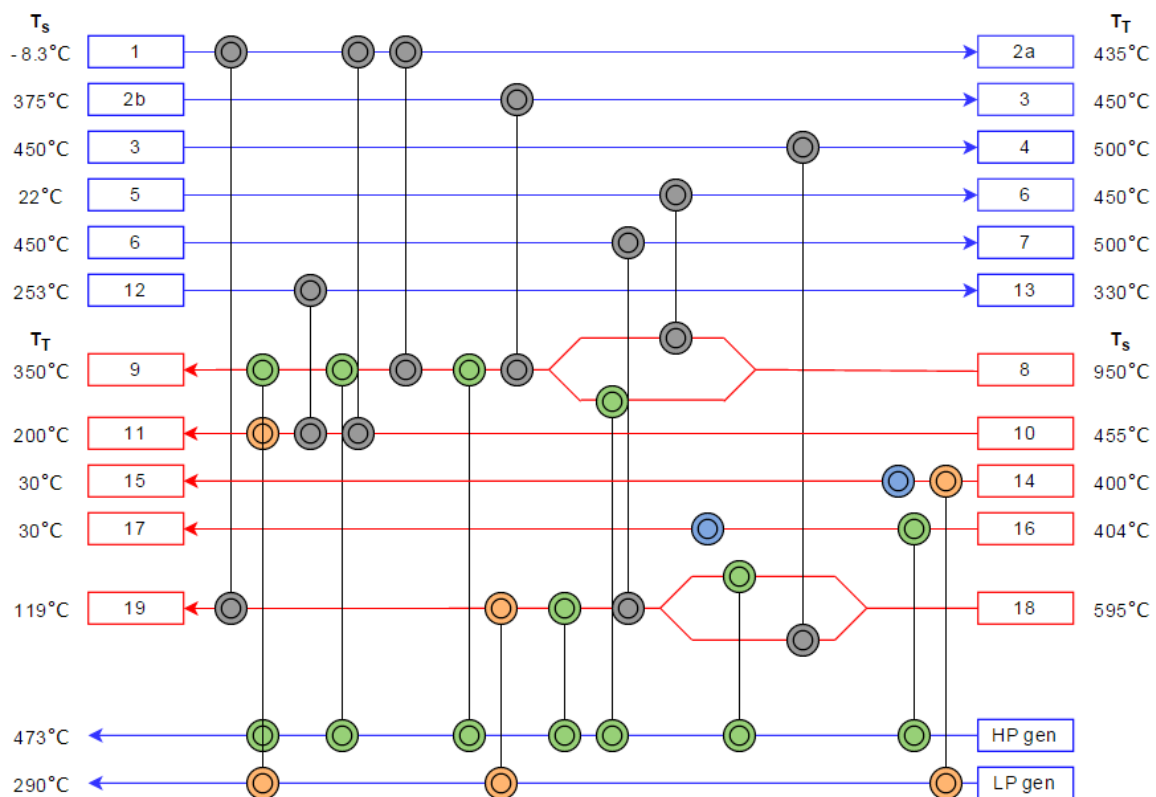


Figure 9.11: HEN case II-3

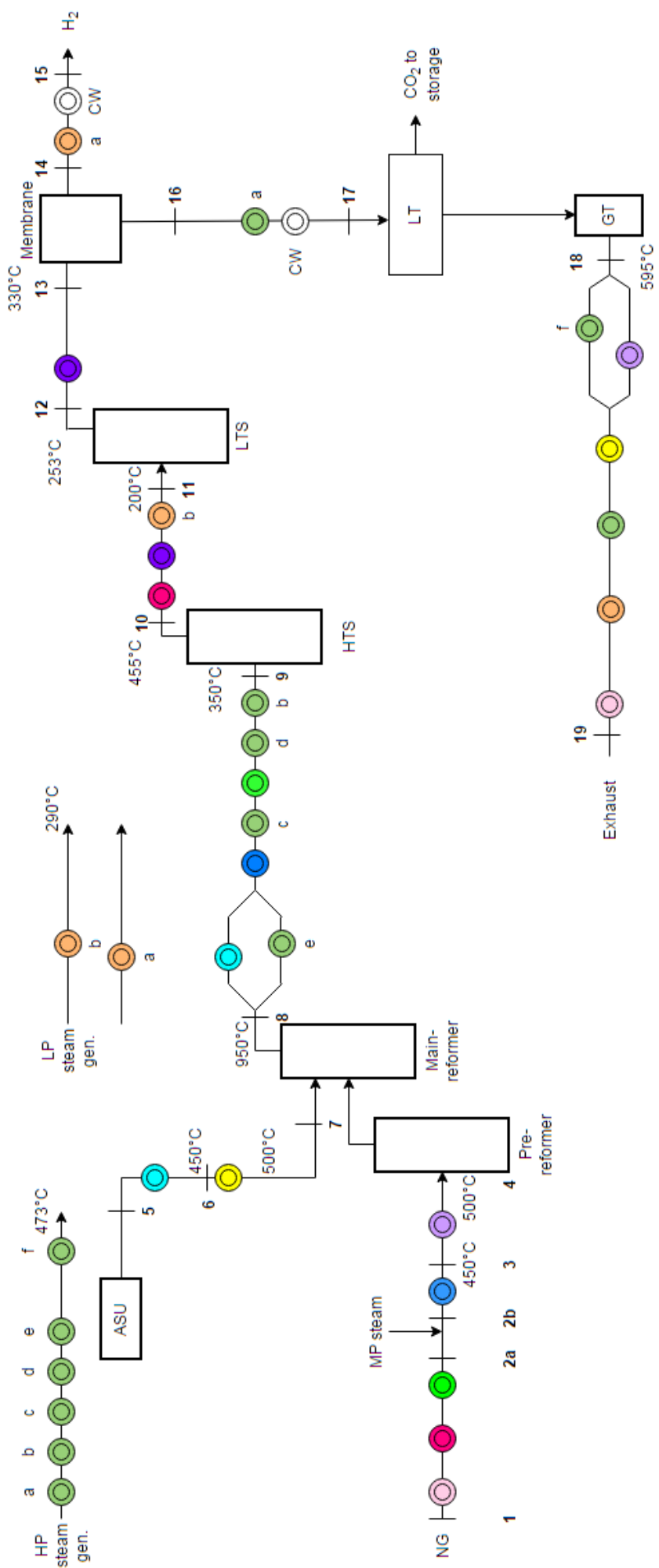


Figure 9.12: Heat-integrated case II-3

Results

Table 9.8 gives the resulting targets, respectively from AEA and HYSYS. As seen, less than 5% deviates the two values. The values are from the case considering equal amount of produced hydrogen as base case.

Table 9.8: Resulting heat-integrated process for case II-3

	Heating [kW]	Cooling [kW]	Deviation [%]
Aspen Energy Analyzer	0	1.005e+006	1.9
HYSYS	0	9.859e+005	

Power Integration

The power distribution changes for this case as the permeate gas not need compression in order to obey the hydrogen liquefaction specifications. The exact values for the power demanding units are found in Appendix D. As indicated in Figure 9.13, the hydrogen liquefaction unit stands for a bigger share in this diagram than in the others cases. However, that does not mean that it consumes more power. In fact, this case needs less additional natural gas supply to the gas turbine in order to meet the requirements. Compared to case II-1, which produces the same amount of hydrogen as the base case, the required NG supply to the gas turbine decreases from 5.57kg/s to 3.014kg/s, which represent a reduction of 45.9%. This is because the total power consumption decreases in this case.

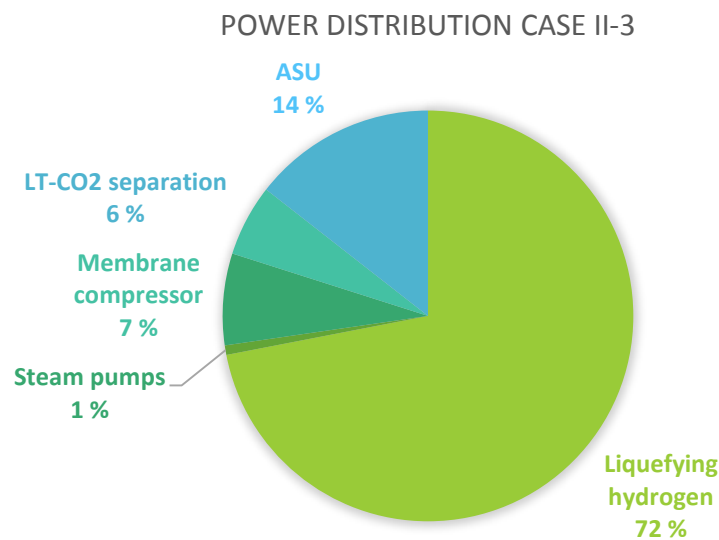


Figure 9.13: Power distribution case II-3

In addition to the case evaluating the process when it produces the same amount of hydrogen as base case, a case with no additional NG supply were developed to see how it impact the amount of produced hydrogen. The results becomes as given in Table 9.9.

Table 9.9: Results case II-3, 36 bar inlet pressure

	HRF	H ₂ production [kg/s] (reduction[%])	Extra NG supply [kg/s]
Case II-3	0.8461	11.72	3.014
Case II-3 : No extra NG	0.7855	10.88 (7.17%)	0

9.2.4 Case II-4 heat- and power integration

Case II-4 deviates from the other cases since this case considers carbon capture in front of the membrane module. As for the other cases, this case is also analyzed with two different feed pressures to the membrane. However, changing the inlet pressure do not affect the design for the heat-integrated process. Figure 9.15 depicts the heat-integrated process.

Cooling of the gas occurs in front of the CO₂-capturing unit in order to separate out liquid water. The heat taken away for this purpose is used to heat up BFW for steam production and to partly preheat the entering natural gas. Due to the cooling upstream the CO₂-capturing unit, the gas must be heated before it enters the membrane. Even though the temperature increases as the gas undergoes compression, the temperature increase is not sufficient to achieve the desired membrane temperature. This applies to both cases considering different membrane inlet pressure.

The corresponding HEN, achieved from Figure 9.15, is as illustrated in Figure 9.14.

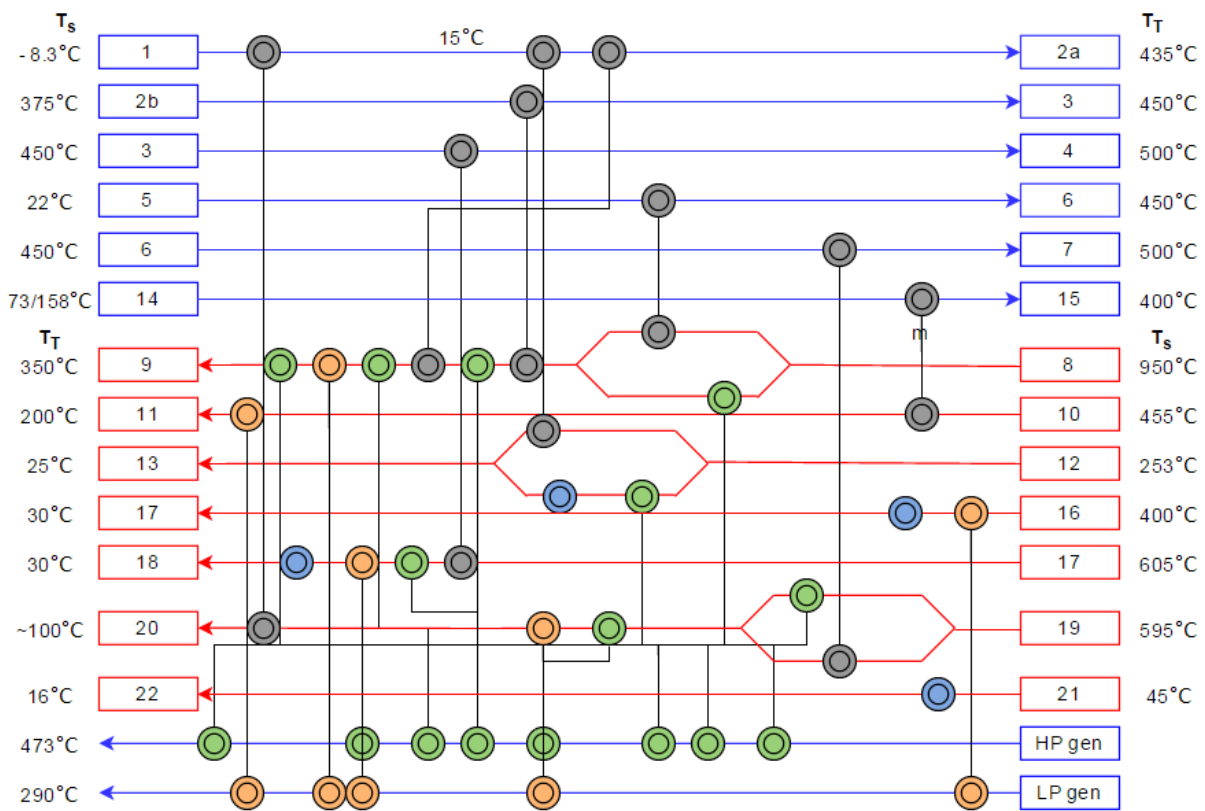


Figure 9.14: HEN case II-4

Results

The deviation between the given heat integrated process and the targets in AEA is provided in Table 9.10. The deviation is below 6%, meaning that the given HEN is rather close to the optimal design. The values are from the case considering equal amount of produced hydrogen as base case.

Table 9.10: Result heat-integration case II-4

	Heating [kW]	Cooling [kW]	Deviation [%]
Aspen Energy Analyzer	0	1.288e+006	5.36
HYSYS	0	1.219e+006	

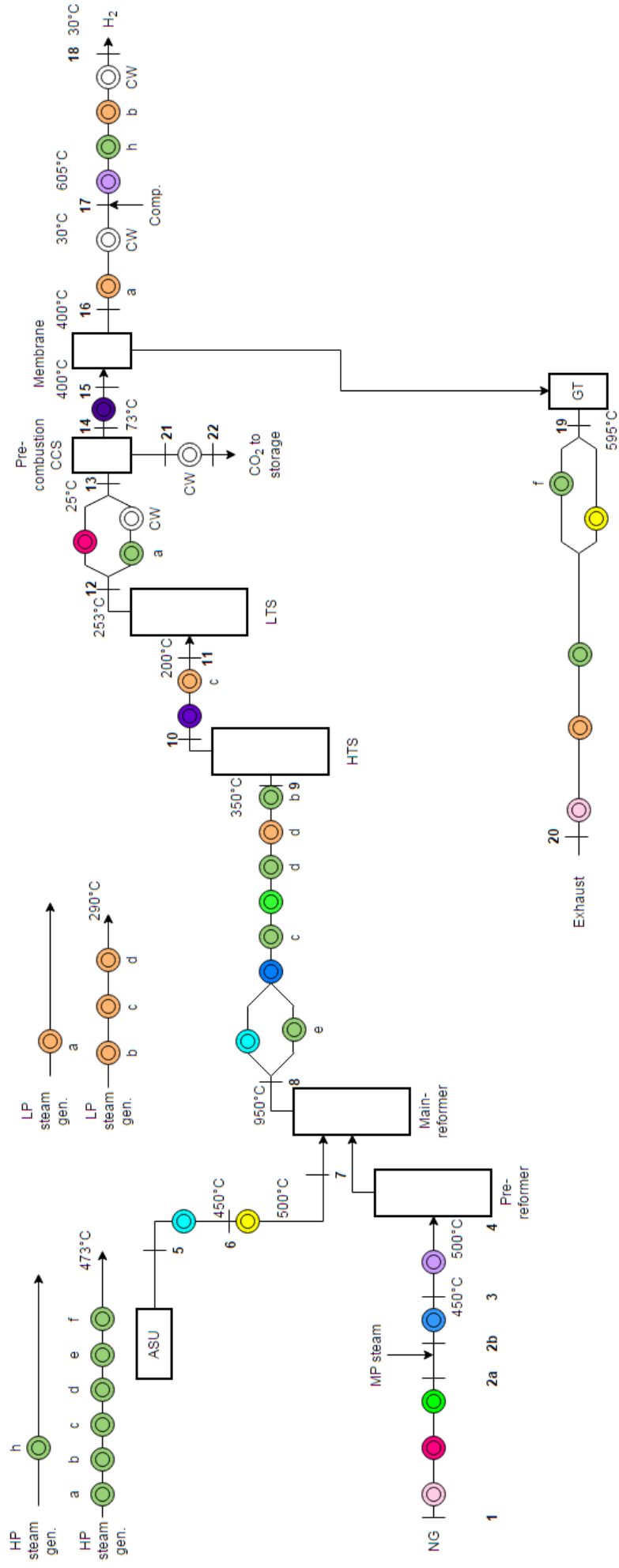


Figure 9.15: Overview of heat-integrated case II-4

Power Integration

The power distribution of this case is as depicted in Figure 9.16. The actual values are found in Appendix D. This case contains different units than the other membrane cases, making the power distribution a bit different.

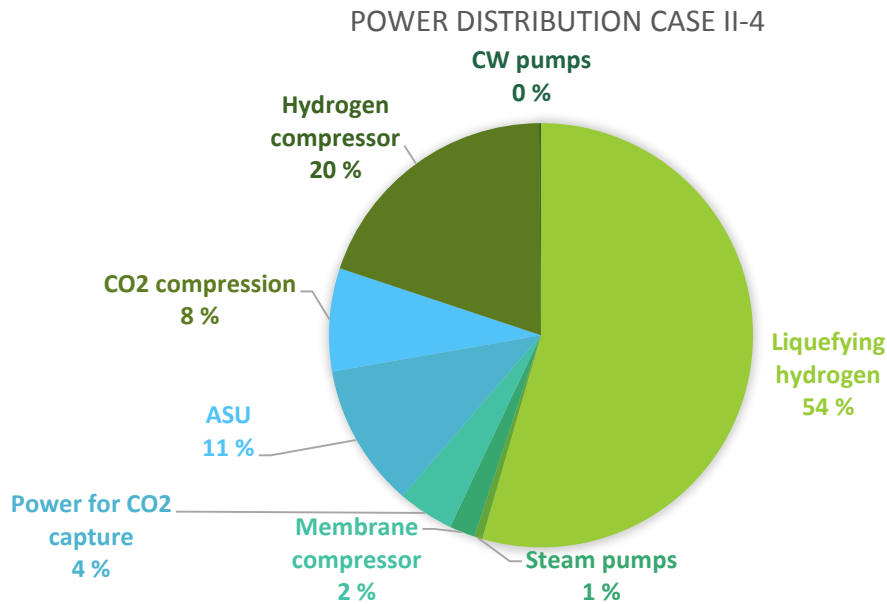


Figure 9.16: Power distribution case II-4

To be able to satisfy a power balancing process when the amount of produced hydrogen equals the base case, this case needs, as the other single membrane cases, additional NG supply to the gas turbine. The amount is given in Table 9.11. However, this case is also considered without any extra NG supply. This affects the amount of produced hydrogen since the HRF-value must be adjusted to cover the needs for energy rich fuel to the gas turbine. The results are provided in Table 9.11.

Table 9.11: Results case II-4, 36 bar inlet pressure

	HRF	H ₂ production [kg/s] (reduction [%])	Extra NG supply [kg/s]
Case II-4 with equal amount of produced H ₂	0.85	11.72	6.76
Case II-4 with no extra NG supply	0.7198	9.93 (15.3%)	0

9.3 Heat and power-integrated membrane cases with 66 bar inlet pressure

An increased pressure level in front of the membrane results in a higher power demand for the cases considering 66 bar membrane inlet pressure. However, increasing the pressure also reduces the power demand for the LT-separation of CO₂. As for the cases with 36 bar inlet pressure, the main cases with 66 bar also produce the same amount of hydrogen as the base case. However, there will also be of interest to look at cases where the HRF-value is adjusted such that the process is in power balance when no additional natural gas is supplied to the gas turbine.

The membrane cases considering 66 bar membrane feed pressure do not deviate largely from the 36 bar inlet pressure-cases when it comes to the heat-integrated process design. This means that the deviation between the targets found in AEA and the achieved targets in the HYSYS simulation will not differ significantly. It is therefore decided to not spend any more time on implementing all cases into AEA, as it is rather time consuming.

9.3.1 Case II-1 heat- and power integration

The compression in front of the membrane ensures high enough inlet temperature to the membrane without any additional heating after the LT-WGS. In fact, the inlet membrane temperature becomes 425°C instead of the specified 400°C. This is however assumed to be all right, since it is in the range of appropriate operating membrane temperatures, which was discussed in Chapter 5. This leads to a small increase of LP steam production between the HT- and LT-WGS reactors.

The HRF-value is equal to the case with 36 bar inlet pressure since the increased pressure do not affect the separation in the component splitter in HYSYS. In reality however, the increased pressure would affect the performance of the membrane. This is further studied in Chapter 11.

The resulting heat-integrated process is shown in Figure 9.17. As can be observed, not much deviates this case from the case with 36 bar inlet pressure, except for the removed heating unit between the HT- and LT WGS.

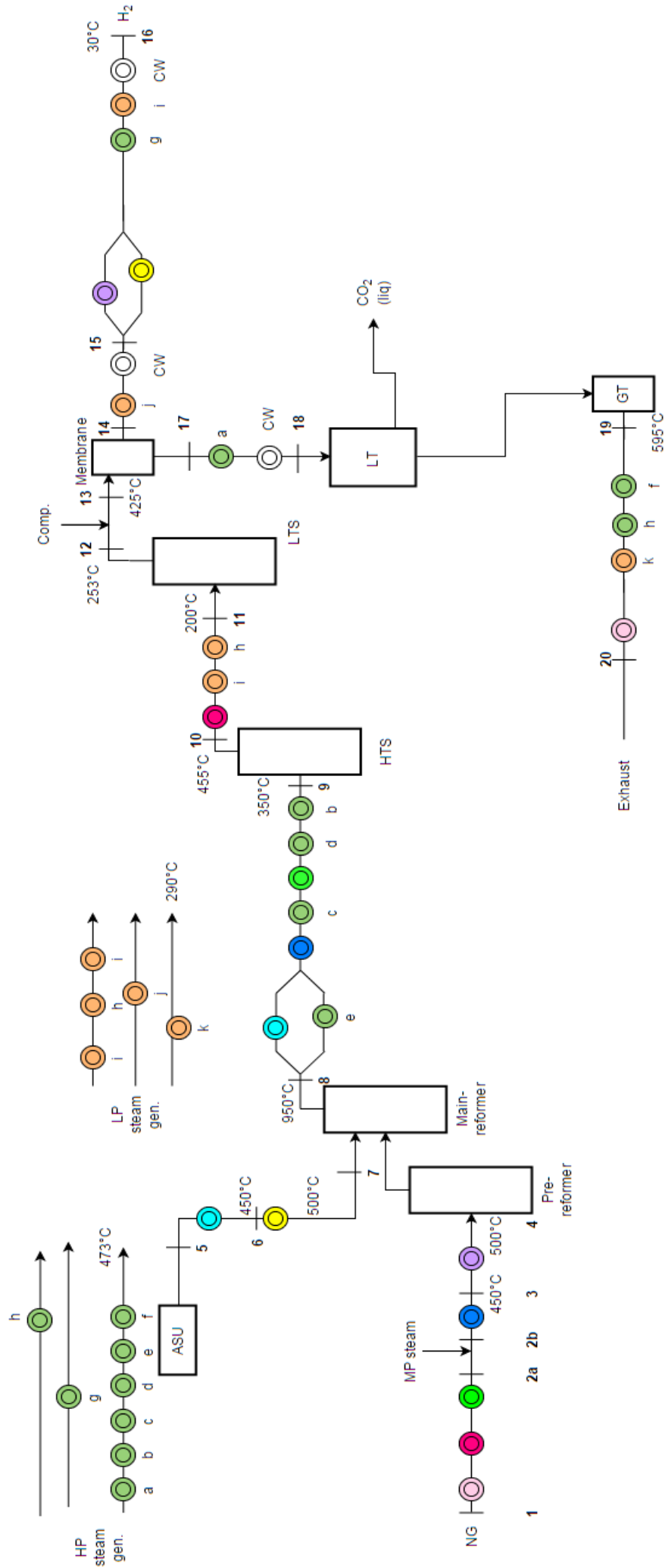


Figure 9.17: Overview of heat integrated case II-1

Corresponding heat-integrated network for this case becomes as depicted in Figure 9.18.

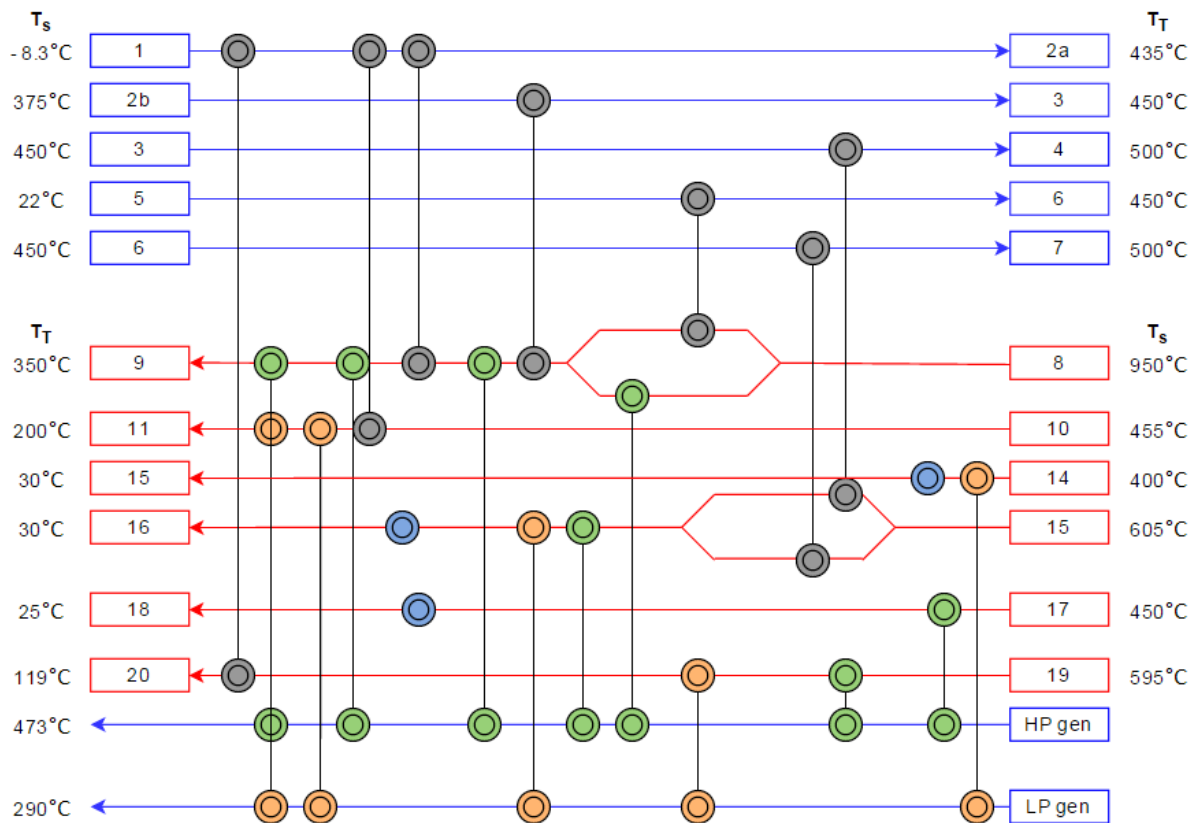


Figure 9.18: HEN case II-1, 66 bar

Power Integration

Due to the increased power requirement for the compressor in front of the membrane, this case needs slightly more natural gas supply to the gas turbine to complete the power balance. The values are given in Table 9.12. As Figure 9.19 depicts, the power distribution in this case is quite similar to the distribution for case II-1 that considers 36 bar inlet pressure to the membrane. However, the membrane compressor now requires 13% of the total power consumption compared to 6% in the previous case.

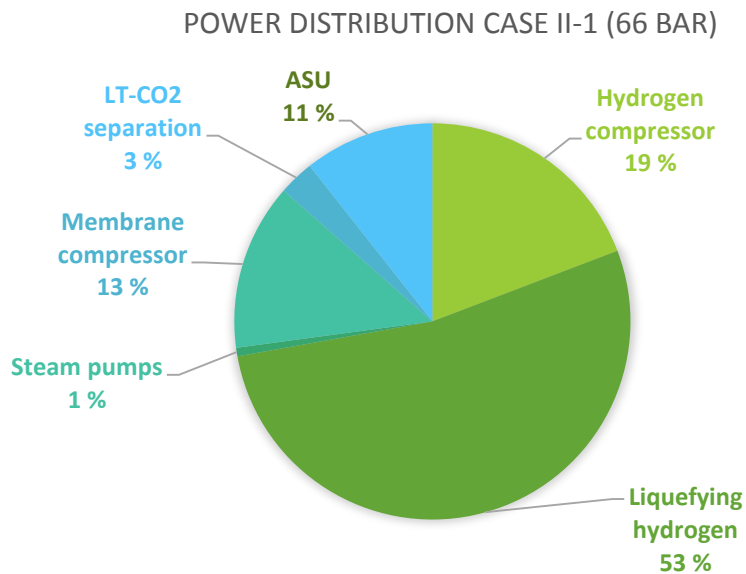


Figure 9.19: Power distribution among the energy demanding units case II-1 and 66 bar inlet pressure

As for the case with 36 bar membrane inlet pressure, a case considering no additional NG supply to the gas turbine is developed for this case as well. The process suffer from power deficit if no additional natural gas supplies the gas turbine. This can, however, be resolved by adjusting the HRF-value in the membrane, such that more hydrogen leaves the membrane along with the retentate gas, and therefore provides the gas turbine with the required amount of energy rich fuel. As in the case with 36 bar inlet pressure, this affects the amount of produced hydrogen. Table 9.12 provides the results for this case.

Table 9.12: Results heat- and power integration case II-1 for 66 bar inlet pressure

	HRF	Hydrogen production [kg/s]	Amount of external NG supply when equal H ₂ production as B.C.
Case II-1	0.8461	11.72	6.58 (14.62% increase in total NG supply)
Case II-1 (no additional NG)	0.7231	10.02	0

9.3.2 Case II-2 heat- and power integration

The main deviation from this case and case II-2 with 36 bar inlet pressure is that this case has less excess power. The amount of available power for export, when the hydrogen production equals the base case, decreases from 71.53 MW to 37.06 MW. However, the process still produces more power than consumed even though the requirements have increased.

The design of the heat integration of this case do not change compared to the case with 36 bar. However, to obtain a membrane temperature of 400°C, the gas must undergo further cooling before the membrane compressor compared to the case with 36 bar. This is because the temperature of the gas increases as the pressure increases, resulting in a higher gas temperature after compression to 69 bar compared to 39 bar. More heat is then available for LP steam generation. The inlet pressure of the first membrane module is 69 bar, due to the same reason as described for the 36 bar-case.

As for the case with 36 bar membrane inlet pressure, this case also considers the power-balanced process. As predicted, this case produces less hydrogen compared to the power-balanced case with 36 bar. The reason is the increased power consumption due to the membrane compressor. Since more hydrogen needs to supply the gas turbine in order to accomplish a power-integrated process, the HRF-value in the membranes are reduced. This decreases the hydrogen production rate. The values are found in Table 9.13.

Table 9.13: Results heat- and power integration case II-2 for 66 bar inlet pressure

	HRF	Hydrogen production [kg/s]	Power deficit / surplus [MW]
Case II-2	0.7 / 0.5472	11.72	+37.06
Case II-2 (no additional NG)	0.7 / 0.5850	11.91	0

9.3.3 Case II-3 heat- and power integration

Heat integration of this process becomes similar to the one having 36 bar inlet pressure, except for the heater upstream the membrane compressor. As for case II-1 considering 66 bar inlet pressure, this unit is removed in order to obtain a sufficient membrane temperature when the gas is compressed.

Increasing the membrane inlet pressure also increases the required amount of NG supply to the gas turbine due to the growing energy demand. The external NG requirement becomes 4.0 kg/s for this case, compared to 6.58 for case II-1 at 66 bar, representing a reduction of 39.2%. Table 9.14 provides the results. To obtain a self-sustained process without any needs for supplementary NG to the gas turbine, the HRF-value in the membrane reduces to provide the gas turbine with more energy rich fuel. The results for this case are given in Table 9.14.

Table 9.14: Results heat- and power integration case II-3 for 66 bar inlet pressure

	HRF	H ₂ production [kg/s] (reduction [%])	Extra NG supply [kg/s]
Case II-3 with equal amount of produced H ₂	0.8461	11.72	4.0
Case II-3 with no extra NG supply	0.7666	10.62 (9.39%)	0

9.3.4 Case II-4 heat- and power integration

A membrane inlet pressure of 66 bar do not change the design of the heat-integrated process for this case. The only difference is that preheating of the gas in front of the membrane requires less heat, meaning that there are more heat available for steam production in the process.

In terms of power integration, the case with 66 bar inlet pressure requires more extra NG supply in order to accomplish the power balance when the process is designed to produce the same amount of hydrogen as the base case. This case is also considered without any additional NG supply. The results are given in Table 9.15.

Table 9.15: Results heat- and power integration case II-4 for 66 bar inlet pressure

	HRF	H ₂ production [kg/s] (reduction [%])	Extra NG supply [kg/s]
Case II-4 with equal amount of produced H ₂	0.85	11.72	7.31
Case II-4 with no extra NG supply	0.71	9.79 (16.47%)	0

9.4 Overview of results

This chapter provides an overview of the given results throughout the chapter. Table 9.16 summarizes the interesting values for all studied cases.

Table 9.16: Overall results of heat-and power integrated processes

	HRF		H ₂ production [kg/S]		Extra NG supply [kg/s]		Energy deficit/surplus whit no extra NG [MW]		Steam production [kg/s]						Specific work for LT unit [kJ/kg]	
	36bar	66bar	36bar	66bar	36bar	66bar	36bar	66bar	HP		MP		LP		36bar	66bar
									36b	66b	36b	66b	36b	66b		
Base case	----	----	11.72	----	5.14	----	- 133.7	----	166	----	0	----	77	----	----	----
Case II-1	0.8461	0.8461	11.72	11.72	5.57	6.58	- 39.53	- 46.58	188	194	0	0	84	100	208.5	144.3
Case II-1 : no additional NG	0.7405	0.7231	10.26	10.02	0	0	0	0	180	185	0	0	75	89	227.6	139.7
Case II-2 with equal amount of produced H ₂	0.7 / 0.5572	0.7 / 0.5472	11.72	11.72	0	0	+ 71.53	+37.06	162	161	0	0	72	87	221.4	144
Case II-2 with power balance	0.7 / 0.6360	0.7 / 0.5850	12.11	11.91	0	0	0	0	161	158	0	0	66	85	202.5	143
Case II-3	0.8461	0.8461	11.72	11.72	3.014	4.0	-76.88	-98.71	154	167	0	0	67	82	208.5	144.3
Case II-3 : no additional NG	0.7855	0.7666	10.88	10.62	0	0	0	0	152	159	0	0	62	76	215.3	148.2
Case II-4	0.85	0.85	11.72	11.72	6.76	7.31	-176.6	-191.3	189	192	0	0	91.25	99	----	----
Case II-4 : no additional NG	0.7198	0.71	9.93	9.79	0	0	0	0	174	178	0	0	83	87	----	----

Figure 9.20 gives the graphical overview of the results obtained in this chapter. As predicted, the power balanced case II-2 produces most hydrogen, while case II-4 with no extra NG supply produces the smallest amount.

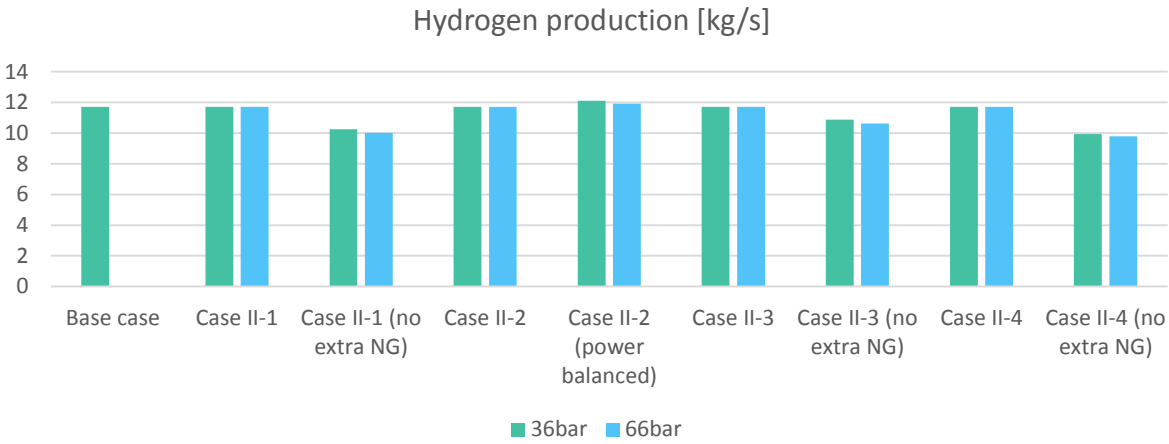


Figure 9.20: Overview hydrogen production

Figure 9.21 outlines the distribution of additional NG supply for the respective cases. Due to the large energy requirements in case II-1 and case II-4, these cases requires most additional fuel supply in order to achieve the desired amount of produced hydrogen.

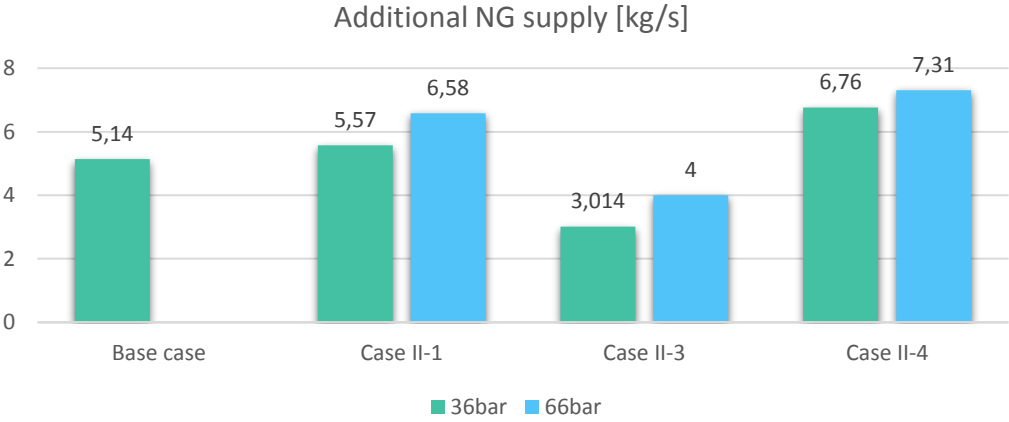


Figure 9.21: Overview additional NG supply

10. Results

This chapter comprises two result sections, of where the first section covers the results from the HYSYS simulations of the studied cases, and the second part provides results from the membrane parametric study. A parametric study was carried out in order to investigate the membranes behavior according to changes in operating conditions. The membrane module is borrowed from SINTEF Materials and Chemistry, and provides a detailed analysis of the membrane reactor. All relevant parameters affecting the membranes performance can be adjusted in the model. The first section, however, comprises a brief overview of the basic calculations employed to find the results.

10.1 Calculations

Calculations of the overall plant performance, as well as the environmental impact of the plant, are required in order to provide the process results.

Overall plant efficiency

Calculations of the overall performance for the hydrogen producing plant is obtained by using the general formula provided in equation 10.1

$$\eta = \frac{\text{Energy output}}{\text{Energy input}} \quad (10.1)$$

The energy output and input to the process can be studied through a control volume sketch, like depicted in Figure 10.1. Since the general goal is to achieve a heat- and power integrated process, the only energy input is natural gas and the only energy output is hydrogen. Liquid CO₂ is also a product from the process, but do not contain any useful energy and is therefore not considered when calculating the plant efficiency.



Figure 10.1: Control volume

A common way to estimate the thermal energy stored in respectively natural gas and hydrogen, is by using the higher heating value, HHV, and the mass flow. Heating value tells how much energy the fuel contains per unit of substance, usually mass. The following equations describe how the energy content in the entering- and leaving gas are calculated.

$$E_{NG} = \dot{m}_{NG} \cdot HHV_{NG} \quad (10.2)$$

$$E_{H2} = \dot{m}_{H2} \cdot HHV_{H2} \quad (10.3)$$

Table 10.1 provides the higher heating values for natural gas and hydrogen. For the cases considering extra fuel supply to the gas turbine, the two mass flows of natural gas must be added.

Table 10.1: Higher heating value natural gas and hydrogen

	Higher heating value, HHV, [kJ/kg]
Hydrogen	1.404e+005
Natural Gas	5.113e+004

Environmental impact

Another result of interest is the environmental impact of the plant. With that in mind, it is useful to find the amount of emission to atmosphere per kg hydrogen produced. The way of calculating total emission is to look at the CO₂ equivalent for all greenhouse gases included in the exhaust gas. Environmental impact is measured in Global Warming Potentials, GWP, which is given as CO₂ equivalents. Table 10.2 gives the relevant CO₂-equivalents for this thesis.

Table 10.2: CO₂-equivalents (EPA, 2014)

<i>CO₂ – equivalents</i>	
<i>CO₂</i>	1
<i>CO</i>	0.5
<i>CH₄</i>	23

The mass flow of CO₂, CO and CH₄ in the exhaust gas is multiplied with the CO₂-equivalent to find the total emitted amount of greenhouse gases in each case. However, as the combustion in the gas turbine runs with excess air, the exhaust gas will not contain any CH₄ and CO. This results in simpler calculations to achieve the environmental impact. The results are provided in the next section, and the calculations can be found in Appendix C.

10.2 Process results

The following section provides the results from the different cases described. Important basis for comparison are the overall efficiency of the plant, how much required natural gas input per hydrogen output and the amount of CO₂ captured. In addition to these results, the amount of required steam per kg hydrogen produced and the amount of emitted CO₂ per kg hydrogen produced are studied. In many countries, water can be a limiting factor. It is therefore interesting to see how the different cases respond to steam consumption per kg hydrogen produced as well.

10.2.1 Results base case

Table 10.3 gives the relevant results for the base case.

Table 10.3: Results base case

Base case				
Overall plant efficiency	Kg NG per kg produced H ₂	Total captured CO ₂	Kg steam input per kg H ₂ produced	Kg CO ₂ emitted per kg H ₂ produced
64.11%	4.282	77.57%	6.266	2.545

10.2.2 Results case II

Case II contains of four membrane cases, respectively case II-1, case II-2, case II-3 and case II-4. Two approaches are investigated for all cases. Accordingly, an approach where the hydrogen production equals the base case and an approach where no additional NG supplies the process. In addition, all membrane cases are studied with two different membrane inlet pressures, respectively 36 bar and 66 bar. The results are based on the calculations provided in Appendix C. First, the results of the membrane cases that produces the same amount of hydrogen as base case.

Results for case II – with equal amount of H₂ production as base case

As stated in Chapter 9, case II-1, with equal hydrogen production as base case, requires additional NG supply in order to cover the energy demand, for both the case with 36 bar – and 66 bar inlet membrane pressure.

The control volume for this case becomes equal as the control volume for the base case, and the plant efficiency is therefore calculated in the same manner. The results are given in Table 10.4.

Table 10.4: Results case II-1

Case II-1 (same H ₂ amount as base case)					
	Overall plant efficiency	Kg NG per kg produced H ₂	Total captured CO ₂	Kg steam input per kg H ₂ produced	Kg CO ₂ emitted per kg H ₂ produced
36 bar	63.57%	4.318	76.39%	6.266	2.679
66 bar	62.32%	4.405	74.87%	6.266	2.909

Case II-2, with the same hydrogen production as base case, deviates from case II-1 since this case produces more power than it consumes, without any additional fuel supply. This enables the process to export power. The control volume for this case becomes as depicted in Figure 10.2.



Figure 10.2: Control volume case II-2

The efficiency of this plant is therefore calculated in the following way:

$$\eta = \frac{\text{Hydrogen energy [MW]} + \text{Excess power energy [MW]}}{\text{Natural gas energy [MW]}} \quad (10.4)$$

For comparison reasons, the efficiency without considering the excess power is also calculated. This value is the efficiency placed in the bottom line in Table 10.5.

Table 10.5: Results case II-2

Case II-2 (same H₂ amount as base case)					
	Overall plant efficiency	Kg NG per kg produced H ₂	Total captured CO ₂	Kg steam input per kg H ₂ produced	Kg CO ₂ emitted per kg H ₂ produced
36 bar	74.53% / 71.42%	3.845	87.56%	6.266	1.253
66 bar	73.03% / 71.42%	3.845	89.20%	6.266	1.085

The results for case II-3, considering 20 bar permeate pressure and equal H₂-production as base case, are given in Table 10.6.

Table 10.6: Results case II-3

Case II-3 (same H₂ amount as base case)					
	Overall plant efficiency	Kg NG per kg produced H ₂	Total captured CO ₂	Kg steam input per kg H ₂ produced	Kg CO ₂ emitted per kg H ₂ produced
36 bar	66.94%	4.101	80.51%	6.266	2.097
66 bar	65.59%	4.185	78.86%	6.266	2.323

The result for case II-4 when the amount of produced hydrogen equals the base case are given in Table 10.7 below.

Table 10.7: Results case II-4

Case II-4 (same H₂ amount as base case)					
	Overall plant efficiency	Kg NG per kg produced H ₂	Total captured CO ₂	Kg steam input per kg H ₂ produced	Kg CO ₂ emitted per kg H ₂ produced
36 bar	62.10%	4.420	75.13%	6.266	2.914
66 bar	61.45%	4.467	74.33%	6.266	3.039

Results for case II – 1, II-3 and II-4 with no extra NG

When no additional NG supplies the gas turbine, case II-1, 3 and 4 need to reduce the HFR-value in order to provide the gas turbine with the sufficient amount of fuel. This affects the amount of produced hydrogen. The control volume is equal to the base case, and the results are as followed in Table 10.8, Table 10.9 and Table 10.10.

Table 10.8: Results case II-1, no extra NG supply

Case II-1 (no extra NG)					
	Overall plant efficiency	Kg NG per kg produced H ₂	Total captured CO ₂	Kg steam input per kg H ₂ produced	Kg CO ₂ emitted per kg H ₂ produced
36 bar	62.51%	4.391	83.29%	7.159	1.930
66 bar	61.04%	4.497	82.84%	7.332	2.030

Table 10.9: Results case II-3, no extra NG supply

Case II-3 (no extra NG)					
	Overall plant efficiency	Kg NG per kg produced H ₂	Total captured CO ₂	Kg steam input per kg H ₂ produced	Kg CO ₂ emitted per kg H ₂ produced
36 bar	66.31%	4.140	84.44%	6.759	1.691
66 bar	64.71%	4.242	83.97%	6.916	1.787

Table 10.10: Results case II-4, no extra NG supply

Case II-4 (no extra NG)					
	Overall plant efficiency	Kg NG per kg produced H ₂	Total captured CO ₂	Kg steam input per kg H ₂ produced	Kg CO ₂ emitted per kg H ₂ produced
36 bar	60.48%	4.539	86.42%	7.399	1.633
66 bar	59.66%	4.601	86.41%	7.501	1.657

Results for case II – 2 with power balance

Instead of having excess power available for export, this case adjusts the HFR-values in the membranes such that the produced hydrogen amount increases. This gives less suitable fuel to the gas turbine, and the amount of excess power decreases. The results for the power-integrated process, where the demand equals the production, become as depicted in Table 10.11.

Table 10.11: Results case II-4, power balanced

Case II-2 (power balanced)					
	Overall plant efficiency	Kg NG per kg produced H ₂	Total captured CO ₂	Kg steam input per kg H ₂ produced	Kg CO ₂ emitted per kg H ₂ produced
36 bar	73.82%	3.719	88.36%	6.062	1.133
66 bar	72.57%	3.783	89.58%	6.167	1.028

Chapter 11 provides graphical illustrations of the results.

10.2.3 Comments

In addition to the results provided in the previous section, it is interesting to see how the cases perform when it comes to the purity of the produced hydrogen and captured CO₂, as well as the conversion rate through the reformer. The conversion rate is equal in all cases since the amount of entering natural gas and steam to the reformer are similar for all cases. The value is given in Table 10.12 below together with the hydrogen- and CO₂ purity.

Table 10.12: General results

	Base Case	Membrane case producing equal amount of H ₂ as base case	Membrane cases, no extra NG supply
Hydrogen purity	99.65%	100%	100%
CO ₂ purity	98.40%	99%	Given in table below
Reformer conversion	94.21%	94.21%	94.21%

The purity of the captured CO₂ is equal in all membrane cases considering the same amount of produced hydrogen as base case. The reason is that the gas entering the LT-separation unit has the same CO₂ concentration in all the relevant cases since the amount of removed hydrogen is similar. For the cases with no extra NG supply, this will not be the case since the HRF-value changes in order to obtain a self-sustained process. Table 10.13 below therefore provides the values for the CO₂-purity in these cases. As depicted, all cases achieves the specification of a CO₂ purity of 95%.

Table 10.13: CO₂ purity for membrane cases with no extra NG supply

Case	CO ₂ purity (36 bar / 66 bar membrane inlet pressure)
Case II-1	98.40 %
Case II-2	99.16 / 99.14 %
Case II-3	98.40 / 98.94 %
Case II-4	99.24 / 99.26 %

10.3 Parametric study of the membrane module – results and analysis

Membrane implementation in HYSYS occurs through a component splitter. The component splitter do not take any other parameters than the defined split ratio and outlet temperature and pressure into account. A membrane reactor, however, is more complex, and many parameters affect the performance of the membrane. This parametric study analyzes how membrane feed pressure and permeate pressure affects the performance and size of the membrane. Changing the pressure difference in the membrane affects the driving forces, which will affect the amount of hydrogen flowing through the membrane. To cope with to small pressure differences, the membrane area can be increased to obtain the desired HRF-value. This will however increase the investment cost for the membrane. Increased pressure difference provides increased driving forces, which makes it possible to reduce the membrane area in order to achieve the desired HRF-value. As indicated, this becomes a tradeoff between operational – and investment costs.

An important factor for comparison is the HRF-value. Respectively, most of the graphical illustrations given in this section concerns how different operating parameters for the membrane influence the HRF-value. However, it is also interesting to study how the inlet pressure and membrane area correlates in order to obtain a fixed HRF-value. All studied membrane cases has a required HRF-value in order to obtain either the required amount of produced hydrogen or the required amount of hydrogen supply to the gas turbine. The inlet gas temperature to the membrane is in all simulations assumed to be 400°C.

The first graph illustrates the relation between the HRF-value and the membrane length, respectively for the two studied inlet pressures. The permeate pressure is defined to be 1 bar in this simulation.

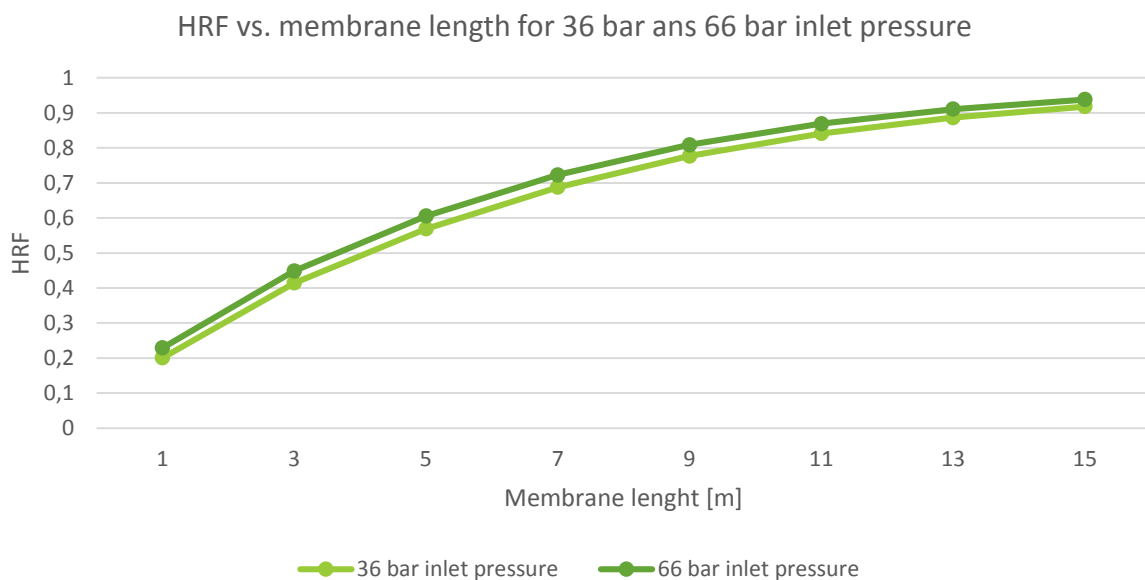


Figure 10.3: changes in HRF according to changes in membrane length

As observed from Figure 10.3, the 66 bar inlet pressure-line lies at all-time slightly above the line for 36 bar inlet pressure. This means that 66 bar inlet pressure ensures a higher HRF-value in the membrane compared

to 36 bar inlet pressure, for the same membrane length. However, increasing the pressure from 36 bar to 66 bar in front of the membrane do not gain any big advantageous when it comes to increases in the HRF-value.

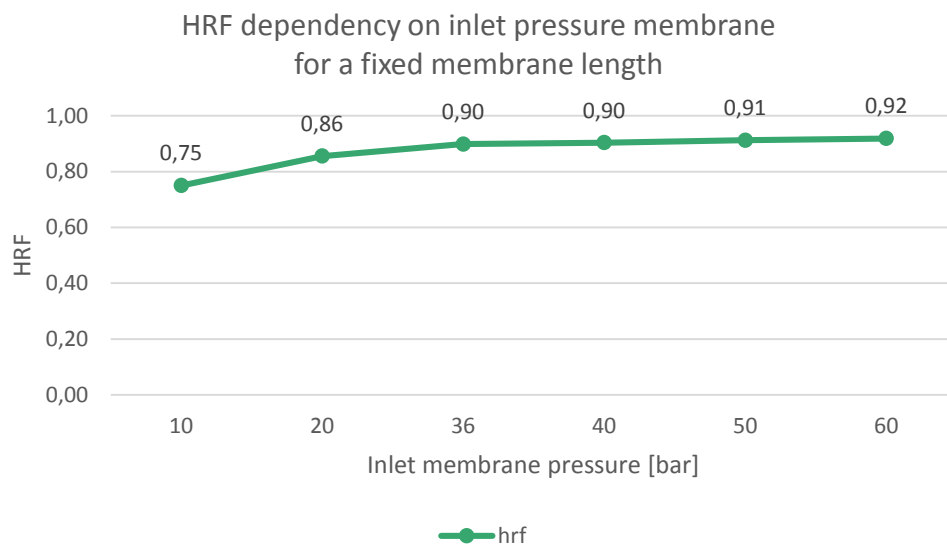


Figure 10.4: Changes in HRF according to changes in inlet membrane pressure

Figure 10.4 illustrates, for a given membrane length and a permeate pressure of 1 bar, the inlet pressure of the membrane against the HRF value. Increasing inlet membrane pressure increases the HRF-value, but flattens out.

Figure 10.5 depicts how the membrane length changes according to the inlet pressure. For this simulation, the required HRF-value in the single membrane case, case II-1, is fixed, as well as a permeate pressure of 1 bar. This graph illustrates the same trend as the previous figures. The required length for the membrane decreases as the membrane inlet pressure increases. This is due to the increase in driving forces across the membrane. However, the reduction in required membrane length declines as the inlet pressure increases. This implies, again, that compression to such high-pressure levels probable will be more costly than advantageous for the process, as it gives little effect on the membrane performance.

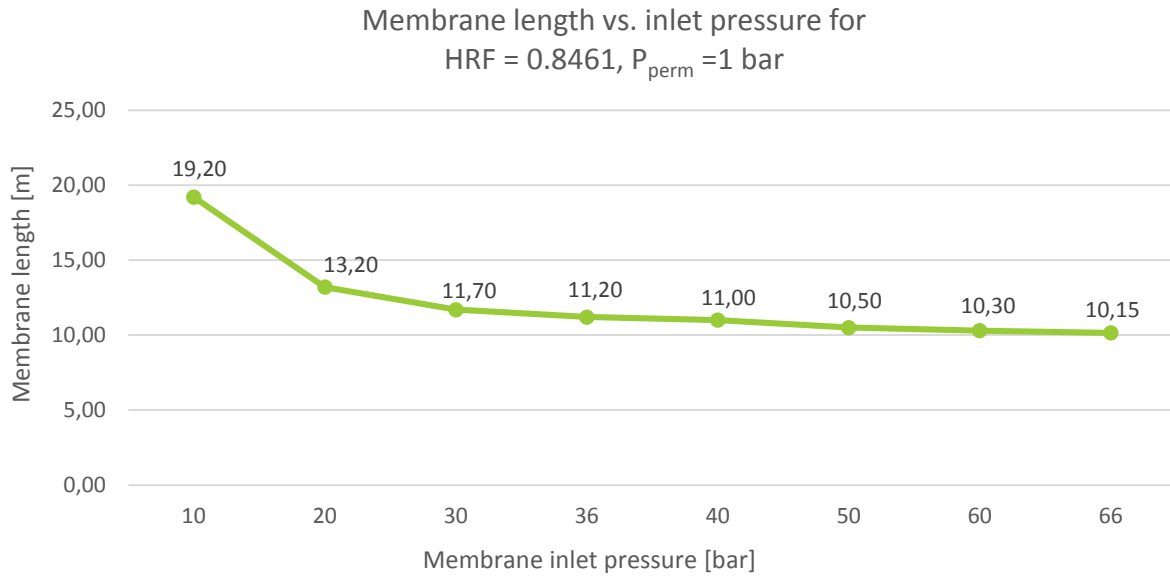


Figure 10.5: Changes in membrane length according to membrane inlet pressure for a fixed HRF value

Another interesting study would be to investigate the consequences of letting the permeate pressure be 20 bar, as was done in case II-3. Figure 10.6 depicts how the pressure-increase on the permeate side impacts the membrane performance. The two lines show how the HRF-value changes according to the permeate pressure for respectively 36 – and 66 bar inlet pressure. The membrane length is fixed in this simulation. This figure shows that compression of the feed gas is advantageous when the permeate pressure increases. When the permeate pressure is set to 1 bar, compression up to 66 bar in front of the membrane only gives slightly better HRF-value. However, as the permeate pressure increases, the HRF-value diminishes much faster when the inlet pressure is 36 bar contra 66 bar. In order to maintain sufficient driving forces, the inlet pressure must increase according to the increase in permeate pressure. If the inlet pressure is 36 bar, and the permeate pressure is decided to be 20 bar, the HRF-value, for the given length, is below 10%, meaning that less than 10% of the produced hydrogen will be able to pass through the membrane.

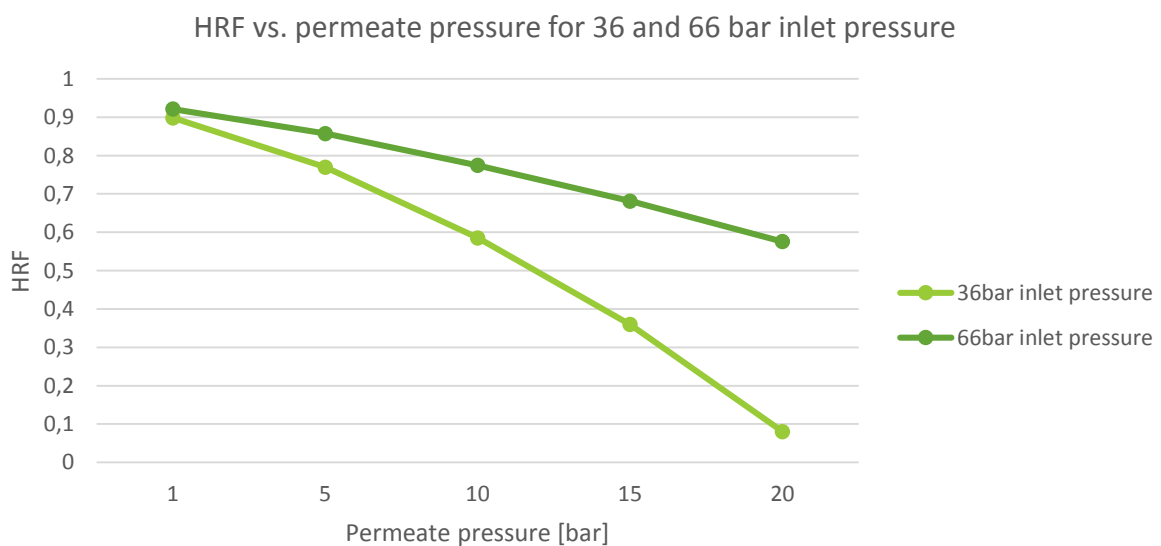


Figure 10.6: Changes in HRF according to changes in permeate pressure

Case II-4 introduced the possibility of having CO₂-separation in front of the membrane. Figure 10.7 below illustrates how the change in inlet gas composition affects the membrane performance, for both studied feed pressures.

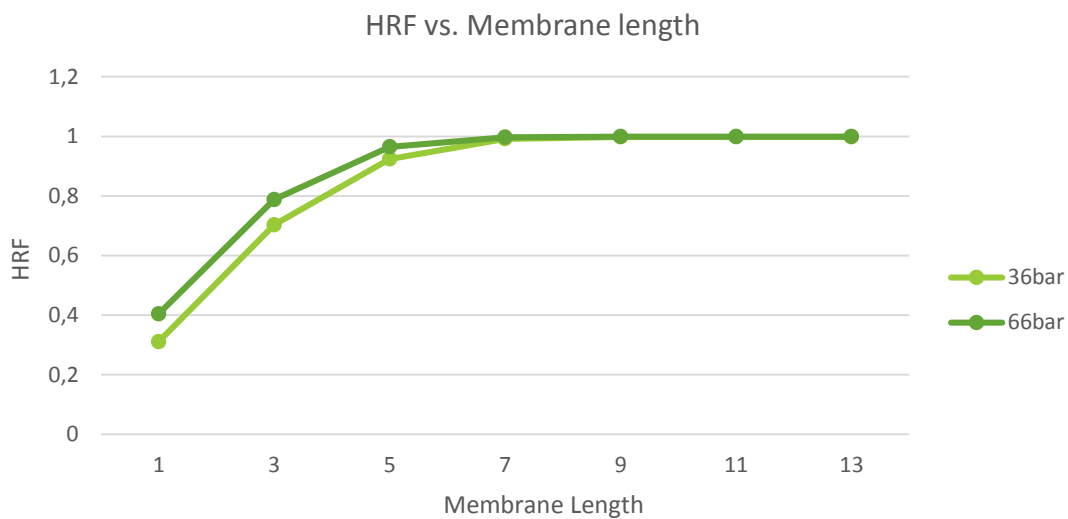


Figure 10.7: Changes in HRF according to changes in membrane length for case II-4

Removal of CO₂ upstream the membrane reduces the amount of gas entering the membrane, and makes the hydrogen fraction in the gas increase. Figure 10.7 illustrates how the HRF-value changes with the membrane length for respectively 36 bar and 66 bar inlet pressure of the hydrogen-rich gas. The permeate pressure is defined to be 1 bar in this case. This case gives considerably better HRF-values for shorter membranes. For comparison, the installed membrane in case II-1, with 36 bar membrane feed pressure, requires a membrane length of 11.2m to obtain the desired HRF-value of 0.8461, which can be seen from Figure 10.5. Figure 10.7 indicates that the increased hydrogen content in the entering gas reduces the required area for obtaining the desired HRF. To achieve a HRF-value value of 0.8461, with 36 bar inlet pressure, in this case, a sufficient membrane length will be around 4.2m. This represents a significant reduction in required membrane area. However, it has to be mentioned that the CO₂-removing unit requires more energy in this case compared to the cases using LT-separation. Table 10.14 provides the values for the required amount of power for the respective CO₂-separation processes. The energy consumption in the pre-combustion CO₂-capturing unit is distributed between thermal requirements of 900 kJ/kg CO₂ and power requirements of 140 kJ/kg CO₂. The specific work required in the LT-separation is found from the simulation results provided by SINTEF. The values in Table 10.14 is for case II-4 and case II-1 where the two cases produce the same amount of hydrogen.

Table 10.14: Power consumption CO₂-capturing units

	36 bar	66 bar
Pre-combustion CO ₂ -capture [MW _{TH}]	92.84	92.84
Pre-combustion CO ₂ -capture [MW _E]	14.44	14.44
LT-separation case II-1	21.2	14.7

Reduced membrane area decreases the investment costs. However, increased energy requirement for CO₂-separation increases the operational costs. Meaning, the favorable process design becomes a tradeoff.

Figure 10.7 also indicates the effect of compressing the gas up to 66 bar instead of 36 bar. Both feed pressures reaches almost 100% HRF when the membrane length becomes around 7m. At this length, there

will be no benefit of compress the gas further in front of the membrane. However, for shorter membranes, the pressure increase gives a better HRF-value. Compared to Figure 10.3, which gave the same relation for the cases not considering CO₂-removal in front of the membrane, this case increases the benefit of compression upstream the membrane until the length of the membrane reaches around 7m. Another observation is that the HRF-value in this case increases more rapidly with increased membrane length compared to the other cases.

Area overview

Table 10.15 gives an overview of the studied cases and the respective membrane length and total membrane area in order to obtain the required HRF-value, provided in Chapter 9. Only the cases who produce the same amount of hydrogen as the base case is considered, due to comparable reasons. As Table 10.15 indicates, the membrane area in case II-3 is huge. For case II-3, with 36 bar inlet pressure, the membrane model was not able to calculate the required membrane length in order to achieve the desired HRF-value for this case. The reason is the lack of driving forces. For case II-3 studied with 66 bar membrane feed pressure, the area was calculated, but as seen, very large.

Table 10.15: Area overview membrane cases

	Membrane length [m]		Total membrane area [m ²]	
	36 bar	66 bar	36 bar	66 bar
Case II-1	11.2	10.15	12335	11179
Case II-2	7.4 + 6,7	6.8 + 5.72	8150 + 4571 = 12721	7489+3881 = 11370
Case II-3	-----	1730	-----	1905379
Case II-4	4.15	3,5	2855	2408

11. Discussion and analysis of process results

Based on the results given in the previous chapter, it has been seen that case II-2 outperforms the other cases when it comes to both the overall plant efficiency and the total CCR. Figure 11.1 below, gives an overview of the calculated plant efficiencies for the studied cases. Case II-2, which implemented a sequential membrane and WGS module with two steps, has considerably better plant efficiency than the other studied cases. The process with two membrane modules do not need any additional NG supply to the gas turbine in order to obtain a power-balanced process. In fact, the process considering equal amount of produced hydrogen as base case, has excess power, resulting in an increased plant efficiency. A big share of the produced hydrogen is removed in the first membrane, causing the equilibrium in the LT-WGS to shift against the product. This means a higher hydrogen conversion in the WGS-stage, and therefore more produced hydrogen in this case than the other cases. With more produced hydrogen, a bigger share can be sent for fuel supply to the gas turbine, making it independent on extra NG feed. This makes case II-2 the most efficient process solution.

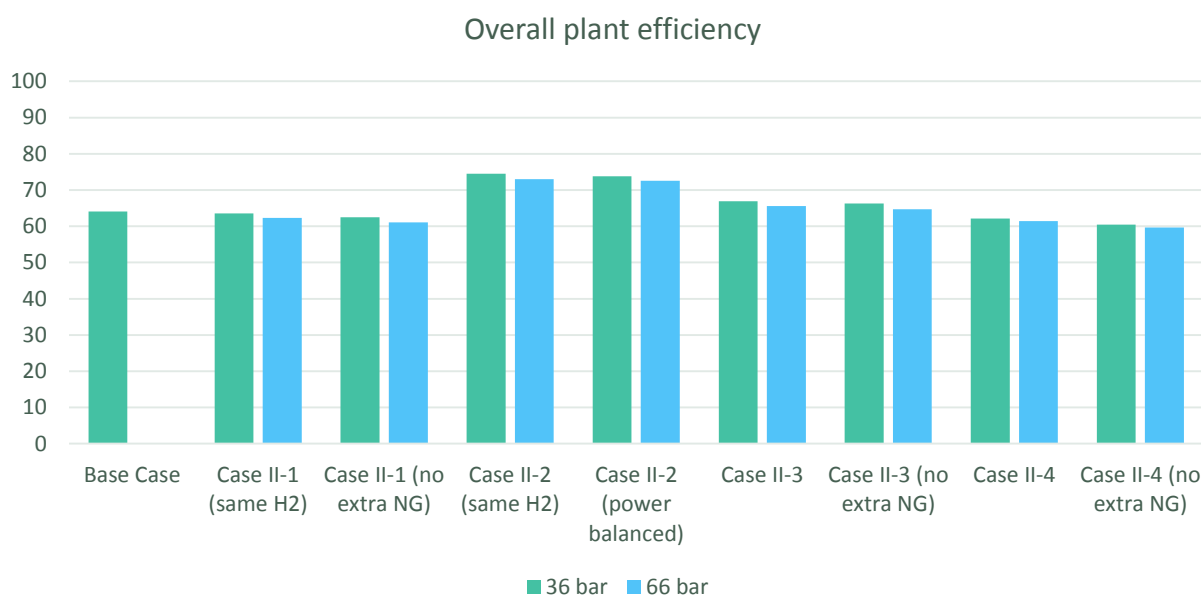


Figure 11.1: Overall plant efficiency

Case II-2, which produces the same amount of hydrogen as the base case, has the highest efficiency of all the studied cases. This plant has excess power, which increases the efficiency considerably. However, this thesis studies a hydrogen producing plant, and it therefore makes little sense to have a hydrogen facility that works as a power plant. With that in mind, the power balanced case II-2 is a more realistic process. Even though the efficiency of this case is less than for the case producing the same amount of hydrogen as base case, it is considerably higher than the other cases. It can also be seen from Figure 11.2 that this case uses the smallest amount of natural gas per kg hydrogen produced.

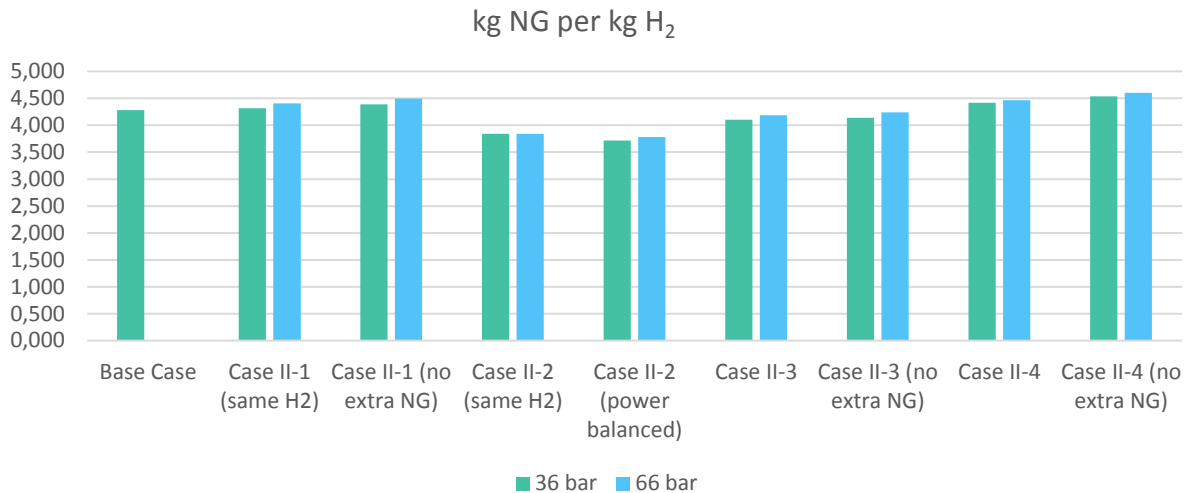


Figure 11.2: kg natural gas per kg hydrogen produced

Figure 11.2 shows the same tendency as Figure 11.1. The cases with the highest overall efficiency use less natural gas per kg hydrogen produced. This is logical since the only two parameters affecting the plant efficiency are the amount of entering natural gas and the amount of hydrogen leaving. This is, however, not the case for case II-2 with same hydrogen production as base case, due to the excess power. The power-balanced case II-2 uses the smallest amount of natural gas per kg hydrogen produced, while case II-4, with no extra NG supply, uses most. No case has larger energy demand than case II-4, which can be seen in Appendix D. To be able to fulfil the power requirements in the case of no extra NG, the HRF-value in the membrane must be adjusted such that the gas turbine gets a sufficient amount of energy-rich fuel. This reduces the amount of produced hydrogen, which leads to a big consumption of natural gas for each kg of produced hydrogen. The power-balanced case II-2, on the other hand, produces the largest amount of hydrogen, which results in the smallest natural gas consumption per kg hydrogen produced. It has to be mentioned that case II-1, with no extra NG supply, follows closely on case II-4, due to the same reason. This is interesting since case II-1 is the most basic membrane case, and it is therefore important to emphasize the performance of this process.

Investigation of the impact of increased membrane inlet pressure shows a tendency of decreased plant efficiency. This is, however, no surprise as the only contribution the increased pressure has on the process, is the increased power demand. The reason is that HYSYS uses component splitters as membranes. Nevertheless, as indicated in the previous chapter, increasing the inlet membrane pressure to 66 bar when the permeate pressure is equal to 1 bar, has small impact on the overall plant efficiency for all cases except case II-4. In other words, an increase in feed pressure will only increase the hydrogen flow through the membrane to a small amount. As depicted in Figure 10.4, increasing the inlet pressure from 36 bar to 60 bar only increases the HRF by 2%, while increasing it from 10 bar to 36 bar increases the HRF by 15%. These results indicate that increasing the membrane pressure further than 36 bar, when the permeate pressure is 1 bar, will not be advantageous when the increased amount of produced hydrogen is compared to the increased power demand for compression. However, Figure 10.7 indicates that increasing the feed pressure for membranes shorter than approximately 5m, increases the HRF-value significantly for case II-4. For longer membranes, the HRF-value will approach 100% for both pressures, meaning no advantages of an eventual pressure increase above a certain membrane length for case II-4.

Figure 11.2 shows that for all membrane cases the amount of required natural gas per produced hydrogen increase, to a various amount, as the membrane inlet pressure increases. The reason is the increased power

demand. For the cases producing the same amount of hydrogen as base case, the increased power demand makes it necessary to increase the amount of NG supply to the gas turbine. Regarding the cases with no additional NG supply, the HRF-value in the membranes are reduced in order to provide the gas turbine with the sufficient amount of fuel, making the amount of produced hydrogen less.

The previous chapter illustrated the effect of changing the permeate pressure to 20 bar for respectively 36- and 66 bar inlet pressure to the membrane. In case II-3, where this was studied, the required HRF-value in order to produce the same amount of hydrogen as base case is 0.8461 for both inlet pressure cases. After testing this membrane in the model borrowed from SINTEF, it was seen that the membrane area would be huge in order to achieve the desired HRF-value. For the case considering 36 bar inlet pressure, the model was not able to calculate the required area. It seems like it reaches a maximum HRF-value, where increasing the length will only increase the HRF-value to a small extent. For this case, a membrane length of 1000m gives a HRF-value of 0.14 while a membrane length of 3000m gives a HRF-value of 0.15. Obviously, this case will not be considered built. The case with 66 bar inlet pressure experiences the same trend. However, the achieved HRF-value for this case is considerably higher than for the 36 bar-case. The required membrane length in order to achieve a HRF-value of 0.8461 is 1730m, found from the membrane model. Construction of such a long membrane will not be practically feasible, which makes this case invalid. Case II-3 was also considered with no extra fuel supply to the gas turbine. In this case, the desired HRF-value decreased compared to the case investigated above. However, with 36 bar inlet pressure, the membrane model were not able to calculate an appropriate membrane area, due to the lack of driving forces. For 66 bar inlet pressure, the required membrane length is 1000m in order to obtain the desired HRF-value of 0.7666 in this case. A membrane length of 1000m is not convenient for construction, which makes this case invalid as well. From Figure 11.1, it can be seen that the plant efficiency for case II-3 is rather good for both approaches. Actually, case II-3 performs better than case II-1 and case II-4. However, due to case II-3 being practically impossible, these results will not be valid. This result emphasizes the drawback of using simplified unit implementations in HYSYS. Since HYSYS only considers the membrane as a stream splitter, it will not give any warnings of the too small driving forces.

Water consumption for hydrogen production can in some parts of the world act as a limiting factor. In some countries, water is an expensive resource, which makes it important to minimize the utilization. The graphical illustration in Figure 11.3 shows the correlation between water consumption and the amount of produced hydrogen for each case.

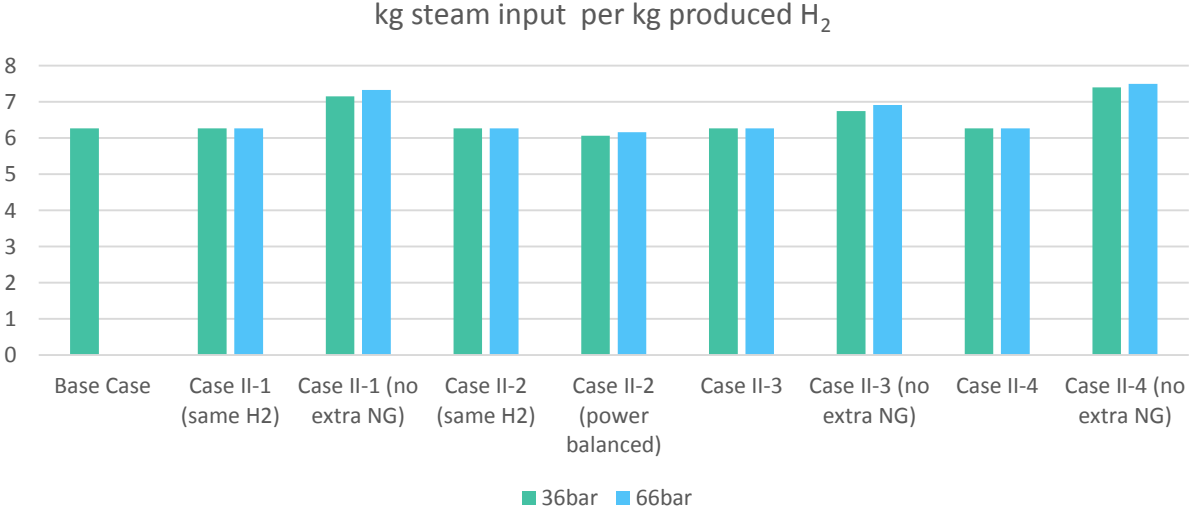


Figure 11.3: Steam consumption per kg hydrogen produced

Again, case II-2 performs best, closely followed by case II-4. Case II-1 and case II-4 with no extra fuel supply has the largest steam consumption per kg hydrogen produced. This is related to the decreased HRF-value in the membranes in order to provide the gas turbine with the required amount of fuel. Case II-1 and case II-4 are the two cases with the largest energy consumption, meaning that the HRF- values in these cases declines the most when the processes are in power balance with no additional fuel supply. Decreasing the HRF-value decreases the amount of produced hydrogen. Since the amount of entering steam to the process is equal in all cases, case II-1 and case II-4 scores poorly. In order to keep the S/C-value in all reformers at 1.5, and the amount of entering natural gas to the reformer is constant, the steam supply must be equal in all cases. Case II-2, in power balance, uses the smallest amount of steam per kg hydrogen produced. This is simply because this case produces the highest amount of hydrogen due to the increased HRF-value when the process is in power balance.

Discussion of environmental impact

When it comes to the total CCR of the cases, Figure 11.4 gives an overview of the results. The trend shows that the cases with no additional NG supply to the gas turbine have the highest total CCR. This is because a smaller quantity of hydrocarbons participate in the combustion, resulting in less CO₂ creation and therefore less emission. The fuel mix from the membrane retentate contains primarily hydrogen, which produces water vapor during combustion. However, the gas also contains small amounts of methane that form CO₂ under combustion. Due to this, and the fact that the LT-separation process for CO₂ capture is not able to capture 100% of the CO₂, the cases not supplied with additional fuel will also have some CO₂-emission, but in smaller amounts than the other cases. Since post-combustion CO₂-capture is not included in this process, the CO₂ created during combustion of natural gas will be emitted. This is the reason why the cases with additional NG supply has lower CCR than the cases that rather supply the gas turbine with some of the produced hydrogen. As indicated, it results in a tradeoff between the amount of produced hydrogen and the amount of emitted CO₂. For the process to be environmentally friendly, it is not advantageous to burn natural gas without any capturing units downstream.

Yet again, Case II-2 comes out as the best alternative. The reason is that none of the cases considering implementation of two membranes needs additional NG supply, and the HRF-value in the membranes are therefore not reduced. In the other cases considering no extra NG supply, the HRF-value declines in order to achieve a power-balanced process. This means a higher hydrogen share in the retentate gas and therefore a lower CO₂ concentration in the gas entering the LT-separation process. This leads to a lower total CCR since the capture rate of the LT-process decreases as a result of the fact that separation becomes easier when the concentration of the component to be separated increases. Due to the increased HRF-value in the power balanced case II-2, the CO₂ concentration of the retentate entering the LT-separation unit is higher than in the other cases, resulting in a higher capture rate for this process.

The previous figures indicated that the single membrane cases with no additional NG supply, performed poorer when it comes to NG supply – and steam supply per kg hydrogen produced, due to the reduced amount of produced hydrogen. The overall performance was also slightly reduced for these cases. However, the CCR results for these cases are much better than for the single membrane cases producing the same amount of hydrogen as base case. It should therefore definitely be considered to employ the cases with no extra NG supply if a single membrane module is used.

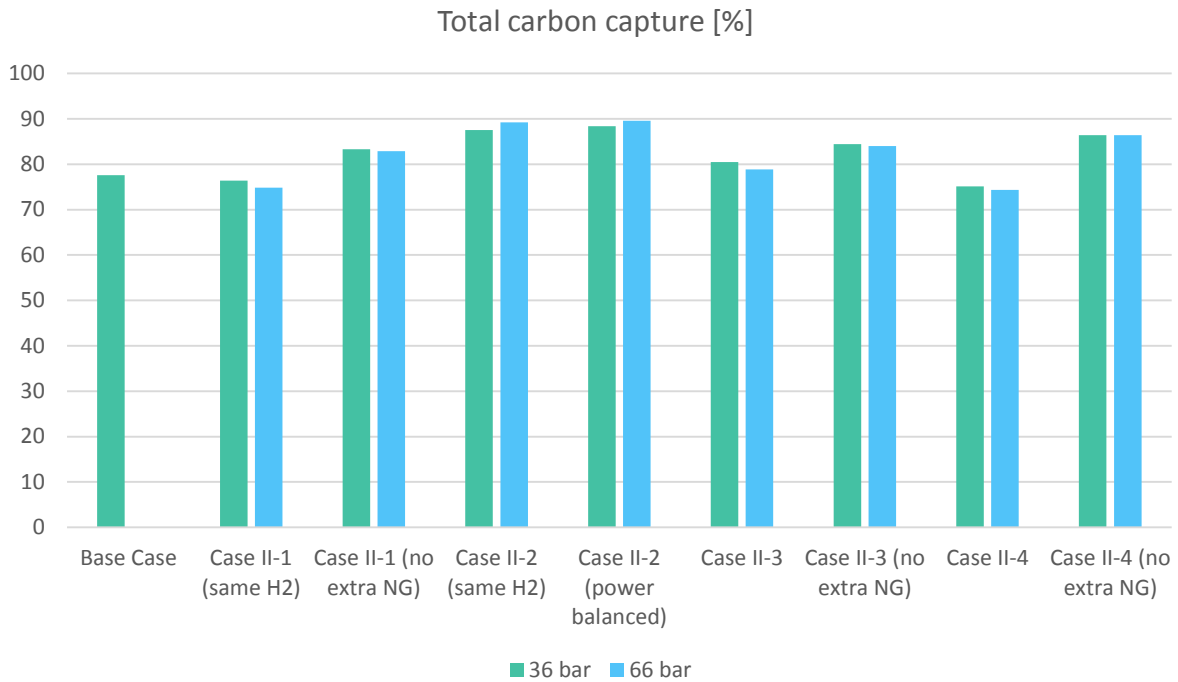


Figure 11.4: Total CCR

Another observation from Figure 11.4 is that the cases considering 66 bar membrane inlet pressure gives slightly less total CCR, except for case II-2. The reason is the increased power consumption in the process when the pressure increases. For the cases considering equal hydrogen production as base case, it becomes necessary to increase the amount of additional NG supply to the gas turbine, which results in a larger amount of emitted CO₂. For the cases considering no additional NG supply, the CCR will not change much as the inlet pressure of the membrane changes. However, as the pressure increases, the power demand increases, which again reduces the HRF-value in order to obtain a power-balanced process. This leads to a bigger share of hydrogen in the retentate gas and therefore a smaller concentration of CO₂, which results in a smaller capture ratio in the LT-process, and thus a smaller total CCR.

For case II-2, the CCR increases when the membrane inlet pressure increases. This is because the conversion rate in the LTS increases, which reduces the amount of CO in the process. A smaller amount of CO results in less CO₂ emitted since CO reacts with oxygen in the complete combustion in the gas turbine and generates CO₂. Since the shift-reaction has equal amount of moles on each side, one could believe that increasing the pressure should not have influenced the conversion rate. However, the equilibrium reactor used in HYSYS converts more CO in the case with increased pressure. The LTS conversion rate in the case with 36 bar inlet pressure is 90.84%, while for the case with 66 bar inlet pressure it reaches 97.54%. Apparently, the increased pressure shifts the shift-reaction against the product and/or increases the rate of the reaction. Section 4.2.4 indicated that increased pressure increases the rate of the reaction, which might be the solution to why the conversion rate increases.

To illustrate the environmental impact of each case, Figure 11.5 represent how much CO₂ the process emits per kg produced hydrogen. This Figure illustrates the same tendency as Figure 11.4, and again, case II-2 has the best result. Case II-2, in power balance, emits less CO₂ per kg hydrogen produced. This is due to two reasons; (1) this case produces the largest amount of hydrogen and (2) the case need no additional NG supply. The cases with external NG supply has the largest emission per kg hydrogen produced, not surprisingly. Case II-1 and case II-4 emits most CO₂ per kg H₂ produced, which again is explained by the high power demand in these cases, see Appendix D, and therefore requires large amount of extra NG supply.

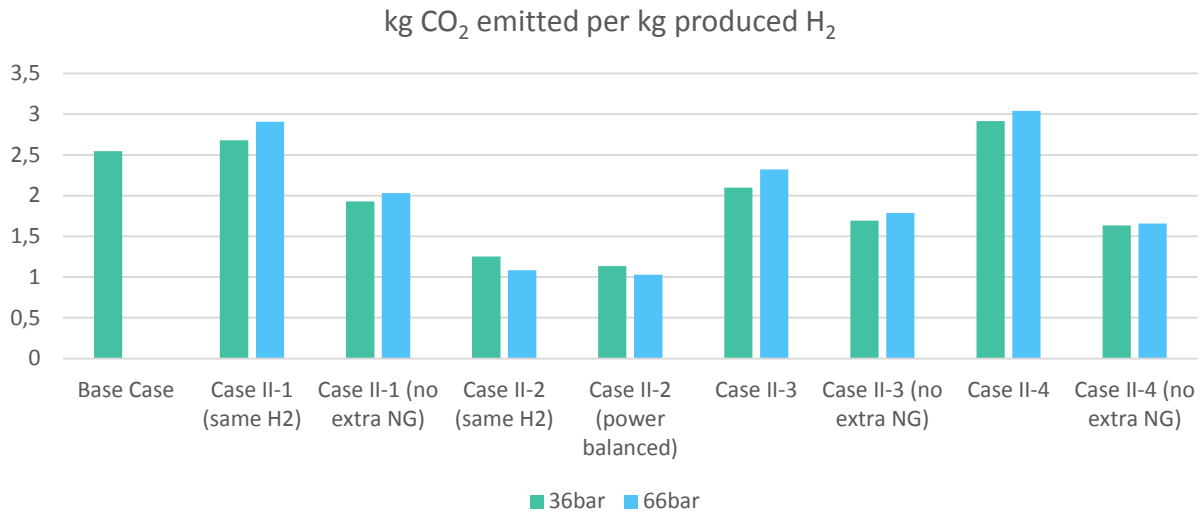


Figure 11.5: Total emission per kg hydrogen produced

Discussion of total membrane area

In terms of the total membrane area, the hypothesis for the membrane analysis performed through the SINTEF model, was that case II-1 and case II-3 would require the largest membrane area in order to obtain the desired HRF-value of 0.8461, while case II-2 and case II-4 would require a smaller area. To obtain a comparative analysis, all studied cases produce the same amount of hydrogen. Case II-3 requires an unrealistically large membrane area. This case is therefore not further discussed. For case II-2, the results show that the total required membrane area did not decrease compared to the single membrane case. This contradicts the hypothesis in front of the study, which was based on literature. Figure 11.6 and 11.7 illustrate the total membrane area required in order to produce the same amount of hydrogen as base case, for respectively 36- and 66 bar feed pressure to the membrane.

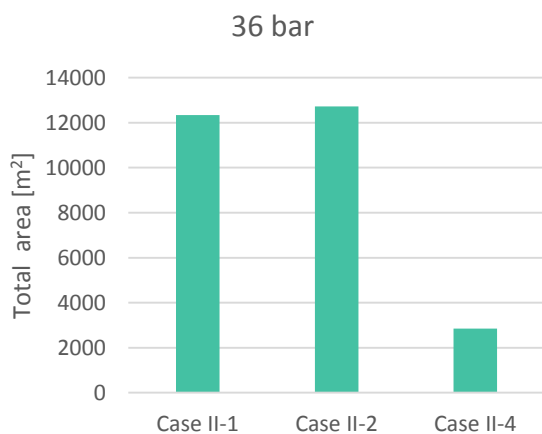


Figure 11.6: Total membrane area, 36 bar inlet pressure

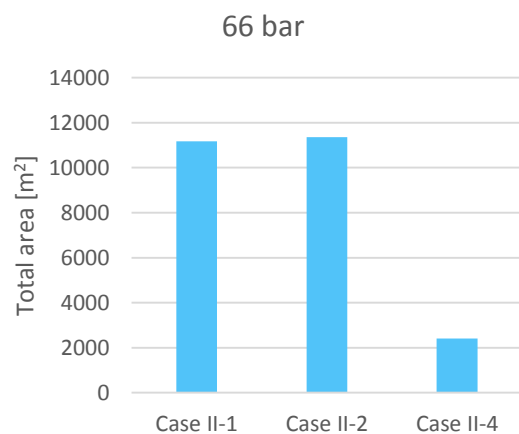


Figure 11.7: Total membrane area, 66 bar inlet pressure

Figure 5.10 indicated that implementation of a sequential membrane and WGS module would decrease the required total membrane area. However, as Figure 11.6 and 11.7 depict, this is not the case in this study. These figures indicate that implementation of two membrane modules requires approximately the same total membrane area as implementing a single membrane. However, the area of each membrane in case II-2 will be less than the area demanded in case II-1. A possible reason for the unreduced membrane area in

case II-2, can be the distribution of the HRF-value between the two membranes in case II-2. At present, the HRF-value for the first membrane is 0.7, while it is 0.6360 for the 36 bar case and 0.5850 for the 66 bar case in the second membrane. In order to see if the HRF-distribution had any effect on the required area, a case with equal HRF-distribution among the membranes, and the same amount of produced hydrogen, was developed. The resulting HRF-value is 0.6262, and the total membrane area required in this case is 12 323m², in other words a reduction of 3.13% compared to the original case. This calculation is conducted only for the case considering 36 bar inlet pressure. For comparison reasons, the required area for case II-1 with 36 bar inlet pressure is 12 335m². The total membrane area becomes smaller when the HRF-values are equal. However, it is not greatly reduced compared to case II-1, which was the assumption before the analysis. It might exist another HRF-distribution that gives a better result in terms of a smaller total membrane area, but it seems like the anticipated reduction is not occurring in this work. Nevertheless, implementation of two membranes score better than case II-1 in all areas, and the required membrane area for case II-2 is not far from the required area in case II-1, meaning that, overall, case II-2 performs better.

Case II-4, on the other hand, decreases the required total membrane area significantly. For 36 bar membrane inlet pressure, the reduction in required area compared to case II-1 is 77.6% and 76.8% for case II-2. In the cases considering 66 bar, the reduction in total area is 78.5% compared to case II-1, and 78.8% compared to case II-2. This implies that the investment costs of constructing case II-4 will be significantly lower compared to the other membrane cases. On the other side, case II-4 has performed relatively poorly considering the overall plant efficiency and emission per kg hydrogen produced. The large energy demand in this case makes the operational costs increase compared to case II-2, where no additional NG is needed. This results in a tradeoff between investment costs and operating costs for producing the same amount of hydrogen.

12. Discussion of process simulations

This process is considered without pre-treatment of the gas, as it is assumed to be free of all sulfur-containing compounds. The main argument for this simplification is the fact that natural gas from the Norwegian Continental Shelf contains small amounts of sulfur containing-compounds. Integrating pre-treatment will only complicate the process, and make no big changes regarding the amount of produced hydrogen. It will, however, affect the required energy input for the process, as the separation unit needs both electric power and heat. By adding pre-treatment, the pressure drop in the process increases, and more equipment leads to bigger process losses.

All process equipment is more or less simplified in the HYSYS drawings for this hydrogen production facility, but the results for the different cases will give a fairly comparable situation as the same simplifications are done to all cases. Simulations in HYSYS do not consider practical limitations, like distance between units, metal dusting, temperature and pressure drop during pipeline transportation etc. This can, however, be considered if the user is aware of the limitations, and implement it to the program. The simulations done in this work has taken pressure drop throughout the process into consideration, and the efficiencies of the different components are changed according to the EBTF-document (DECABRit, 2009). Metal dusting issues are also considered, and the heat exchangers postponed for metal dusting do not exchange heat with high temperature streams. Distance between the units are not taken into account, and could potentially pose problems in reality. For example, to obtain a heat integrated system, preheating of the incoming natural gas partly occurs through heat exchange with the gas turbine exhaust gas, which in practice probably will be located some distance away. There will in reality be several additional forbidden matches.

As discussed in the last chapter, another limitation affecting the process results is the simplification done in the membrane implementation in HYSYS. Since this thesis implements the membrane as a stream splitter, the properties affecting the membrane area and HRF-value, is not taken into concern. This problem was highlighted when the membrane in case II-3 were studied. HYSYS calculated a rather good overall plant efficiency for this case, but the requirements of large membrane area makes it impossible to build this plant in practice.

Simplifications done to the other separation units as well might influence the reliability of the process. This applies to the PSA unit and the pre-combustion carbon-capturing unit. Designing these units in HYSYS would be complicated, and is not the scope for this assignment. Instead, estimated values for separation efficiency and energy requirements are used. This could be a potential source of error. If some small modifications are done to the system, this will not affect the separation units the way it would do in reality, due to the fixed assumed values.

All heat exchangers are assumed to work without any heat loss. This is not the case in reality, and actual heat exchangers need to be built larger or have bigger driving forces.

It seems like the decided mass flow in the current study is a bit unrealistic. This can be seen through the required work output from the gas turbine and the required size of the plant for liquefaction of the produced hydrogen. In the base case, the net power output from the gas turbine is 260 MW, and approximately the same for the membrane cases. The net value increases for the cases concerning 66 bar membrane pressure due to the increased power demand in the process. According to SIEMENS, a power output above 232 MW for this type of gas turbine makes it necessary to implement two turbines (Siemens, 2015). However, the value of 260 MW is not that far away from the existing limits for the gas turbine, and

it might be possible to arrange the gas turbine such that it is able to generate the required output in this study.

Most current plants for hydrogen liquefaction can produce around 10.5tons liquid hydrogen per day. However, the largest plant, situated in USA, can produce up to 36tons/day (Walnum et al., 2012). This thesis introduced processes with a hydrogen production ranging between 9.93 and 12.11 kg/s, which represents 875.9tons/day and 1046.3tons/day, respectively. With the current technology for liquefaction, it requires over a 100 liquefaction plants to be able to liquefy all the produced hydrogen, in the latter case, in one day. However, hydrogen can be stored as gas, and be liquefied whenever. It is also ongoing research trying to develop large-scale liquefaction plants such that the energy requirement reduces per kg hydrogen liquefied. It is assumed that these large-scale liquefaction plants can liquefy up to around 100tons/day (Walnum et al., 2012). Despite the possible scale-up of this technology, the amount of produced hydrogen in this thesis is unrealistic. The amount of produced hydrogen in the current process equals around 420MMscfd, assuming that 1 kg hydrogen equals 415.6 standard cubic feet. According to Ritter & Ebner, a hydrogen production site of around 150-200MMscfd is large, making the process in this thesis impractical for the current technology (Ebner and Ritter, 2009). Although the process studied in this thesis is larger than practically possible, the results would be the same if the whole process were scaled down. It will therefore not change any of the results, but it can be useful to have in mind when studying the relevant mass flows and power consumptions, as they might be a bit unrealistically large.

Heat-and power integration

Chapter 9 provided the resulting heat-integrated case study. The obtained cooling targets in HYSYS were in all cases lower than the calculated targets in AEA. However, the deviations were not significant, which implies that the heat-integration of the processes is acceptable. One possible reason for the deviation between the achieved targets in HYSYS and the targets calculated by AEA can be the algorithms used in the AEA calculations. Since this program is intended for the industry, it calculates the targets by being on “the safe side”. This means that AEA calculates the targets based on a conservative linearization of the cooling- and heating curve of the process, which Figure 12.1 illustrates. The red curve is the hot composite curve, while the blue curve is the cold composite curve.

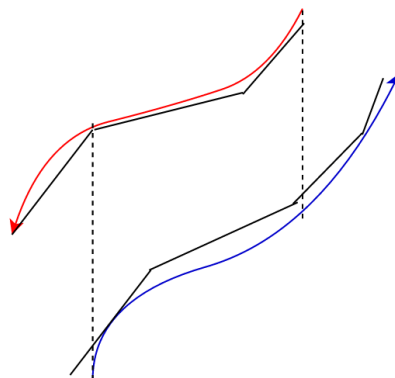


Figure 12.1: Illustration of conservative linearization

As described in previous chapters, it is important to adhere the ΔT_{\min} -rule when heat integrating a process network. When AEA linearizes the cooling- and heating curves, it can occur that the ΔT_{\min} between the lines are less than the defined value. Since the linearization is conservative, this can occur even though the driving forces are sufficient in reality. Once AEA linearizes the composite curves, it shift the curves in order to obey the ΔT_{\min} -rule between the lines, which means an increase in calculated target values.

13. Conclusion

This report suggests an alternative production plant for hydrogen, where the conventional PSA technology for hydrogen purification is replaced with the new and interesting membrane technology. A case study was developed in order to accomplish the desired survey. The objective was to investigate if new technology may result in advantageous effects on the process for hydrogen production, in form of increased efficiency and reduced emission.

As the results from the HYSYS simulations indicated, implementation of one single membrane module and low-temperature CO₂-capture will not provide any great benefits compared to the case considering a conventional ATR process. In fact, for the single membrane case, case II-1, producing the same amount of hydrogen as the base case, the overall plant efficiency is slightly reduced compared to base case. Case II-1 also performs poorer in terms of total CCR, consumption of NG per kg hydrogen produced and amount of CO₂-emission per kg hydrogen produced. With that in mind, implementation of a single membrane module and a LT-separation process seems uninteresting. However, liquefaction of hydrogen requires a 100% pure hydrogen, which is obtained from the membrane process.

In order to accomplish a power-balanced process, the base case needs additional NG supply to the gas turbine. This is similar for all single membrane cases when the hydrogen production equals the base case. The single membrane cases were also studied without any additional NG supply, which reduced the amount of produced hydrogen. For case II-1, considered without any additional NG, the overall plant efficiency slightly decreases compared to the case with extra NG supply. However, the CCR increases considerably. Rest of the single membrane cases follow the same trend.

The difference, in terms of efficiency, for the various single membrane cases and the base case are limited. However, for the cases considering a single membrane module, case II-3 generally scores better. Case II-3 introduced the possibility of elevated permeate pressure, making hydrogen compression superfluous. As a result of the sensitivity analysis, it was, however, seen that this case is not practically possible due to the lack of driving forces in the membrane, applying to both feed pressures studied.

Two membrane feed pressures were investigated, respectively 36 bar and 66 bar. The HYSYS simulations generally calculated a poorer overall plant efficiency for increased membrane feed pressure, due to the increased power demand. Higher inlet membrane pressure provides increased membrane driving forces, resulting in a higher hydrogen flux through the membrane. Increasing the membrane pressure was therefore assumed to affect the HRF-value of the membrane in a way that more hydrogen were produced. The sensitivity analysis of the single membrane module indicated however that a pressure increase from 36 bar inlet pressure to 66 bar only increased the HRF-value in the membrane to a small amount. This makes it an optimization question, since increasing the feed pressure increases the operational costs of the process but ensures a slightly better HRF-value, which leads to a potential reduction in required membrane area.

Case II-2 introduced the possibility of implementing two membrane modules, accordingly on each side of the LT-WGS. This process design outperforms the other cases when it comes to both overall plant efficiency and total CCR. The great performance of this process ensures excess power in the case that consider equal amount of produced hydrogen as base case. Excess power from a hydrogen producing facility should, however, be used for further hydrogen production. The process considering this case, where all excess power is used for further hydrogen production, stands out as the best solution in this case study. Compared to the conventional ATR process, the power balanced case with two membranes increase the overall plant

performance with 15.15% for 36 bar membrane feed pressure, and 13.2% for 66 bar membrane feed pressure. At the same time, this case also increases the overall CCR with 13.9% and 15.5%, respectively for 36 bar and 66 bar membrane feed pressure, compared to base case. Implementation of two membrane modules will however be more costly than implementation of a single membrane.

A result that was not quite as expected was the area requirements for case II-2. According to literature, the total membrane area should decrease as the process includes two membranes instead of one. However, results from the sensitivity analysis gave small deviations between the required area in case II-1 and case II-2. The results for the membrane area required in the single membrane cases were as expected. Despite the fact that the membrane area for case II-2 was greater than expected, case II-2 outperforms the single membrane cases in terms of efficiency and CCR. Meaning, replacing the conventional PSA unit and CO₂-capturing unit with the more unconventional membrane technology and a LT-process for CO₂-capture, contributes to a more efficient hydrogen producing plant if two membrane modules are included. Implementation of a single membrane module, however, will not provide any benefits compared to the base case other than the high purity of the produced hydrogen.

Case II-4 introduced the possibility of CO₂-removal in front of the membrane module. This reduces the membrane area considerably. Compared to case II-1, the area decreases with 76.85% and 78.46% for 36- and 66 bar membrane feed pressure, respectively. However, case II-4 performs poorly in terms of overall plant efficiency. Due to the large energy demand for this process, it emits more CO₂ than the other comparable cases as well. Employment of this process reduces the investment costs due to the decreased membrane area, but the operational cost increases because of the big power demand. Consequently, employment of this process solution is a tradeoff between investment costs and operating costs.

14. Further work

For hydrogen to become competitive to fossil fuels, the production of hydrogen must be economically viable and efficient. Hydrogen attracts much attention due to its environmental profile, as it has the ability to make the society less dependent on fossil fuels. This is of great interest in the carbon-restricted society the world is facing in order to reduce the climate impact. However, for hydrogen production from natural gas to be environmentally friendly, the production plant must include CO₂-capture, and the process must be as efficient as possible. With that in mind, future work will consist of continuing to develop hydrogen production plants, such that it becomes more effective. An interesting technology for this purpose is the use of membranes. This thesis introduced the possibility of implementing a single membrane module, or a sequential membrane and WGS module, instead of the traditional PSA unit. The hydrogen producing plant were also considered with the more immature low-temperature technology for CO₂-capture. As was seen, implementing one single membrane module did not give any advantage compared to base case. However, using two membranes for hydrogen purification gave significantly better results. Future work should therefore focus on develop this scenario.

Other possibilities for improving the plant efficiency will be to adopt more advanced technology, like the membrane reformer or the water-gas shift membrane-reactor, which was briefly discussed in Chapter 5. As Figure 14.1 illustrates, these technologies can make it possible to produce hydrogen and simultaneously separate CO₂, in the same unit. The reformer membrane reactor includes reforming, water-gas shift and hydrogen purification. If this unit proves to be efficient, it can make hydrogen production more economical and lead to a more competitive hydrogen production technology.

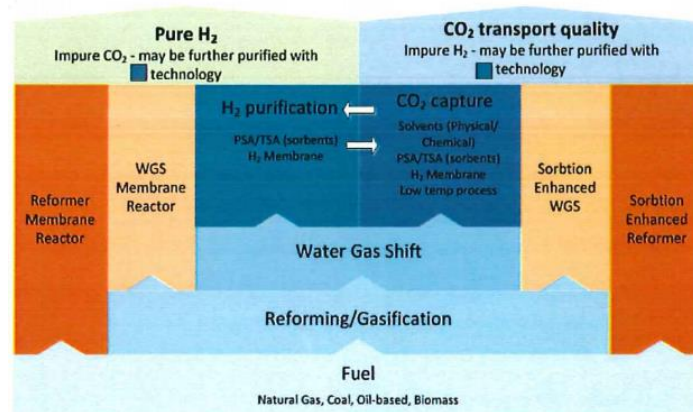


Figure 14.1: Possible production routes for hydrogen with CO₂ capture from hydrocarbon feedstock (Jordal and Anantharaman, 2013)

Another challenge for a hydrogen driven society is the low energy per kg hydrogen when it is at ambient condition. Future work should consequently emphasize possible reduction initiatives in cost for hydrogen compression and/or liquefaction, in order to make hydrogen as commercial available as fossil fuels.

It could have been interesting to study the impact on the process performance when increasing the membrane feed pressure further, in order to see if a 20 bar permeate-pressure is achievable with an acceptable membrane area. This thesis showed that 66 bar inlet pressure was not sufficient.

Heat integration of the processes in this thesis were primarily done by hand, since Aspen Energy Analyzer did not give the desired network design for the relevant cases. Even though heat-integration done manually

can obtain good results, it becomes complicated, time consuming and will probably not achieve the same results as if the integration was done by utilizing computer simulation programs. Since the heat- and power integration only was a sub task for this thesis, possible future work can be emphasized on complementary studies regarding heat integration of the processes. Future work can be to optimize the integration further, and make the integration more realistic by introducing more forbidden matches according to an actual process plant. It was not possible to become completely familiar with all possible opportunities in AEA due to a limited time scope. Further investigation of the program can result in important discoveries that make it suitable for use in this context as well.

15. References

- ASPENTECH. 2004. *Aspen HYSYS - Operations Guide* [Online]. Cambridge, USA. Available: <https://www.ualberta.ca/CMENG/che312/F06ChE416/HysysDocs/AspenHYSYSOperationsGuide.pdf> [Accessed 28. May 2015].
- ATSONIOS, K., KOUMANAKOS, A. K., PANOPOULOS, K. D., DOUKELIS, A. & KAKARAS, E. 2015. 12 - Using palladium membranes for carbon capture in natural gas combined cycle (NGCC) power plants: process integration and techno-economics. In: DOUKELIS, A., PANOPOULOS, K., KOUMANAKOS, A. & KAKARAS, E. (eds.) *Palladium Membrane Technology for Hydrogen Production, Carbon Capture and Other Applications*. Woodhead Publishing.
- ATSONIOS, K., PANOPOULOS, K. D., DOUKELIS, A., KOUMANAKOS, A. & KAKARAS, E. 2012. Exergy analysis of a hydrogen fired combined cycle with natural gas reforming and membrane assisted shift reactors for CO₂ capture. *Energy Conversion and Management*, 60, 196-203.
- BELLONA. 2014. *Pre-combustion* [Online]. Available: <http://bellona.org/ccs/technology/capture/post-combustion.html> [Accessed 17. October 2014].
- BERSTAD, D., ANANTHARAMAN, R. & NEKSÅ, P. Low-temperature CCS from an IGCC power plant and comparison with physical solvents. 11th International Conference on Greenhouse Gas Control Technologies, GHGT 2012, 2013a Kyoto. 2204-2211.
- BERSTAD, D., ANANTHARAMAN, R. & NEKSÅ, P. 2013b. Low-temperature CO₂ capture technologies - Applications and potential. *International Journal of Refrigeration*, 36, 1403-1416.
- BERSTAD, D., BÖRSCH, M., DECKER, L., ELLIOTT, A., HABERSTROH, C., LOUIS, J., LOWESMITH, B., MORTIMER, N., NEKSÅ, P., QUACK, H., SEEMAN, I., STOLZENBURG, K. & WALNUM, H. T. 2013c. *IDEALHY - Integrated Design for Demonstration of Efficient Liquefaction of Hydrogen* [Online]. Available: http://www.hydrogen.no/Kalender/2013/HFCNordic_2013/presentations/c2/IDEALHY_HFCNordic2013.pdf [Accessed 04. May 2015].
- BERSTAD, D., STANG, J. & NEKSÅ, P. 2009. A future energy chain based on liquefied hydrogen. *Hydrogen and Fuel Cells in the Nordic Countries*. Oslo: SINTEF Energy Research.
- BESANCON, B. M., HASANOV, V., IMBAULT-LASTAPIS, R., BENESCH, R., BARRIO, M. & MOLNVIK, M. J. 2009. Hydrogen quality from decarbonized fossil fuels to fuel cells. *International Journal of Hydrogen Energy*, 34, 2350-60.
- BOLLAND, O. 2013. *Natural Gas Technology - Thermal Power Generation*, Department of Energy and Process Engineering - NTNU.
- BRACHA, M., LORENZ, G., PATZELT, A. & WANNER, M. 1994. Large-scale hydrogen liquefaction in Germany. *International Journal of Hydrogen Energy*, 19, 53-59.
- CARAVELLA, A., HARA, S., DRIOLI, E. & BARBIERI, G. 2013. Sieverts law pressure exponent for hydrogen permeation through Pd-based membranes: Coupled influence of non-ideal diffusion and multicomponent external mass transfer. *International Journal of Hydrogen Energy*, 38, 16229-16244.
- CHANG, H.-F., PAI, W.-J., CHEN, Y.-J. & LIN, W.-H. 2010. Autothermal reforming of methane for producing high-purity hydrogen in a Pd/Ag membrane reactor. *International Journal of Hydrogen Energy*, 35, 12986-12992.
- CHEN, C.-H. & MA, Y. H. 2010. The effect of H₂S on the performance of Pd and Pd/Au composite membrane. *Journal of Membrane Science*, 362, 535-544.
- CHUN, C. M. & RAMANARAYANAN, T. A. 2009. Metal dusting resistant alumina forming coatings for syngas production. *Corrosion Science*, 51, 2770-2776.
- COLLODI, G. 2010. Hydrogen production via steam reforming with CO₂ capture. *Chemical Engineering Transactions*.

- DECABRIT. 2009. *D 1.4.1 Common Framework Definition Document* [Online]. Sintef Available: http://www.sintef.no/globalassets/project/decarbit/d-1.4.1-common_framework-0605091.pdf [Accessed 03. september 2014].
- EBNER, A. D. & RITTER, J. A. 2009. State-of-the-art adsorption and membrane separation processes for carbon dioxide production from carbon dioxide emitting industries. *Separation Science and Technology*, 44, 1273-1421.
- ENERGILINK. 2008a. *Energitetthet* [Online]. Available: <http://energilink.tu.no/leksikon/energitetthet.aspx> [Accessed 27. May 2015].
- ENERGILINK. 2008b. *Hydrogen, stadig underveis* [Online]. Available: <http://energilink.tu.no/no/hydrogen.aspx> [Accessed 27. May 2015].
- EPA. 2014. *Overview of greenhouse gases* [Online]. United States Environmental Protection Agency. Available: <http://www.epa.gov/climatechange/ghgemissions/gases/co2.html> [Accessed 03. November 2014].
- FU, C. 2015. *RE: Air Separation Unit*. Type to SKREBERGENE, K.
- GRABKE, H. J. 2003. Metal dusting. *Materials and Corrosion*, 54, 736-746.
- GUPTA, R. B. 2008. *Hydrogen fuel: production, transport, and storage*, Boca Raton, CRC Press.
- HIGGINBOTHAM, P., WHITE, V., FOGASH, K. & GUVELIOGLU, G. 2011. Oxygen supply for oxyfuel CO₂ capture. *International Journal of Greenhouse Gas Control*, 5, Supplement 1, S194-S203.
- IEA. 2012. *Energy Technology Perspectives 2012* [Online]. Available: http://www.iea.org/publications/freepublications/publication/ETP2012_free.pdf [Accessed 01. June 2015].
- IEA. 2014. *Key World Energy Statistics* [Online]. Available: <http://www.iea.org/publications/freepublications/publication/key-world-energy-statistics-2014.html> [Accessed 06. October 2014].
- IEAGHG. 2012. *CO₂ Capture at Gas Fired Power Plants* [Online]. Available: http://ieaghg.org/docs/General_Docs/Reports/2012-08.pdf [Accessed 18. October 2014].
- INTERGOVERNMENTAL PANEL ON CLIMATE CHANGE 2005. *Carbon Dioxide Capture and Storage*. Cambridge University Press: Cambridge.
- JECHEM. 2014. *Gas separation by Pressure Swing Adsorption (PSA)* [Online]. Available: http://www.jechem.co.jp/shirasagi_e/tech/psa.html [Accessed 20. September 2014].
- JONES, D., BHATTACHARYYA, D., TURTON, R. & ZITNEY, S. E. 2011. Optimal design and integration of an air separation unit (ASU) for an integrated gasification combined cycle (IGCC) power plant with CO₂ capture. *Fuel Processing Technology*, 92, 1685-1695.
- JORDAL, K. & ANANTHARAMAN, R. 2013. Production and use of Hydrogen in a CCS context.
- KUROKAWA, H., SHIRASAKI, Y. & YASUDA, I. Energy-efficient distributed carbon capture in hydrogen production from natural gas. *Energy Procedia*, 2011. 674-680.
- KYRIAKIDES, A. S., IPSAKIS, D., VOUTETAKIS, S., PAPADOPOULOU, S. & SEFERLIS, P. 2013. Modelling and simulation of a membrane reactor for the low temperature methane steam reforming. *Chemical Engineering Transactions*. Italian Association of Chemical Engineering - AIDIC.
- LENNTECH. 2015. *Chemical elements listed by boiling point* [Online]. Available: <http://www.lennotech.com/periodic-chart-elements/boiling-point.htm> [Accessed 01. June 2015].
- LINDE. 2009. *Hydrogen Recovery by Pressure Swing Adsorption* [Online]. Available: http://www.linde-engineering.com/internet.global.lindeengineering.global/en/images/HA_H_1_1_e_12_150dp_i19_6130.pdf [Accessed 20. September 2014].
- LIU, K., SONG, C. & SUBRAMANI, V. 2010. *Hydrogen and syngas production and purification technologies*, Hoboken, NJ, Wiley.
- MAIYA, P. S., ANDERSON, T. J., MIEVILLE, R. L., DUSEK, J. T., PICCIOLO, J. J. & BALACHANDRAN, U. 2000. Maximizing H₂ production by combined partial oxidation of CH₄ and water gas shift reaction. *Applied Catalysis A: General*, 196, 65-72.
- MANUM, S. B. 2009. *Kull. I Store norske leksikon* [Online]. Available: <https://snl.no/kull> [Accessed 02. October 2014].

- MARTELLI, E., NORD, L. O. & BOLLAND, O. 2012. Design criteria and optimization of heat recovery steam cycles for integrated reforming combined cycles with CO₂ capture. *Applied Energy*, 92, 255-268.
- MILJØDIREKTORATET. 2014. *Karbondioksid CO₂, utslipp* [Online]. Miljøstatus. Available: <http://www.miljostatus.no/Tema/Klima/Klimanorge/Utslipp-av-klimagasser/Karbondioksid-CO2-utslipp/> [Accessed 02. November 2014].
- MORAN, M. J. & SHAPIRO, H. N. 2010. *Fundamentals of engineering thermodynamics*, Hoboken, N.J., Wiley.
- MOULIJN, J. A., MAKKEE, M. & DIEPEN, A. V. 2013. *Chemical process technology*, Chichester, Wiley.
- MULDER, M. 1996. *Basic principles of membrane technology*, Dordrecht, Kluwer.
- NATIONAL ENERGY TECHNOLOGY LABORATORY. 2014. *A Faster Way to Reduce Carbon Footprints* [Online]. Available: <http://www.netl.doe.gov/newsroom/labnotes/apr-2014> [Accessed 14. February 2015].
- NATIONAL PROGRAMME ON TECHNOLOGY ENHANCED LEARNING. 2012. *Grand Composite Curve* [Online]. Available: <http://nptel.ac.in/courses/103107094/module4/lecture3/lecture3.pdf> [Accessed 23. March 2015].
- NAVARRO, R. M., PEÑA, M. A. & FIERRO, J. L. G. 2007. Hydrogen production reactions from carbon feedstocks: Fossil fuels and biomass. *Chemical Reviews*, 107, 3952-3991.
- OCKWIG, N. W. & NENOFF, T. M. 2007. Membranes for Hydrogen Separation. *Chemical Reviews*, 107, 4078-4110.
- ORMESTAD, H. 2009. *Membran* [Online]. Store norske leksikon. Available: <https://snl.no/membran> [Accessed 03. February 2015].
- PASQUALI, I. & BETTINI, R. 2008. Are pharmaceuticals really going supercritical? *International Journal of Pharmaceutics*, 364, 176-187.
- SIEMENS. 2015. *Gas turbine SGT6-5000F* [Online]. Available: <http://www.energy.siemens.com/hq/en/fossil-power-generation/gas-turbines/sgt6-5000f.htm#content=Description> [Accessed 28. May 2015].
- SMART, S., LIN, C. X. C., DING, L., THAMBIMUTHU, K. & DINIZ DA COSTA, J. C. 2010. Ceramic membranes for gas processing in coal gasification. *Energy & Environmental Science*, 3, 268-278.
- SMITH, A. R. & KLOSEK, J. 2001. A review of air separation technologies and their integration with energy conversion processes. *Fuel Processing Technology*, 70, 115-134.
- SMITH, R. 2005. *Chemical process design and integration*, Chichester, Wiley.
- SOLBRAA, E. 2013. *Natural Gas Technology - Gas Processing*, Department of Energy and Process Engineering - NTNU.
- THE ENGINEERING TOOLBOX. 2015. *Boiling Points of some common Fluids and Gases* [Online]. Available: http://www.engineeringtoolbox.com/boiling-points-fluids-gases-d_155.html [Accessed 01. June 2015].
- THE MCILVANE COMPANY. 2014. *Pressure Swing Adsorption plants* [Online]. Available: http://www.mcilvanecompany.com/DECISION_TREE/SUBSCRIBER/TREE/DESCRIPTIONTEXTLINKS/PRESSURE%20SWING%20ADSORPTION%20OF%20HYDROGEN.HTM [Accessed 12. November 2014].
- THE UNIVERSITY OF WAIKATO. 2014. *Industrial Energy Efficiency Division* [Online]. Available: http://www.energyefficiencynz.com/#!_capability/pinch-anaylsis [Accessed 08. May 2015].
- WALNUM, H. T., BERSTAD, D., DREACHER, M., NEKSÅ, P., QUACK, H., HABERSTROH, C. & ESSLER, J. 2012. Principles for the liquefaction of hydrogen with emphasis on precooling processes.
- WESTERN OREGON UNIVERSITY. 2006. *Energy from Fossil Fuels* [Online]. Available: https://www.wou.edu/las/physci/GS361/Energy_From_Fossil_Fuels.htm [Accessed 10. September 2014].
- ZERO EMISSION RESOURCE ORGANISATION. 2014. *What is CCS* [Online]. Available: <http://www.zeroco2.no/introduction/what-is-ccs> [Accessed 18. September 2014].
- ZUMDAHL, S. S. 2009. *Chemical principles*, Houghton Mifflin Company.

16. Appendix

Appendix A – Derivations

This Appendix provides the derivation of how and why the temperature affects respectively exothermic and endothermic reactions.

With high temperature and low pressure, the equilibriums in the reformer shifts towards the products, H₂ and CO. The equilibrium constant explains why the reformer stage is best suited with high temperatures. For a given equilibrium, $aA + bB = cC + dD$, the equilibrium constant is defined as:

$$K = \frac{C^c \cdot D^d}{A^a \cdot B^b} \quad (\text{A.1})$$

The exponential elements in this equation are the stoichiometric coefficients and the big letters are in the case of gas the partial pressure. A large K-value indicates that there is more product than reactants, meaning the equilibrium is shifted towards the product. K depends on temperature. This is seen from the Gibbs free energy equation:

$$\Delta G = -RT \ln K \quad (\text{A.2})$$

Solving for K gives:

$$K = e^{-\frac{\Delta G}{RT}} \quad (\text{A.3})$$

ΔG is the change in Gibbs energy, and is equal to $\Delta H - T\Delta S$. Putting this into the equation for K gives:

$$K = e^{-\frac{\Delta H}{RT}} \cdot e^{\frac{\Delta S}{R}} \quad (\text{A.4})$$

ΔS and ΔH changes very little compared to temperature, such that K increases when T increases for endothermic reactions since $\Delta H > 0$ for endothermic reactions. For exothermic reactions where $\Delta H < 0$, it is opposite (Zumdahl, 2009).

Appendix B – Unit Specifications

Unit specifications

The process equipment needs to work within some specific limits, as clarified in Table A.1. The specifications are a result of discussions with the supervisors and values from the DeCARBit's manual (DECABRit, 2009).

Table A.1: Unit specifications

<i>Pre-reformer specifications</i>	
T_{out} pre-reformer [°C]	400
ΔP [%]	5

<i>Reformer specifications</i>	
T_{out} reformer [°C]	950
P [bar]	30
ΔP [%]	5
S/C-ratio reformer	1.5

<i>Water – Gas shift specifications</i>	
T_{in} HTS [°C]	350
T_{in} LTS [°C]	200
ΔP [bar]	0.5

<i>PSA specifications</i>		
	<i>Hydrogen stream</i>	<i>Off-gas</i>
Hydrogen	0.85	0.15
Hydrocarbons	0	1
H ₂ O	0	1
CO	0	1
CO ₂	0	1
Nitrogen	0.08	0.92
Argon	0.34	0.66
NO	1	0
NO ₂	1	0

<i>Energy consumption pre-combustion CO₂ – capture</i>	
Specific reboiler energy (kJ/kg CO ₂)	900
Specific power consumption (kJ/kg CO ₂)	140

<i>ASU specifications</i>	
Specific separation energy [kWh/ton O ₂]	225
Compression energy [kWh/ton O ₂]	84.9

H₂ Liquefaction specifications

<i>Energy consumption [kWh/kg H₂]</i>	6.4
--	-----

Gas turbine specifications

<i>η_{pol} Compressor [%]</i>	90
<i>η_{pol} Turbine [%]</i>	85.7
<i>Max temp. after combustion chamber [°C]</i>	1318

Steam turbine specifications

<i>η_{HP} [%] (Isentropic)</i>	92
<i>η_{MP} [%]</i>	94
<i>η_{LP} [%]</i>	88

Pump specifications

<i>$\eta_{adiabatic}$ Pumps [%]</i>	75
--	----

Heat exchanger specifications

<i>ΔP, gas phase for cold and hot side [%]</i>	2
<i>ΔP, liquid phase for cold and hot side [MPa]</i>	0.04
<i>ΔT_{min} [°C]</i>	10

Membrane specifications

<i>Inlet pressure [bar] (starting point)</i>	36 / 66
<i>Inlet temperature [°C]</i>	400
<i>ΔP [bar]</i>	1

LT-process specifications

<i>Inlet pressure [bar]</i>	35 / 65
<i>Separation temperature [°C]</i>	-55
<i>Separation pressure [bar]</i>	110
<i>Specific CO₂ separation and compression work [MJ/kgCO₂(liq)]</i>	Depends on CO ₂ -cons.
<i>Compressor efficiency range [%]</i>	80-85
<i>Turbine efficiency range [%]</i>	84-88
<i>Assumed cooling circuits</i>	Propane and ethane

Appendix C - Calculations

This section gives a more complementary description of the results from the HYSYS models.

Results base case

Plant efficiency

Results of base case with hydrogen liquefaction

Natural Gas [A]

NG entering flow	kg/s	45.06
NG fuel	kg/s	5.136
NG HHV	kJ/kg	5.113e+004

Thermal energy input of natural gas – HHV basis		2566.52MW _{th}
---	--	-------------------------

Hydrogen output [B]

Hydrogen flow	kg/s	11.72
HHV hydrogen	kJ/kg	1.404e+005

Hydrogen output – HHV basis		1645.49MW _{th}
-----------------------------	--	-------------------------

<i>Overall efficiency [B / A · 100]</i>		64.11%
---	--	---------------

How much NG per H2

Hydrogen product [kg/s]	11.72
-------------------------	-------

NG input [kg/s]	50.18
-----------------	-------

Kg NG / kg H2	4.282
---------------	--------------

Total CCR

CO ₂ captured [kg/s]	103.15
---------------------------------	--------

CO ₂ emitted [kg/s]	29.82
--------------------------------	-------

CO ₂ Capturing Rate	77.57%
--------------------------------	---------------

Environmental impact

Stream	Mass fraction	CO ₂ equivalent	Equivalent CO ₂ flow (kg/h)
Exhaust gas			
CH ₄	0	23	0
CO	0	0.5	0
CO ₂	0.0506	1	107360.62
Total emission (tonCO ₂ /h)			107.36
Kg CO ₂ emitted per kg H ₂			2.545

Results case II-1, 36 bar membrane pressure

Plant efficiency

Natural Gas [A]

NG entering flow	kg/s	45.06
NG fuel	kg/s	5.56
NG HHV	kJ/kg	5.113e+004

Thermal energy input of natural gas – HHV basis 2588.20MW_{th}

Hydrogen output [B]

Hydrogen flow	kg/s	11.72
HHV hydrogen	kJ/kg	1.404e+005

Hydrogen output – HHV basis 1645.49MW_{th}

Overall efficiency $[B / A \cdot 100]$ **63.57%**

How much NG per H2

Hydrogen product [kg/s] 11.72

NG input [kg/h] 50.61

Kg NG / kg H2 **4.318**

Total CCR

CO₂ captured [kg/s] 101.55

CO₂ emitted [kg/s] 31.39

CO₂ Capturing Rate **76.39%**

Environmental impact

Stream	Mass fraction	CO ₂ equivalent	Equivalent CO ₂ flow (kg/h)
Exhaust gas			
CH ₄	0	23	0
CO	0	0.5	0
CO ₂	0.0538	1	113013.97
Total emission exhaust (ton/h)			113.01
Kg CO ₂ emitted per kg H ₂			2.679

Results case II-1, 36 bar membrane pressure, no extra NG

Plant efficiency

Natural Gas [A]

NG entering flow	kg/s	45.06
NG fuel	kg/s	0
NG HHV	kJ/kg	5.113e+004

Thermal energy input of natural gas – HHV basis 2303.92MW_{th}

Hydrogen output [B]

Hydrogen flow	kg/s	10.26
HHV hydrogen	kJ/kg	1.404e+005

Hydrogen output – HHV basis 1440.50MW_{th}

Overall efficiency $[B / A \cdot 100]$ **62.51%**

How much NG per H2

Hydrogen product [kg/s] 10.26

NG input [kg/h] 45.06

Kg NG / kg H2 **4.391**

Total CCR

CO₂ captured [kg/s] 98.65

CO₂ emitted [kg/s] 19.79

CO₂ Capturing Rate **83.29%**

Environmental impact

Stream	Mass fraction	CO ₂ equivalent	Equivalent CO ₂ flow (kg/h)
Exhaust gas			
CH ₄	0	23	0
CO	0	0.5	0
CO ₂	0.0394	1	71271.40
Total emission exhaust (ton/h)			71.3
Kg CO ₂ emitted per kg H ₂			1.93

Results case II-2, 36 bar membrane pressure

Plant efficiency

Natural Gas [A]

NG entering flow	kg/s	45.06
NG fuel	kg/s	0
NG HHV	kJ/kg	5.113e+004

Thermal energy input of natural gas – HHV basis 2303.92MW_{th}

Hydrogen output [B]

Hydrogen flow	kg/s	11.72
HHV hydrogen	kJ/kg	1.404e+005

Hydrogen output – HHV basis 1645.49MW_{th}

Excess power [C] 71.53MW_e

Overall efficiency [B + C / A · 100] **74.53%**

How much NG per H2

Hydrogen product [kg/s] 11.72

NG input [kg/h] 45.06

Kg NG / kg H2 **3.843**

Total CCR

CO₂ captured [kg/s] 103.36

CO₂ emitted [kg/s] 14.69

CO₂ Capturing Rate **87.56%**

Environmental impact

Stream	Mass fraction	CO ₂ equivalent	Equivalent CO ₂ flow (kg/h)
Exhaust gas			
CH ₄	0	23	0
CO	0	0.5	0
CO ₂	0.0429	1	52882.17
Total emission exhaust (ton/h)			52.9
Kg CO ₂ emitted per kg H ₂			1.253

Results case II-2, 36 bar membrane pressure, power balanced

Plant efficiency

Natural Gas [A]

NG entering flow	kg/s	45.06
NG fuel	kg/s	0
NG HHV	kJ/kg	5.113e+004

Thermal energy input of natural gas – HHV basis 2303.92MW_{th}

Hydrogen output [B]

Hydrogen flow	kg/s	12.11
HHV hydrogen	kJ/kg	1.404e+005

Hydrogen output – HHV basis 1700.24MW_{th}

Overall efficiency $[B / A \cdot 100]$ **73.82%**

How much NG per H2

Hydrogen product [kg/s] 12.11

NG input [kg/h] 45.06

Kg NG / kg H2 **3.719**

Total CCR

CO₂ captured [kg/s] 104.14

CO₂ emitted [kg/s] 13.72

CO₂ Capturing Rate **88.36%**

Environmental impact

Stream	Mass fraction	CO ₂ equivalent	Equivalent CO ₂ flow (kg/h)
Exhaust gas			
CH ₄	0	23	0
CO	0	0.5	0
CO ₂	0.0460	1	49391.18
Total emission exhaust (ton/h)			49.4
Kg CO ₂ emitted per kg H ₂			1.133

Results case II-3, 36 bar membrane pressure

Plant efficiency

Natural Gas [A]

NG entering flow	kg/s	45.06
NG fuel	kg/s	3.015
NG HHV	kJ/kg	5.113e+004

Thermal energy input of natural gas – HHV basis 2458.07MW_{th}

Hydrogen output [B]

Hydrogen flow	kg/s	11.72
HHV hydrogen	kJ/kg	1.404e+005

Hydrogen output – HHV basis 1645.49MW_{th}

Overall efficiency [B / A · 100] **66.94%**

How much NG per H2

Hydrogen product [kg/s] 11.72

NG input [kg/h] 48.06

Kg NG / kg H2 **4.101**

Total CCR

CO₂ captured [kg/s] 101.54

CO₂ emitted [kg/s] 24.58

CO₂ Capturing Rate **80.51%**

Environmental impact

Stream	Mass fraction	CO ₂ equivalent	Equivalent CO ₂ flow (kg/h)
Exhaust gas			
CH ₄	0	23	0
CO	0	0.5	0
CO ₂	0.0518	1	88490.07
Total emission exhaust (ton/h)			88.5
Kg CO ₂ emitted per kg H ₂			2.097

Results case II-3, 36 bar membrane pressure, no extra NG

Plant efficiency

Natural Gas [A]

NG entering flow	kg/s	45.06
NG fuel	kg/s	0
NG HHV	kJ/kg	5.113e+004

Thermal energy input of natural gas – HHV basis 2303.92MW_{th}

Hydrogen output [B]

Hydrogen flow	kg/s	10.88
HHV hydrogen	kJ/kg	1.404e+005

Hydrogen output – HHV basis 1527.55MW_{th}

Overall efficiency [B / A · 100] **66.31%**

How much NG per H2

Hydrogen product [kg/s] 10.88

NG input [kg/h] 45.06

Kg NG / kg H2 **4.140**

Total CCR

CO₂ captured [kg/s] 99.87

CO₂ emitted [kg/s] 18.40

CO₂ Capturing Rate **84.44%**

Environmental impact

Stream	Mass fraction	CO ₂ equivalent	Equivalent CO ₂ flow (kg/h)
Exhaust gas			
CH ₄	0	23	0
CO	0	0.5	0
CO ₂	0.0423	1	66242.01
Total emission exhaust (ton/h)			66.2
Kg CO ₂ emitted per kg H ₂			1.691

Results case II-4, 36 bar membrane pressure

Plant efficiency

Natural Gas [A]

NG entering flow	kg/s	45.06
NG fuel	kg/s	6.757
NG HHV	kJ/kg	5.113e+004

Thermal energy input of natural gas – HHV basis 2648.70MW_{th}

Hydrogen output [B]

Hydrogen flow	kg/s	11.72
HHV hydrogen	kJ/kg	1.404e+005

Hydrogen output – HHV basis 1645.49MW_{th}

Overall efficiency [B / A · 100] **62.10%**

How much NG per H2

Hydrogen product [kg/s] 11.72

NG input [kg/h] 51.80

Kg NG / kg H2 **4.420**

Total CCR

CO₂ captured [kg/s] 103.15

CO₂ emitted [kg/s] 34.15

CO₂ Capturing Rate **75.13%**

Environmental impact

Stream	Mass fraction	CO ₂ equivalent	Equivalent CO ₂ flow (kg/h)
Exhaust gas			
CH ₄	0	23	0
CO	0	0.5	0
CO ₂	0.0518	1	122934.47
Total emission exhaust (ton/h)			122.9
Kg CO ₂ emitted per kg H ₂			2.914

Results case II-4, 36 bar membrane pressure, no extra NG

Plant efficiency

Natural Gas [A]

NG entering flow	kg/s	45.06
NG fuel	kg/s	0
NG HHV	kJ/kg	5.113e+004

Thermal energy input of natural gas – HHV basis 2303.92MW_{th}

Hydrogen output [B]

Hydrogen flow	kg/s	9.925
HHV hydrogen	kJ/kg	1.404e+005

Hydrogen output – HHV basis 1392.99MW_{th}

Overall efficiency [B / A · 100] **60.48%**

How much NG per H2

Hydrogen product [kg/s] 9.925

NG input [kg/h] 45.06

Kg NG / kg H2 **4.539**

Total CCR

CO₂ captured [kg/s] 103.15

CO₂ emitted [kg/s] 16.21

CO₂ Capturing Rate **86.42%**

Environmental impact

Stream	Mass fraction	CO ₂ equivalent	Equivalent CO ₂ flow (kg/h)
Exhaust gas			
CH ₄	0	23	0
CO	0	0.5	0
CO ₂	0.0284	1	58352.7
Total emission exhaust (ton/h)			58.4
Kg CO ₂ emitted per kg H ₂			1.633

Results case II-1, 66 bar membrane pressure

Plant efficiency

Natural Gas [A]

NG entering flow	kg/s	45.06
NG fuel	kg/s	6.58
NG HHV	kJ/kg	5.113e+004

Thermal energy input of natural gas – HHV basis 2640.69MW_{th}

Hydrogen output [B]

Hydrogen flow	kg/s	11.72
HHV hydrogen	kJ/kg	1.404e+005

Hydrogen output – HHV basis 1645.49MW_{th}

Overall efficiency [B / A · 100] **62.32%**

How much NG per H2

Hydrogen product [kg/s] 11.72

NG input [kg/h] 51.63

Kg NG / kg H2 **4.405**

Total CCR

CO₂ captured [kg/s] 101.54

CO₂ emitted [kg/s] 34.09

CO₂ Capturing Rate **74.87%**

Environmental impact

Stream	Mass fraction	CO ₂ equivalent	Equivalent CO ₂ flow (kg/h)
Exhaust gas			
CH ₄	0	23	0
CO	0	0.5	0
CO ₂	0.0544	1	122718
Total emission exhaust (ton/h)			122.7
Kg CO ₂ emitted per kg H ₂			2.909

Results case II-1, 66 bar membrane pressure, no extra NG

Plant efficiency

Natural Gas [A]		
NG entering flow	kg/s	45.06
NG fuel	kg/s	0
NG HHV	kJ/kg	5.113e+004
<hr/>		
Thermal energy input of natural gas – HHV basis		2303.92MW _{th}
Hydrogen output [B]		
Hydrogen flow	kg/s	10.02
HHV hydrogen	kJ/kg	1.404e+005
<hr/>		
Hydrogen output – HHV basis		1405.40MW _{th}
Overall efficiency [B / A · 100]		61.04%

How much NG per H2

Hydrogen product [kg/s]	10.02
NG input [kg/h]	45.06
<hr/>	
Kg NG / kg H2	4.497

Total CCR

CO ₂ captured [kg/s]	98.18
CO ₂ emitted [kg/s]	20.33
<hr/>	
CO ₂ Capturing Rate	82.84%

Environmental impact

Stream	Mass fraction	CO ₂ equivalent	Equivalent CO ₂ flow (kg/h)
Exhaust gas			
CH ₄	0	23	0
CO	0	0.5	0
CO ₂	0.0384	1	73189.34
Total emission exhaust (ton/h)			73.2
Kg CO ₂ emitted per kg H ₂			2.030

Results case II-2, 66 bar membrane pressure

Plant efficiency

Natural Gas [A]

NG entering flow	kg/s	45.06
NG fuel	kg/s	0
NG HHV	kJ/kg	5.113e+004

Thermal energy input of natural gas – HHV basis 2303.92MW_{th}

Hydrogen output [B]

Hydrogen flow	kg/s	11.72
HHV hydrogen	kJ/kg	1.404e+005

Hydrogen output – HHV basis 1645.49MW_{th}

Excess power [C] 37.06MW_e

Overall efficiency [B + C / A · 100] **73.03%**

How much NG per H2

Hydrogen product [kg/s] 11.72

NG input [kg/h] 45.06

Kg NG / kg H2 **3.844**

Total CCR

CO₂ captured [kg/s] 104.96

CO₂ emitted [kg/s] 12.71

CO₂ Capturing Rate **89.20%**

Environmental impact

Stream	Mass fraction	CO ₂ equivalent	Equivalent CO ₂ flow (kg/h)
Exhaust gas	CH ₄	0	0
	CO	0	0
	CO ₂	0.0374	45768.23
Total emission exhaust (ton/h)			45.8
Kg CO ₂ emitted per kg H ₂			1.085

Results case II-2, 66 bar membrane pressure, power balanced

Plant efficiency

Natural Gas [A]

NG entering flow	kg/s	45.06
NG fuel	kg/s	0
NG HHV	kJ/kg	5.113e+004

Thermal energy input of natural gas – HHV basis 2303.92MW_{th}

Hydrogen output [B]

Hydrogen flow	kg/s	11.91
HHV hydrogen	kJ/kg	1.404e+005

Hydrogen output – HHV basis 1672.16MW_{th}

Overall efficiency [B / A · 100] **72.57%**

How much NG per H2

Hydrogen product [kg/s] 11.91

NG input [kg/h] 45.06

Kg NG / kg H2 **3.783**

Total CCR

CO₂ captured [kg/s] 105.33

CO₂ emitted [kg/s] 12.25

CO₂ Capturing Rate **89.58%**

Environmental impact

Stream	Mass fraction	CO ₂ equivalent	Equivalent CO ₂ flow (kg/h)
Exhaust gas			
CH ₄	0	23	0
CO	0	0.5	0
CO ₂	0.0384	1	44084.96
Total emission exhaust (ton/h)			44.1
Kg CO ₂ emitted per kg H ₂			1.028

Results case II-3, 66 bar membrane pressure

Plant efficiency

Natural Gas [A]

NG entering flow	kg/s	45.06
NG fuel	kg/s	4.004
NG HHV	kJ/kg	5.113e+004

Thermal energy input of natural gas – HHV basis 2507.95MW_{th}

Hydrogen output [B]

Hydrogen flow	kg/s	11.72
HHV hydrogen	kJ/kg	1.404e+005

Hydrogen output – HHV basis 1645.49MW_{th}

Overall efficiency [B / A · 100] **65.59%**

How much NG per H2

Hydrogen product [kg/s] 11.72

NG input [kg/h] 49.05

Kg NG / kg H2 **4.185**

Total CCR

CO₂ captured [kg/s] 101.55

CO₂ emitted [kg/s] 27.22

CO₂ Capturing Rate **78.86%**

Environmental impact

Stream	Mass fraction	CO ₂ equivalent	Equivalent CO ₂ flow (kg/h)
Exhaust gas			
CH ₄	0	23	0
CO	0	0.5	0
CO ₂	0.0527	1	97999.74
Total emission exhaust (ton/h)			98
Kg CO ₂ emitted per kg H ₂			2.323

Results case II-3, 66 bar membrane pressure, no extra NG

Plant efficiency

Natural Gas [A]

NG entering flow	kg/s	45.06
NG fuel	kg/s	0
NG HHV	kJ/kg	5.113e+004

Thermal energy input of natural gas – HHV basis 2303.92MW_{th}

Hydrogen output [B]

Hydrogen flow	kg/s	10.62
HHV hydrogen	kJ/kg	1.404e+005

Hydrogen output – HHV basis 1490.43MW_{th}

Overall efficiency [B / A · 100] **64.71%**

How much NG per H2

Hydrogen product [kg/s] 10.62

NG input [kg/h] 45.06

Kg NG / kg H2 **4.242**

Total CCR

CO₂ captured [kg/s] 99.34

CO₂ emitted [kg/s] 18.97

CO₂ Capturing Rate **83.97%**

Environmental impact

Stream	Mass fraction	CO ₂ equivalent	Equivalent CO ₂ flow (kg/h)
Exhaust gas			
CH ₄	0	23	0
CO	0	0.5	0
CO ₂	0.0409	1	68299.68
Total emission exhaust (ton/h)			68.3
Kg CO ₂ emitted per kg H ₂			1.787

Results case II-4, 66 bar membrane pressure

Plant efficiency

Natural Gas [A]

NG entering flow	kg/s	45.06
NG fuel	kg/s	7.307
NG HHV	kJ/kg	5.113e+004

Thermal energy input of natural gas – HHV basis 2676.85MW_{th}

Hydrogen output [B]

Hydrogen flow	kg/s	11.72
HHV hydrogen	kJ/kg	1.404e+005

Hydrogen output – HHV basis 1645.49MW_{th}

Overall efficiency [B / A · 100] **61.45%**

How much NG per H2

Hydrogen product [kg/s] 11.72

NG input [kg/h] 52.35

Kg NG / kg H2 **4.467**

Total CCR

CO₂ captured [kg/s] 103.15

CO₂ emitted [kg/s] 35.62

CO₂ Capturing Rate **74.33%**

Environmental impact

Stream	Mass fraction	CO ₂ equivalent	Equivalent CO ₂ flow (kg/h)
Exhaust gas			
CH ₄	0	23	0
CO	0	0.5	0
CO ₂	0.0521	1	128226.82
Total emission exhaust (ton/h)			128.2
Kg CO ₂ emitted per kg H ₂			3.039

Results case II-4, 66 bar membrane pressure, no extra NG

Plant efficiency

Natural Gas [A]

NG entering flow	kg/s	45.06
NG fuel	kg/s	0
NG HHV	kJ/kg	5.113e+004

Thermal energy input of natural gas – HHV basis 2303.92MW_{th}

Hydrogen output [B]

Hydrogen flow	kg/s	9.79
HHV hydrogen	kJ/kg	1.404e+005

Hydrogen output – HHV basis 1374.02MW_{th}

Overall efficiency [B / A · 100] **59.66%**

How much NG per H2

Hydrogen product [kg/s] 9.79

NG input [kg/h] 45.06

Kg NG / kg H2 **4.601**

Total CCR

CO₂ captured [kg/s] 103.15

CO₂ emitted [kg/s] 16.22

CO₂ Capturing Rate **86.41%**

Environmental impact

Stream	Mass fraction	CO ₂ equivalent	Equivalent CO ₂ flow (kg/h)
Exhaust gas			
CH ₄	0	23	0
CO	0	0.5	0
CO ₂	0.0276	1	58380.56
Total emission exhaust (ton/h)			58.4
Kg CO ₂ emitted per kg H ₂			1.657

Appendix D - Power distribution

Base case

Unit	Demand [MW]	Unit	Production [MW]
Power for pre-comb.	14.4	Gas turbine	512.3
H ₂ liquefaction	287.9	HP steam turbine	51.4
Gas turbine compressor	252.1	MP steam turbine	38.8
Pump work Steam cycle	2.9	LP steam turbine	66.9
CO ₂ compression	39		
Pump work CW	0.7		
Fuel compression	18.2		
ASU	54.2		
SUM	669.4	SUM	669.4

Base case, without hydrogen liquefaction

Unit	Demand [MW]	Unit	Production [MW]
Power for pre-comb.	14.4	Gas turbine	322.3
Gas turbine compressor	156.8	HP steam turbine	10.3
Pump work Steam cycle	1.1	MP steam turbine	32.8
CO ₂ compression	39	LP steam turbine	44.6
Pump work CW	0.7		
Fuel compression	18.2		
ASU	54.2		
SUM	285.4	SUM	410
Difference	124.6 MW		

Membrane case II-1 36 bar

Unit	Demand [MW]	Unit	Production [MW]
Hydrogen compression	97.79	Gas turbine	507.74
H ₂ liquefaction	270	HP steam turbine	59.6
Gas turbine compressor	248.8	MP steam turbine	50
Pump work Steam cycle	3.4	LP steam turbine	105.15
Membrane compressor	27.1		
CO ₂ sep. work	21.2		
ASU	54.2		
SUM	722.49	SUM	722.49

Membrane case II-1 36 bar, without hydrogen liquefaction

Unit	Demand [MW]	Unit	Production [MW]
Hydrogen compression	86.1	Gas turbine	301.9
Gas turbine compressor	145.4	HP steam turbine	46.9
Pump work Steam cycle	2.8	MP steam turbine	32.6
Membrane compressor	25.5	LP steam turbine	84
CO ₂ sep. work	21.2		
ASU	54.2		
SUM	335.2	SUM	465.4
Difference	130.2		

Membrane case II-1 66 bar

Unit	Demand [MW]	Unit	Production [MW]
Hydrogen compression	97.85	Gas turbine	545.2
H ₂ liquefaction	270	HP steam turbine	61.5
Gas turbine compressor	267.6	MP steam turbine	52.8
Pump work Steam cycle	3.5	LP steam turbine	117.7
Membrane compressor	69.43		
CO ₂ sep. work	14.6		
ASU	54.2		
SUM	777.2	SUM	777.2

Membrane case II-2 36 bar – same H₂ amount as base case

Unit	Demand [MW]	Unit	Production [MW]
Hydrogen compression	97.85	Gas turbine	300.5
H ₂ liquefaction	270	HP steam turbine	51.4
Gas turbine compressor	144.8	MP steam turbine	38.8
Pump work Steam cycle	2.87	LP steam turbine	300.5
Membrane compressor	28.1		
CO ₂ sep. work	21.86		
ASU	54.2		
SUM	619.7	SUM	691.2
Difference	71.5 MW		

Membrane case II-2 36 bar – power balanced

Unit	Demand [MW]	Unit	Production [MW]
Hydrogen compression	101.16	Gas turbine	261.5
H ₂ liquefaction	279.1	HP steam turbine	51.1
Gas turbine compressor	125.96	MP steam turbine	38.36
Pump work Steam cycle	2.85	LP steam turbine	261.5
Membrane compressor	28.1		
CO ₂ sep. work	21.09		
ASU	54.2		
SUM	612.46	SUM	612.46

Membrane case II-2 66 bar – same H₂ amount as base case

Unit	Demand [MW]	Unit	Production [MW]
Hydrogen compression	97.83	Gas turbine	299.6
H ₂ liquefaction	269.96	HP steam turbine	51.1
Gas turbine compressor	144.4	MP steam turbine	38.4
Pump work Steam cycle	2.86	LP steam turbine	299.6
Membrane compressor	67.26		
CO ₂ sep. work	15.1		
ASU	54.2		
SUM	651.6	SUM	688.7
Difference	37.1 MW		

Membrane case II-2 66 bar – power balanced

Unit	Demand [MW]	Unit	Production [MW]
Hydrogen compression	99.43	Gas turbine	280.7
H ₂ liquefaction	274.4	HP steam turbine	50.1
Gas turbine compressor	135.3	MP steam turbine	36.98
Pump work Steam cycle	2.8	LP steam turbine	280.7
Membrane compressor	67.3		
CO ₂ sep. work	15.06		
ASU	54.2		
SUM	648.5	SUM	648.5

Membrane case II-3, 36 bar inlet pressure

Unit	Demand [MW]	Unit	Production [MW]
H ₂ liquefaction	270	Gas turbine	413.4
Gas turbine compressor	201.4	HP steam turbine	48.9
Pump work Steam cycle	2.8	MP steam turbine	35.4
Membrane compressor	27.1	LP steam turbine	79
CO ₂ sep. work	21.2		
ASU	54.2		
SUM	576.7	SUM	576.7

Membrane case II-3, 66 bar inlet pressure

Unit	Demand [MW]	Unit	Production [MW]
H ₂ liquefaction	270	Gas turbine	450
Gas turbine compressor	219.8	HP steam turbine	51.6
Pump work Steam cycle	2.9	MP steam turbine	39
Membrane compressor	69.4	LP steam turbine	90.4
CO ₂ sep. work	14.7		
ASU	54.2		
SUM	631	SUM	631

Membrane case II-4 36 bar

Unit	Demand [MW]	Unit	Production [MW]
Hydrogen compression	97.85	Gas turbine	572.4
H ₂ liquefaction	270	HP steam turbine	59.9
Gas turbine compressor	282.1	MP steam turbine	50.5
Pump work Steam cycle	3.06	LP steam turbine	88.3
Membrane compressor	9.7		
CO ₂ sep. work	14.4		
ASU	54.2		
CO ₂ compression	39		
Pump work CW	0.7		
SUM	771	SUM	771

Membrane case II-4 66 bar

Unit	Demand [MW]	Unit	Production [MW]
Hydrogen compression	97.9	Gas turbine	593
H ₂ liquefaction	270	HP steam turbine	60.8
Gas turbine compressor	292.5	MP steam turbine	51.8
Pump work Steam cycle	3.1	LP steam turbine	94.2
Membrane compressor	28		
CO ₂ sep. work	14.4		
ASU	54.2		
CO ₂ compression	39		
Pump work CW	0.7		
SUM	799.8	SUM	799.8

Appendix E – Stream Data

This section provides stream data for the relevant case study. Overview pictures of the plant illustrates the stream numbers used in the data tables. Stream data is given for the base case, case II-1, case II-2 and case II-4, and for the membrane cases, the tables only provides data for cases producing the same amount of hydrogen as base case, and for 36 bar membrane inlet pressure. This is because the deviation between the cases are limited. However, after each case, a table will highlight the streams that differ from the focused case. First, the stream data of the base case is given.

Base Case

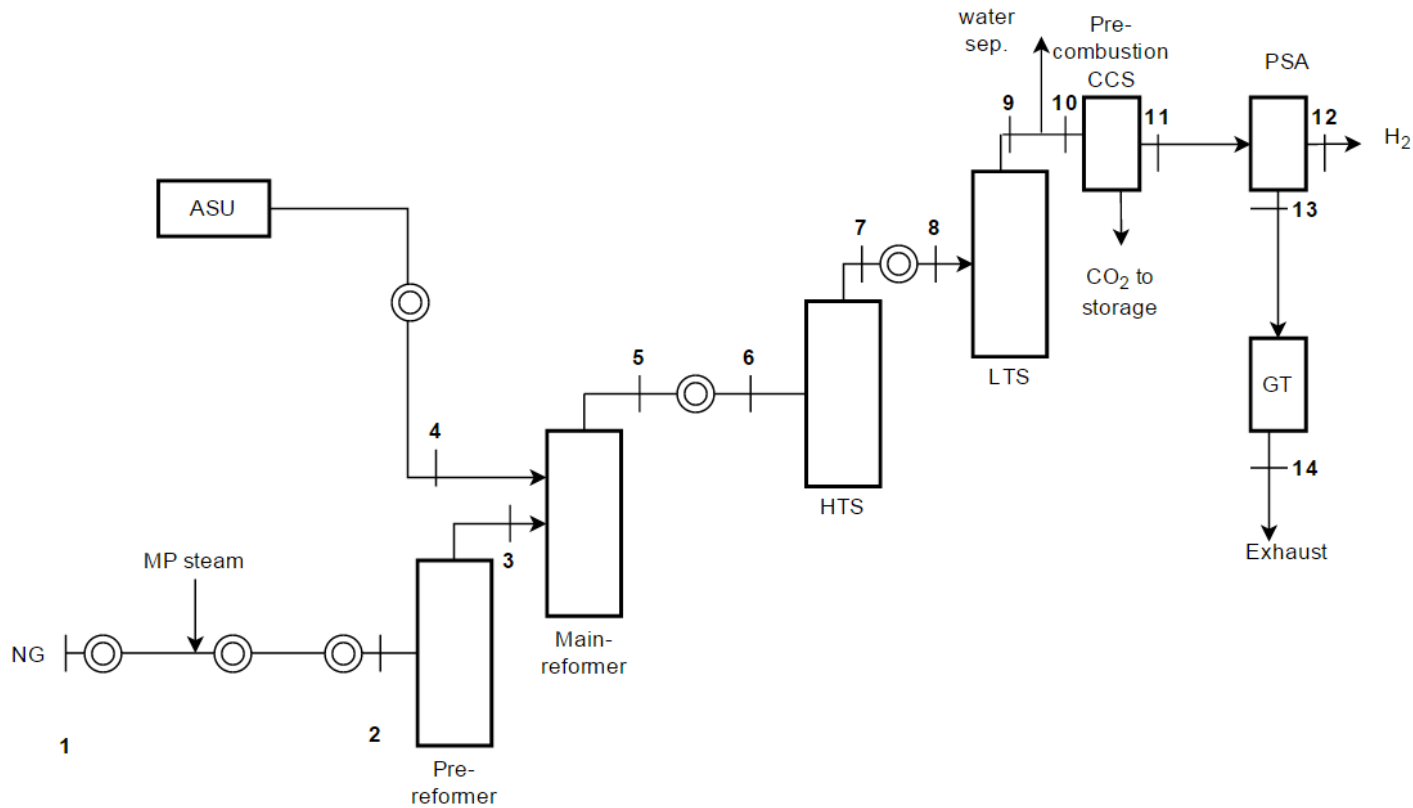


Figure 16.1: Overview base case

Table 16.1: HYSYS stream data, base case

		1	2	3	4	5	7	9	10	11	12	13	14
Temperature	°C	10	500	447.2	500	950	455	253.3	25	27	30	15	595
Pressure	Bar	70	34.18	32.47	29.95	29.95	28.53	27.27	26.26	24.80	20	1.35	1.04
Flow	Kgmole/h	9000	2.368e+004	2.495e+004	5434	4.207e+004	4.207e+004	4.207e+004	3.488e+004	2.628e+004	2.100e+004	5276	7.535e+004
Mass flow	Kg/h	1.622e+005	4.265e+005	4.265e+004	1.749e+005	6.015e+005	6.015e+005	6.015e+005	4.715e+005	9.893e+004	4.498e+004	5.396e+004	2.122e+006
Composition	Mol fraction												
	Methane	0.8900	0.3383	0.3583	0.0000	0.0123	0.0123	0.0123	0.0148	0.0197	0.0000	0.0981	0.0000
	Ethane	0.0700	0.0266	0.0000	0.0000	0.0000	0.0000	0.0000	0.0000	0.0000	0.0000	0.0000	0.0000
	Propane	0.0100	0.0038	0.0000	0.0000	0.0000	0.0000	0.0000	0.0000	0.0000	0.0000	0.0000	0.0000
	i-Butane	0.0005	0.0002	0.0000	0.0000	0.0000	0.0000	0.0000	0.0000	0.0000	0.0000	0.0000	0.0000
	n-Butane	0.0005	0.0002	0.0000	0.0000	0.0000	0.0000	0.0000	0.0000	0.0000	0.0000	0.0000	0.0000
	i-Pentane	0.0001	0.0000	0.0000	0.0000	0.0000	0.0000	0.0000	0.0000	0.0000	0.0000	0.0000	0.0000
	n-Pentane	0.0000	0.0000	0.0000	0.0000	0.0000	0.0000	0.0000	0.0000	0.0000	0.0000	0.0000	0.0000
	n-Hexane	0.0000	0.0000	0.0000	0.0000	0.0000	0.0000	0.0000	0.0000	0.0000	0.0000	0.0000	0.0000
	H2O	0.0000	0.6199	0.5374	0.0000	0.3131	0.2177	0.1717	0.0015	0.0001	0.0000	0.0003	0.1001
	CO	0.0000	0.0000	0.0000	0.0000	0.1496	0.5420	0.0083	0.0100	0.0132	0.0000	0.0658	0.0000
	Hydrogen	0.0000	0.0000	0.0682	0.0000	0.4466	0.1654	0.5879	0.7091	0.9370	0.9955	0.7001	0.0000
	CO2	0.0200	0.0076	0.0323	0.0000	0.0701	0.0042	0.2114	0.2545	0.0167	0.0000	0.0831	0.0324
	Nitrogen	0.0089	0.0034	0.0032	0.0176	0.0042	0.0000	0.0042	0.0050	0.0000	0.0007	0.0305	0.7300
	Oxygen	0.0000	0.0000	0.0000	0.9500	0.0000	0.0000	0.0000	0.0000	0.0000	0.0000	0.0000	0.1258
	H2S	0.0000	0.0000	0.0000	0.0000	0.0000	0.0000	0.0000	0.0000	0.0000	0.0000	0.0000	0.0000
	M-Mercaptan	0.0000	0.0000	0.0000	0.0000	0.0000	0.0000	0.0000	0.0000	0.0000	0.0000	0.0000	0.0000
	SO2	0.0000	0.0000	0.0000	0.0000	0.0000	0.0000	0.0000	0.0000	0.0000	0.0000	0.0000	0.0000
	Argon	0.0000	0.0000	0.0000	0.0324	0.0042	0.0042	0.0042	0.0050	0.0067	0.0029	0.0220	0.0103
	NO	0.0000	0.0000	0.0000	0.0000	0.0000	0.0000	0.0000	0.0000	0.0000	0.0000	0.0000	0.0014
	NO2	0.0000	0.0000	0.0000	0.0000	0.0000	0.0000	0.0000	0.0000	0.0000	0.0000	0.0000	0.0000

Case II-1

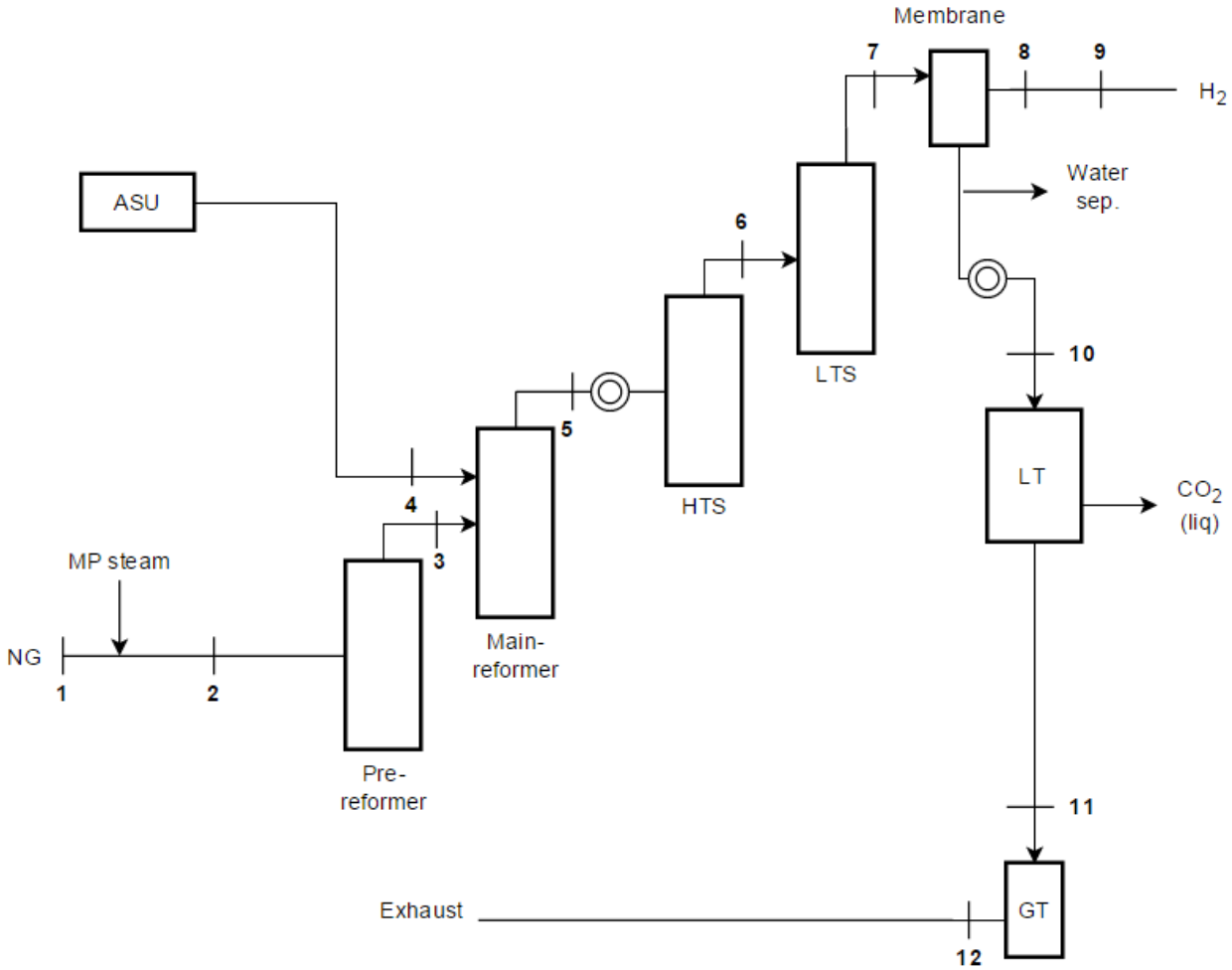


Figure 16.2: Overview case II-1

Table 16.2: HYSYS stream data, case II-1

		1	2	3	4	5	6	7	8	9	10	11	12
TEMPERATURE	°C	10	500	447.2	500	950	455	253.3	400	30	25	20	595
PRESSURE	Bar	70	34.18	32.47	29.95	29.95	28.53	27.27	1	20	35	23	1.04
FLOW	Kgmole/h	9000	2.368e+004	2.495e+004	5434	4.207e+004	4.207e+004	4.207e+004	2.093e+004	2.093e+004	1.388e+004	5477	7.464e+004
MASS FLOW	Kg/h	1.622e+005	4.265e+005	4.265e+004	1.749e+005	6.015e+005	6.015e+005	6.015e+005	4.219e+004	4.219e+004	4.270e+005	5.949e+004	2.101e+006
COMPOSITION													
	MOL FRACTION												
	Methane	0.8900	0.3383	0.3583	0.0000	0.0123	0.0123	0.0123	0.0000	0.0000	0.0373	0.0838	0.0000
	Ethane	0.0700	0.0266	0.0000	0.0000	0.0000	0.0000	0.0000	0.0000	0.0000	0.0000	0.0000	0.0000
	Propane	0.0100	0.0038	0.0000	0.0000	0.0000	0.0000	0.0000	0.0000	0.0000	0.0000	0.0000	0.0000
	i-Butane	0.0005	0.0002	0.0000	0.0000	0.0000	0.0000	0.0000	0.0000	0.0000	0.0000	0.0000	0.0000
	n-Butane	0.0005	0.0002	0.0000	0.0000	0.0000	0.0000	0.0000	0.0000	0.0000	0.0000	0.0000	0.0000
	i-Pentane	0.0001	0.0000	0.0000	0.0000	0.0000	0.0000	0.0000	0.0000	0.0000	0.0000	0.0000	0.0000
	n-Pentane	0.0000	0.0000	0.0000	0.0000	0.0000	0.0000	0.0000	0.0000	0.0000	0.0000	0.0000	0.0000
	n-Hexane	0.0000	0.0000	0.0000	0.0000	0.0000	0.0000	0.0000	0.0000	0.0000	0.0000	0.0000	0.0000
	H2O	0.0000	0.6199	0.5374	0.0000	0.3131	0.2177	0.1717	0.0000	0.0000	0.0014	0.0000	0.1032
	CO	0.0000	0.0000	0.0000	0.0000	0.1496	0.5420	0.0083	0.0000	0.0000	0.0251	0.0632	0.0000
	Hydrogen	0.0000	0.0000	0.0682	0.0000	0.4466	0.1654	0.5879	1.0000	1.0000	0.2742	0.6946	0.0000
	CO2	0.0200	0.0076	0.0323	0.0000	0.0701	0.0042	0.2114	0.0000	0.0000	0.6366	0.0974	0.0344
	Nitrogen	0.0089	0.0034	0.0032	0.0176	0.0042	0.0000	0.0042	0.0000	0.0000	0.0127	0.0315	0.7273
	Oxygen	0.0000	0.0000	0.0000	0.9500	0.0000	0.0000	0.0000	0.0000	0.0000	0.0000	0.0000	0.1228
	H2S	0.0000	0.0000	0.0000	0.0000	0.0000	0.0000	0.0000	0.0000	0.0000	0.0000	0.0000	0.0000
	M-Mercaptan	0.0000	0.0000	0.0000	0.0000	0.0000	0.0000	0.0000	0.0000	0.0000	0.0000	0.0000	0.0000
	SO2	0.0000	0.0000	0.0000	0.0000	0.0000	0.0000	0.0000	0.0000	0.0000	0.0000	0.0000	0.0000
	Argon	0.0000	0.0000	0.0000	0.0324	0.0042	0.0042	0.0042	0.0000	0.0000	0.0127	0.0295	0.0108
	NO	0.0000	0.0000	0.0000	0.0000	0.0000	0.0000	0.0000	0.0000	0.0000	0.0000	0.0000	0.0014
	NO2	0.0000	0.0000	0.0000	0.0000	0.0000	0.0000	0.0000	0.0000	0.0000	0.0000	0.0000	0.0000

Case II-2

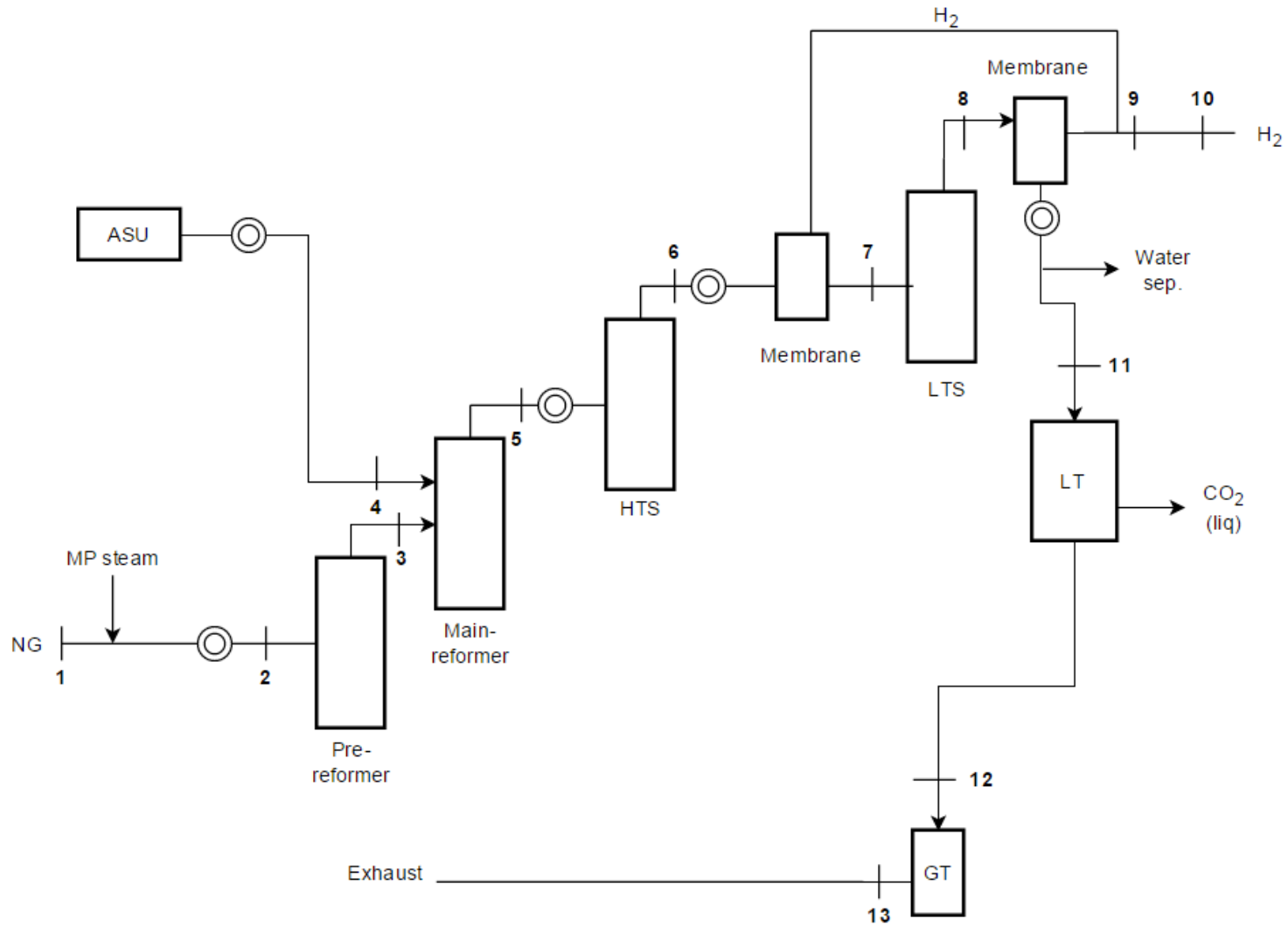


Figure 16.3: Overview case II-2

Table 16.3: HYSYS stream data case II-2

		1	2	3	4	5	6	7	8	9	10	11	12	13
TEMPERATURE	°C	10	500	447.2	500	950	455	200	280.8	400	30	25	20	595
PRESSURE	Bar	70	34.18	32.47	29.95	29.95	28.53	37.34	36.74	1	20	35	23	1.04
FLOW	Kgmole/h	9000	2.368e+004	2.495e+004	5434	4.207e+004	4.207e+004	2.611e+004	2.611e+004	2.093e+004	2.093e+004	1.402e+004	5464	4.417e+004
MASS FLOW	Kg/h	1.622e+005	4.265e+005	4.265e+004	1.749e+005	6.015e+005	6.015e+005	5.693e+005	5.693e+005	4.219e+004	4.219e+004	4.296e+005	5.541e+004	1.232e+006
COMPOSITION														
MOL FRACTION														
	Methane	0.8900	0.3383	0.3583	0.0000	0.0123	0.0123	0.0198	0.0198	0.0000	0.0000	0.0369	0.0835	0.0000
	Ethane	0.0700	0.0266	0.0000	0.0000	0.0000	0.0000	0.0000	0.0000	0.0000	0.0000	0.0000	0.0000	0.0000
	Propane	0.0100	0.0038	0.0000	0.0000	0.0000	0.0000	0.0000	0.0000	0.0000	0.0000	0.0000	0.0000	0.0000
	i-Butane	0.0005	0.0002	0.0000	0.0000	0.0000	0.0000	0.0000	0.0000	0.0000	0.0000	0.0000	0.0000	0.0000
	n-Butane	0.0005	0.0002	0.0000	0.0000	0.0000	0.0000	0.0000	0.0000	0.0000	0.0000	0.0000	0.0000	0.0000
	i-Pentane	0.0001	0.0000	0.0000	0.0000	0.0000	0.0000	0.0000	0.0000	0.0000	0.0000	0.0000	0.0000	0.0000
	n-Pentane	0.0000	0.0000	0.0000	0.0000	0.0000	0.0000	0.0000	0.0000	0.0000	0.0000	0.0000	0.0000	0.0000
	n-Hexane	0.0000	0.0000	0.0000	0.0000	0.0000	0.0000	0.0000	0.0000	0.0000	0.0000	0.0000	0.0000	0.0000
	H2O	0.0000	0.6199	0.5374	0.0000	0.3131	0.2177	0.3507	0.2713	0.0000	0.0000	0.0014	0.0000	0.1194
	CO	0.0000	0.0000	0.0000	0.0000	0.1496	0.5420	0.0874	0.0080	0.0000	0.0000	0.0149	0.0379	0.0000
	Hydrogen	0.0000	0.0000	0.0682	0.0000	0.4466	0.1654	0.2620	0.3414	1.0000	1.000	0.2814	0.7216	0.0000
	CO2	0.0200	0.0076	0.0323	0.0000	0.0701	0.0042	0.2666	0.3460	0.0000	0.0000	0.6403	0.0960	0.0272
	Nitrogen	0.0089	0.0034	0.0032	0.0176	0.0042	0.0000	0.0067	0.0067	0.0000	0.0000	0.0125	0.0315	0.7168
	Oxygen	0.0000	0.0000	0.0000	0.9500	0.0000	0.0000	0.0000	0.0000	0.0000	0.0000	0.0000	0.0000	0.1231
	H2S	0.0000	0.0000	0.0000	0.0000	0.0000	0.0000	0.0000	0.0000	0.0000	0.0000	0.0000	0.0000	0.0000
	M-Mercaptan	0.0000	0.0000	0.0000	0.0000	0.0000	0.0000	0.0000	0.0000	0.0000	0.0000	0.0000	0.0000	0.0000
	SO2	0.0000	0.0000	0.0000	0.0000	0.0000	0.0000	0.0000	0.0000	0.0000	0.0000	0.0000	0.0000	0.0000
	Argon	0.0000	0.0000	0.0000	0.0324	0.0042	0.0042	0.0067	0.0067	0.0000	0.0000	0.0126	0.0294	0.0122
	NO	0.0000	0.0000	0.0000	0.0000	0.0000	0.0000	0.0000	0.0000	0.0000	0.0000	0.0000	0.0000	0.0014
	NO2	0.0000	0.0000	0.0000	0.0000	0.0000	0.0000	0.0000	0.0000	0.0000	0.0000	0.0000	0.0000	0.0000

Case II-3, equals case II-1 in all streams except the permeate leaving the membrane. Instead of having 1 bar pressure, it is 22 bar. However, the composition, temperature and flow are equal. Meaning, no additional stream data is provided for this case.

Case II-4

When it comes to case II-4, this case equals the base case, inclusive stream 11. Rest of the stream data is provided in the Table 16.4 below.

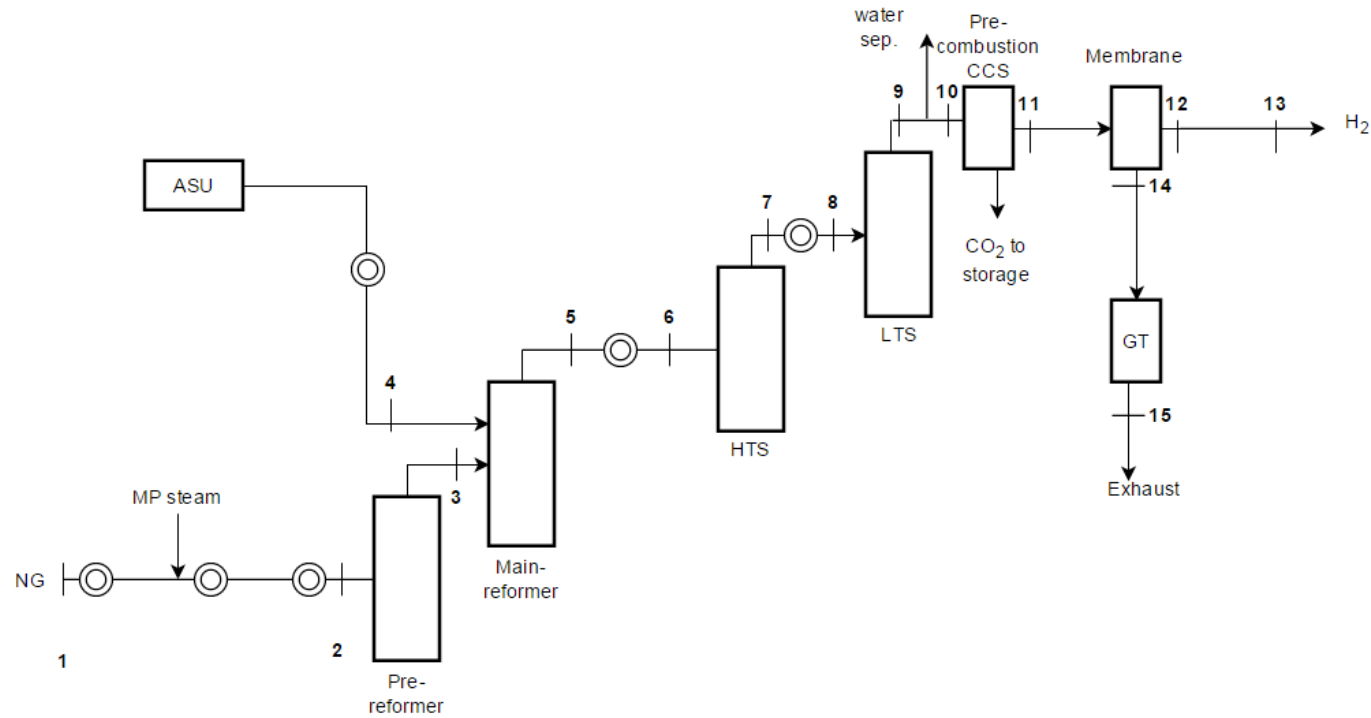


Figure 16.4: Overview case II-4

Table 16.4: HYSYS stream data, case II-4

		12	13	14	15
TEMPERATURE	°C	400	30	406.2	594
PRESSURE	Bar	1	20	35	1.05
FLOW	Kgmole/h	2.093e+004	2.093e+004	5349	8.420e+004
MASS FLOW	Kg/h	4.219e+004	4.219e+004	5.674e+004	2.374e+006
COMPOSITION					
	MOL FRACTION				
	Methane	0.0000	0.0000	0.0967	0.0000
	Ethane	0.0000	0.0000	0.0000	0.0000
	Propane	0.0000	0.0000	0.0000	0.0000
	i-Butane	0.0000	0.0000	0.0000	0.0000
	n-Butane	0.0000	0.0000	0.0000	0.0000
	i-Pentane	0.0000	0.0000	0.0000	0.0000
	n-Pentane	0.0000	0.0000	0.0000	0.0000
	n-Hexane	0.0000	0.0000	0.0000	0.0000
	H2O	0.0000	0.0000	0.0003	0.0985
	CO	0.0000	0.0000	0.0649	0.0000
	Hydrogen	1.0000	1.0000	0.6904	0.0000
	CO2	0.0000	0.0000	0.0820	0.0332
	Nitrogen	0.0000	0.0000	0.0327	0.7309
	Oxygen	0.0000	0.0000	0.0000	0.1253
	H2S	0.0000	0.0000	0.0000	0.0000
	M-Mercaptan	0.0000	0.0000	0.0000	0.0000
	SO2	0.0000	0.0000	0.0000	0.0000
	Argon	0.0000	0.0000	0.0329	0.0108
	NO	0.0000	0.0000	0.0000	0.0014
	NO2	0.0000	0.0000	0.0000	0.0000

Case II-1, no extra NG

Deviation for the membrane cases with no extra NG supply is summarized in Table 16.5-16.8.

For case II-1 with no extra NG, all stream data including stream 7 is equal to Table 16.2. Table 16.5 below gives the different stream.

Table 16.5: HYSYS stream data case II-1, no extra NG

		8	9	10	11	12
TEMPERATURE	°C	400	30	25	20	595
PRESSURE	Bar	1	20	35	23	1.04
FLOW	Kgmole/h	1.832e+004	1.832e+004	1.651e+004	8353	6.509e+004
MASS FLOW	Kg/h	3.693e+004	3.693e+004	4.327e+005	7.597e+004	1.810e+006
COMPOSITION						
	MOL FRACTION					
	Methane	0.0000	0.0000	0.0313	0.0568	0.0000
	Ethane	0.0000	0.0000	0.0000	0.0000	0.0000
	Propane	0.0000	0.0000	0.0000	0.0000	0.0000
	i-Butane	0.0000	0.0000	0.0000	0.0000	0.0000
	n-Butane	0.0000	0.0000	0.0000	0.0000	0.0000
	i-Pentane	0.0000	0.0000	0.0000	0.0000	0.0000
	n-Pentane	0.0000	0.0000	0.0000	0.0000	0.0000
	n-Hexane	0.0000	0.0000	0.0000	0.0000	0.0000
	H2O	0.0000	0.0000	0.0014	0.0000	0.1226
	CO	0.0000	0.0000	0.0211	0.0415	0.0000
	Hydrogen	1.0000	1.0000	0.3889	0.7680	0.0000
	CO2	0.0000	0.0000	0.5360	0.0931	0.0249
	Nitrogen	0.0000	0.0000	0.0106	0.0208	0.7158
	Oxygen	0.0000	0.0000	0.0000	0.0000	0.1242
	H2S	0.0000	0.0000	0.0000	0.0000	0.0000
	M-Mercaptan	0.0000	0.0000	0.0000	0.0000	0.0000
	SO2	0.0000	0.0000	0.0000	0.0000	0.0000
	Argon	0.0000	0.0000	0.0107	0.0198	0.0014
	NO	0.0000	0.0000	0.0000	0.0000	0.0000
	NO2	0.0000	0.0000	0.0000	0.0000	0.0000

Case II-2, no extra NG

The stream data for case II-2 that not produces the same amount of hydrogen as base case is provides in Table 16.6. Inclusive stream 8, this case equals case II-2 that produces the same hydrogen amount as base case, given in Table 16.3.

Table 16.6: HYSYS stream data, case II-2, power balanced

		9	10	11	12	13
TEMPERATURE	°C	400	30	25	20	595
PRESSURE	Bar	1	20	35	23	1.04
FLOW	Kgmole/h	2.163e+004	2.163e+004	1.332e+004	4681	3.843e+004
MASS FLOW	Kg/h	4.361e+004	4.361e+004	4.280e+005	5.074e+004	1.074e+006
COMPOSITION						
	MOL FRACTION					
	Methane	0.0000	0.0000	0.0388	0.0953	0.0000
	Ethane	0.0000	0.0000	0.0000	0.0000	0.0000
	Propane	0.0000	0.0000	0.0000	0.0000	0.0000
	i-Butane	0.0000	0.0000	0.0000	0.0000	0.0000
	n-Butane	0.0000	0.0000	0.0000	0.0000	0.0000
	i-Pentane	0.0000	0.0000	0.0000	0.0000	0.0000
	n-Pentane	0.0000	0.0000	0.0000	0.0000	0.0000
	n-Hexane	0.0000	0.0000	0.0000	0.0000	0.0000
	H2O	0.0000	0.0000	0.0014	0.0000	0.1170
	CO	0.0000	0.0000	0.0157	0.0442	0.0000
	Hydrogen	1.0000	1.0000	0.2436	0.6923	0.0000
	CO2	0.0000	0.0000	0.6740	0.0977	0.0242
	Nitrogen	0.0000	0.0000	0.0132	0.0366	0.7172
	Oxygen	0.0000	0.0000	0.0000	0.0000	0.1226
	H2S	0.0000	0.0000	0.0000	0.0000	0.0000
	M-Mercaptan	0.0000	0.0000	0.0000	0.0000	0.0000
	SO2	0.0000	0.0000	0.0000	0.0000	0.0000
	Argon	0.0000	0.0000	0.0132	0.0338	0.0126
	NO	0.0000	0.0000	0.0000	0.0000	0.0014
	NO2	0.0000	0.0000	0.0000	0.0000	0.0000

Case II-3, no extra NG

Case II-3, with no extra NG supply equals case II-1 inclusive stream 7. Table 16.7 below gives the stream data for the respective streams.

Table 16.7: HYSYS stream data, case II-3 with no extra NG supply

		8	9	10	11	12
TEMPERATURE	°C	400	30	25	20	595
PRESSURE	Bar	22	20	35	23	1.04
FLOW	Kgmole/h	1.943e+004	1.953e+004	1.539e+004	7126	5.625e+004
MASS FLOW	Kg/h	3.917e+004	3.917e+004	4.303e+005	6.892e+004	1.568e+006
COMPOSITION						
	MOL FRACTION					
	Methane	0.0000	0.0000	0.0336	0.0657	0.0000
	Ethane	0.0000	0.0000	0.0000	0.0000	0.0000
	Propane	0.0000	0.0000	0.0000	0.0000	0.0000
	i-Butane	0.0000	0.0000	0.0000	0.0000	0.0000
	n-Butane	0.0000	0.0000	0.0000	0.0000	0.0000
	i-Pentane	0.0000	0.0000	0.0000	0.0000	0.0000
	n-Pentane	0.0000	0.0000	0.0000	0.0000	0.0000
	n-Hexane	0.0000	0.0000	0.0000	0.0000	0.0000
	H2O	0.0000	0.0000	0.0014	0.0000	0.1203
	CO	0.0000	0.0000	0.0227	0.0486	0.0000
	Hydrogen	1.0000	1.0000	0.3448	0.7440	0.0000
	CO2	0.0000	0.0000	0.5747	0.0945	0.0268
	Nitrogen	0.0000	0.0000	0.0114	0.0243	0.7161
	Oxygen	0.0000	0.0000	0.0000	0.0000	0.1239
	H2S	0.0000	0.0000	0.0000	0.0000	0.0000
	M-Mercaptan	0.0000	0.0000	0.0000	0.0000	0.0000
	SO2	0.0000	0.0000	0.0000	0.0000	0.0000
	Argon	0.0000	0.0000	0.0114	0.0230	0.0114
	NO	0.0000	0.0000	0.0000	0.0000	0.0014
	NO2	0.0000	0.0000	0.0000	0.0000	0.0000

Case II-4, no extra NG

Case II-4, with no extra NG supply deviates from the case producing equal amount of hydrogen as base case, in the following streams, provided in Table 16.8.

Table 16.8: HYSYS stream data, case II-4 with no extra NG supply

		12	13	14	15
TEMPERATURE	°C	400	30	403.4	592
PRESSURE	Bar	1	20	35	1.04
FLOW	Kgmole/h	1.772e+004	1.772e+004	8555	7.402e+004
MASS FLOW	Kg/h	3.573e+004	3.573e+004	6.320e+004	2.056e+006
COMPOSITION					
	MOL FRACTION				
	Methane	0.0000	0.0000	0.0605	0.0000
	Ethane	0.0000	0.0000	0.0000	0.0000
	Propane	0.0000	0.0000	0.0000	0.0000
	i-Butane	0.0000	0.0000	0.0000	0.0000
	n-Butane	0.0000	0.0000	0.0000	0.0000
	i-Pentane	0.0000	0.0000	0.0000	0.0000
	n-Pentane	0.0000	0.0000	0.0000	0.0000
	n-Hexane	0.0000	0.0000	0.0000	0.0000
	H2O	0.0000	0.0000	0.0002	0.1168
	CO	0.0000	0.0000	0.0406	0.0000
	Hydrogen	1.0000	1.0000	0.8064	0.0000
	CO2	0.0000	0.0000	0.0513	0.0179
	Nitrogen	0.0000	0.0000	0.0205	0.7230
	Oxygen	0.0000	0.0000	0.0000	0.1298
	H2S	0.0000	0.0000	0.0000	0.0000
	M-Mercaptan	0.0000	0.0000	0.0000	0.0000
	SO2	0.0000	0.0000	0.0000	0.0000
	Argon	0.0000	0.0000	0.0206	0.0110
	NO	0.0000	0.0000	0.0000	0.0014
	NO2	0.0000	0.0000	0.0000	0.0000

The stream data for the cases with 66 bar membrane inlet pressure is not given. For the cases considering equal hydrogen production as base case, the only stream data that changes is the exhaust gas due to the extra NG supply. For the self-sustained cases without any additional NG supply, the stream data will change to some extent due to the change in HRF-value. The actual HRF-values in each case is provided in the thesis, and there will not be necessary to give all stream data for these cases.

Appendix F – LT-process simulation results

Values achieved from David Berstad, SINTEF, for estimating the specific work consumed in the LT-process.

For 35 bar initial pressure

Feed CO2 concentration	0,544465								
CCR	77,9949	82,08742	84,88976	86,8965	88,38226	89,50969	90,38088	91,06297	91,60174
w [kWh/kgCO2]	182,3934	187,6044	193,9251	200,4856	206,919	213,1886	219,2005	225,0288	230,7599
FUEL LP 1 - Master Comp Mole Frac (CO)	3,72E-02	3,86E-02	3,97E-02	4,05E-02	4,11E-02	4,15E-02	4,19E-02	4,21E-02	4,23E-02
FUEL LP 1 - Master Comp Mole Frac (Hydrogen)	0,662662	0,689951	0,710045	0,725314	0,737181	0,746567	0,754092	0,760185	0,765152
FUEL LP 1 - Master Comp Mole Frac (Methane)	5,42E-02	5,59E-02	5,71E-02	5,79E-02	5,83E-02	5,86E-02	5,88E-02	5,88E-02	5,88E-02
FUEL LP 1 - Master Comp Mole Frac (Nitrogen)	1,88E-02	1,95E-02	2,00E-02	2,04E-02	2,08E-02	2,10E-02	2,12E-02	2,13E-02	2,14E-02
FUEL LP 1 - Master Comp Mole Frac (Oxygen)	0	0	0	0	0	0	0	0	0
FUEL LP 1 - Master Comp Mole Frac (Argon)	1,85E-02	1,92E-02	1,96E-02	1,99E-02	2,01E-02	2,02E-02	2,03E-02	2,03E-02	2,04E-02
FUEL LP 1 - Master Comp Mole Frac (CO2)	0,208701	0,176828	0,153518	0,136001	0,12256	0,112082	0,103815	9,72E-02	9,20E-02

Feed CO2 concentration	0,614641								
CCR	83,39723	86,45829	88,54929	90,04367	91,14702	91,98111	92,62236	93,12099	93,50878
w [kWh/kgCO2]	175,9969	181,2189	187,0291	192,6888	198,1085	203,0216	207,8493	212,4319	217,1115
FUEL LP 1 - Master Comp Mole Frac (CO)	4,95E-02	5,15E-02	5,29E-02	5,39E-02	5,47E-02	5,52E-02	5,57E-02	5,60E-02	5,63E-02
FUEL LP 1 - Master Comp Mole Frac (Hydrogen)	0,619289	0,645003	0,664075	0,678658	0,690068	0,699156	0,70649	0,712464	0,717123
FUEL LP 1 - Master Comp Mole Frac (Methane)	7,15E-02	7,37E-02	7,50E-02	7,59E-02	7,63E-02	7,65E-02	7,65E-02	7,64E-02	7,63E-02
FUEL LP 1 - Master Comp Mole Frac (Nitrogen)	2,50E-02	2,60E-02	2,67E-02	2,72E-02	2,76E-02	2,79E-02	2,82E-02	2,84E-02	2,85E-02
FUEL LP 1 - Master Comp Mole Frac (Oxygen)	0	0	0	0	0	0	0	0	0
FUEL LP 1 - Master Comp Mole Frac (Argon)	2,45E-02	2,53E-02	2,59E-02	2,62E-02	2,64E-02	2,65E-02	2,66E-02	2,66E-02	2,66E-02
FUEL LP 1 - Master Comp Mole Frac (CO2)	0,210186	0,178549	0,155456	0,138147	0,124913	0,114643	0,10659	0,100233	9,52E-02

Feed CO2 concentration	0,65698								
CCR	86,11043	88,65397	90,3892	91,62726	92,53923	93,22399	93,74943	94,15536	94,47023
w [kWh/kgCO2]	172,5254	177,8497	183,1778	188,2869	192,9247	197,2328	201,2909	205,3592	208,751
FUEL LP 1 - Master Comp Mole Frac (CO)	5,94E-02	6,17E-02	6,34E-02	6,46E-02	6,55E-02	6,62E-02	6,67E-02	6,71E-02	6,74E-02
FUEL LP 1 - Master Comp Mole Frac (Hydrogen)	0,584797	0,609374	0,627699	0,641803	0,652919	0,661615	0,668813	0,674704	0,679547

FUEL LP 1 - Master Comp Mole Frac (Methane)	8,52E-02	8,76E-02	8,91E-02	8,99E-02	9,02E-02	9,04E-02	9,03E-02	9,00E-02	8,96E-02
FUEL LP 1 - Master Comp Mole Frac (Nitrogen)	3,00E-02	3,12E-02	3,20E-02	3,27E-02	3,32E-02	3,35E-02	3,38E-02	3,40E-02	3,42E-02
FUEL LP 1 - Master Comp Mole Frac (Oxygen)	0	0	0	0	0	0	0	0	0
FUEL LP 1 - Master Comp Mole Frac (Argon)	2,93E-02	3,02E-02	3,08E-02	3,11E-02	3,13E-02	3,15E-02	3,15E-02	3,15E-02	3,14E-02
FUEL LP 1 - Master Comp Mole Frac (CO2)	0,211345	0,179897	0,156982	0,139846	0,126784	0,116702	0,108834	0,102671	9,78E-02
Feed CO2 concentration	0,705584								
CCR	88,8376	90,86362	92,243	93,22156	93,94124	94,48048	94,88997	95,203	95,44222
w [kWh/kgCO2]	169,1338	174,0887	178,9683	183,3611	187,2261	190,5739	193,7672	196,5555	199,2809
FUEL LP 1 - Master Comp Mole Frac (CO)	7,43E-02	7,72E-02	7,93E-02	8,08E-02	8,20E-02	8,28E-02	8,34E-02	8,39E-02	8,42E-02
FUEL LP 1 - Master Comp Mole Frac (Hydrogen)	0,533377	0,556346	0,573643	0,586883	0,597575	0,606252	0,613383	0,619287	0,624188
FUEL LP 1 - Master Comp Mole Frac (Methane)	0,105437	0,108143	0,109655	0,110522	0,11069	0,110477	0,110009	0,109376	0,108644
FUEL LP 1 - Master Comp Mole Frac (Nitrogen)	3,75E-02	3,90E-02	4,01E-02	4,09E-02	4,15E-02	4,20E-02	4,23E-02	4,26E-02	4,28E-02
FUEL LP 1 - Master Comp Mole Frac (Oxygen)	0	0	0	0	0	0	0	0	0
FUEL LP 1 - Master Comp Mole Frac (Argon)	3,63E-02	3,74E-02	3,80E-02	3,85E-02	3,86E-02	3,87E-02	3,86E-02	3,85E-02	3,83E-02
FUEL LP 1 - Master Comp Mole Frac (CO2)	0,213038	0,181878	0,159239	0,142386	0,129603	0,119797	0,112225	0,106374	0,101876
Feed CO2 concentration	0,74997								
CCR	91,03872	92,64747	93,74123	94,51656	95,08243	95,50325	95,81942	96,05739	96,23515
w [kWh/kgCO2]	166,2124	170,8751	175,2251	178,9759	182,2104	184,7279	186,8798	188,7287	190,9643
FUEL LP 1 - Master Comp Mole Frac (CO)	9,30E-02	9,67E-02	9,94E-02	0,101353	0,102795	0,103856	0,104623	0,105158	0,105505
FUEL LP 1 - Master Comp Mole Frac (Hydrogen)	0,469419	0,490293	0,506307	0,519006	0,529334	0,537885	0,545049	0,551084	0,556173
FUEL LP 1 - Master Comp Mole Frac (Methane)	0,130344	0,133394	0,134887	0,13534	0,135094	0,134381	0,133366	0,132166	0,130869
FUEL LP 1 - Master Comp Mole Frac (Nitrogen)	4,70E-02	4,89E-02	5,03E-02	5,14E-02	5,22E-02	5,28E-02	5,32E-02	5,35E-02	5,38E-02
FUEL LP 1 - Master Comp Mole Frac (Oxygen)	0	0	0	0	0	0	0	0	0
FUEL LP 1 - Master Comp Mole Frac (Argon)	4,51E-02	4,63E-02	4,70E-02	4,74E-02	4,75E-02	4,74E-02	4,72E-02	4,69E-02	4,65E-02
FUEL LP 1 - Master Comp Mole Frac (CO2)	0,215083	0,184305	0,162036	0,145546	0,133143	0,123734	0,116581	0,111173	0,107147

For 65 bar initial pressure

Feed CO2 concentration	0,544465									
CCR	87,93416	88,80858	89,53808	90,15041	90,66763	91,10668	91,48073	91,80018	92,07335	
w [kWh/kgCO2]	122,2363	126,4359	130,3807	134,1456	137,7448	141,2168	144,6332	148,0618	151,3414	
FUEL LP 1 - Master Comp Mole Frac (CO)	4,09E-02	4,12E-02	4,15E-02	4,18E-02	4,20E-02	4,22E-02	4,23E-02	4,24E-02	4,25E-02	
FUEL LP 1 - Master Comp Mole Frac (Hydrogen)	0,733501	0,740672	0,74679	0,752055	0,756606	0,760556	0,763992	0,766988	0,769602	
FUEL LP 1 - Master Comp Mole Frac (Methane)	5,82E-02	5,85E-02	5,86E-02	5,87E-02	5,88E-02	5,88E-02	5,88E-02	5,88E-02	5,87E-02	
FUEL LP 1 - Master Comp Mole Frac (Nitrogen)	2,07E-02	2,08E-02	2,10E-02	2,11E-02	2,12E-02	2,13E-02	2,14E-02	2,15E-02	2,15E-02	
FUEL LP 1 - Master Comp Mole Frac (Oxygen)	0	0	0	0	0	0	0	0	0	
FUEL LP 1 - Master Comp Mole Frac (Argon)	2,00E-02	2,01E-02	2,02E-02	2,03E-02	2,03E-02	2,03E-02	2,04E-02	2,04E-02	2,04E-02	
FUEL LP 1 - Master Comp Mole Frac (CO2)	0,126674	0,118628	0,111816	0,106018	0,101063	9,68E-02	9,32E-02	9,00E-02	8,73E-02	

Feed CO2 concentration	0,614641									
CCR	90,81447	91,46253	92,00176	92,45277	92,8321	93,15242	93,42358	93,65337	93,84799	
w [kWh/kgCO2]	126,6347	129,698	132,5359	135,2473	137,8199	140,1953	142,7224	145,1032	147,5061	
FUEL LP 1 - Master Comp Mole Frac (CO)	5,44E-02	5,49E-02	5,53E-02	5,56E-02	5,58E-02	5,60E-02	5,62E-02	5,63E-02	5,64E-02	
FUEL LP 1 - Master Comp Mole Frac (Hydrogen)	0,686467	0,693418	0,699347	0,704471	0,708918	0,712792	0,716173	0,719128	0,721709	
FUEL LP 1 - Master Comp Mole Frac (Methane)	7,63E-02	7,64E-02	7,65E-02	7,65E-02	7,65E-02	7,64E-02	7,63E-02	7,61E-02	7,59E-02	
FUEL LP 1 - Master Comp Mole Frac (Nitrogen)	2,75E-02	2,78E-02	2,80E-02	2,81E-02	2,83E-02	2,84E-02	2,85E-02	2,85E-02	2,86E-02	
FUEL LP 1 - Master Comp Mole Frac (Oxygen)	0	0	0	0	0	0	0	0	0	
FUEL LP 1 - Master Comp Mole Frac (Argon)	2,64E-02	2,65E-02	2,65E-02	2,66E-02	2,66E-02	2,66E-02	2,66E-02	2,65E-02	2,65E-02	
FUEL LP 1 - Master Comp Mole Frac (CO2)	0,128961	0,121055	0,114385	0,108732	0,103925	9,98E-02	9,63E-02	9,34E-02	9,08E-02	

Feed CO2 concentration	0,65698									
CCR	92,26527	92,79913	93,24306	93,61321	93,92337	94,18406	94,4006	94,58488	94,73945	
w [kWh/kgCO2]	128,0329	130,4449	132,6884	134,7879	136,6618	138,576	140,3596	142,1588	144,0274	
FUEL LP 1 - Master Comp Mole Frac (CO)	6,53E-02	6,58E-02	6,62E-02	6,66E-02	6,69E-02	6,71E-02	6,73E-02	6,75E-02	6,76E-02	
FUEL LP 1 - Master Comp Mole Frac (Hydrogen)	0,649341	0,656172	0,661998	0,667054	0,671463	0,67532	0,678445	0,68138	0,683948	
FUEL LP 1 - Master Comp Mole Frac (Methane)	9,03E-02	9,03E-02	9,03E-02	9,02E-02	9,01E-02	8,98E-02	8,97E-02	8,95E-02	8,92E-02	
FUEL LP 1 - Master Comp Mole Frac (Nitrogen)	3,30E-02	3,33E-02	3,35E-02	3,37E-02	3,39E-02	3,40E-02	3,42E-02	3,42E-02	3,43E-02	
FUEL LP 1 - Master Comp Mole Frac (Oxygen)	0	0	0	0	0	0	0	0	0	
FUEL LP 1 - Master Comp Mole Frac (Argon)	3,13E-02	3,14E-02	3,14E-02	3,15E-02	3,14E-02	3,14E-02	3,14E-02	3,13E-02	3,13E-02	

FUEL LP 1 - Master Comp Mole Frac (CO2)	0,130777	0,122988	0,116438	0,110909	0,106228	0,102262	9,89E-02	9,61E-02	9,37E-02
Feed CO2 concentration	0,705584								
CCR	93,73036	94,14895	94,49427	94,78294	95,02319	95,22344	95,3902	95,52861	95,64277
w [kWh/kgCO2]	128,768	130,4884	132,0724	133,4004	134,5252	135,6222	136,6503	137,8198	139,221
FUEL LP 1 - Master Comp Mole Frac (CO)	8,16E-02	8,23E-02	8,28E-02	8,33E-02	8,36E-02	8,39E-02	8,41E-02	8,43E-02	8,44E-02
FUEL LP 1 - Master Comp Mole Frac (Hydrogen)	0,594288	0,60102	0,606479	0,611456	0,615828	0,619678	0,623069	0,626056	0,628679
FUEL LP 1 - Master Comp Mole Frac (Methane)	0,110675	0,11049	0,110466	0,110165	0,109777	0,109325	0,10883	0,108307	0,107768
FUEL LP 1 - Master Comp Mole Frac (Nitrogen)	4,13E-02	4,17E-02	4,20E-02	4,22E-02	4,24E-02	4,26E-02	4,27E-02	4,29E-02	4,29E-02
FUEL LP 1 - Master Comp Mole Frac (Oxygen)	0	0	0	0	0	0	0	0	0
FUEL LP 1 - Master Comp Mole Frac (Argon)	3,86E-02	3,86E-02	3,87E-02	3,86E-02	3,86E-02	3,85E-02	3,83E-02	3,82E-02	3,81E-02
FUEL LP 1 - Master Comp Mole Frac (CO2)	0,133494	0,12589	0,11955	0,114223	0,109752	0,106004	0,102871	0,100268	9,81E-02
Feed CO2 concentration	0,74997								
CCR	94,91216	95,24318	95,51433	95,73759	95,9217	96,07332	96,19762	96,29867	96,37971
w [kWh/kgCO2]	128,7951	129,9269	130,748	131,2823	131,7202	132,0835	132,7512	133,4929	134,4729
FUEL LP 1 - Master Comp Mole Frac (CO)	1,02E-01	1,03E-01	1,04E-01	0,104425	0,104855	0,105187	0,105434	0,105606	0,105714
FUEL LP 1 - Master Comp Mole Frac (Hydrogen)	0,526111	0,532485	0,538111	0,5431	0,547537	0,551488	0,555006	0,558131	0,560898
FUEL LP 1 - Master Comp Mole Frac (Methane)	0,13523	0,134892	0,134358	0,133685	0,132914	0,132075	0,131193	0,130289	0,12938
FUEL LP 1 - Master Comp Mole Frac (Nitrogen)	5,19E-02	5,24E-02	5,28E-02	5,31E-02	5,33E-02	5,35E-02	5,37E-02	5,38E-02	5,39E-02
FUEL LP 1 - Master Comp Mole Frac (Oxygen)	0	0	0	0	0	0	0	0	0
FUEL LP 1 - Master Comp Mole Frac (Argon)	4,75E-02	4,75E-02	4,74E-02	4,73E-02	4,71E-02	4,69E-02	4,66E-02	4,64E-02	4,61E-02
FUEL LP 1 - Master Comp Mole Frac (CO2)	0,136907	0,129578	0,123499	0,118455	0,114278	0,110836	0,108024	0,105755	0,10396

Appendix G – HYSYS screenshots

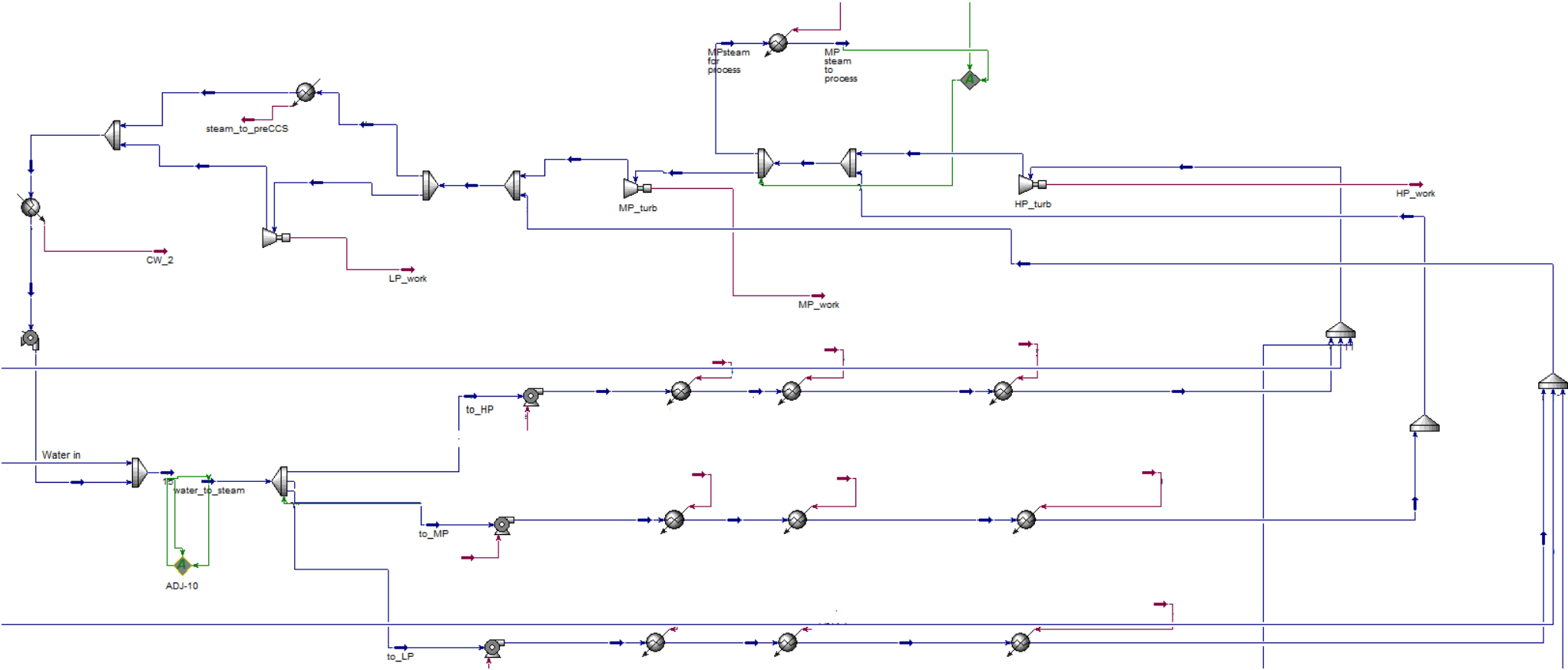


Figure A 1: Steam cycle HYSYS

Appendix H – Grand Composite Curves and AEA – networks

This appendix gives the relevant grand composite curves for all cases, except the membrane cases considering 66 bar membrane inlet pressure. However, the grand composite curves for these cases will not deviate much from the 36 bar membrane cases. Aspen Energy Analyzer recommended network design for all cases, which were used as inspiration for the developed heat-integrated cases. Some of the recommended designs are provided in this Appendix.

Base Case

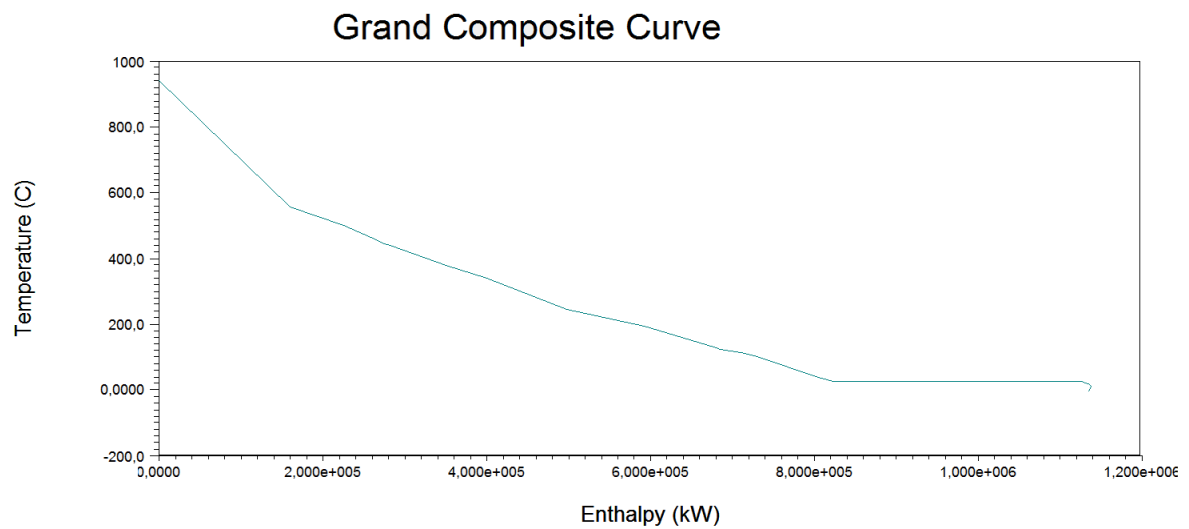


Figure A 2: GGC Base case

Figure A.3 provides one of the recommended network design according to Aspen Energy Analyzer.

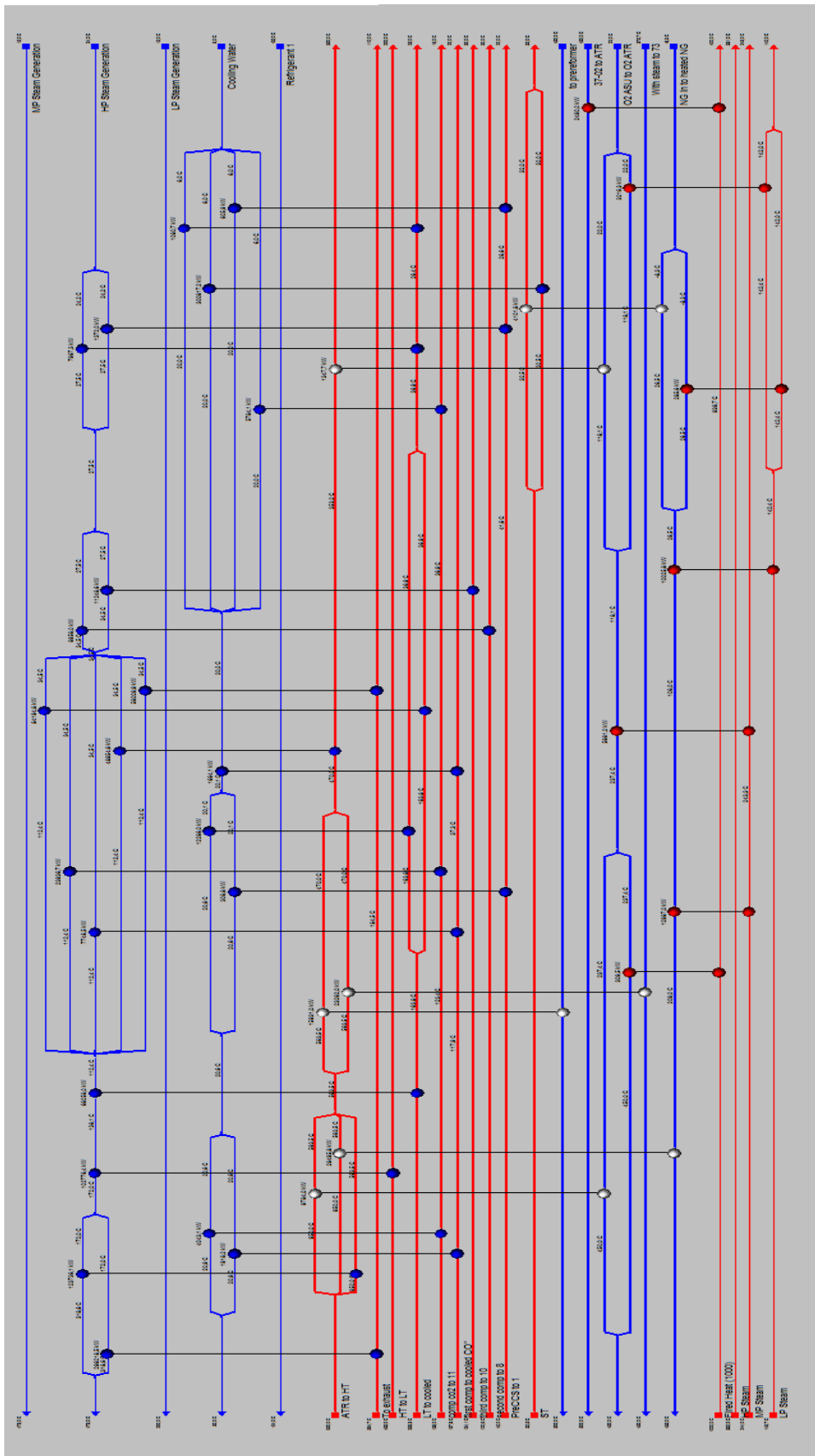


Figure A 3: One of the recommended designs from AEA

Case II-1

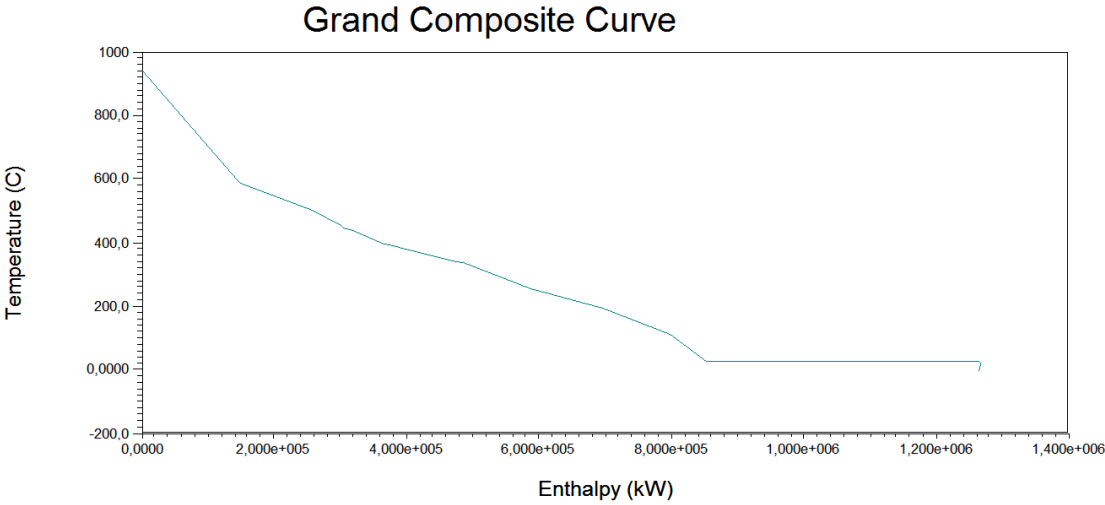


Figure A 4: GCC Case II-1

Case II-2

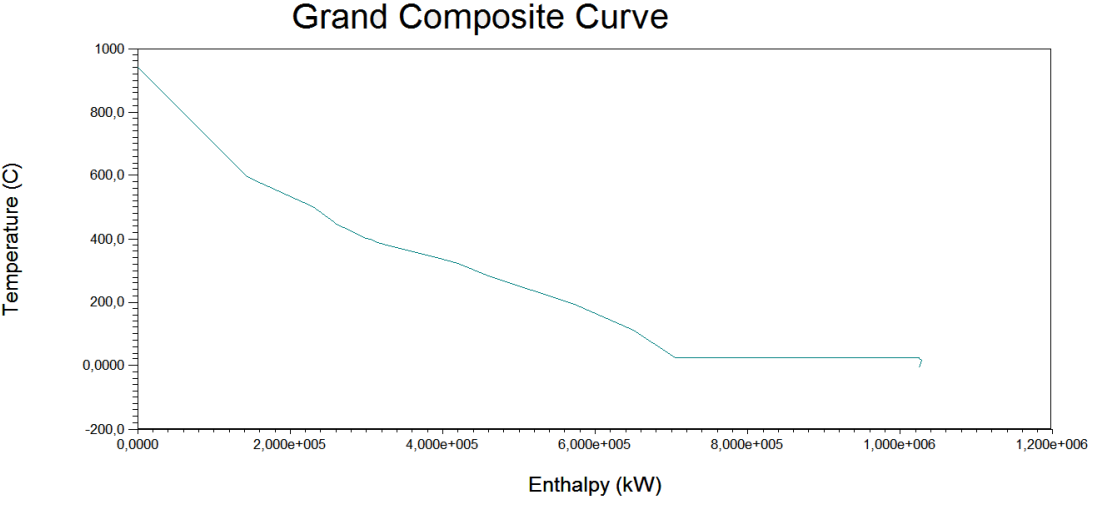


Figure A 5: GCC Case II-2

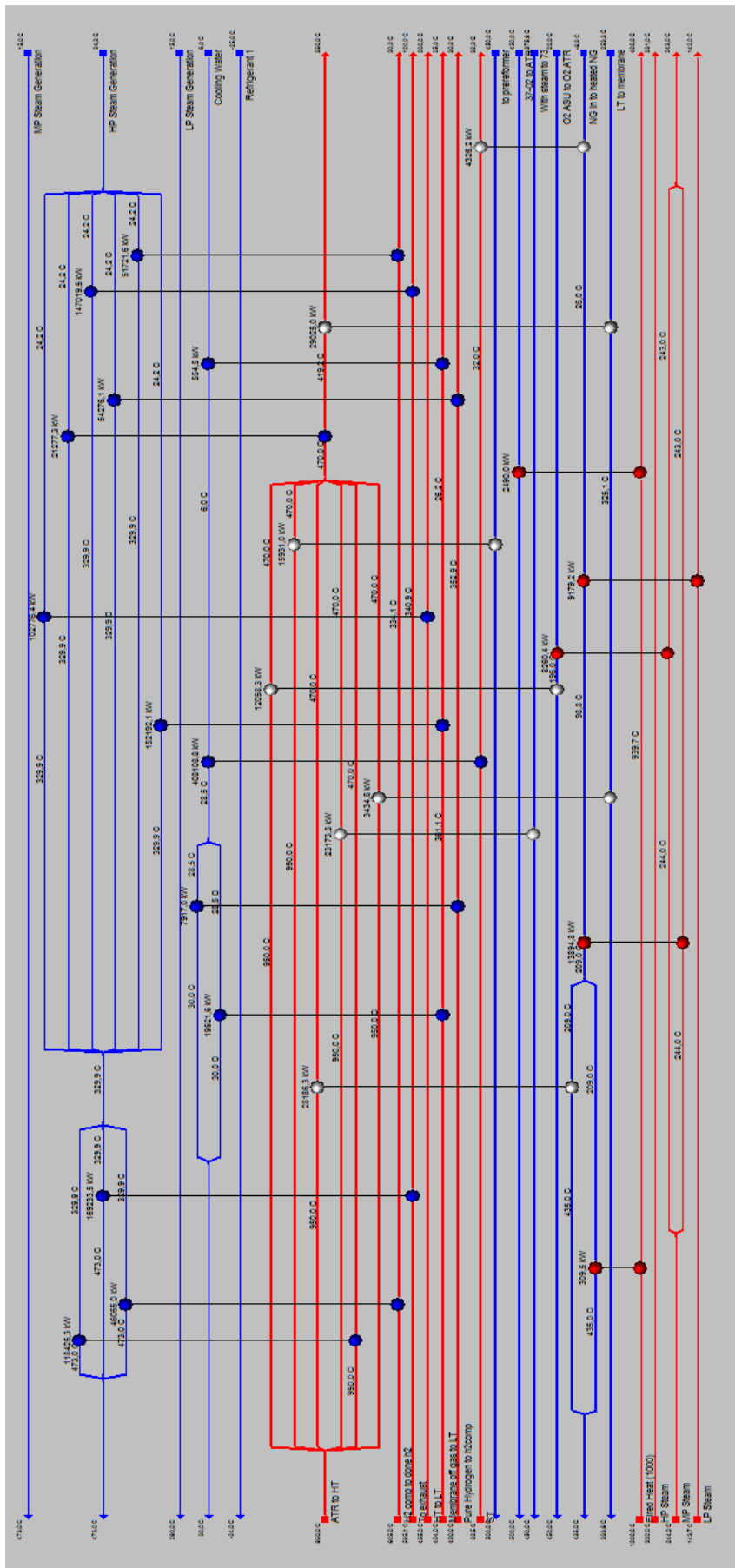


Figure A 6: One of the generated network designs for case II-1

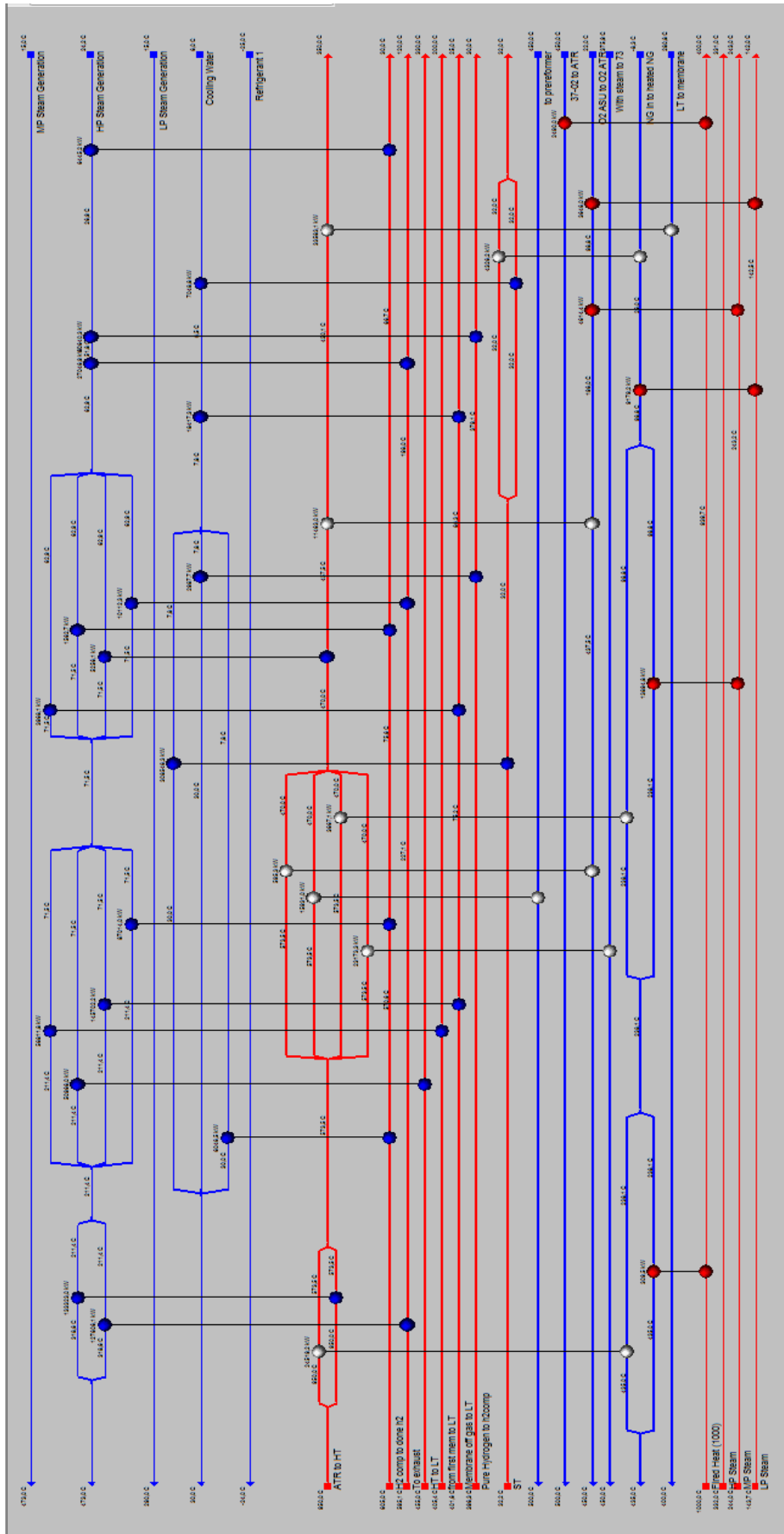


Figure A 7: One of the recommended designs for case II-2

Case II-3

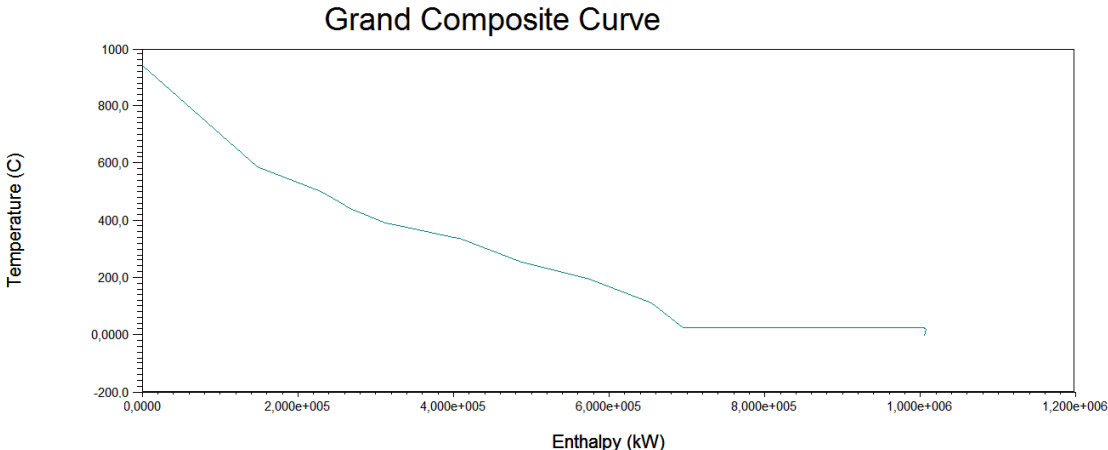


Figure A 8: GCC Case II-3

Case II-4

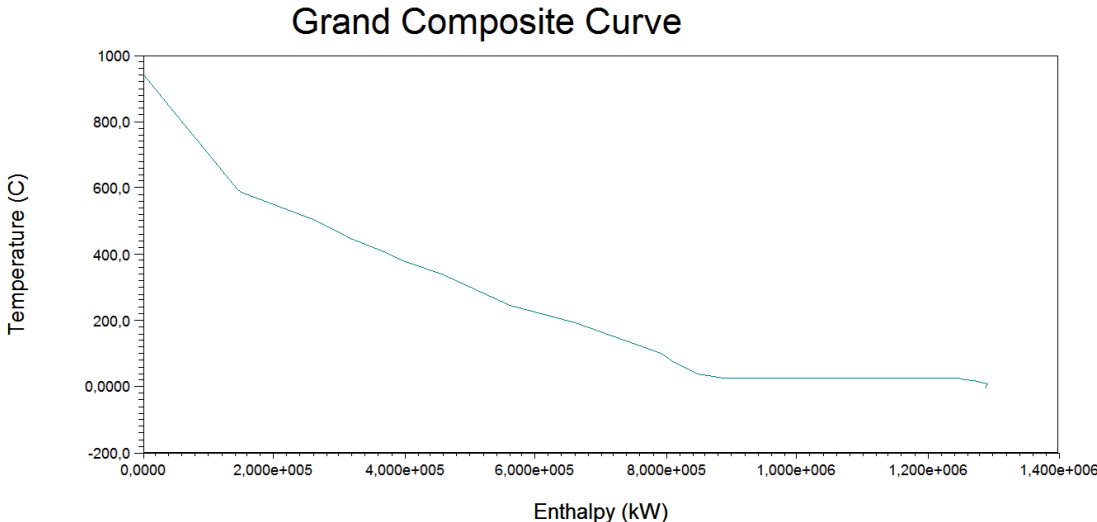


Figure A 9: GCC Case II-4

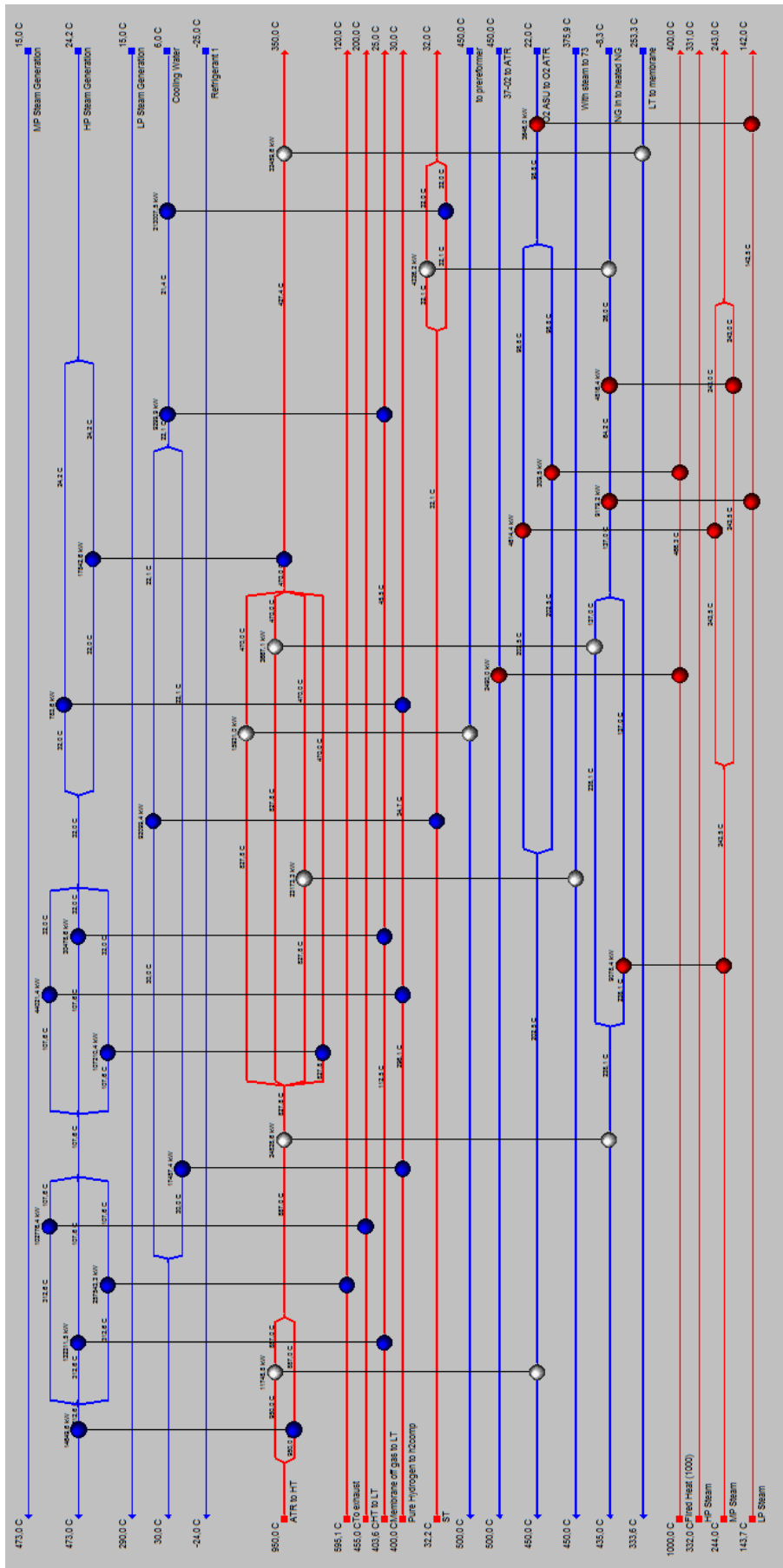


Figure A 10: One of the recommended designs for case II-3

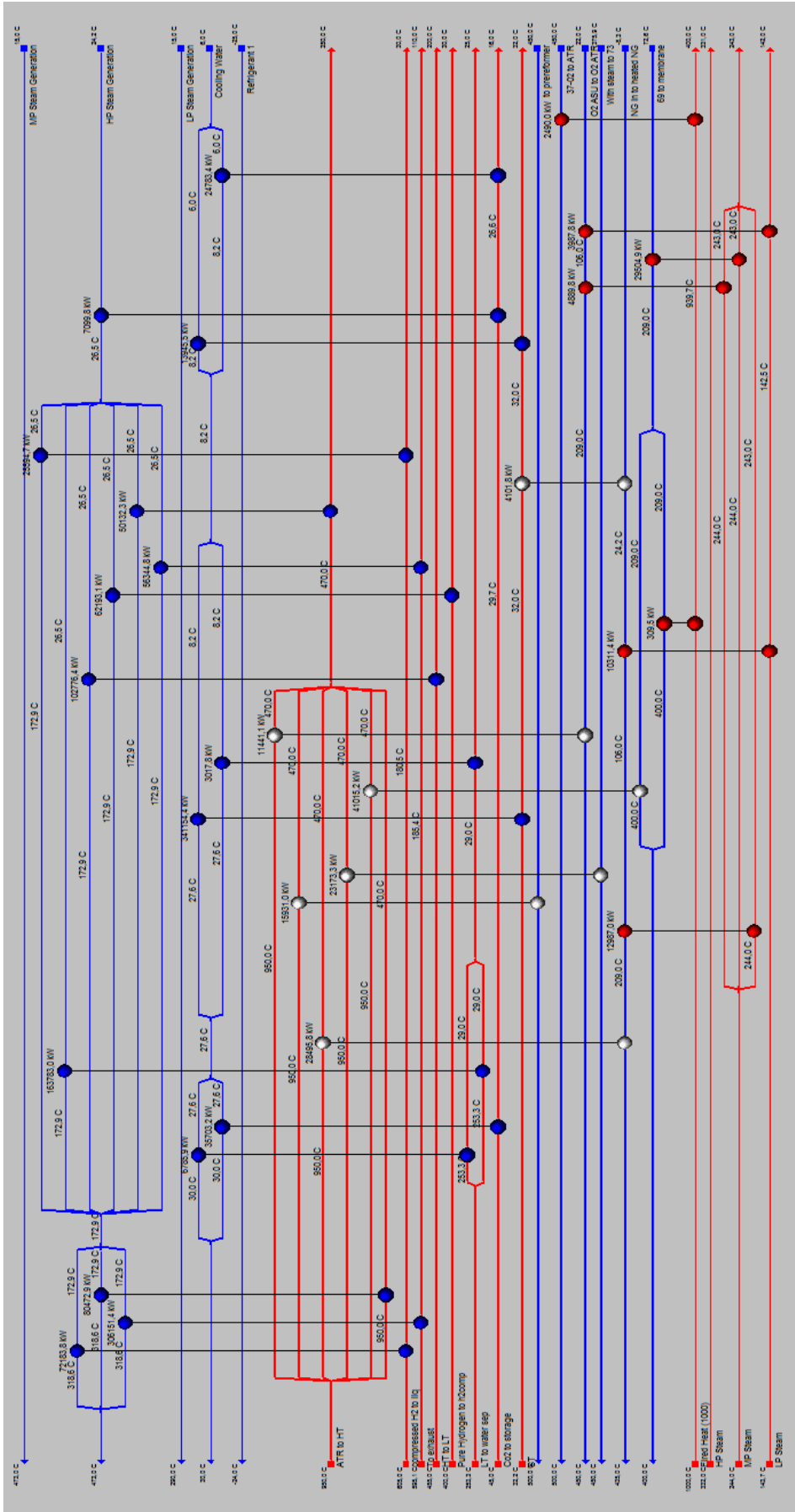


Figure A 11: One of the recommended designs for case II-4

